Green Infrastructure in the City of Vancouver: Performance Monitoring of Stormwater Tree Trenches and Bioswales

by

Osvaldo Miguel Vega

B.A.Sc. Mining Engineering, The University of British Columbia, 2016

A THESIS SUBMITTED IN PARTIAL FULFILLMENT OF

THE REQUIREMENTS FOR THE DEGREE OF

MASTER OF APPLIED SCIENCE

in

THE FACULTY OF GRADUATE AND POSTDOCTORAL STUDIES

(Civil Engineering)

THE UNIVERSITY OF BRITISH COLUMBIA

(Vancouver)

April 2019

The following individuals certify that they have read, and recommend to the Faculty of Graduate and Postdoctoral Studies for acceptance, a thesis/dissertation entitled:

Green Infrastructure in the City of Vancouver: Performance Monitoring of Stormwater Tree Trenches and Bioswales

submitted by Osvaldo Miguel Vega in partial fulfillment of the requirements for

the degree of Master of Applied Science

in Civil Engineering

Examining Committee:

Steven Weijs, PhD
Supervisor

Hanspeter Schreier, PhD
Supervisory Committee Member

Supervisory Committee Member

Additional Examiner

Additional Supervisory Committee Members:

Supervisory Committee Member

Supervisory Committee Member

Abstract

Green infrastructure (GI) is an approach that aims to reduce the amount of stormwater that reaches the combined or stormwater sewer networks and protect receiving waterbodies in urban watersheds. Cities across North America and the world are devoting resources to implement different types of GI to showcase their use. As it is a new approach, the field of GI research is emerging. The main objective of this thesis is to contribute to the GI literature by assessing the water quantity and water quality performances of three green infrastructure practices constructed in 2018 by the City of Vancouver. A stormwater tree trench and two bioswales were monitored. The soil moisture levels in the structural soil stormwater tree trench and one of the bioswales were monitored to assess the drought resistance of these practices and to evaluate the salt migration. This research introduced low cost monitoring options that can simplify the monitoring of stormwater tree trenches and bioswale practices. This research concluded that structural soil stormwater tree trenches and bioswale practices are effective in treating heavy metals, suspended solids, and other pollutants harmful street pollutants. These practices are also effective tools in removing stormwater from the stormwater/sewer networks by promoting infiltration to native soils.

Lay Summary

Green infrastructure is a tool that can be used by engineers to unseal the urban landscape. Green infrastructure aims to mimic pre-development conditions by allowing the stormwater to be used by plants and/or infiltrating the stormwater into the native soils. Green infrastructure is typically referred in literature as low impact development (LID) or best management practice (BMP), however they all fall under the umbrella of green infrastructure. This thesis assessed the performance of a structural soil stormwater tree trench and two bioswales practices from the perspective of hydrology, water quality treatment, drought resistance and salt tracking in order to get a full-spectrum perspective on the performance of green infrastructure at the City of Vancouver. This will study will help determine if green infrastructure is effective in the Pacific Northwest. In addition, this thesis introduced low cost monitoring options that can simplify the monitoring of stormwater tree trenches and bioswale practices.

Preface

This dissertation is original, unpublished and independent work by the author, Osvaldo Vega.

The field and office work for this thesis was completed by utilizing resources of the Green Infrastructure Implementation Branch of the City of Vancouver. This includes the automated sampling equipment, payment of the water quality analysis, transportation, and other supporting equipment necessary to conduct the research.

A preliminary version of Chapter 4 has been published. Vega, O., & Lukes, R. (2018). *Application of Stormwater Tree Trenches in the City of Vancouver*. University of British Columbia Sustainability. Vancouver. Appendix G contains the earlier version of Chapter 4 and it was solely drafted by this author.

The Simple Method described in Chapter 4 utilized to corroborate the total flows estimated by the SWMM® models make use of the modifications recommended by the Credit Valley Conservation (CVC) in order to include the green infrastructure footprint in the calculation and to estimate the total event's rainfall instead of the annual rainfall, which is the typical form of employment for this method.

The water quality analysis described in Chapter 4 was performed at a third-party laboratory called: CARO Labs. The samples were collected and composited by this author according to the quality standards required by the laboratory. The laboratory fees were paid in full by the Green Infrastructure Implementation Branch of the City of Vancouver.

Table of Contents

List of Tables

List of Figures

List of Symbols

'	Feet
"	Inches
%	Percent
<	Less Than
>	Greater Than
≤	Less Than or Equal
≥	Greater than or Equal
°	Degrees
°C	Degrees Celcius
A	Area
cm	centimeter
CO_2	Carbon Dioxide
C_u	Unit Conversion Coefficient
dS/m	DeciSiemens per Meter
E	Specific Energy (m)
Ecsol	Paste Extract Electrical Conductivity
g/m	gallons per minute
h	hour
Hz	Hertz
i	Precipitation
Ia	Impervious Fraction

km	Kilometer
kPa	Kilopascal
L/s	Liters per second
m	Meter
M	Mega
mL	Mililiters
mm	Milimiters
mS	MilliSiemens
mS/m	MiliSiemens per Meter
n	Number of Samples
N/A	Not Available
q	Unit Discharge
Rv	Runoff Coefficient
T	Temperature
W	West
Y	Water Elevation (m)

List of Abbreviations

ADP	Antecedent Dry Period
Al	Aluminum
ASTM	American Society of Testing and Materials
AUS	Australia
BC	British Columbia
BMP	Best Management Practices
Ca	Calcium
CA	Canada
CALA	Canadian Association for Laboratories Accreditation
CB	Catch Basin
CCME	Canadian Council of Ministers of Environment
Cd	Cadmium
CEC	Cation Exchange Capacity
CH	China
CI	Confidence Interval
CoV	City of Vancouver
Cr	Chromium
CSO	Combined Sewer Overflows
Cu	Copper
CVC	Credit Valley Conservation
DCIA	Directly Connected Impervious Area

DO	Dissolved Oxigen
EC	Electrical Conductivity
EIA	Effective Impervious Area
EMC	Event Mean Concentrations
ENG	England
FAO	Food and Agriculture Organization
FC	Field Capacity
Fe	Iron
FISRWG	Federal Interagency Stream Restoration Working Group
GI	Green Infrastructure
GI CB	Green Infrastructure Catch Basin
HEC-HMS	Hydrologic Modeling System
IARC	International Agency for Research of Cancer
ICPMS	Inductively Coupled Plasma Mass Spectrometry
IDF	Intensity Duration Frequency
IDF	Intensity Duration Curves
ISMP	Integrated Stormwater Management Plans
ISO	International Organization for Standardization
LID	Low Impact Development
Mg	Manganese
MK	Mann-Kendall
MV	Metro Vancouver

N	Nitrogen
NH DES	New Hampshire Department of Environmental Services
Ni	Nickel
NOx	Nitrate and Nitrogen Combination
OH	Ohio
ON	Ontario
P	Phosphorus
PA	Pennsylvania
PAH	Polyaromatic Hydrocarbons
Pb	Lead
pH	Potential of Hydrogen
PVC	Polyvinyl Chloride
PWD	Philadelphia Water Department
ROW	Right of Way
SA	Sacramento
SEFC	Southeast False Creek
STT	Stormwater Tree Trench
SWMM	Storm Water Management Model
TIA	Total Impervious Area
TKN	Total Kjeldahl Nitrogen
TOC	Total Organic Carbon
TP	Total Phosphorus

TS14	Toughsonic 14
TSS	Total Suspended Solids
UC	University of California
US (USA)	United States (United States of America)
US EPA	United States Environmental Protection Agency
VOC	Volatile Organic Compounds
VWC	Volumetric Water Content
WP	Wilting Point
WSUD	Water Sensitive Design
Zn	Zinc

Acknowledgements

I want to acknowledge that all the work conducted for this master thesis was done on the traditional and un-ceded territories of the Musqueam, Squamish, and Tsleil-Waututh people. With this work, I aim to help restore and protect the beauty of these watersheds.

I thank Dr. Steven Weijs for being my supervisor and supporting me on this journey. Your encouragement and willingness to commute far from UBC to our initial meetings with the City of Vancouver helped me get this master's thesis kickstarted. I am also deeply grateful for my second reader, Dr. Hanspeter Schreier, for agreeing to be part of my examining committee and for providing valuable feedback during the revision stage. Your dedication to protect the environment is remarkable and truly inspiring.

This research could have not been completed without the institutional, technical and financial support of the Green Infrastructure Implementation (GI) Branch of the City of Vancouver. I am extremely grateful for Melina Scholefield, manager of the GI branch, for opening the door to her group. I feel fortunate to have met you at the CWRA seminar, where you got me excited about the work that your branch does and for believing in me to pursue this research. I would also like to thank Robb Lukes for trusting me with the GI monitoring program and for providing invaluable mentorship since my Greenest City Scholar days to this date. Your support has played an immense role in the success of this research and I am excited to continue to learn from you in my new role at the city. I want to also thank Paul Lightfoot and David Flatt for their countless support, input and company. Thank you for being with me in the field to deploy the instruments, perform inspections, and for building part of the monitoring equipment: experimental flume (Paul) and cutting of the PVC weir caps (David). I want to thank Alexandra Couillard, Sara Pour, Chris Despins and Jesse Neufeld for volunteering your time to chat with me about my research and sharing your expertise with me. I also want to thank everyone at the branch who has made my time at the office so enjoyable: Kristen, Tim, Cameron, Yette, Wendy, Arzina, Karline and Cherie. Thank you to Thomas Gallos (Environmental Services Branch) for letting us borrow the automatic samplers and the work space to clean the samplers. Thank you to Nima Najafi (Integrated Rainwater Branch) for providing the rain gauge.

Lastly, I want to thank my family: my partner Cheryl Inkster. Thank you for being so loving, patient, accommodating and supportive this past year. I would have not been able to survive the early mornings, sleepless nights and non-existent weekends without you. Your love and support have been my bedrock for the last 7 years (and counting). To my brother Alonso, thank you for being my unconditional friend these past 14 years. Your friendship is something I hold very dear. To my parents and sister, thank you for your love and support. To my grandparents, cousins and aunts/uncles both in Canada and El Salvador, thank you for your love and support.

Dedication

I want to dedicate my thesis to all the people in this world tackling the climate change problem. Your research and passion inspired me to take action in my personal life and to contribute to the body of research dedicated for this cause. This is truly a defining moment in history as we need to correct the mistakes and negligence of past and current generations so that we can save and protect the environment.

We only have one planet to live and we must do everything in our control to not let misinformation and greed destroy the only home we have. We, the youth of this planet, are the ones who will suffer from the consequences of inaction and misinformation. This thesis is my contribution to help protect this world for the benefit of current and future generations.

Chapter 1: Introduction

1.1 Historical Background on Urban Hydrology

Archeologist theorize that the origin of communities is associated with the development of agriculture in the period known as the "Neolithic Revolution", which began about 11,500 years ago (Balter, 2005). The Neolithic period marks one of the two most important events in human history along with the "Industrial Revolution" (Scanes, 2018). The importance of the Neolithic Revolution is that it marked the transition from hunter-gather bands to settlements that domesticated plants and animals for their benefit (Zimmer, 2016). These early forms of communities settled in geographically advantageous locations. These locations could be near a source of water and accompanied by fertile lands to produce crops. The transition from the nomadic life, was accompanied by an increase in the population where these settlements occurred (Scanes, 2018). The stable food supply enabled the smaller communities to grow into kingdoms that spanned hundreds of miles (Zimmer, 2016). This period sets the base of what we call today: urban areas.

Fast forwarding to the 12^{th} BC, these small settlements have grown into large, complex empires. Within these empires exist intricate city systems that were developed to accommodate the expanding population. The pervious landscape that once dominated the small settlements was replaced with impervious surfaces, i.e. intricate paved road systems, plazas, buildings, etc. Civilizations such as the Greeks and the Romans were among the first civilizations to identify and solve how to deal with the excess runoff generated by the impervious surfaces. For example, the Greeks used ditches and clay pipes to drain and collect rain water (Delleur, 2003). The Greeks went as far as reusing the water collected during storms for household use during periods of water scarcity. They stored the stormwater in cisterns (Angelakis, Koutsoyiannis, &

Tchobanoglous, 2005). The romans disposed of the water depending on the location. Households would drain the water towards cisterns, street rainwater would be collected at strategic locations based on the grades of the roads, using gutters in some cases. Once the Romans mastered the practice of drainage and stormwater management, the newer cities in the empire would be planned strategically to incorporate sewage networks and inspection locations (Delleur, 2003). The approaches of the Romans and Greeks, of course, began to reduce the amount of water that could return to the soil.

In present day, our cities have continued to evolve on a scale unprecedented in human history. The global population has grown to approximately 7.6 billion people as of 2017 and it is estimated that about 55% of the global population lives in cities according to the UN. This number is expected to increase to 68% when the population is projected to be at 9.8 billion people across the world by 2050 (UN, 2017, 2018). The population increase and the migration to urban areas mean that our cities will have to continue to expand to accommodate current and future generations. This expansion implies that more impervious surfaces will be constructed in the new developments.

Urban watersheds approximately allow between 15% to 35% of the stormwater to infiltrate into ground, depending of the impervious surface cover. Under the same premise, between 30% to 50% becomes runoff (FISRWG, 1998). The hydrological conditions of urban watersheds and the ever-increasing population makes me reflect on the following: *How are our cities managing the ever-increasing stormwater runoff generated by the infrastructure built to house and connect millions of people?* The answer to this question is that after thousands of years, the great majority of cities across the globe still use the same approach employed in ancient times: *Collect the stormwater and pipe it out of the way as fast as possible somewhere else without caring much about the downstream effects.*

1.2 Restoring the Natural Flow of Water in the XXI Century

Collecting and piping stormwater is very engrained in our history, hence the difficulty to look at different approaches and to believe that these new approaches might be a solution to the increasing stormwater runoff problem. After the industrial revolution, cities in Europe (and soon after in North America) began discharging the stormwater runoff into the sewer systems. However, this approach backfired as the sewer systems would reach capacity during heavy rain periods. A flow regulator system was devised which would allow the combined flow in the sewer system to be diverted to a nearby waterbody when the capacity of the sewer system was exceeded. The regulator system became known as combined sewer overflows (CSO) (Liu, Bralts, & Engel, 2015; Wojtenko, Minamyer, Tafuri, Field, & Lai, 2004).

Mid XX century, scientists in the United States researched and demonstrated the health and environmental hazards of CSO practices (Wojtenko et al., 2004). The combined stormwater/sewer water was contaminated with oxygen demanding pollutants, suspended solids, nutrients (Phosphorus and Nitrogen), pathogens, heavy metals, among others (US EPA, 1999b). This contaminated water cocktail affects the aquatic environments of the receiving waters, creating a public health and aquatic life endangerment concerns.

Cities are currently addressing the CSO problem by separating the combined systems and have separate mains for sanitary and stormwater. The city of Vancouver as of 2019, has managed to separate ~54% of the combined sewer system (City of Vancouver, 2018d). Despite the sewer separation efforts, new approaches are required to tackle the stormwater issues of the XXI century. A decrease in the amount of stormwater that ends at the combined sewer system is necessary to reduce the impacts of our cities in their respective watersheds. Scientists have recognized that "unsealing" urban watersheds by increasing the perviousness of the watersheds can provide hydrological benefits to cities. The approaches to unseal cities has many names: best management practices (BMP), low impact development (LID), water sensitive urban design (WSUD), among other names. However, now they are all known collectively as green infrastructure (GI) (Schifman et al., 2017).

Green infrastructure can be used as a complement or as an alternative to centralized gray infrastructure networks by offering additional retention and diversion capacity to an overloaded system. Green infrastructure uses soils, vegetations and other elements to enhance water retention, infiltration, and evapotranspiration (Schifman et al., 2017). This ultimately delivers environmental, social and economic benefits.

1.3 Research and Monitoring Objectives

Green infrastructure is an emerging field of research. Cities across North America are devoting resources into pilot projects that demonstrate the application of GI in their cities. In general, the field of GI suffers from a scarcity of monitoring studies. Monitoring studies are necessary to adequately assess the performance of GI practices. A 2016 report surveyed 35 cities across North America and found that rain gardens, infiltration bulges and absorbent landscapes are typically the most common GI practices used as they are perceived as highest performing (Jin, 2016). Consequently, these types of practices are associated with the majority of monitoring studies available in the literature. The shortage of monitoring studies is very evident in the field of stormwater tree trenches (STT) practices. The monitoring efforts on GI, including STT, in the field will be covered in Section 2.2 of this thesis.

The main objective of this research is to assess the hydrological and water quality treatment performance of GI in the City of Vancouver (CoV). As a secondary objective, thesis aims to contribute to the literature of GI performance monitoring and propose low cost monitoring alternative for bioswales and STT. The findings of this research will provide city planners, designers and engineers with a set of applicable performance standards for the design of future GI at the CoV. An additional benefit of this study is the possibility to extrapolate the findings from this research to the rest of the Lower Mainland as the cities within the region share similar climatic and soil conditions. The Lower Mainland is a region of municipalities located in the Southwest of British Columbia (BC). It includes cities in the Greater Vancouver Urban area (Vancouver, Burnaby, Surrey, Richmond, etc.) and the valley rural areas (Chilliwack, Abbotsford, Langley, etc.) (Province of British Columbia, 2018).

1.4 Scope and Methodology Overview

The scope of this research includes the performance monitoring of three different GI practices which include a STT and two bioswales located in Vancouver, BC and the introduction of monitoring method that facilitate the monitoring of bioswales and STT. The three GI practices will be monitored for water quantity and water quality performance from the month of September of 2018 to February of 2019. This monitoring period only covers the wet period and it will not provide enough information on the pollution loading problem related to the first flush. The first flush is not captured during the wet season as it is more persistent in the dry months.

The STT design is a structural soil practice. The two bioswales practices have similar designs but use different soil mediums: One bioswale uses a proprietary soil blend from Veratec© and the other bioswale uses the standard turf blend used by the CoV as of 2018. Three of the practices are in the Mount Pleasant neighborhood, at the intersection of Quebec Street and

1st Avenue. This area will be further referenced to as "Quebec & 1st." A more detailed description of the practices and their respective sites is available in Section 3.3 of this thesis.

For the monitoring of the hydrological parameters, the study made use of different sensors to continuously track the water inflows, the migration of the stormwater through the practices, and water outflows from the practices to the stormwater sewer system. The rainfall information was obtained from a nearby rain gauge, property of the CoV, located within a maximum of ~266m distance from all the practices.

The water quality monitoring was conducted by the collection of a limited number of samples. The samples were acquired by using automatic water quality samplers loaned from the CoV. The short timeframe of this thesis did not allow for the collection of more samples to achieve statistical significance by site. However, a total of 12 discrete time weighted composite samples from the practices (inflows and outflows), one rainwater sample and two field blank samples were analyzed during the water quality study. The sampling method chosen has the main limitation of not capturing the entire pollutant loading behavior of each storm, including the first flush. The water quality study monitored for heavy metals, nutrients, total suspended sediment, among other parameters. The samples were independently assessed by a third-party laboratory based at the City of Richmond. The samples were delivered to the laboratory within a two-hour period from the collection time. No parameters were measured on site due to equipment limitations.

Below is a summary of all the performance parameters that this thesis aims to monitor:

- Water quantity: peak flow reduction, volume reduction and lag time
- Water quality: pollutant removal efficiencies
- Drought resistance and salt flushing: soil moisture and electrical conductivity monitoring

Green infrastructure is difficult to monitor as they come in various shapes and sizes. The last objective of this thesis is to recommend and introduce monitoring methods that can help simplify the performance monitoring of STT and bioswales. For the STT GI method, this thesis introduces a novel inflow monitoring method that can accurately measure flows from catch basins (CB), which are typically used as pre-treatment STT.

Chapter 2: Literature Review

The literature review was conducted to provide an insight on:

- The impact of urban development in cities from the perspective of:
    - Hydrology
    - Water quality
    - Urban vegetation health
- The impact of climate change in the urban environment: How will this further affect the hydrology, water quality and tree health of our cities?
- What is GI, and what can we expect from its use based on the experience of other cities across the Lower Mainland, North America and the rest of the world?

2.1 Watersheds Overview: Impacts of Urbanization

The pressures from population growth and the immigration of people to cities create an inevitable push towards the rapid urbanization of watersheds. This situation has a myriad of negative consequences in urbanized watersheds. This section of the literature review will focus on the impact that urbanization has from a hydrological, urban vegetation and water quality perspective.

2.1.1 Hydrological Impacts

The Lower Mainland has undergone massive development since the 19th century with the arrival of European settlers to the region, affecting the hydrological regimes of the different watersheds that belong to the region. The impact of development in the Lower Mainland was reflected by a report prepared for the Ministry of Fisheries and Oceans in 1997. The main conclusion of the report was: “the development footprint … has left devastating impacts on most streams, many of which historically supported, and some of which still support, viable salmon populations." The survey of this report identified that the surviving streams are under stress due to alterations in the watershed landscape, pollution, and riparian zone destruction (Precision Identification Biological Consultants, 1997).

2.1.1.1 Natural Hydrological Flows

In a natural, undisturbed forest, infiltration depends on a variety of factors that include: vegetation cover, rainfall intensity and duration, and soil characteristics (D. Booth, 1991). Most of the water is either intercepted by the vegetation canopy, evapotranspired by the flora, or infiltrated into the soil, eventually making its way into the deep groundwater. Very little stormwater leaves the site as runoff (D. Booth, 1991; Stephens, 2002). These interception opportunities are lost with urbanization.

2.1.1.1.1 Interception

The vegetation in a catchment plays an important role in the hydrological cycle. A portion of the precipitation never reaches the ground as it is intercepted by the vegetation in the catchment. The water storage capacity of the flora is a function of the plant type, the shape of the leaves, the texture of the leaves, the time of the year, among other factors (FISRWG, 1998). According Dunne and Leopold (1978), forests can intercept between 13% to 28% and grasses have an interception efficiency between 10% to 20% depending on climate. Urban trees can intercept more rain water than trees in forested areas due to the exposure of the trees to higher temperatures and winds. The continuous canopy of the forested areas protects the trees from the conditions encountered by urban trees (Asadian, 2010).

2.1.1.1.2 Evapotranspiration

Evapotranspiration is a complex process that is part of the water cycle. It refers to all the processes where liquid water returns to the atmosphere as vapor (Margulis, 2017). However it is one of the most difficult and uncertain components to quantify in the water balance (Blight, 2003; Fatahi, Khabbaz, & Indraratna, 2014; Margulis, 2017). Evapotranspiration is composed of transpiration and evaporation components. Transpiration refers to the diffusion of water vapor that returns to the atmosphere from the plant leaves. Transpiration originates from the water taken up by the roots, which are part of the vascular system of the plant (FISRWG, 1998; Margulis, 2017). In the root system, the non-woody roots have the main function to absorb water and nutrients (Fatahi et al., 2014). More specifically, this function takes place in the most active parts, which are the young roots and root hairs (Radcliffe, Hayden, Walson, Crowley, & Phillips, 1980). Trees located in urban areas were found to have higher transpiration rates than trees located in forest as urban trees are more exposed to wind and higher temperatures than trees in forests (Asadian, 2010). Evaporation takes place when water is transformed to vapor from liquid water in open water surfaces, such as lakes and rivers, and from the soil (Margulis, 2017). The soil evaporation is a complicated process that depends on capillarity and osmotic forces (FISRWG, 1998).

2.1.1.1.3 Infiltration

Rainwater that is not intercepted by the mechanisms described before can be infiltrated into the ground. The rates at which water infiltrates into the ground depends on the rainfall intensity, the depth of the water table, the antecedent moisture content, and the hydraulic properties of the soil (Ferré & Warrick, 2005). Among other processes, gravity is the main force that drives water into the pores of the soil, especially the macro pores. Not all soils have the same amounts of pores available. Porosity is highly dependent on the texture of the soil (Dunne & Leopold, 1978). The size, connectivity and quantity of pore openings will determine the movement of water within the soil. Air and water favor large, continuous pores (Holthusen, Brandt, Reichert, & Horn, 2018). Below the surface, gravity is still the main force driving the water down, however, capillarity forces eventually take over and can make the water move in any direction. This process will continue until the water reaches the zone called as the capillary fringe. The capillary fringe is a water saturated zone held by capillarity forces. The capillary fringe is located above the ground water table, which is a phreatic surface. This surface will fluctuate with the seasons by either being recharged or discharged by natural factors (FISRWG, 1998).

2.1.1.1.4 Runoff

Runoff occurs when the rain water cannot infiltrate into the soil. Factors that affect the runoff process include topography, geology, soil characteristics, vegetation, climate, among other factors (FISRWG, 1998). Runoff can be grouped into to two core categories: surface (overland) flow and subsurface flow (FISRWG, 1998; Horton, 1933; Margulis, 2017; Rinderer & Seibert, 2012). Surface flow can be further broken down as infiltration excess surface runoff and saturation excess runoff flow (D. B. Booth & Jackson, 1997; FISRWG, 1998; Margulis, 2017). Infiltration excess surface runoff occurs when the rate of precipitation exceeds the infiltration capacity of the soil. In hydrology infiltration excess runoff is known as “Hortonian” runoff, after Robert Horton (1933). The rainwater will begin to accumulate in depressions in the soil, ponding until the water is either infiltrated later or evaporated, if the climatic conditions allow. Otherwise, depending on the slope of the topography, the rainwater can run down the slope as runoff (FISRWG, 1998; Margulis, 2017). Horton argued that antecedent soil moisture conditions and soil properties played important role in the infiltration capacity of a soil (Horton, 1933; Margulis, 2017).

Water can pond at the surface and runoff downslope, even if the soil beneath it is not saturated. The second form of runoff is known as saturation excess runoff or “Dunne” runoff. Saturation excess runoff occurs when the ground water table reaches the surface, protruding from the soil. This is can occur due to recharge from higher ground or from the local precipitation. This happens generally when the water table is relatively shallow, typically near a receiving water body (Dunne, 1975; Margulis, 2017).

Subsurface flow refers to lateral movement of the water in the soil. Water in the soil pores moves from “A” to “B” due to differences in hydraulic head, also known as hydrostatic pressure differences, due to elevation changes (FISRWG, 1998). There are two kinds of subsurface processes. The first process is known as baseflow. This relates to the downhill lateral flow of groundwater towards a stream. The second process known as interflow is focused on the lateral flow of water in the unsaturated zone known as “Vadose Zone” (Margulis, 2017). Rainwater infiltrating through the Vadose Zone might not reach the groundwater table due the presence of an aquitard, which can create a perched water table or the presence of macropores that transport water more effectively (FISRWG, 1998; Margulis, 2017). In both situations, and if the gradient permits, the water can be slowly discharged into a stream directly.

2.1.1.2 Watershed Urbanization Impacts

The urbanization of a watershed completely changes the natural regime (D. B. Booth & Jackson, 1997; Henshaw & Booth, 2000; Kokkonen, Grimmond, Christen, Oke, & Järvi, 2018; T. R. Oke, Mills, Christen, & Voogt, 2017; Stime, 2014) explored in section 2.1.1.1. Urbanization is tied with the increase in impervious areas, associated with a consequential decrease in infiltration and evaporation in the watershed (D. B. Booth & Jackson, 1997; Kokkonen et al., 2018). The impacts of this change in the hydrological regime can be seen in the form of high peak flows, reduced time to reach the peak, and a decrease in return period of storm flows of certain magnitude (D. B. Booth & Jackson, 1997; Klein, 1979; Pour, 2013; Stime, 2014).

2.1.1.2.1 Impervious Area

Impervious surfaces are commonly used in hydrology to assess the impact of urbanization on water resources (Ebrahimian, Wilson, & Gulliver, 2016). Efforts have been made in the past to find ways to quantify the impervious area of a watershed. Previously, the concept of Total Impervious Area (TIA), was considered a key definition that characterized the decline of a watershed, where streams in watersheds that reach 15% imperviousness begin to show signs of decline. This constraint was more stringent on streams with self-sustaining fish populations, where a 10% watershed imperviousness should not be exceeded (D. B. Booth & Jackson, 1997; Klein, 1979). However, TIA is deficient in two areas, which were brought up by Booth and Jackson (1997):

The first component has to do with the assumption that TIA does not account for the compaction on certain pervious surfaces, which might in fact have low perviousness, effectively acting as impervious surfaces. TIA can also discriminate surfaces such as rooftops that can drain directly into the channel though downspout systems. Both exclusions would cause TIA to underestimate runoff.

Secondly, TIA includes impervious surfaces that might not be hydraulically connected to the downstream channel, contributing nothing to the runoff response. This would cause TIA to overestimate runoff. On the same note,

Effective Impervious Area (EIA) is an index that circumvents the issues previously emphasized. Effective impervious area is an indicator of urbanization effects, much more accurate than TIA for determining alterations to urban streams (Ebrahimian, Gulliver, & Wilson, 2016). The EIA index includes only the impervious area that has "direct hydraulic connection to the downstream drainage system" (D. B. Booth & Jackson, 1997; Ebrahimian, Gulliver, et al., 2016; Ebrahimian, Wilson, et al., 2016; Walsh, 2004). The relationship between EIA and TIA will vary greatly on local factors that depend on the storm drainage and flood attenuation features of a watershed (Miller et al., 2014).

In watersheds such as the Lower Mainland of BC, were natural forests dominate the region and the rainfall patters are on average low intensity rainfalls, subsurface flow regimes tend to govern in the watershed (D. Booth, 1991; D. B. Booth & Jackson, 1997; Pour, 2013). Under this regime, most of the precipitation is usually absorbed and infiltrated in the soils where it moves laterally downstream (D. Booth, 1991; Pour, 2013). The incidence of impervious surfaces is clearly detrimental as it changes the dominant hydrological regime for the Southwest BC region. Under the index of EIA, researchers determined that humid watersheds such as Western Washington State, which resembles the conditions of the Lower Mainland of BC, suffer loss of aquatic-system function, perhaps at an irreversible level, when EIA reaches ~10% (D. B. Booth & Jackson, 1997; Klein, 1979).

2.1.1.2.2 Higher Peak Flows and Reduced Time to Peak

Urbanization alters the watershed regime described in Section 2.1.1.1. For the Lower Mainland, infiltration is an important component of the hydrological balance. The subsurface flow regime formerly described for the Lower Mainland can change to a surface flow (runoff) dominated regime (D. Booth, 1991; D. B. Booth & Jackson, 1997; Henshaw & Booth, 2000; Pour, 2013). This impacts the watershed two ways: increase in volume of runoff (more runoff and higher peak flows) and increase in speed at which runoff reaches streams (time to peak).

The first impact deals with quantity of runoff produced. Groundwater is negatively impacted as, post-development, a larger portion of the rainfall is converted to runoff directly and a smaller portion can infiltrate in the soils (Klein, 1979; Pour, 2013). This effectively lowers the base flow as less water infiltrates (Klein, 1979; T. R. Oke et al., 2017; Stime, 2014). Hence, more water will be conveyed downstream, effectively increasing the runoff volumes and flow rates (Ebrahimian, Gulliver, et al., 2016). From a hydrological point of view, the larger volume of runoff also increases the size of flood peak during storm periods (Leopold, 1968). Previous peaks are now magnified due to the larger quantities of runoff produced. Runoff increases in proportion to the cover of impervious area (T. R. Oke et al., 2017; White & Greer, 2006). When comparing natural against urbanized watersheds, peak runoff from urban catchments are characteristically higher than natural catchments. This comparison links to a direct, but not necessarily linear relationship, between impervious surfaces and the ratio to peak increase (Stime, 2014). Researchers Spinello and Simmons (1992) found a direct correlation between magnitude of high flows and imperviousness. A 2003 Boulder, Colorado modelling study made a link between directly connected impervious area (DCIA), another imperviousness index similar to EIA, and runoff production during small rainfall events. The researchers concluded that there was a direct relationship between peak discharge and DCIA (Lee & Heaney, 2003).

The second effect of the impervious cover is that water can move downstream more efficiently. Engineered conveyance systems play an important role in reducing the time it takes to reach a peak flow by reducing the time of concentration. Because the full drainage area now contributes already during shorter, more intense storms, the peak flow magnitudes will also increase. The faster, larger flow is evident in the sheet flow and gutter flow conditions observed on the impervious urban surfaces during rainfall events. Engineered systems successfully act as "smooth" surfaces, assisting runoff to move faster overland (D. B. Booth & Jackson, 1997; Leopold, 1968; Stime, 2014). This type of hydrological response is often referred to as "flashy" flows (Henshaw & Booth, 2000). The increase efficiency of the connected surfaces and conveyance systems, can allow runoff to reach an outlet more rapidly (between 5 to 20 minutes) when compared to a natural, forested catchment which can take several hours (Leopold, 1968; Ligtenberg, 2017; T. R. Oke et al., 2017). A 2014 study in the United Kingdom assessing the urbanization impacts on a peri-urban watershed that was historically rural found that the increase in peak flow (by over 400% increase in magnitude from historical data) was accompanied by a decrease in time to reach peak flows (Miller et al., 2014) on average by about 58% between the years of 1960 to 2010 (calculated based on data provided by the study).

2.1.1.2.3 Flood Return Frequency

Accompanying the changes in runoff volumes and consequent decrease in time to reach peak flows due to a decrease in time to reach concentration, storms of smaller size can produce flooding events that were not possible during undeveloped conditions. Booth (1991) argued that urbanization accomplishes more than just magnifying peak discharges; urbanization creates entirely new peaks in the system. Urban watersheds become more sensitive to shorter, intense storm events. All these changes result in more frequent occurrence of floods of any given discharge post-urbanization (D. Booth, 1991; Pour, 2013).

The firsts attempt to characterize the impact of urbanization on flood return intervals was done by Luna Leopold (1968). Leopold developed practical curves that summarized several studies at the time. From his curves, one could conclude, for example, that in a 20% impervious and 20% sewered catchment, overbank flows increase by twice the magnitude of the peak discharge of an un-urbanized watershed; and in a 100% sewered and 60% impervious, overbank flows could almost be 6 times the magnitude of the peak discharge of an un-urbanized watershed for the same return interval. However, Hollis (1975) expanded the work that Leopold initiated and concluded that urbanization does not affect floods of different recurrence intervals by the same extent. For example, smaller, more frequent events are indeed affected by urbanization as Leopold suggested, however, a large flood that will inflict damage regardless might not experience significant alterations from the impervious areas within the catchment area. To account for this situation, Hollis (1975) developed a non-linear curve example for a basing with 20% paving (impervious) that reflects his premise. From this curve, it can still be concluded that urbanization affects the lower end of the return intervals. For the 20% paved basin, the peak flow of a 1-year return interval event is magnified by 10 times when compared to predevelopment conditions. In the Pacific Northwest, Booth (1991) concluded that depending on the percentage of urbanization in the catchment, the greatest percent increases in peak flow magnitudes were observed for the most frequent flood events.

All these researchers conclude the same principle in the end: urbanization affects the flows, especially for the most frequent flow events. Storms magnitudes that produced little to no runoff before urbanization can have their peak flows magnified once urbanization is introduced. The degree of the impact will vary depending on the specifics of the watershed in question.

2.1.2 Urban Vegetation Impacts

The first casualty in the introduction of urbanization are plants. When soils are compacted or covered with impervious surfaces, plants are either removed or planted near compacted soils, effectively killing them. Designers, such as urban planners, architects and engineers, nowadays incorporate vegetative elements into their plans and designs as we now appreciate the beauty and benefits of including plants in streets, buildings, etc. However, very little is known by the average designer on what a plant requires to survive. This leaves the vegetation in a position of struggle to survive.

2.1.2.1 Root Space

One of the most important qualities that is often overlooked is the element of rooting space. It is common knowledge that a plant requires soil, water and nutrients to live, but often too little of those components are included in designs. Plants require space to spread their roots. Roots play an important part in the overall structure of a plant. Vegetation requires roots to obtain water and nutrients; nonetheless, roots also provide a structural support component that allows the growth of a plant. The "root architecture" of the plant vary between species, soil composition and nutrient availability (Hodge, Berta, Doussan, Merchan, & Crespi, 2009) as plants seek within the soil where to feed.

Designers introduce compacted surfaces around the designated vegetation areas, which limit the space where the roots of the plants can expand to. Plants are often relegated as decorative elements, making them non-essential in the overall design. When roots encounter dense soils (such as soil compacted to 95% proctor density for example) or root barriers, plants adapt by changing the direction of the root growth. The biggest downside of this is that trees are "containerized" by the compacted soil or root barriers (Bassuk, Grabosky, & Trowbridge, 2005).

The containerization problem is very evident in hurricane/monsoon prone areas where urban trees are toppled by high winds, nonetheless this problem is persistent in all urban watersheds. When assessing the cause of failures of the trees in hurricane affected areas, researchers often find that trees were installed too close to compacted surfaces. The more rooting space a tree has, the more resistant the trees are to wind toppling. The deflection of roots by curbs, sidewalks, roads, etc. increase the failure rates by wind toppling (Gilman, Edward F.;Partin, 2007). This leaves large vegetation such as trees vulnerable to stability problems.

2.1.2.2 Soil Moisture

As the volume of search is reduced, trees experience stress related to the lack of water and nutrients. A consequence of lack of water is that trees must work harder to obtain it. The introduction of impermeable surfaces reduces the amount of water that is available to infiltrate as explored in Section 2.1.1.2.1.

Water enters the plant via an osmosis process in the roots. The suction pressure (negative pressure) applied by the root hairs acts against the gravitation pull of earth and the suction pressure known as “matric potential” of the pores in the soil. If the moisture content is low, the suction in the soil pores is higher than the root’s osmotic pressure, making it more difficult, if not impossible, for the roots to extract the liquid. By increasing the suction pressure around the roots of the plant, to an unsustainable point, the overall structure of the plant will fail. This will cause wilting. This phenomenon is directly related to the soil wilting point (Margulis, 2017). If the plant does not succumb to this stress, they will show signs of water stress (Bartens, Wiseman, & Smiley, 2010).

Depending on the soil properties, the amount of water available for the plants varies. Figure 2.1 shows the volumetric water content (VWC) for a wide range of soils and it relates them to their corresponding level on the field capacity (FC) and wilting point (WP) curve. This curve relates the different matric potential points against the soil’s moisture content by soil type classification. This curve was developed by Saxton and Rawls (2006) with extensive soil water characteristic data from the United States Department of Agriculture. The data includes over 4,000 data points that include soil water content at matric potentials of 33kPa and 1,500kPa, soil composition, among other parameters. The table summarizing their findings can be found in Appendix A. The main drawback of this table is that the soil organic matter content in the samples used to develop the table averaged 2.5%. Higher quantities of organic matter on soil have been shown to increase the water retention capacity of soils by acting like sponges (Franzluebbers, 2002; Fundenburg, 2001). This would shift both the FC and WP curves to higher values of WVC.

Curves of this kind make the process of identifying suitable moisture levels by soil type more intuitively for irrigation plans. Nevertheless, it is important to highlight that this model would be consider a static one. Academics recommend using more dynamic models that incorporate soil, plant and atmosphere interactions into account when determining the appropriate soil moisture values. This can be achieved through numerical models (Dane, Topp, Romano, & Santini, 2002). However, for the scope of this thesis, a static model approach will be used to evaluate the drought resistance of the GI practices.

In short, the curve can be interpreted in the following fashion:

- The moisture content values above the FC are typically moved by gravity. The water may be available for the plant for a short period of time after the storm as gravity will drain the soil. It is important to highlight that too much water can also induce stress on a plant.
- The moisture content between the FC curve and the WP is the moisture available for plant absorption.
- The moisture values below the WP curve reflect the stage where the plants can no longer absorb water from the soil, inducing permanent damage to the plant if not corrected in time.

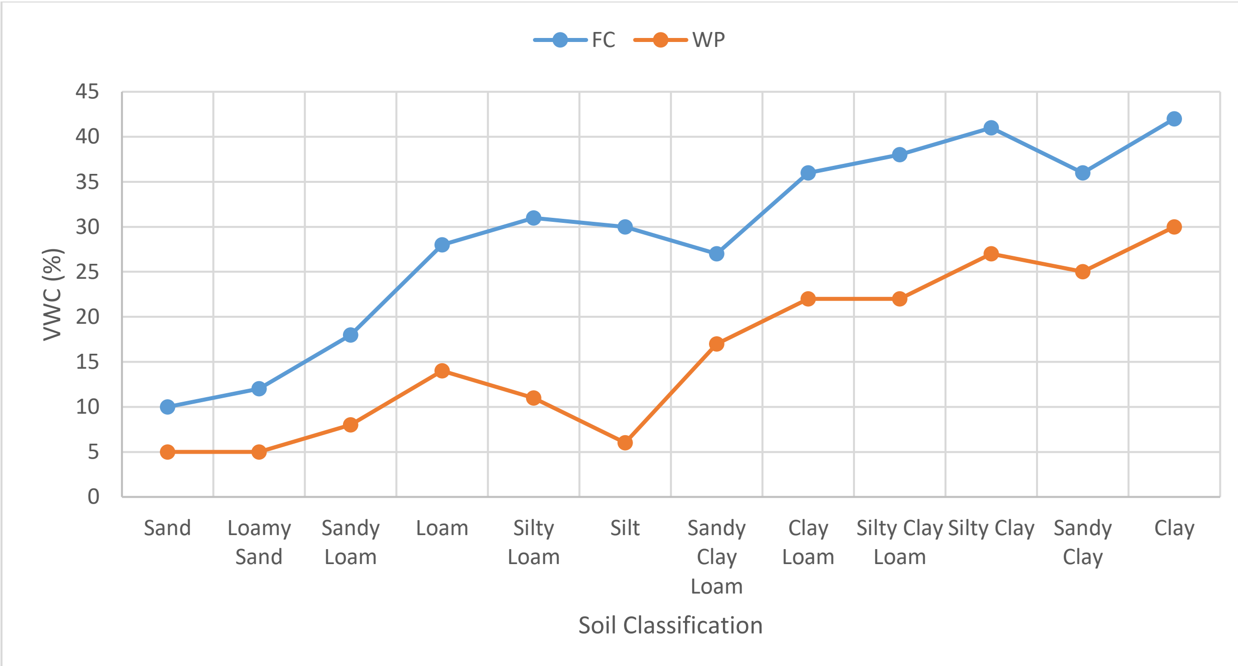

Figure 2.1: Field water capacity and permanent wilting point by soil type (Saxton & Rawls, 2006).

2.1.2.3 Soil Salinity

Salts are an issue in urban watersheds exposed to severe winter conditions. The problem with salts is that commonly overused and become detrimental to the flora (Ordóñez-Barona, Sabetski, Millward, & Steenberg, 2018). Salt of the NaCl form is commonly used by municipalities to preemptively or reactively melt the snow/ice from roads, sidewalks, plazas, etc. (Kimbrough, 2006; Marosz & Nowak, 2008). Their use began in the 1930s and they became common practice by the 1960s. The de-icing salt can be deployed either by spreading manually by workers or equipment can be used in some cases. The salts can be utilized as a solid (in crystal form) or dissolved in the form of a brine. There are variations of the salts that are used nowadays which include substitutes such as magnesium chloride ($MgCl_2$), calcium chloride ($CaCl_2$). In some cases the salt substitutes are diluted in cane sugar or beet sugar molasses to improve the salt's retention time on the surface (Kimbrough, 2006). Utilizing molasses-based salt solutions can be also detrimental from a water quality perspective. The injection of nutrients will be further discussed in Section 2.1.3.3.

The salts used during the snow storm events, or even during cold days, tends to stay in place unless the ambient temperatures rise, and the snow begins to melt. Once runoff begins to occur, the salts are either transported to the stormwater/sewer system or to the urban vegetation. Once salts begin to infiltrate into the soils of the urban vegetation, the salt concentrations begin to rise. After certain thresholds are met, which highly depend on the plant species, the vegetation will begin showing damage. This damage can be shown in the form of leaf and root necrosis, hinder growth, water deficit and cause death (Munck, Bennett, Camilli, & Nowak, 2010; Ordóñez-Barona et al., 2018).

2.1.3 Water Quality Impacts

Water bodies in proximity to urban areas have historically been used as sinks. The concept of discharging untreated, contaminated water during periods of excess stormwater was the basis of CSO systems. Section 1.2 of this thesis went into more detail on their purpose and functionality. In a nutshell, once the sewer is overwhelmed by the rain event, the CSO system is activated and by design, the system's overflow diverts the untreated, excess stormwater into the strategically selected nearby water body. This water body could be in the form of a lake, river, among other forms (Liu, Ahiablame, Bralts, & Engel, 2015). All the street pollutants that were accumulated during the runoff process ultimately end up in the water body. Despite efforts by engineers to incorporate sediment retention units, such as CB, sediments are still a prominent water in stormwater and sewer systems.

Separating sewers and stormwater systems is a new direction that many municipalities are currently taking. This recent strategy was developed by municipalities to address the CSO events that are very common nowadays. Smaller storm events are now triggering CSO events. The stormwater collected in the separated stormwater systems is discharged directly into a receiving water body untreated. In the case of Vancouver, these water bodies are the Burrard Inlet and the North arm of the Fraser River (Hall & Schreier, 1996). These separation programs are a start but not a “fix all problems” solution.

The sewer separation process is slow and expensive, not to mention that they are not 100% effective. Firstly, cross-contamination is a risk even after the sewers are separated (US EPA, 1999a). Every building in the sewershed must be connected to the appropriate sewer connections to be effective. This is a problem for buildings that have not been affected by newer bylaws that require buildings to have separated sewer connections. Secondly, these separation programs do not include stormwater treatment facilities in the program. The stormwater is discharged directly into receiving water bodies. This direct discharge approach is due to the misconception that stormwater is cleaner than sewer water and it does not need to be treated. Adding to the misconception are costs implications. Adding another treatment facility for stormwater alone would raise the costs of any sewer separation program. Therefore, regardless of the sewer separation program, the water quality treatment problem is still not addressed.

Urban areas are a non-point source of contamination (Hall & Schreier, 1996). The pollutant accumulation process is summarized as the following: pollutants are picked by the stormwater when it lands on hard (or impervious) surfaces and runs off downstream. It has been documented that urbanization contributes in adding nutrients, heavy metals, pesticides, oils, road salts, detergents, among other contaminants (Klein, 1979; T. R. Oke et al., 2017). The following sections will discuss the different pollutants and their impact on the receiving waterbodies. The concept of first flush will also be introduced.

2.1.3.1 First Flush

The concentration of pollutants that is carried in the stormwater runoff process is not constant throughout the rain event. The prevalent theory is that concentration decreases as the rain event progresses. Nonetheless, the definition of first flush is inconclusive among researchers. Earlier researchers established that between 70 to 80% of the total pollutants are transported during the first 25 to 30% of total runoff volume (Bach, McCarthy, & Deletic, 2010). Another definition places the emphasis on the first 20% of the total runoff (Deletic, 1998). More recent definitions, place emphasis on time: the first 6 to 30 minutes of a rainfall event (Huber, Welker, & Helmreich, 2016). All in all, some researchers do agree on the fact that the pollutant concentrations are at least higher at the beginning of a rainfall event when compared to the rest of the event.

On the other hand, many researchers have also found that this effect if present in only a portion of rainfall events. Sage et al. (1996), for example, analyzed 197 storm events and found that only one of the studied events fit the 80% of pollutants in the first 30% of total runoff definition. Bertrand-Krajewski et al. (1998) adopted the same definition and they did not found first flush effects in their analysis.

A possible explanation to the lack of first flush findings is to the concept known as antecedent dry period (ADP). This concept accounts for the pollutants that were accumulated during the dry period that preceded a storm event. Nevertheless, this concept should be used as an indicator as there is still inconclusive evidence that all pollutants accumulate gradually during the ADP. A 16-month highway study in Texas, U.S. which studied two curbless highways, one in Austin and another in College Station, concluded that ADP was a significant indicator for the College Station highway but not the other. This same studied also concluded that a longer ADP does not correlate to a higher accumulation of pollutant. Factors such as wind, vehicle induced wind, biodegradation and chemical decay process can eliminate the pollutants away from the catchment (M.-H. Li & Barrett, 2008). A German study conducted a spatial and temporal study for the solid-phase concentration of Polyaromatic Hydrocarbons (PAH) in road dust. Polyaromatic Hydrocarbons are a known cancerogenic pollutant. The study found strong evidence of traffic and ADP dominating PAH accumulation. Researcher Deletic (1998) concluded that ADP does not have an influence on total suspended solids (TSS) for the two catchments that were included in the study. A Canadian study's conclusions best characterize the concept of ADP, in this thesis author's opinion. The study concluded that for most pollutants, the load seems to be a function of the mobilizing effects of storms and not necessarily controlled by the ADP accumulation concept.

All things considered; the first flush effect is still a concept of contention. The ADP concept can be used as an indicator to assess the period between events to determine what occurred in the catchment prior to the storm event, but it is not an infallible indicator of pollutant accumulation in urban catchments.

2.1.3.2 Metals

The presence of high metal concentrations in aquatic environments is of concern. Metals can be naturally present in the environment. Metals are found on Earth's crust and the composition of metals vary globally (Jaishankar, Tseten, Anbalagan, Mathew, & Beeregowda, 2014). The weathering process on rocks and soils can cause the natural increase in concentration of heavy metals. In urban watersheds, however, human activity is associated with the significant increase in heavy metals (T. Li, 2007). Stormwater runoff has been studied widely to assess the impact of human activity. Heavy metals such as zinc (Zn), copper (Cu), lead (Pb), cadmium

(Cd), chromium (Cr), Iron (Fe), Aluminum (Al), etc. have been found in urban stormwater runoff (T. Li, 2007; McKenzie, Money, Green, & Young, 2009). Heavy metals are found in dissolved forms and adhered to solids in the water (T. Li, 2007).

Heavy metals can be sourced from industrial and domestic effluents, atmospheric deposition, and soils (T. Li, 2007; Mccallum, 1995). The main source of heavy metals in urban watersheds is mostly associated to vehicles. In vehicles, the exhaust fumes and the wearing of bearings, bushings, brakes, etc. are the main contributors of Zn, Pb, Cu, Fe and manganese (Mg) (Stime, 2014). Tire and brakes were of specific interest for a 2009 study. These two components of the vehicle are under constant wearing, leaving particulates behind during the braking motion of the car. The study concluded that breaks are a source of Fe, Cu, and barium (Ba). On the other hand, tires were characterized as contributors of Zn, Pb and Cu (McKenzie et al., 2009). Other sources of heavy metals can be found in hard surfaces and water conveyance systems. Asphalt used to pave roads has been found to be a source of nickel (Ni) (Stime, 2014). Infrastructure that is buried or exposed is subject to weathering can be a source of Fe (Stime, 2014) and Cu coated material can be a source of Cu (T. Li, 2007). Table 2.1 summarizes the expected concentrations for the most common metals in urban stormwater runoff.

Table 2.1: Expected metal concentrations in urban stormwater (Stime, 2014; US EPA, 2004)

Land Use	**Pollutant Concentration (ppm)**						
	Al	**Cd**	**Cu**	**Fe**	**Pb**	**Ni**	**Zn**
Residential	0.026-7.1	0.04-1.7	14-221	0.2-20.8	120-1000	0.0226	47-1170
Street	N/A	0.22-3.90	22-220	N/A	N/A	N/A	44-480
Highway	N/A	0.6-4.3	90-281	N/A	130-4800	N/A	250-336
Industrial	N/A	0.7-3.4	228	N/A	488-1410	N/A	665-1445
Commercial	N/A	0.02-1.06	10.4	N/A	160-220	N/A	53-1065
City - Downtown	N/A	2.6-7.0	143-390	N/A	1880-2550	N/A	470-534
Parking lot	N/A	1.0-14.6	206	N/A	2000-1500	N/A	1600

2.1.3.2.1 Impacts of Metals on Receiving Waterbodies and the Fauna

Metals in very low concentrations are necessary to carry necessary biochemical and physiological functions in organisms (Jaishankar et al., 2014; Mccallum, 1995). Nevertheless, they can quickly become toxic if certain threshold concentrations are exceeded, exposure times are prolonged, or if certain ambient conditions are met.

The ambient conditions are essential in determining the toxicity of metals. Certain metals in low concentrations do not pose a threat to the environment. Studies have determined conditions such as hydrologic conditions, pH, salinity, hardness, metal chemistry and the properties of the sediments in the water bodies affect the bioavailability and metal concentrations (Jaishankar et al., 2014; T. Li, 2007; Stime, 2014; Straus & Tucker, 1993).

For example, metals such as Cu are needed by organisms, including humans, to carry out biological functions. However, the concentrations required are extremely low. Studies have found that Cu at even low concentrations in water can cause brain damage in mammals (T. Li, 2007). Water pH and hardness were found to control the toxicity to catfish in a study in Mississippi at a fish farm. At the time of the study, copper sulphate was used as an algicide and parasiticide. The copper treated waters were studied to determine the toxicity of the Cu substance in the fish. The study determined that pH between the range of 7 to 9 and the higher hardness, calcium (Ca) hardness, reduce the copper concentrations available for uptake by the fish. The downside of the alkaline water is that the effectiveness of the substance on the parasite decreases, for the same reason that it affects the fish to a lesser extent. The symptoms that the researchers noted before fish fatality were convulsions, lethargy and loss of balance (Straus & Tucker, 1993). Iron is another example of an metal that is essential for organisms and it is one of the most abundant elements on earth. Iron can be found in the blood in the form of oxygen transporting proteins such as myoglobin and hemoglobin. High concentrations of iron can lead to overdose effects. Excess iron intake has been linked to increase the risk of cancer. The toxicity of iron in mammals has do with the corrosive effects of unbound iron (free radicals) in the gastrointestinal tract and biological fluids, which in turn compromises other organs (Jaishankar et al., 2014).

Closer to the Lower Mainland, in the Puget Sound, two research studies in the State of Washington (in the US) have investigated the effect of stormwater in important regional fish populations. Researchers studied the impact of urban stormwater runoff in populations of salmonid species and the rates of mortality. Both studies concluded that the exposure of fish species to stormwater proved fatal. The dilution of the stormwater into the receiving water bodies, has demonstrated to be insufficient to protect the salmonid species from death (Scholz et al., 2011; Spromberg et al., 2016). The symptoms that the salmonid fish demonstrated include gaping, pectoral fin splaying, surface swimming, and loss of equilibrium. The symptoms aforementioned occurred rapidly and the fish typically died within a few hours (Scholz et al., 2011). These symptoms are similar to those shown in the previously discussed fish farm study in Mississippi, US. Very recently, a 2018 study conducted by the Washington State University investigate the effect of stormwater in the larvae development of zebra fish and Coho salmon. The study exposed the fish larvae to sub-lethal doses of untreated stormwater. The researchers concluded that both fish species experience permanent damage to the neuromast. The researchers conclude that this might affect the survival chances of the affected fish in the future. The researchers theorize that metals such as Cu and Cd, known neurotoxins, are responsible of affecting the salmonids (Young, Kochenkov, McIntyre, Stark, & Coffin, 2018).

2.1.3.3 Nutrients and Oxygen

Nutrients such as nitrogen (N) and phosphorus (P) are important for the flora of a watershed (Mccallum, 1995). Both the flora and fauna of a watershed require N and P to flourish. However, an excess concentration of P can lead to a process known as eutrophication, which is the excess growth of plants and algae, and the consequent death of the fauna of a waterbody. The presence of certain forms of N can be toxic to the fauna and aid in the eutrophication process. The transport of N and P has to do with the stormwater runoff process from various zones within the watershed to the waterbody (T. Li, 2007).

Point and non-point source can be attributed to the contribution of nutrients in an urban and semi-urban watershed (Stime, 2014). Anthropogenic sources such as agriculture (fertilizers), industry and urban activities (runoff, wastewater treatment plants and CSO discharges) have been identified as the main contributors of excess nutrients to aquatic ecosystems (FISRWG, 1998; T. Li, 2007; Mccallum, 1995; Stime, 2014).

2.1.3.3.1 Nitrogen and its Impact

Nitrogen can be found in two in the form of ammonia, nitrite and nitrate (T. Li, 2007; Mccallum, 1995; Stime, 2014). Nitrogen does not adhere strongly to the sediments and it is easily soluble. Nitrate is the most soluble form of N.

The natural sources of N are attributed to the natural decomposition of the flora and dead fauna. Ammonia is released during the decay process and it is converted to nitrate and nitrite (FISRWG, 1998). Among the anthropogenic sources, the discharge of sewer water to waterbodies, which happens during CSO events, and leaky septic systems can increase the amount of nutrients to the aquatic ecosystem (Mesner & Geiger, 2010; Wojtenko et al., 2004). In agriculture, fertilizers are used to increase the yield of crops. Improper management of fertilizer uses can lead to excess of N. Manure from livestock is another source of N (FISRWG, 1998). The easily soluble N from these agricultural sources is easily transported in the runoff process.

Similar to heavy metals, aquatic background conditions can increase the toxicity of the diverse forms of N. Un-ionized ammonia and nitrates have been shown to be detrimental to fish under certain pH conditions (T. Li, 2007; Mccallum, 1995; Stime, 2014). Temperature is another factor to consider for the toxicity of ammonia. Certain fish species are more tolerant to ammonia at lower ambient temperatures (Stime, 2014).

Methods have been developed to examine the levels of N in a watershed. Nitrate and Nitrite are in inorganic forms of nitrogen that can be measured individually. Organic sources of nitrogen and ammonia are quantify by an indicator known as Total Kjeldahl Nitrogen (TKN) (Stime, 2014). Table 2.2 summarizes the expected concentrations of nitrogen in its diverse forms in urban stormwater or waterways. The term NOx encompasses the concentration of nitrate and nitrite

Table 2.2: Expected nitrogen concentrations in urban watersheds (Novotny & Olem, 1994; Stime, 2014)

Land Use	**Pollutant Concentration (ppm)**		
	TN	**TKN**	**NOx**
Residential	0.34-22.38	0.48-11	0.096-81.9
Untreated Wastewater	35	N/A	N/A
Treated Wastewater	30	N/A	N/A
Urban Runoff	3-10	N/A	N/A

2.1.3.3.2 Phosphorus and its Impact

Phosphorus is an important nutrient. In aquatic systems it can be found in many chemical forms that are non-toxic to the fauna or the flora. Phosphorus can be found dissolved or solid forms (Mesner & Geiger, 2010).

Phosphorous can be sourced from natural and anthropogenic sources just as N. Fertilizers from agricultural and urban landscape practices can be a significant source of P. Sewer discharges and poorly functioning also are a significant source of P (Mesner & Geiger, 2010; Wojtenko et al., 2004). Phosphorus travels within the watershed adhered to particles, including sediments and organic matter (FISRWG, 1998). The erosion of stream banks due to the loss of riparian zones and the consequent high TSS loadings in the water increase the chances of P transport.

Natural factors can change the availability of P in aquatic environments. Orthophosphate (O-PO_4) is of particular interest in monitoring programs at it is readily biologically available (Mesner & Geiger, 2010; Stime, 2014). Due to this bioavailability, orthophosphate can be taken out of circulation naturally. It can combine with minerals and metals in the water and soil that contain Al and Ca (FISRWG, 1998; Mesner & Geiger, 2010). Inorganic P can be present in aquatic systems and be processed by plants. Sources of inorganic P can be found in rocks and minerals. Excess of this form of P can also lead to eutrophic conditions (Mesner & Geiger, 2010). Both organic and inorganic forms of P are measured in the Total Phosphorus (TP) tests (Stime, 2014). This concentration index is used to measure the levels of P in the aquatic system. The eutrophication consequence of P in the fauna of a watershed will be discussed in Section 2.1.3.3.3. Table 2.3 summarizes the expected concentrations of phosphorus in urban stormwater or waterways.

Table 2.3: Expected phosphorus concentrations in urban watersheds (Novotny & Olem, 1994; Stime, 2014)

Land Use	TP (ppm)
Residential	0.22-4.41
Untreated Wastewater	10
Treated Wastewater	10
Urban Runoff	0.2-1.7

2.1.3.3.3 Oxygen and its Impact

The oxygen levels in the water fluctuate naturally. These changes can be due to oxygen consuming processes either natural or anthropogenic.

Reaeration is the primary method of oxygen introduction to watersheds. The process is driven by internal mixing and turbulence, temperature, wind mixing, rapid changes in water speed (rapids, falls, dams) and the water column depth (FISRWG, 1998). Temperature, internal mixing and turbulence are associated to seasonal and diurnal changes. Lakes, for example, suffer from stratification. The amount of oxygen available decreases with depth. Depending on the region, a process known as overturning takes place. During the late summer and early fall, the surface water cools, increasing the density of the water. This causes the cooler, denser water to sink down until reaching equilibrium: when similar density water is encountered. The upper region of the lake (known as the epilimnion) contains the highest amount of dissolved oxygen (DO) due to the aeration process, previously discussed. The overturning process naturally increases the amount of oxygen available in the lower depths of stratified lakes (Smith & Bella, 1973).

Anthropogenic sources can influence greatly the amount of oxygen available in a waterbody. The excess introduction of nutrients can cause eutrophication in the watershed. Eutrophication will cause the death of the fauna in the watershed. Animals depend on the respiration process to conduct the biological functions that release of energy stored in their food. Respiration consumes the DO to carry oxidation-reduction reactions (FISRWG, 1998). The surplus and die-off of plants and organisms (algae) that developed from the eutrophication process decrease the amount of oxygen available for marine fauna, effectively suffocating them. Organisms that have low tolerance to low oxygen levels will not survive (T. Li, 2007). The die-off of marine animals can affect the aviary and surviving marine fauna as the carcass decomposition process consumes DO. The die-off is further magnified when animals feed from contaminated carcasses that contain maggots that have concentrated a bacterium known as *Clostridium botulinum*. The infected animals die from a condition known as botulism. This process is known as the carcass-maggot cycle (Espelund & Klaveness, 2014; Wurtsbaugh, n.d.). This cycle increases the mortality in the fauna further reducing the DO available.

Oxygen demanding waste can also decrease the amount of readily available oxygen (FISRWG, 1998). Combined sewer overflows introduce a wide array of contaminants that include organic material (including fecal waste). The introduction of bacteria, such as fecal coliforms, has shown to decrease the amount of available DO in streams. The addition degradable organic matter by CSO or urban runoff in the waterbodies decrease the amount of oxygen that is available (Erickson, Weiss, & Gulliver, 2013; T. Li, 2007; Mccallum, 1995).

Overall, low levels of oxygen in waterbodies are detrimental to the survival of the fauna of a watershed’s aquatic ecosystem. Fish and benthic invertebrate suffer from increase competition for resources, inhibit growth and decrease in survival rates. The die-off of certain populations can increase the growth of less desirable species (Wojtenko et al., 2004).

2.1.3.4 Organic Matter: Organic Carbon

Carbon, just as water, has a cycle which begins inland. Organic carbon can be found in both dissolved and solid phase, and it can be sourced from natural and anthropogenic sources. The presence of certain forms of organic carbon are toxic for both the flora and fauna of a watershed.

Organic matter is naturally abundant in terrestrial environments. Plants themselves are a natural are source of carbon. The same can be said about the fauna as all are carbon-based life forms. Carbon can also be present in the atmosphere, most commonly in the form of carbon dioxide (CO_2) which can be sourced from natural and anthropogenic sources of combustion, respiration, etc. Plants absorb the CO_2 and process it through photosynthesis. In marine environments, estuaries and continental shelf have been considered as the dominant reservoirs of organic carbon. Carbon is transported to these sinks by rivers in the form of sediment (He et al., 2010). Organic carbon can be dissolved in marine environments. The dissolved carbon is used as an energy source by microbes, which in turn make it bioavailable. According to their food web, these microbes are consumed by predators and the process continues. Abiotic process can also turn dissolved carbon into bioavailable forms (Sickman, Zanoli, & Mann, 2007).

Urbanized watersheds suffer from altered carbon cycles. The alteration of natural landscapes to agricultural and urban land is changing both the quantity and composition of the organic matter delivered to water environments (He et al., 2010; Sickman et al., 2007). The anthropogenic sources of organic carbon include pesticides, detergents, pharmaceuticals, and hydrocarbons (Stime, 2014). Of special interest to researchers are hydrocarbons.

2.1.3.4.1 Hydrocarbons

Higher than normal concentrations of hydrocarbons can occur naturally. Canada, for example, is home to a peculiar hydrocarbon deposit in Northern Alberta (Fort McMurray) known as oil sands. Due to geological factors, the oil sand deposits daylight in some areas due to the erosion of the Athabasca River. The erosion process washes tar bearing sediments into the stream naturally, which elevates the hydrocarbon concentration levels in the water (Conly, Crosley, & Headley, 2002; Timoney & Lee, 2011).

The presence of hydrocarbons in urban watersheds have to do primarily with the incomplete combustion of fossil fuels (Dutta et al., 2017; Han et al., 2015), vehicles, leakages, oils, etc. (Hall & Schreier, 1996; T. Li, 2007; Spromberg et al., 2016). Hydrocarbons are hydrophobic and can attach easily to sediments, particularly fine sediment (Conly et al., 2002). These properties make hydrocarbons easily transported in urban effluents, especially in combined sewers. Combined sewers are a major source of sediment in urban watersheds (Wojtenko et al., 2004). Wastewater discharge and urban runoff were identified in a 2007 study in the Sacramento River as one of the causes of elevated sources of organic carbon. The TOC concentrations in urban runoff were between 4 to 20 times greater than in the downstream portions of the Sacramento River (Sickman et al., 2007; Stime, 2014).

2.1.3.4.2 Hydrocarbon Toxicity: PAH and VOC

Hydrocarbons are toxic to both the flora and the fauna of the urban watershed. Volatile organic compounds (VOC), ethylene in particular, can trigger various plant and microbial processes that mimic plant hormones. This can negatively impact seed germination rates, weed response, herbivore resistance and nutrient uptake. Polyaromatic hydrocarbons (PAH) combined with the presence of biochar, which is artificially added in landscape practices to reduce nutrient leaching, can further the phytotoxic effects of PAH. In addition, biochar leaches VOC (Dutta et al., 2017), which induce the negative effects aforementioned.

The fauna is negatively impacted as well. In humans alone, PAH are classified as cancerogenic and toxic by the International Agency for Research of Cancer (IARC). Different forms of PAH have been linked as possible and probable human carcinogens (Conly et al., 2002; IARC, 1983). Polyaromatic hydrocarbons are bioavailable due to their lipophilic nature. This property allows PAH to be metabolized by biotic systems (Conly et al., 2002). In waterbodies, fish exhibit severe reactions to PAH, regardless if the PAH occur naturally. Fish in the Athabasca river that are naturally exposed to PAH display spinal malformations, cardiac dysfunction, edema, skeletal deformations, high mortality rates, liver lesions and alterations to DNA (Conly et al., 2002; Timoney & Lee, 2011). The findings of the Athabasca river coincide with the findings of studies regarding the salmon pollutions of the Puget Sound in Washington State. The source of hydrocarbons for the fish studied were anthropogenic in nature, but the effects were the similar. The researchers identified the toxic cocktail of heavy metals and PAH that are present in urban stormwater as the cause of the high mortality syndrome that is affecting anadromous fish such as the adult Coho salmon which is declining in population numbers (Scholz et al., 2011; Spromberg et al., 2016; Young et al., 2018).

2.1.3.5 Sediments

The United States Environmental Protection agency (US EPA) identified suspended sediment composed of organic and inorganic material as the most widespread pollutant in rivers and streams (US EPA, 2005). As explored in the previous sections, nutrients, metals and hydrocarbons can be adhered to sediment and are transported across the system. Sediments can have a variety of sources, both natural and anthropogenic.

Erosion is an indicator that the flow velocities are too large, this could be because excess stormwater is entering the system. The channelization erodes the sediment and increases the suspended solids concentration in the system. The erosion process occurs in the outside bends of natural streams. An opposite effect occurs in the inside of the bends, where the stream velocities are slower: the sediment is deposited (FISRWG, 1998). Once the sediment enters the waterway, excess sediment can affect the aquatic habitat by increasing turbidity and produce clogging due to deposition of sediment (FISRWG, 1998; T. Li, 2007).

Urban watersheds suffer the loss of riparian integrity, which compromises the stability of the embankments of streams. Stream erosion due to encroachment increases when the buffer zone is less than 30m wide (Finkenbine, 1998). Other urban sources of sediments are associated to construction, pavement wear, vehicle wear and tear, among others (Klein, 1979; T. Li, 2007; Stime, 2014). The increase of impervious surfaces and consequent increase in stormwater runoff in urban watersheds facilitates the transport of sediments and attached contaminants to waterbodies. The sediment collected during the runoff process is typically collected by the stormwater or combined sewer systems. During CSO events, the untreated water is discharged to the receiving waterbody, causing sediment deposition around the outfalls. The solids washed by CSO are conformed by street dust, dirt of eroded materials from pervious areas, solids washed from impervious areas, re-entrainment within the conveyance system, atmospheric deposition and sanitary waste. The sediments in the outfall areas accumulate the majority of pollutants (Wojtenko et al., 2004).

Studies on Pacific Salmon have shown a decline in population. The reasons cited for the fatality are anthropogenic in nature. Salmonid populations are susceptible to the impact on substrate quality, namely the increase in sediment on stream beds. Salmonid fish migrate inland to return to their original spawning ground. They spawn by depositing eggs among clear gravel that is well oxygenated (FISRWG, 1998). The increase in sediment, can induce changes to the stream geomorphology, clogging the spawning grounds, and introduce particle bound contaminants that can prove fatal to the salmonid species.

2.1.3.6 Water Quality Guidelines

Monitoring a watershed is complicated in nature. Government agencies across the world use concentration indices based on research to monitor the water quality issues that arise from human activity and act according to the findings. Monitoring programs are developed based on the monitoring goals established by the agencies.

In the Lower Mainland, Metro Vancouver (MV) is a federation, empowered by provincial legislation, that is comprised of 21 municipalities, one Electoral area and one Treaty Frist Nation (Metro Vancouver, 2018). The BC Ministry of Environment requires that all member municipalities develop integrated stormwater management plans (ISMP) in coordination with MV. This requirement includes biennial reports that contain water quality performance reports that evaluate each municipalities' ISMP (Metro Vancouver, 2010). As part of this provincial requirement, MV created an adaptive management framework that will help municipalities monitor watershed health, track ISMP performance, identify impacts and threats to watershed health, and to select and track the effectiveness of their management practices.

Metro Vancouver classified the water quality parameters of relevance to the reporting as primary and secondary. This classification is according to their relative impact to the overall health of a watershed. (Metro Vancouver, 2014). Table 2.4 summarizes MV's water quality requirements for their adaptive management framework.

Table 2.4: Summary of Metro Vancouver's adaptive management framework water quality requirement table (Metro Vancouver, 2014)

Group	Parameter	Level		
		Good	**Satisfactory**	**Requires Attention**
Metals in µg/L (Hardness approximating 100 mg/L CaCO3)	Al	N/A	N/A	N/A
	Cd	<0.06	0.06 -0.34	>0.34
	Cu	<3	3 - 11	>11
	Fe	<800	800 - 5000	>5000
	Ni	N/A	N/A	N/A
	Pb	<5	5 - 30	>30
	Zn	<6	6 - 40	>40
Nutrients (mg/L)	Nitrate	<2	2 - 5	>5
	Nitrite	N/A	N/A	N/A
	TKN	N/A	N/A	N/A
	TP	N/A	N/A	N/A
Other Parameters	DO	≥ 11	6.5 - 11	<6.5
	pH	6.5 - 9.0	6.0 - <6.5 or >9.0 - 9.5	<6 or >9.5
	EC (µS/cm)	<50	50 - 200	>200
	TSS	N/A	N/A	N/A

It is important to highlight that the values compiled by MV include parameters compiled from the BC Ministry of Environment, US EPA, and Canadian Council of Ministers of Environment (CCME) for the protection of aquatic life that is relevant to fresh water sources. The limits shown on Table 2.4 will vary depending on the type of water in the waterbody in question. This choice in parameters is because the majority of MV members have salmon (fish) bearing forest streams. This is not the case for municipalities such as Richmond, Vancouver, Burnaby, and Surrey which have a low incidence of fresh water streams, non-existing in some cases. In addition, a city such as Vancouver discharges all its water/wastewater in to the marine waterbodies surrounding the city boundaries: Fraser River, Burrard Inlet, False Creek, and English Bay (City of Vancouver, 2016b).

Table 2.5: Water quality guidelines compiled from the BC Ministry of Environment and CCME. Marine and estuary parameters shown in blue, freshwater parameters shown in black (CCME, 2014; Water Protection & Sustainability Branch, 2018).

Group	Parameter	Unit	British Columbia Water Quality Guideline for Aquatic Life		CCME Water Quality Guideline for the Protection of Aquatic Life	
			Long Term Average	**Short Term Maximum**	**Long Term**	**Short Term**
Metals	**Al**	mg/L	If pH≥6.5 then 0.05; otherwise WQG=e[1.6−3.327(median pH)+0.402(median pH)^2]	If pH≥6.5 then 0.1; otherwise WQG = e[1.209−2.426(pH)+0.286(pH)^2]	N/A	N/A
	Cd	µg/L	WQG = e[0.736 × ln(hardness) – 4.943]; applies to water hardnesses (mg/L CaCO3) between 3.4 – 285 mg/L.	WQG = e[1.03 × ln(hardness) – 5.274] when hardnesses (mg/L CaCO3) is between 7 – 455 mg/L. If >455, site-specific assessment required.	<1	<0.12
	Cu	µg/L	≤ 2	<3	When the water hardness is 0 to < 82 mg/L, the CWQG is 2 µg/L; when hardness ≥82 to ≤180 mg/L then -> CWQG (µg/L) = 0.2 * e{0.8545[ln(hardness)]-1.465}; when hardness >180 mg/L, the CWQG is 4 µg/L; if unknown then: 2 µg/L	N/A
	Fe	mg/L	N/A	Total Fe = 1 (Dissolved = 0.35)	N/A	N/A
	Ni	N/A	N/A	N/A	N/A	N/A
	Pb	µg/L	≤ 2 total lead (80% of values ≤ 2 total lead)	140	When the hardness is 0 to ≤ 60 mg/L, the CWQG is 1 µg/L; when hardness is >60 to ≤ 180 mg/L then -> WQG (µg/L) = e{1.273[ln(hardness)]-4.705}; when hardness is >180 mg/L, the CWQG is 7 µg/L; If hardness is unknown, then: 1 µg/L	N/A
	Zn	µg/L	<10	<55	When water hardness is 0 to ≤ 60 mg/L, the CWQG is 25 µg/L; when hardness > 60 to ≤ 180 mg/L then -> CWQG (µg/L) = e{0.76[ln(hardness)]+1.06}; when hardness >180 mg/L, the CWQG is 150 µg/L; if hardness is unknown, the CWQG is 25 µg/L	N/A
Nutrients	**Nox**	mg/L	Nitrate = 3.7; non-proposed for Nitrite	N/A	Nitrate: <200,000 µg/L or <200 mg/L; Nitrite: N/A	Nitrate: 1,500,000 µg/L or 1500 mg/L; Nitrite: N/A
	TKN	mg/L	Refer to Table 26E (of BC's WQ Guidelines)	Refer to Table 26F (of BC's WQ Guidelines)	Refer for CCME website for table	N/A
	TN	mg/L	N/A	N/A	N/A	N/A
	TP	µg/L	(5 -15)	N/A	N/A	N/A
Others	**pH**	N/A	(7.0-8.7) (Unrestricted change within this range (for protection of mollusc embryo development)		The pH of marine and estuarine waters should fall within the range of 7.0 – 8.7 units unless it can be demonstrated that such a pH is a result of natural processes. Human activity should not change pH by 0.2 units from background pH	
	TOC	N/A	The 30-day median for both DOC and TOC shall be within 20% of seasonally-adjusted median background levels as measured historically or at appropriate reference sites.		N/A	N/A
	DO	mg/L	>8; Buried Embryo Aleving Life Stages (11)	>5; Buried Embryo Aleving Life Stages (>9)	≥ 8.0; should decrease more than 10% from background by human activities	
	TSS		Change from background of 25 mg/L (< 24 h) in all waters during clear flows or in clear waters. Change from background of 5 mg/L (<30 d) in all waters during clear flows or in clear waters.		Maximum average increase of 5 mg/L from background levels of receiving waterbody (>24h)	Maximum increase of 25 mg/L from background levels of receiving waterbody (<24h)

Table 2.5 summarizes some of the most relevant water quality parameters for the Lower Mainland. This includes the short-term and long-term exposures for marine and estuarine aquatic life. According to the BC Ministry of Environment, short term maximum and long-term average exposures are defined as the maximum concentration under 96 hours and a minimum of 5 averages in 30 days respectively (Water Protection & Sustainability Branch, 2018). The CCME defines short-term exposure as the maximum concentration for the protection against intermittent, transient events and the long-term exposure as the maximum concentrations for long-term events (CCME, 2007). The fresh water aquatic life parameter is provided if a marine/estuarine parameter is not available. The list of agencies that this table includes encompass the BC Ministry of Environment, and CCME. The parameters shown in Table 2.5 will be used to complement the parameters shown in Table 2.4.

2.2 Green Infrastructure

Green infrastructure aims to mimic pre-development conditions by allowing the stormwater to be used by plants and/or infiltrating the stormwater into the native soils (Vega & Lukes, 2018). Green infrastructure can also be defined from an economic standpoint as a set of approaches to manage wet weather impacts in a cost-effective, resilient manner with the goal of reducing and treating stormwater at its source (US EPA, 2018). Green infrastructure practices are nimble as they vary in shape, space requirements and functionality. The greatest applicability of GI is that it can be used in new and retrofit locations (Hopton et al., 2015). The combination of versatility and applicability allow each GI method to achieve different objectives. Green Infrastructure can deliver environmental, social and economic benefits (University of the West of England, 2012; US EPA, 2018). Communities implementing GI must identify the number of ecosystem services, besides stormwater management, when deciding which GI method to use (Hopton et al., 2015).

Green Infrastructure was developed because of the conclusion that typical grey infrastructure is not enough to address current and future needs water management needs. For centuries, engineers have focused on only grey solutions to manage stormwater, which can only provide one function at the time: the fast conveyance of water downstream (University of the West of England, 2012). Green Infrastructure methods are a response to the change in paradigm on how engineers can use natural processes to be less disruptive in the natural hydrological cycle by 1) reducing the amount of water that enters grey infrastructure, 2) addressing flooding issues, 3) treating stormwater at its source, and 4) targeting multiple objectives parallelly: such as the mitigation of urban heat island, the access to green spaces and the protection of urban watersheds. Among the reported benefits, GI can address: water quality issues, peak flow reduction, peak flow delays and total runoff reduction (CVC, 2015; Hopton et al., 2015; Miller et al., 2014; Stime, 2014; Welker, Mandarano, Greising, & Mastrocola, 2013; Winston, Dorsey, & Hunt, 2016). These properties will be evaluated in the City of Vancouver context by this thesis.

A broad definition of GI includes natural features such as parks, forests, and wetlands (University of the West of England, 2012; Yang & Li, 2013). Typically, manmade structures such as LID or BMP structures fall under the umbrella of GI. Examples of typical GI are: green roofs, bioretention and constructed wetlands, infiltration trenches, among other methods (Yang & Li, 2013). Of special attention for this thesis are the bioswale and STT GI practices.

2.2.1 Bioswales

Bioswales are one of the most common and most studied GI practices. Bioswales are vegetated and typically in the shape of a trapezoidal channel which conveys stormwater (Caltrans, 2011; Erickson et al., 2013). The soils in the bioswale are the main filtration system which temporarily stores and filters the stormwater. The soil used in bioswales is typically engineered soil media that increases the pollutant removal efficiencies of the practice (Bradford, 2016). Water can enter the bioswale practices directly through curb openings (Bradford, 2016) or permeable structures such as dams which might be utilized to decrease the flow velocity (Erickson et al., 2013).

Bioswales are flexible in the design and can be installed as part of new construction or in retrofit projects (Caltrans, 2011). The pleasantly aesthetic qualities of bioswales is what makes them a more attractive, easy to sell option with respect to other GI methods. Tall meadow grasses, sod, decorative herbaceous cover, or even trees can be used in bioswales. Compared to the role of the soils, plants do not have a significant effect in pollutant removal, but they host and foster the microbes that do play a significant role in the pollutant removal efficiencies of the practice (Bradford, 2016).

The maintenance cost associated throughout the life of the project can make bioswale practices more costly than other GI methods. A 2018 report compared the life cycle cost associated with a bioswale practice option against a typical boulevard reconstruction method and three GI methods. The results of this report showed that the maintenance costs associated with bioswales practices increase significantly the total costs of bioswales, making them the least cost-effective GI option regardless of their aesthetical appeal (Vega & Lukes, 2018). Involving the public in the maintenance operations for bioswales could be a solution to lower the life cycle costs of these practices.

Bioswales have the highest impacts on the runoff sequestration and water quality treatment capabilities among GI practices. Pollutants are removed by the filtration process of the stormwater through the bioswale vegetation (plant uptake), adsorption on the soil particles and lastly by the infiltration of the stormwater through engineered soils (Caltrans, 2011). The pollutant removal efficiencies of bioswales increase when the dimensions of the practice are extended (Caltrans, 2011; Erickson et al., 2013; Schmidt, 2017). Bioswales are effective in targeting TSS, and particulate bound nutrients and metals (Caltrans, 2011; Erickson et al., 2013). The hydrological impacts of bioswales is also tied to the dimensions of the channel. Increasing the soil media depth can ensure that the practice has enough capacity to infiltrate to the native soils (Schmidt, 2017). However, factors such as drainage area, storm duration, storm intensity and low infiltrating native soils can also control the performance of the practice.

2.2.1.1 Bioswale Monitoring

GI performance monitoring is an emerging field of research. Bioswales are the most common form of GI that has been studied academically. Table 2.6 summarizes average reduction efficacies for total runoff volume reduction and peak flow reduction found in the water quantity performance literature for bioswales. The water quality performance of bioswales can be found on Appendix B, Section B.1. All in all, bioswales can be effective tools to positively address water quality and water quantity issues in urbanized watersheds. Bioswale practices are considered the gold standard in terms of water quality and water quantity performance.

Table 2.6: Summary of hydrological performance of bioswale practices

Location	Site	Storms Size	Average Reduction Efficiencies		Source
			Total Runoff (%)	**Peak Flow (%)**	
Langley, BC (CA)	Routley	2-60mm	30%	41%	(Stime, 2014)
Mississauga, ON (CA)	Lakeview Drive (LV-2)	<25mm	81%	N/A	(Bradford, 2016)
	Lakeview Drive (LV-4)	<25mm	100%	N/A	
		33-71mm	N/A	24.7-100%	
	Elm Drive	>2mm	92%	N/A	(CVC, 2016c)
		33-71mm	N/A	66-94.8%	
	IX-2	2-25mm	90%	76%	(CVC, 2016e)
		>30mm	72%	N/A	
	IX-3	2-25mm	78%	69%	
		>30mm	59%	N/A	
	IX-4	2-25mm	64%	69%	
		>30mm	62%	N/A	
	Riverwood	0-25mm	51-79%	69-90%	(CVC, 2016d)
		≥ 25mm	55%	65%	
Maryland (USA)	Savage	1.5-173.2mm	20-40%	Reduced	(Davis, Stagge, Jamil, & Kim, 2012)
Davis, SA (USA)	UC Davis	>9mm	89%	Reduced	(Xiao & Mcpherson, 2011)
Melbourne (AUS)	Lynbrook	N/A	51-100%	Reduced	(Lloyd, Wong, & Chesterfield, 2002)
Tongde Jiayuan, Xi'an (CH)	Bioswale A	2-98.15mm	98%	N/A	(Jiang, Li, Li, Li, & Chen, 2017)
	Bioswale A	2-98.15mm	78%	N/A	
Pike, OH (USA)	UC, HA South, HA North	2-14mm	36-59%	24-96%	(Winston et al., 2016)

2.2.2 Stormwater Tree Trenches

Stormwater tree trenches are modified tree trenches. Typical tree trenches are confined planter boxes that make use of structural components or aggregate to bear the surface loadings and allow the soil in the planter box to not be compacted, hence, these why these methods are often referred to as suspended pavement methods. Because of the load bearing capacity of the added elements, the tree trenches can be extended under sidewalks where typically only compacted soils are utilized and trees cannot access due to compaction. Trees installed in small spaces and next to confined soils experience a variety of stress factors such as: water stress, difficulty of roots to expand, restricted aeration, and imbalanced nutrition (Bartens et al., 2010; Bassuk, 2013; Bassuk et al., 2005). Tree trenches can exist in the form of structural soils and soil cells.

2.2.2.1 Structural Soils

Structural soils consist of a mix of soil, crushed coarse stone, and additives, which may or may not be added depending on the method employed. The stone matrix can be compacted to engineering standards while maintaining the porosity within the matrix and all the benefits that come with it: aeration, hydration and rooting space. Typical ratios of stone to soil (stone:soil) range between 3:1 to 4:1(Bartens et al., 2010). The porosity after compaction can vary between 20% and 30% (Bassuk, 2013; Urban, 2013). Many proprietary and non-proprietary methods exist such as the CU-Structural Soil®, Stockholm method, Carolina Stalite® based structural soil, among other methods (Bartens et al., 2010; Bassuk et al., 2005; Vega & Lukes, 2018).

2.2.2.2 Soil Cells

Soil cells utilize structures to bear the surface loadings to engineering standards while providing loose soil for the trees. The engineered structures can be made out of plastic (in the form of crates), and concrete (Vega & Lukes, 2018). The void space for soil is up to 92% (Urban, 2013); however, this void space will vary depending on the technology employed and the manufacturer that builds the soil cell crates. Nowadays, there is a variety of manufacturers that have made the use of plastic crates more accessible. Examples of these are: Silva Cells™, Citygreen™, Stormtank ™, among other manufacturers (Bartens et al., 2010; Urban, 2013; Vega & Lukes, 2018).

2.2.2.3 Stormwater Tree Trench Concept

Stormwater tree trenches include a drainage system that allows the tree trench to accept stormwater. Stormwater tree trenches can be utilized to process the runoff from areas such as streets, parking lots, sidewalks, rooftops and plazas. Both soil cell and structural soil tree trench methods can be utilized as stormwater tree trenches (Vega & Lukes, 2018). The term bioretention and suspended pavement is often utilized interchangeably with soil cell STT method.

Water can enter the STT practices through a variety of methods. For open spaces such as plazas, parking lots and sidewalks designers can use permeable pavement or porous pavers over the STT to allow for the direct infiltration of water into the practice (Bassuk et al., 2005). Curb integration and drainage gradients are the biggest challenges for practices installed and designed to accept street stormwater. Designers often utilize conventional CB to overcome this issue (Vega & Lukes, 2018).

The integration of trees is an important component of the STT. Adding to the filtering capacity of the soil employed to treat the stormwater, trees play an important role in absorbing the water, metals and nutrients. In addition, trees bring with them a variety of benefits such canopy cover, CO_2 sequestration, evapotranspiration, etc. A STT literature report conducted by CoV in 2018 concluded that all methods employed for STT practices successfully support tree health (Vega & Lukes, 2018). It is important to note that the study highlights that each manufacturer has recommendations on the type of tree utilized for the practice and the dimensions of the practices. Not all tree species are the same. Some tree species have more aggressive rooting than others, making them not suitable for STT applications. Certain tree species can grow too big for their trench, effectively suffocating them. All in all, the report concludes that trees should be selected according to the recommendations of the manufacturer, and special attention should be given to select species that are resist to variable soil pH and drought conditions (Vega & Lukes, 2018).

2.2.2.4 Stormwater Tree Trench Monitoring

The field of STT research is emerging. The literature available is very limited, however, promising results have been shown from these practices. Table 2.7 summarizes average reduction efficacies for total runoff volume reduction and peak flow reduction found in the water quantity performance literature for STT. The water quality performance results can be found in Appendix B, Section B.2. This result shows that STT can be effective tools to protect urban watersheds. It should be noted that the results on water quality are only for soil cell STT practices. Structural soil STT have not been studied for water quality performance.

Table 2.7: Summary of hydrological performance of stormwater tree trenches practices

Location	**Site**	**STT Type**	**Storms Size**	**Average Reduction Efficiencies**		**Source**
				Total Runoff (%)	**Peak Flow (%)**	
Toronto, ON (CA)	Queensway	Soil Cell	<20mm	Reduced	Reduced	(Cheung & Anderton, 2016)
Toronto, ON (CA)	Mississauga, ON (CA)	Soil Cell	2-15mm	96-100%	97-100%	(CVC, 2016f)
			>25mm	91%	85%	
Raleigh, NC (USA)	Orange St and Anne St	Soil Cell	3-72mm	80%	62%	(Page, Winston, Mayes, Perrin, & Hunt, 2015)
Salford, MAN (ENG)	Howard St	Soil Cell	N/A	60%	70-98%	(City of Trees, 2016; Susdrain, 2018)
Philadelphia, PA (USA)	Various	Structural Soil	<76.2mm	On average 100%	Reduced	(PWD, 2016)

2.2.3 Literature Review Conclusions on Bioswales and Stormwater Tree Trenches

This literature review did in fact confirm that GI is an emerging field of research with very limited sources that have monitored performance. The great majority of the research found was related to the tree health and benefits that increasing the amount of soil does for trees and plants.

Bioswales are the most widely used GI method. The treatment efficiencies of bioswales are considered the target that all other GI practices aim for. Stormwater tree trenches show promising application in highly dense urban environment. Early research on STT has shown that soil cell STT have similar performance to bioswale practices. However, no academic sources out there contained much information regarding the hydrological and water quality treatment properties of structural soil STT. This thesis will aim to contribute in the water quality treatment performance of structural soil STT.

Chapter 3: Site Background

3.1 City of Vancouver

Vancouver is a growing city that is experiencing change at a fast pace. The latest census places the population of Vancouver at more than 630,000 people, making it the most dense city in the province of BC (Statistics Canada, 2017). The CoV (2017) expects that the population will continue to increase at a rate of 1.8% per year in 2019 and 2020. Significant investments will be made to update the current infrastructure and public amenities to support the housing developments in the city (City of Vancouver, 2018a).

As explored in previous chapters, the increase in population is tied to the increase in the production of wastewater and an increase runoff due to the decrease in pervious surfaces. Vancouver's land use as of 2016 is composed of: 15% green (or permeable) in the form parks, open spaces, and golf courses, and the remainder 85% of land use is dominated by impervious surfaces. The highly urbanized landscape of Vancouver makes CSO events more frequent and severe. To tackle this issue, the city is currently investing in a massive sewer separation program which is expected to be completed in 2050 and aims to reduce (or even eliminate) the number of CSO events that occur (City of Vancouver, 2016b). However, the stormwater that is collected in the dedicated stormwater sewer is still discharged directly to the adjacent waterbodies, hence the importance of reducing the runoff in the first place.

In addition to the sewer separation program, the CoV is banking on an unconventional approach to address the water quality issues related to urban stormwater runoff. In 2016, the office of the General Manager recommended to the CoV council to create and adopt a "long-term target to capture and treat 90% of Vancouver's average annual rainfall through the implementation of [GI] on public and private property" (City of Vancouver, 2016b). Green

Infrastructure will allow Vancouver to increase the permeable footprint, which is in current decline, and to treat stormwater at its source.

Streets account for 30% of the total land use of Vancouver and the CoV has direct influence on the street designs and operation. Green Infrastructure is currently being embedded in several boulevard reconstruction projects around the city to the increase permeability in Vancouver. The sites scoped in this thesis are examples of this initiative.

Private properties in Vancouver account for 55% of the total land use. The CoV is encouraging and enforcing new private realm developments to manage and treat the stormwater through bylaws, design standards and guidelines (City of Vancouver, 2016b). This influence on the private realm is crucial in targeting the water quantity and water quality issue.

Vancouver is moving towards treating water as a resource for the community and the watersheds. Green Infrastructure is a powerful tool that is allowing the CoV to align with its corporate goals set by the Greenest City Action plan and Healthy City strategy. Examples of GI in Vancouver include rain gardens, green roofs, infiltration trenches, bioswales, STT, etc. (City of Vancouver, 2016b).

3.2 Climate

Vancouver is located in the southwest of BC. The city experiences a maritime temperate climate (T. Oke & Hay, 1994). Most of the annual precipitation in Vancouver occurs during the winter and fall months as shown in Figure 3.1. Researchers in 1986 determined that the winter time precipitation can be close to four times greater than the summer precipitation (Grimmond & Oke, 1986). This ratio was found to be higher for the last decade (from 2008 to 2018). Based on the information provided by Figure 3.1, the winter to summer total rainfall ratio has increased to

4.5 in the last decade. The changes to the precipitation distribution will be further discussed in Section 3.2.1.

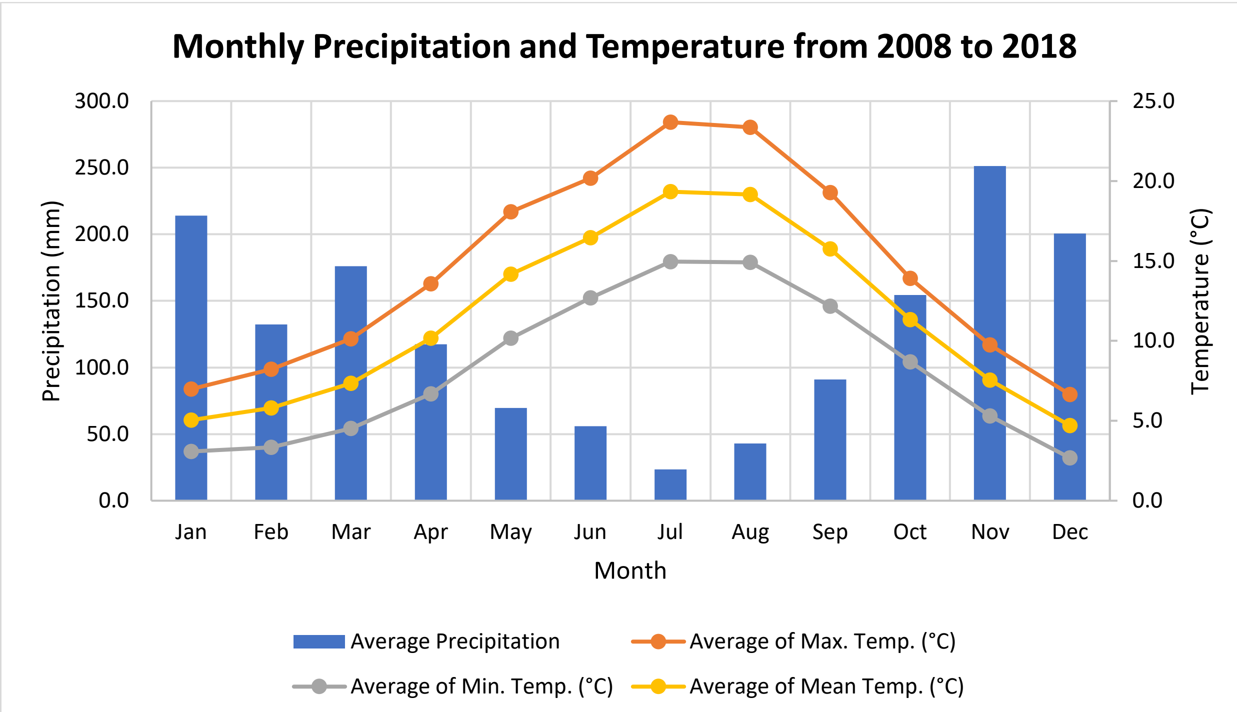

Figure 3.1: Monthly precipitation and temperature summary from 2008 to 2018. Data sourced from Environment Canada's gauge: 1108446, located in Stanley Park at 49°17'43.270" N, 123°07'18.730" W (Environment Canada, 2018).

The rainfall distribution of Vancouver varies within the municipality. The rainfall patterns across the city are influenced by prevailing winds from the Pacific Ocean and the North Shore Mountains. The great majority of storms in an average year fall in the form of light showers or small storms. In hydrological terms, 90% of Vancouver annual precipitation falls in events smaller or equal to a 6 month return storm with a 24h duration which add up to ~48mm. About 10% of the total rainfall in an average year falls under extreme storm event conditions, greater than 48mm. Based on data from 1961 to 1990, the total annual precipitation can be as low as 1,200 mm near the Fraser River, in the south side of the city, or as high as 1,500mm by the shoreline of the Burrard Inlet according to the CoV (City of Vancouver, 2016b). Figure 3.2 summarizes the last decade (from 2008 to 2018) of yearly precipitation near the Burrard Inlet where it shows that the 10-year average precipitation is at 1,505mm.

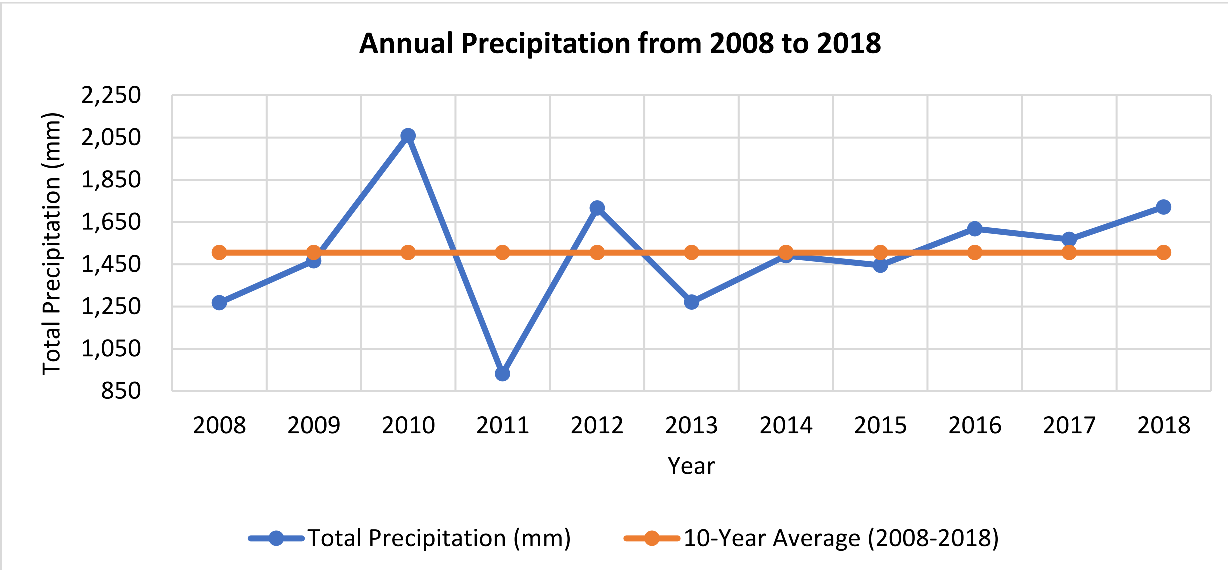

Figure 3.2: Yearly precipitation summary from 2008 to 2018. Data sourced from Environment Canada's gauge: 1108446, located in Stanley Park at 49°17'43.270" N, 123°07'18.730" W (Environment Canada, 2018).

3.2.1 Climate Change

Climate change is global threat. In BC, the changes brought by global warming will be felt in the form of higher precipitation during the winter months, more extreme weather and drier summers.

Climate change is expected to increase the average temperature in the region, increasing the rates of evaporation and plant transpiration. Warm air is known to be able to hold larger amounts of water vapor (BC Ministry of Environment, 2016). For the case of the southwest of BC, the warmer prevalent winds from the Pacific Ocean can effectively pick up more moisture from ocean and carry it to land where it precipitates in the form of snow or rain. In 2016, the BC Ministry of Environment reported climate change projections for the end of the century based on

1961-1990 historical data. The projections cited were based from 15 different GCM models, each developed by a different modelling institution from around the world. Each GCM model used a run of high (A2) and low (B1) greenhouse gas emission scenarios. None of the models include reductions in greenhouse emissions based on international agreements (PCIC, 2012). The main projections are according to the report are (BC Ministry of Environment, 2016):

- Increase in average annual temperature between 1.7ºC to 4.5ºC
    - Glaciers in southern BC will very likely disappear
    - Snow will melt sooner and faster, which will affect fresh water reserves across the province
    - Extremes will become more extreme
- Increase in annual precipitation between 4% to 17%
    - Increasing the runoff generated in urbanized watersheds (cities)
- Decrease in summer base flow
    - Rivers in southern BC may be dry during the summer and early fall months

Based on the projections reported by the Ministry of Environment, it can be expected that the amount of rainfall produced in Vancouver will be higher and more intense during the winter months. The increase in annual mean temperatures and extreme temperatures during the summer months are also an element of risk for the flora at the city. The higher rates of soil evaporation will limit the amount of available water for the plants causing higher mortality rates. The higher temperatures will also exacerbate the heat island effects that are prevalent in highly urbanized or commercial areas with low canopy cover, negatively affecting the people and the fauna in the watershed.

3.3 Site Description

This thesis will evaluate three GI practices located in the False Creek area.

3.3.1 False Creek Site History

False Creek was a tidal flat towards the east. The various streams that were located in the south boundary housed some of the largest trout and salmon runs in Vancouver (City of Vancouver, 2015). Historically, the False Creek area was occupied by the Coast Salish people, which include the Musqueam, Squamish and Tsleil-waututh. The Coast Salish settlements date back at least 3,000 years. European settlers arrived in the 1800's to pursue fishing and logging. Earlier in the 20th century, industrial activities in the area grew to larger operations such as saw and shingle mills, ship building, metal works, among other industries (Sussmann, 2012). Between 1913 and 1917, the tidal flat was filled with the purpose of incentivizing economic growth in the city by increasing economically productive area of False Creek. The materials used to fill in the flat include scraps of lumber, landfill material from development projects, bricks from mills, and general construction waste (City of Vancouver, 2015). The industrial activity in False Creek area began to decline in the 1960s. Much of the area was rezoned to accommodate future housing and parks in the 1970s (Sussmann, 2012).

3.3.2 Quebec Street and 1st Street: Site Description

This site belongs to a community known as Southeast False Creek (SEFC), which is part of the False Creek waterfront sector. Currently, the SEFC area is becoming a high-density residential neighborhood that keeps growing as more high-rise developments are currently being built and planned for the SEFC neighborhood.

Quebec Street in the SEFC recently underwent significant reconstruction. Several GI practices were included between the streets of Central Street and 1st Avenue at Quebec Street.

This thesis will focus on three GI practices that were constructed for the Quebec Street project. The location of the individual practices of interest is shown in Figure 3.3. The practices included are:

- Structural soil STT
- Bioswale with CoV turf blend (will be referred to as Bioswale 1)
- Bioswale with Veratec® bioretention media (will be referred to as Bioswale 2)

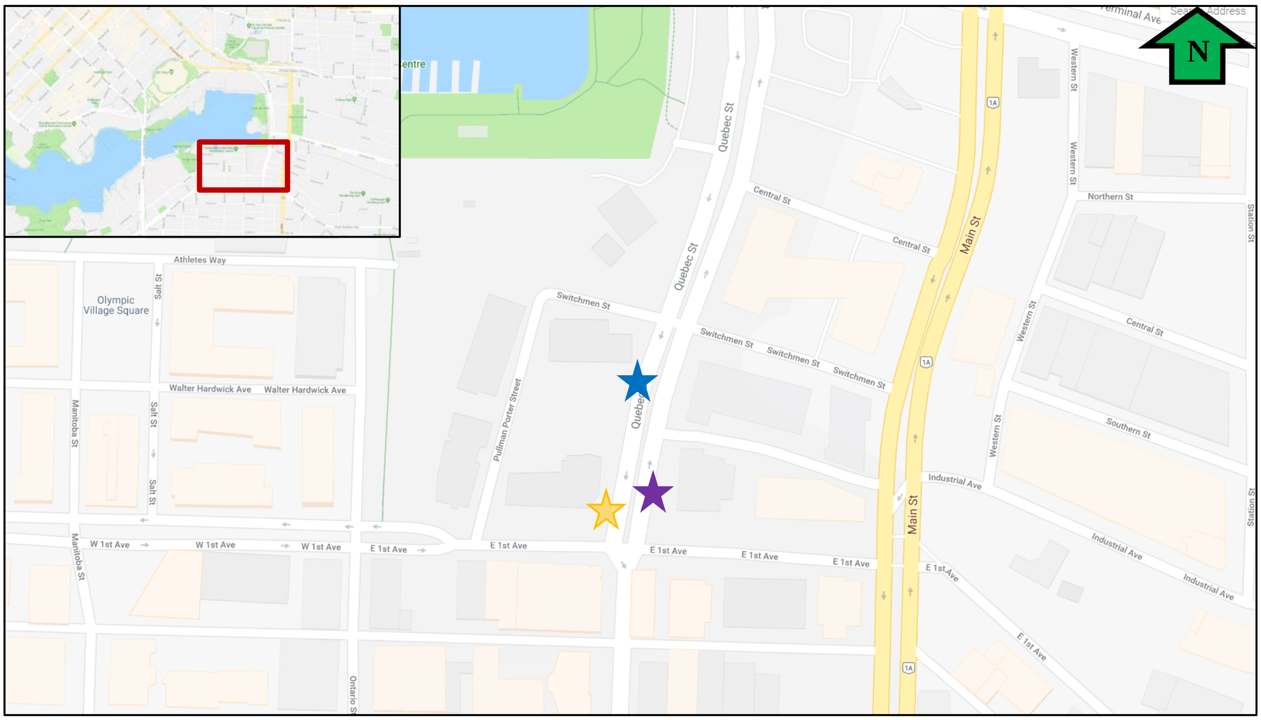

Figure 3.3: Quebec Street and 1st Avenue GI Locations. Structural soil shown by orange star, Bioswale 1 shown by purple star, and Bioswale 2 shown by blue star. Image source: Google Map data ® 2019.

3.3.2.1 Structural Soil Stormwater Tree Trench

The structural soil STT at this location is built under a bicycle lane. This type of application shows the versatility of STT. Structural soil STT can be adapted into locations where utilities are present, and space is limited.

The runoff is collected by a dedicated CB denominated as “GICB”. If the GICB is bypassed, a secondary CB is located 1.7m to the south. The secondary CB is connected to the stormwater sewer directly. The only connection of the GICB is the 6” feeder pipe (at 1% slope) that connects into the 6” distribution pipe laid (at 0% slope) along the length of the practice. The feeder pipe and the distribution pipe are connected by a bend of 135°. Utilizing connection angles not sharper than 135° is important for maintenance reasons. The operation crews of the CoV require large bends in order to use their snaking and scoping equipment when doing regular maintenance. Sharper bends would require the installation of an additional manhole or inspection chamber.

This practice has a 4” perforated underdrain with the function of collecting the exccess stormwater that does not get to infiltrate into the native soils. The underdrain is laid along the length of the STT and it is placed at 0% gradient. At the end of the practice, the underdrain expands to a 6” solid pipe which is sloped at a 1%. This pipe is connected directly to the stormwater sewer. Figure 3.4 shows the cross section of the structural soil STT. The fully detailed engineering drawings can be found in Appendix C.

The practice is approximately 18.24m long and 2.5m wide with a typical depth of 0.85m across the practice. A monitoring well was installed to track the water levels in the practice. This practice uses a custom structural soil and Veratec® bioretention blend as the structural soil in order to increase the water quality treatment efficiencies of this STT. A monitoring manhole was installed and connected to the underdrain pipe. This manhole will be used to monitor the outflows and water quality.

This STT collects and treats an EIA of 415m^2. The catchment area is shown in Figure 3.5. The area includes a section from the sidewalk, bicycle lane and paved boulevard section (not shown in figure). The boundaries were determined and calcualted by the GI Branch during design. I evaluated the boundaries in the field during the water quality sampling days. The runoff drains into the curb's gutter, which in turn is sloped towards the GIBC. Quebec Street is centerline crowned with a slope that varies between 1% to 2%. The water drains to the side gutter and ultimately into the GICB.

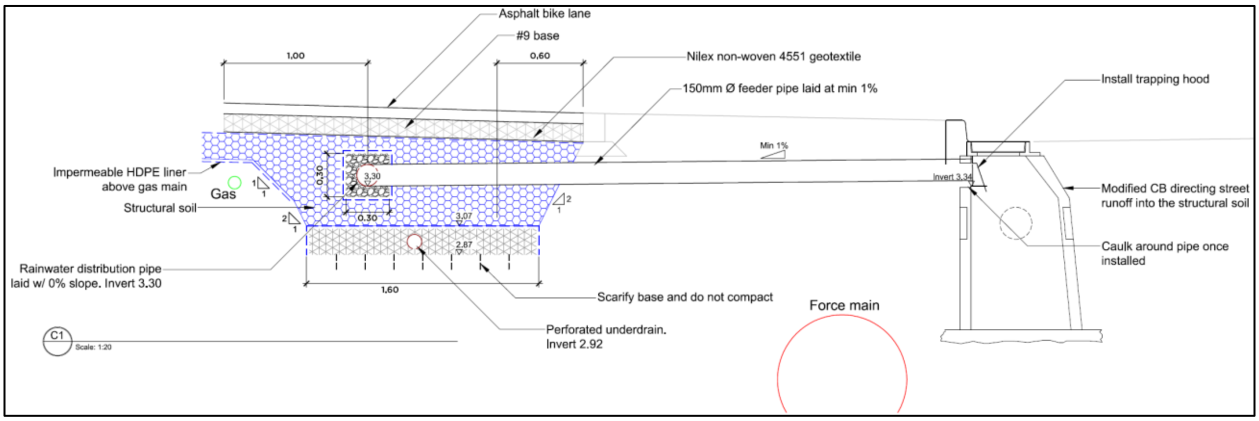

Figure 3.4: Structural soil STT cross-section. Image source: Green Infrastructure Implementation Branch

Figure 3.5: Structural soil stormwater tree trench drainage area. Drainage area shown in red, not drawn to scale. Approximate GICB location shown with green star. Image source: Google Map data ® 2019.

3.3.2.2 Bioswale 1

This is the first of the two bioswales considered for this thesis. Bioswale 1 follows a typical bioswale design with two inlets and one outflow curb openings. The second inlet is to the south of the first one and they are spaced by 6.85m (centerline to centerline). The outlet is located 6.51m (centerline to centerline) to the south of the second inlet. Each inlet has a sediment pad that is composed of a concrete slab surrounded by a river rock apron. The apron has the purpose of slowing down the flow into the bioswale and minimize erosion. Figure 3.6 shows the cross-sections of Bioswale 1. The fully detailed engineering drawings can be found in Appendix C.

The practice is approximately 15.6m long and 1.1m wide (width based on base which is the smallest dimension). This bioswale allows a maximum ponding depth of 15.5cm before overflowing. The average depth of this bioswale is 0.51m. The soil used for this practice is the standard turf blend that is used by the CoV which is used across all landscape activities in the city. This soil mix is does not have any added biofiltration capabilities or nutrient retention additives.

This bioswale practice has a 4” perforated underdrain that is laid at 0% gradient across the majority of the length of the practice. The underdrain is in the middle of the 20cm clear crush aggregate layer that is located between the bioswale soil media and the native soils. The perforated underdrain increases to a solid 6” pipe diameter that discharges to the stormwater sewer. A monitoring manhole was installed and attached to the underdrain in order to have space and access to the flow to monitor the outflows and water quality. A monitoring well was installed in this practice to track the water levels during storm events.

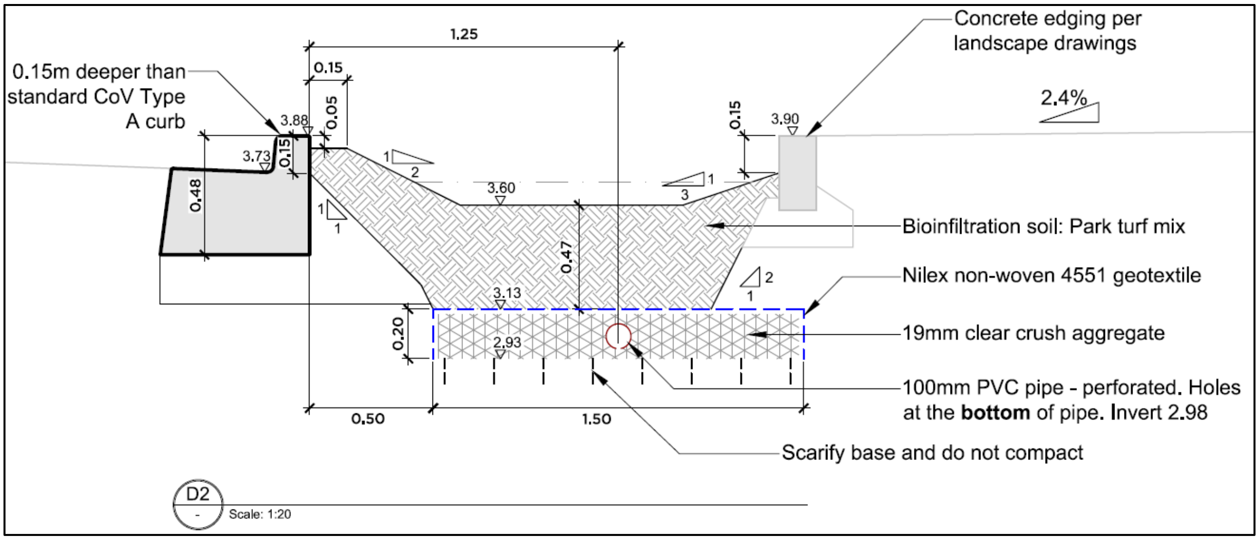

Figure 3.6: Bioswale 1 cross-section. Image source: Green Infrastructure Implementation Branch

Bioswale 1 collects and treats an EIA of 630m^2 in addtion to the approxiamately 17.2m^2 of the bioswale practice itself. The catchment area includes a section from the sidewalk, bicycle lane, paved boulevard section. The boundaries were determined and calcualted by the GI Branch during design. I evaluated the boundaries in the field during the water quality sampling days. The areas are shown in Figure 3.7. The runoff drains to the curb’s gutter, which in turn is sloped towards the inlets. From the bicycle lane, the water drains directly to the practice. Quebec Street is centerline crowned with a slope that varies between 1% to 2%. The water drains to the side gutter and ultimately into the GICB.

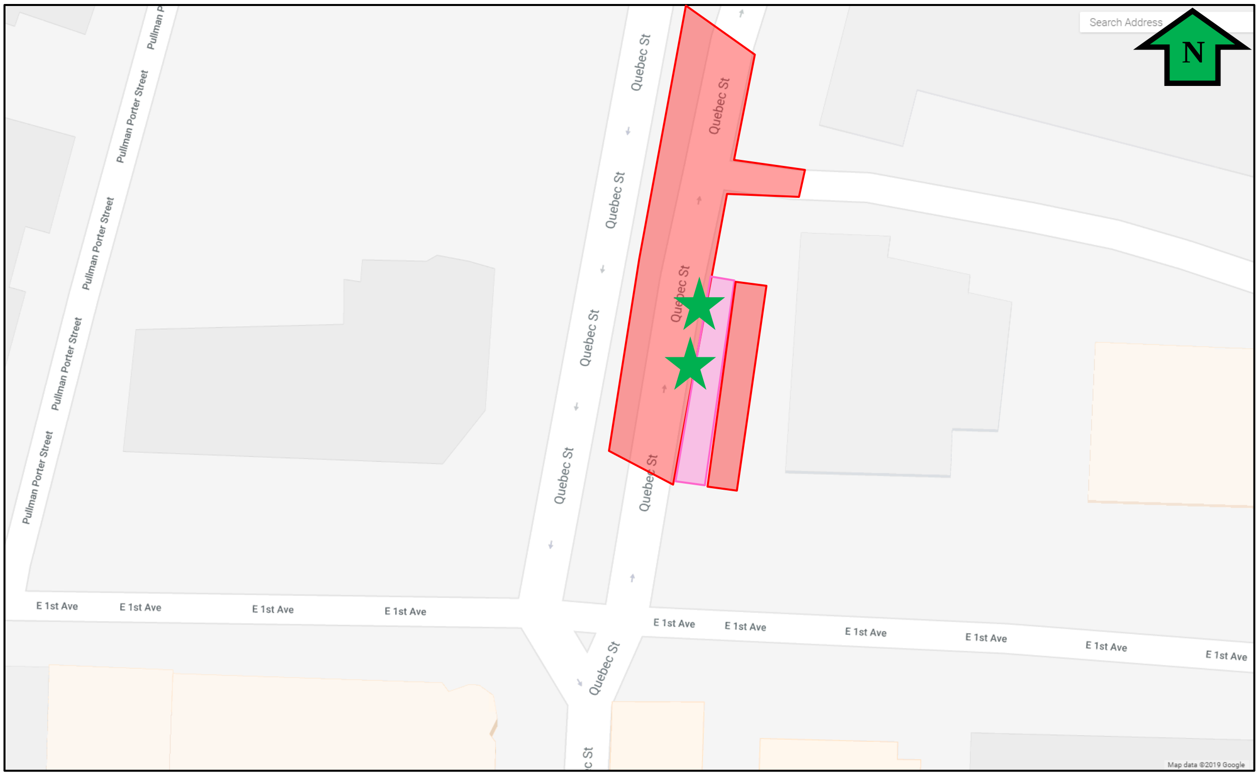

Figure 3.7: Bioswale 1 drainage area. Bioswale 1 practice area. Drainage area shown in red, not drawn to scale. Approximate inlet locations shown with green star. Image source: Google Map data ® 2019.

3.3.2.3 Bioswale 2

Bioswale 2 follows the same design parameters of Bioswale 1. The inlets of this practice are similar to those of Bioswale 1. The second inlet is to the south of the first one and they are spaced by 10.7 m (centerline to centerline). The outlet is located 8.6m (centerline to centerline) to the south of the second inlet. Figure 3.8 shows the cross-sections of Bioswale 2. The fully detailed engineering drawings can be found in Appendix C.

This bioswale allows a maximum ponding depth of 28cm before overflowing. The practice is approximately 18.24m long and 1.4m wide (width based on base which is the smalles dimension). The average depth of this bioswale is 0.50m. The soil used for this practice a custom bioretention mix produced by Veratec®. This soil mix is proprietary, and it does have added biofiltration capabilities or nutrient retention additives. The underdrain and 20cm clear crush layer have the same set-up as Bioswale 1. A monitoring manhole was installed and attached to the underdrain in order to monitor the outflows and water quality. A monitoring well was installed in this practice to track the water levels during storm events.

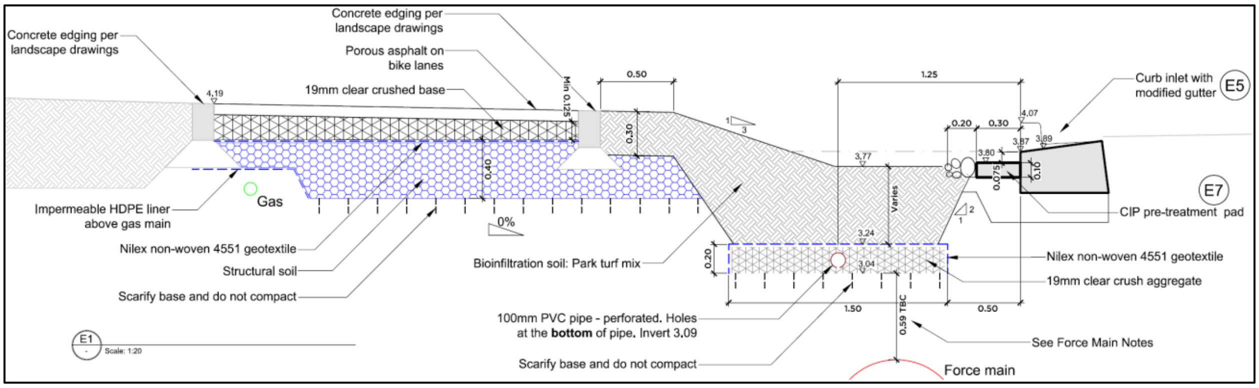

Figure 3.8: Bioswale 2 cross-section. Image source: Green Infrastructure Implementation Branch

Bioswale 2 collects and treats an EIA of 270m^2 in addtion to the approxiamtely 25.5m^2 of the bioswale practice itself. The catchment area includes a section from the sidewalk, bicycle lane, paved boulevard section. The boundaries were determined and calcualted by the GI Branch during design. I evaluated the boundaries in the field during the water quality sampling days. The areas are shown in Figure 3.9. The runoff drains to the curb, which in turn is sloped towards the inlets. From the bicycle lane, the water drains directly to the practice. Quebec Street is centerline crowned with a slope that varies between 1% to 2%. The water drains to the side gutter and ultimately into the GICB.

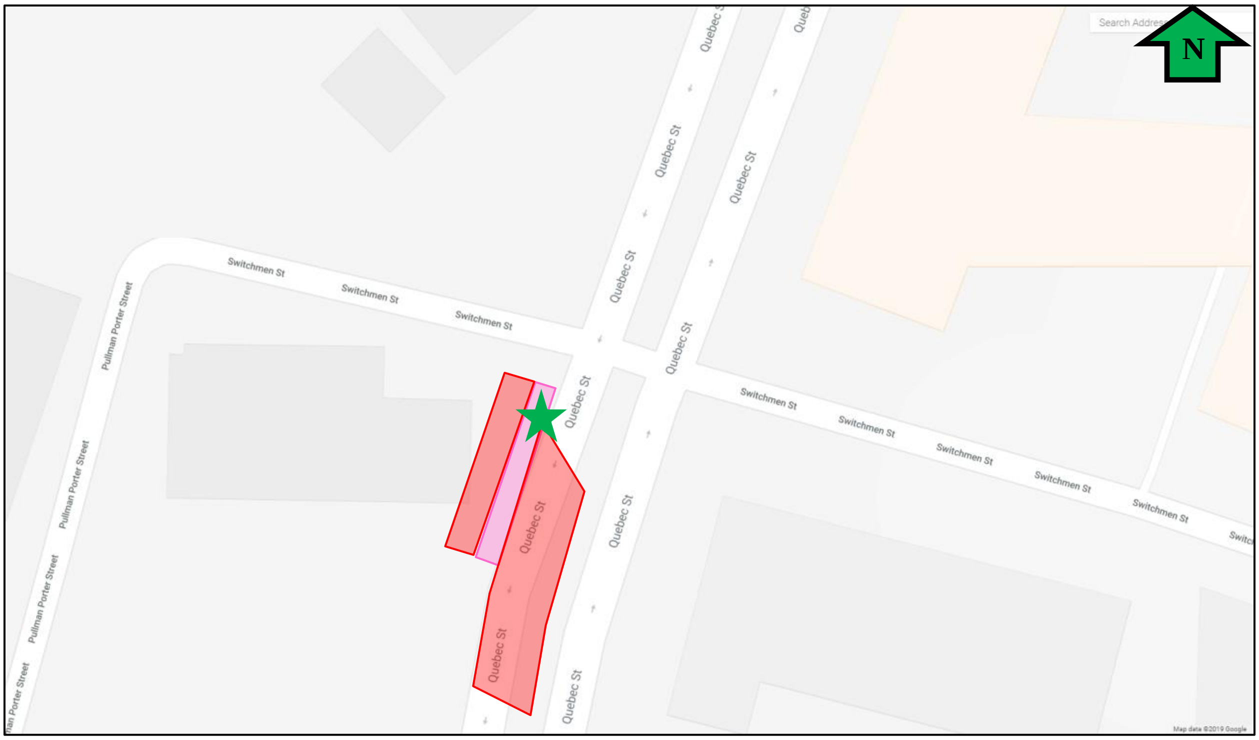

Figure 3.9: Bioswale 2 drainage area. Bioswale 2 practice area. Drainage area shown in red, not drawn to scale. Approximate inlet locations shown with green star. Image source: Google Map data ® 2019.

Chapter 4: Monitoring Plan Methodology and Field Deployment

4.1 Precipitation Monitoring

A rain gauge was installed in July of 2018 at the Creekside Community Recreation Centre in the SEFC neighborhood. The rain gage information is uploaded online and accessible remotely by FlowWorks®. The resolution of the data is in 5-minute intervals. The rain gauge is located at ~266m northwest of the Quebec & 1st site. This study will consider only rainfall events that have a minimum cumulative precipitation of 2mm. Each storm will be differentiated by a minimum 6-hour antecedent dry period (ADP).

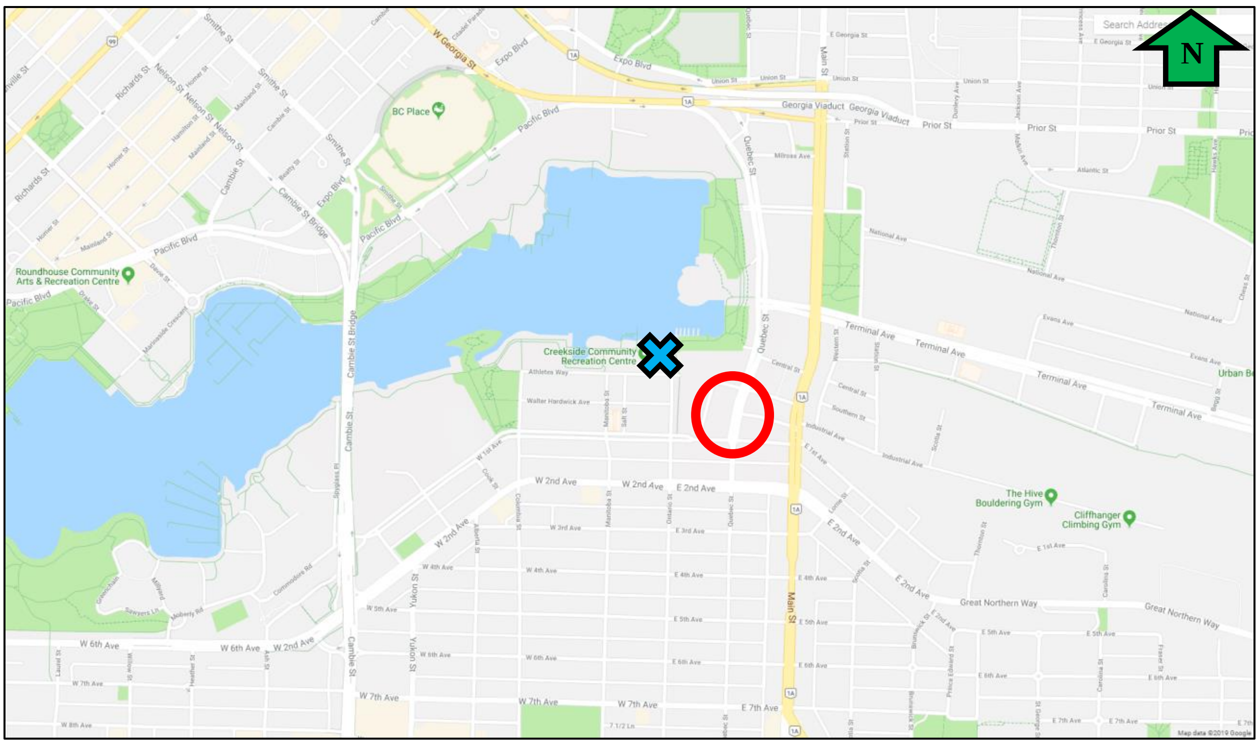

Figure 4.1: Rain gauge location relative to monitoring sites. Quebec Street and 1st site location circled in red. Rain gauge at Creekside Community Recreation Centre shown in blue cross. Image source: Google Map data ® 2019.

4.2 Flow Monitoring

Traditional monitoring programs rely on accurate flow measurement information to determine a variety of factors such as peak flow reduction, volume reduction, loadings, and discharges to streams (Rindosh, 2016). Hydrologically speaking, peak flow and volume reduction are one of the most important and sought-after qualities of GI.

Green infrastructure is very versatile and effective in managing a diversity of landscape changes that occur in the urban environment (Schifman et al., 2017). This versatility is what makes monitoring GI, specifically bioswales, challenging in the field. The construction locations of the GI (i.e. rights-of-way, plazas, among others) also adds to the increase in difficulty in monitoring. Adding field instrumentation to a street inlet is difficult due to installation challenges, data collection equipment and battery life (Rindosh, 2016). The instrumentation chosen for the present work was selected to monitor inflow and outflow drains in accordance to the following constraints:

- Acceptable accuracy to measure low flow scenarios
- Continuous data recording capability with minimal maintenance requirements
- Compact system that can be stored underground in a manhole and has water resistance capability
- Minimize work required on GI catch basins due to proximity to the street and bicycle lanes
- Minimize weights of manhole covers and other lids to protect GI vegetation and minimize required personnel
- Minimize equipment costs: study is budget limited

4.2.1 Inflow Monitoring

GI comes in a variety of shapes and sizes. The inlet designs vary between GI practices. As specified in Section 1.4, this monitoring study includes two bioswale designs and one STT.

4.2.1.1 Bioswales

Bioswales have an inlet design that consists of curb opening. The curb opening for the bioswales of this study is shown in Figure 4.2. A flume system as the one considered by Rindosh (2016) can be an option to accurately measure inflows to a bioswale system. A system such as this is highly recommended by this author to accurately record inflow information. Unfortunately, the bioswales identified for this study did not allow for the installation of a flume system due to space and location restrictions.

Figure 4.2: Bioswale Inlet Design shortly after being completed. Opening is flush with the street curb's gutter. Water flows into the inlet and drops into a concrete slab with the purpose of trapping fine sediment. The water is dispersed radially into river stone to disperse sediment and reduce flow speed.

4.2.1.1.1 Bioswale Inflow Estimation Method 1: US EPA' Storm Water Management® Model

For event based and continuous simulation modes, Mike-Urban®, HEC-HMS and EPA SWMM ® are typically used; however, only HEC-HMS and EPA SWMM ® are publicly available or have free of charge software (Alamdari, Sample, Steinberg, Ross, & Easton, 2017). The free version of the EPA SWMM ® (Version 5.1) was selected to simulate and estimate the runoff in bioswales as it is widely used among researchers to simulate rainfall-runoff events in urban watersheds. It has the capability of simulating runoff, infiltration, evapotranspiration, percolation, snow accumulation and melting, and pollutant load estimations (Alamdari et al., 2017; US EPA, 2019). EPA SWMM ® now has an added feature to simulate the infiltration processes of GI (US EPA, 2019).

EPA SWMM ® was used to model the runoff generated by each storm event. The source of rainfall information was provided by the Creekside rain gauge (refer to Section 4.1). Each practice was modelled in the software. The drainage areas, road grading, and other required information was obtained from the site descriptions provided in Section 3.3.2. The EPA SWMM ® was used as an input to calculate the stormwater volume reduction and peak flow reduction.

The stormwater volume reduction was calculated per practice and by storm event as a percentage. The general formula to be employed is described by Equation (4.1). Where Inflow Volume is the total stormwater runoff generated in liters by each storm event "i" and Outflow Volume is the total underdrain flow measured in liters by each storm event "i".

$$Stormwater\ Volume\ Reduction_{(i)}(\%) = \left(1 - \frac{Outflow\ Volume_{(i)}}{Inflow\ Volume_{(i)}}\right) * 100(\%) \qquad (4.1)$$

In a similar fashion as the stormwater volume reduction, the peak flow reduction will be calculated by comparing a storm's peak runoff against the peak flow out of the underdrain of each GI practice. The process is summarized in Equation (4.2). Where Peak Inflow is in L/s and Peak Outflow is in L/s. Peak flow reduction will be expressed as a percent.

$$Peak\ Flow\ Reduction_{(i)}(\%) = \left(1 - \frac{Peak\ Outflow_{(i)}}{Peak\ Inflow_{(i)}}\right) * 100\% \qquad (4.2)$$

The lag time of each storm into the storm sewer network will be calculated by subtracting the time stamps of the start of the underdrain outflow against the start of the inflow to the GI practice by using each storm's hydrograph. The process summarized in Equation (4.3) is used to convert time stamps in Microsoft EXCEL® to hours.

$$Lag\ Time_{(i)}(h) = \frac{Outflow\ Start\ Time_i - Inflow\ Start\ Time_i}{0.0416666666666667} \qquad (4.3)$$

The methods to calculate the outflows of the GI practices will be further explored in Section 4.2.2.

4.2.1.1.2 Bioswale Inflow and Peak Flow Estimation Method 2: The Simple Method and Rational Method

The Simple Method developed by Schueler (1987) was selected to cross-check the EPA SWMM ® simulated inflows to the bioswales. The simple method provides a flow estimate by accounting for total precipitation, runoff coefficients and drainage area (Schueler, 1987). Adjustments were made to the Simple Method formula to account for individual events and for the GI features. These modifications followed the steps set by the Credit Valley Conservation (CVC) (2016a, 2016b). The modifications steps determined by CVC are the following:

- The bioswale area will be incorporated into the calculations of the Simple Method as an added term without accounting for the runoff coefficient. The runoff coefficient only accounts for impervious surfaces. This assumption is based on the premise that no runoff will occur on the rainfall captured directly by the bioswale.

- The total event precipitation in mm will be used instead of the annual precipitation.

After the incorporation of the adjustments, the modified Simple Method formula components are the following:

$$Q = [(Draiange\ Area\ to\ GI * R_v) + GI\ Area] * [i] \tag{4.4}$$

In Equation (4.4), Q is the discharge to the GI practices in L/s, Rv is the dimensionless runoff coefficient, the area components are in m^2, and "i" is the total storm is in mm.

$$R_v = 0.05 + (0.9 * I_a) \tag{4.5}$$

Equation (4.5) explains the details of the runoff coefficient. The value of 0.9 specifies the fraction of rainfall events that produce runoff (CVC, 2016a, 2016b, 2016c). The term Ia corresponds to the impervious fraction, which is also a dimensionless number. The I_a formula is detailed in equation (4.6).

$$I_a = {}^{Impervious\ Area}\!/_{Drainage\ Area\ to\ GI} \tag{4.6}$$

The catchment areas for the bioswales are small and simple. The Simple method is expected to provide reasonable flow estimates. Nevertheless, the formula has several limitations that need to be accounted for:

- The Simple Method is sensitive to the impervious cover values. Each land use within a watershed has its own coefficient. The coefficients are derived from a linear relationship with significant dispersion. The R^2 value of this linear model equals 0.71. The linear model used 47 samples (NH DES, 2008; Schueler, 1987).

- For small events, the Simple Method over estimates the inflow discharge. This is due to the assumption of equal distribution of rainfall along the drainage area (NH DES, 2008).

The Rational Method is a simple technique for estimating discharge for small watershed (Kuichling, 1889). This method is the basis for the design of small structures. The Rational Method is particularly used in the sizing structures with drainage basins that are limited to a few tens of acres. The formula of the Rational Method relates the peak rainfall intensity for a certain storm duration, watershed drainage area, and runoff producing potential of the watershed (Thompson, 2006) related to the site conditions (land use, permeability of surface, etc.). The formula developed by Kuichling (1889) is:

$$\mathrm{Q} = C_u * C * i * A \tag{4.7}$$

Where Q corresponds to the discharge that depends on the C*u* factor to determine the units. C*u* is a unit conversion coefficient. In this case the desired units of discharge are m^3/s which requires the Cu = 1/3600 in this case. The “i” term corresponds to the design rainfall intensity in mm/h. The “A” term corresponds to the area of the catchment in m^2 (Thompson, 2006). This term of the formula will be modified to include the GI catchment.

The runoff coefficient “C” is a dimensionless term that relates the intensity of a rainfall and the runoff associated to it. According to the site conditions, a runoff coefficient of 0.95 was used for the street catchment calculations. This coefficient value corresponds to asphalt and downtown areas (Thompson, 2006). The runoff coefficient for the GI structures will be treated differently to accommodate the different structures. The bioswales and soil cell will be considered to intercept all precipitation. The structural soil catchment areas are covered in asphalt; hence why the 0.95 coefficient applies.

For Vancouver, the rainfall intensity should be estimated using the updated Intensity Duration Curves (IDF) required by CoV as of 2019. The updated IDF curves were updated in 2017 and their use is mandatory in the design of infrastructure by city staff and developers (City of Vancouver, 2018b). The STT and bioswales for this study have a design life of 50 years. Hence, this sizing exercise was focused on the projections of the IDF curve for the year 2050.

A geospatial tool called VanMap was used to estimate the catchment areas. VanMaps is a public tool created and maintained by CoV to create maps of the city, assess property values, water and sewer utilities, among other uses (City of Vancouver, n.d.).

4.2.1.2 Stormwater Tree Trenches

The STT for this project were designed to treat street runoff. As specified in Section 3.3.2.1, the stormwater collected within the catchment areas of the STT is drained towards a dedicated GICB. The locations of the STT did not allow for the installation of a monitoring manhole in the distribution pipe of the GICB and the reduced space conditions in the GICB did not allow the installation of measuring devices to monitor the inflows to the practice. Therefore, the inflows to the STT will be modelled in the same fashion as the bioswale practices. The inflows will be estimated using the EPA SWMM ® and corroborated using the Simple Method in a similar fashion as the bioswale practices. The total runoff volume reduction, peak flow reduction and lag time will be calculated using Equations (4.1), (4.2) and (4.3) respectively.

4.2.1.2.1 Recommended Inflow Measuring Method

The method hereby proposed is a simple tool that can be used in GI applications to measure inflows to a feeder pipe connected to a CB. In-stream flow measuring devices are more accurate tools; however, the installation of these devices is not always feasible due to budget, space constraints in the CB and flow conditions (low flows, oil pollutant's adhering to sensor, etc.). All of this considered, a low-cost weir made from a rubber lined PVC cap that can fit on the feeder distribution pipe of the GI practice can be an efficient method to measure flows.

Weirs are fairly easy to construct and can measure discharges when built and installed correctly (Van Den Bosch, Snellen, Brouwer, & Hatcho, 1993). Weirs are sharp-crested overflow structures of specified geometries that are typically built across open channels (ASTM, 2013, 2014; Van Den Bosch et al., 1993). The volumetric flow rate is a unique function that is dependent on the water level upstream of the weir structure. The head-discharge relationship has been experimentally determined by American Society of Testing and Materials (ASTM). Figure 4.3 shows a typical thin-plate rectangular weir. ASTM recommends that weirs are used in water and wastewater where head loses can be afforded and low in-stream debris (solids) should be maintained to maximize the accuracy of weir devices (ASTM, 2013).

The PVC weir cap hereby proposed is based on the conditions outlined in the ASTM document named ASTM D5242 – 92: Standard Test Method for Open-Channel Flow Measurement of Water with Thin-Plate Weirs (ASTM, 2013). The main assumption is that the approach conditions inside the GICB are maintained according to the conditions outlined by the ASTM D5242 document. The main reason for this check is that for weirs to work, the approach to the weir constriction must have negligible flow velocity (subcritical conditions). The constriction of the weir forces the flow to go through critical flow at the weir constriction and immediately transition into supercritical flow after the drop.

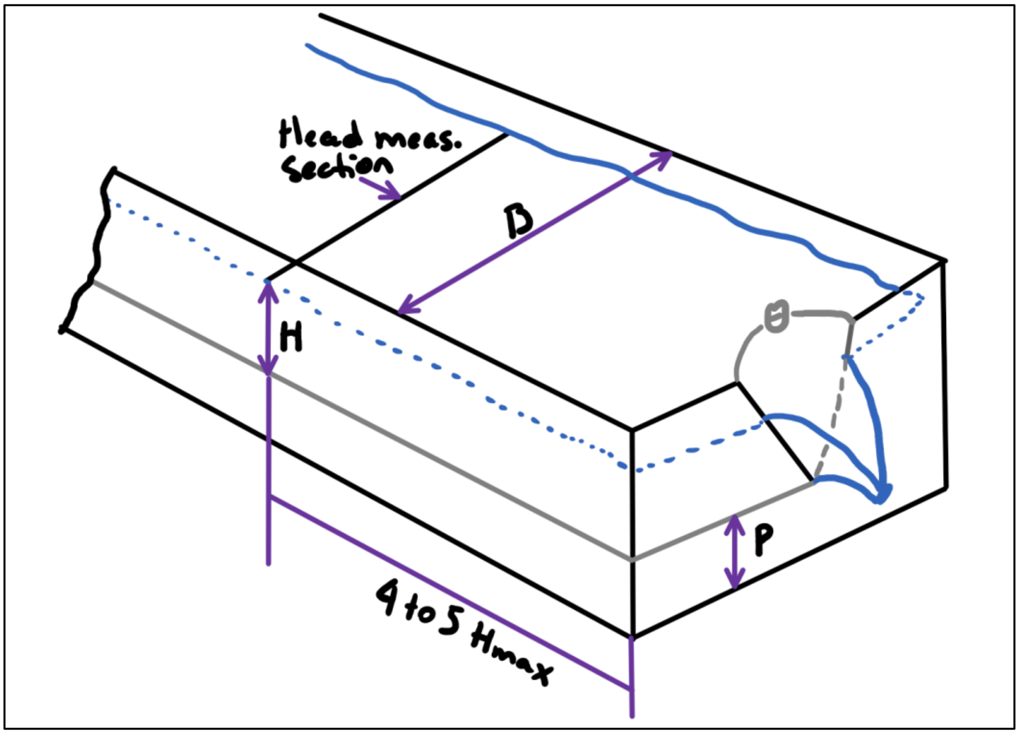

Figure 4.3: Thin-plate rectangular weir diagram. Image adapted from ASTM D5640 – 95 (ASTM, 2014)

The stormwater in the GICB will back up against the weir until it reaches the bottom of the constriction and begin to spill over the weir. The stormwater in the GICB will have a velocity of practically zero, imitating the negligible approach velocity condition required. The constriction will force the flow to go from subcritical to critical. After the constriction, the flow will transition into supercritical flow when it discharges into the feeder distribution pipe. This supercritical flow regime will change due to the constrictions in the pipe connections. Figure 4.4 summarizes the process described.

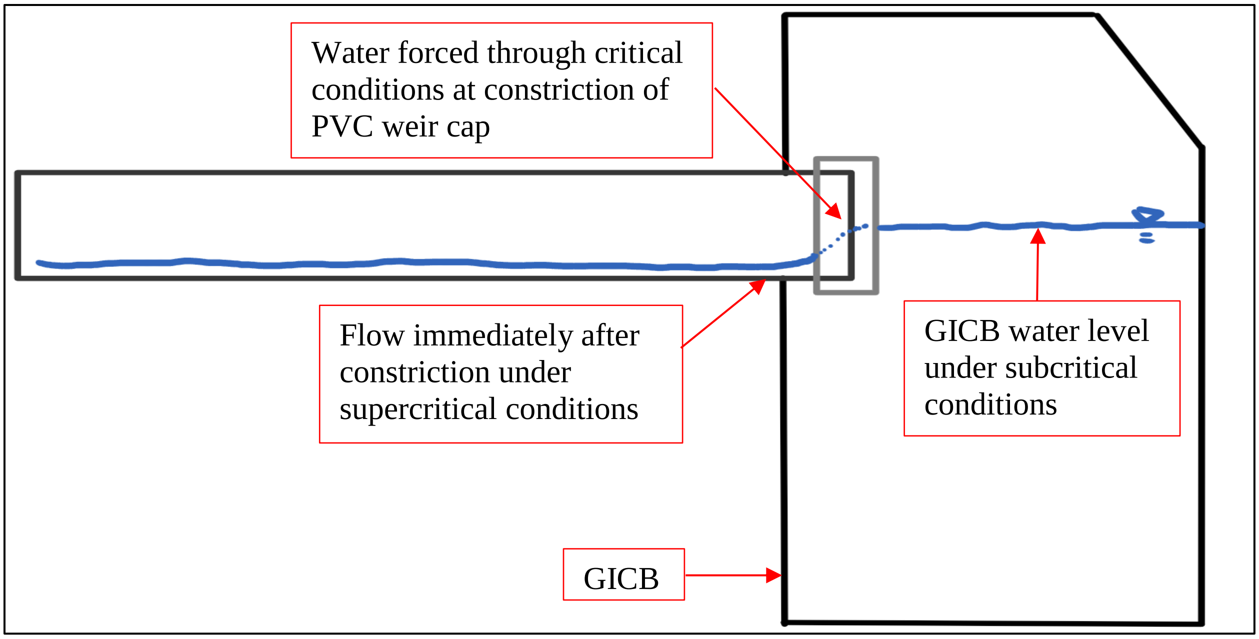

Figure 4.4: Theoretical flow inside GICB and the PVC weir cap

The weir device should not be a bottleneck in the GI practice, so to verifying the maximum capacity of the weir is an important step. The Rational Method can be utilized to study the peak flows expected for the catchment. To demonstrate the potential use of the PVC weir cap in this thesis, the structural soil STT will be evaluated as only STT can use the PVC weir cap method. The design storm utilized had a 10-year return period as this is the required recurrence for structures such as CB in at False Creek area by the CoV (City of Vancouver, 2018c, 2018b). The 2050 IDF curve was utilized as the practice evaluated will have a 50-year life span. The intensities in mm/h to be evaluated are shown in Table 4.1.

Table 4.1: PVC weir cap design storm evaluation intensities for different durations

Design Storm - 2050 IDF Curve			
10-Year (mm/h)			
30 min	**2 hours**	**6 hours**	**24 hours**
38	18	10	4.8

The catchment area of 415m^2 provided in Section 3.3.2.1 was used to estimate the peak flows shown in Table 4.2. This table summarizes the expected peak flows for the structural soil

STT GICB. For other catchments, the same process must be followed in accordance to the applicable municipal guidelines (if assessing municipal assets). The peak flows shown below will be compared to the maximum discharges possible form the PVC weir cap variations.

Table 4.2: Runoff produced at different durations in test location based on 2050 IDF curve

Peak Discharge (m^3/s)			
10-Year			
30 min	**2 hours**	**6 hours**	**24 hours**
4.16E-03	1.97E-03	1.10E-03	5.26E-04

Two weir notches were tested: 90° and 53.13° for the 6" PVC weir cap. The conditions outlined in the ASTM D5242 document used to determine if the GICB meets the approach requirements for each weir v-notch angle in consideration. The evaluation can be found in Appendix E. Both V-notch angles satisfy the approach conditions required.

Table 4.3: PVC weir cap notch selection

Vnotch (Theta)	Tan (theta/2)	Hmax (mm)	Cet	Delta et (mm)	Het (mm)	Q (mm^3/s)	Q (m^3/s)
53.13°	0.5	117.00	0.575	0.98	117.980	3.25E+06	3.25E-03
90°	1.0	81.00	0.578	1.3	82.300	2.65E+06	2.65E-03
Comment	-	-	From curve	From curve	=Hmax+Delta et	From formula	Converted

Table 4.3 summarizes the results of the V-notch selection for the 6" PVC weir cap for a typical CB used by the CoV (refer to Appendix D standard detail drawings). Each notch was evaluated by calculating the maximum discharge possible. This was determined by measuring the maximum distance between the V-notch and the base of the inverted triangle opposite to the V-notch. This was done because the discharge formula from the ASTM D5242 document is only valid within this range.

Based on the results of Table 4.3, the 53.13° V-notch was selected as it provides the greatest maximum discharge out of the 6” PVC cap dimensions. Figure 4.5 shows a PVC weir cap with a 53.13° V-notch which was utilized for a project, outside the scope of this thesis. The maximum discharge is more than capable of tolerating the peak flows calculated in Table 4.2 except for the most intense duration.

Figure 4.5: PVC weir cap with 53.13° V-notch

For cases where the peak flows exceed the maximum discharge of a V-notch, it is important to note that the maximum discharge of the V-notch, as provided in Table 4.3, only includes the area where the formula provided by the ASTM D5242 document is valid. Figure 4.6 shows the same PVC weir cap but deployed in the field. In this vantage point it can be shown that the PVC weir cap has larger opening which provides extra flow capacity, reducing the chances of making the PVC weir cap the bottle neck. The calculations of the extra flow capacity are beyond the scope of this thesis due to the complexity of the analysis.

Figure 4.6: 6” PVC weir cap installed in a 6” distribution pipe inside a typical CoV CB

Once deployed in the field, the water levels in the CB relative to the V-notch can be permanently measured using a pressure transducer as shown in Figure 4.7. The sensor can be secured either to the wall of the CB or suspended by a chain from the grate. A secondary pressure transducer is required to do the atmospheric compensation. This secondary sensor can be installed at a location near the CB to avoid submersion.

The pressure transducer of choice by this study is the HOBO® U20 level logger (shown in Figure 4.8). The HOBO U20® requires minimal maintenance and has the capability of measuring and recording liquid pressure and temperature. The pressure range is from 0 to 145kPa with a resolution of 0.0013kPa. The error for pressure is ±0.075%. The temperature range is from -20° to 50°C with a resolution of 0.10°C at 25°C. The error for temperature is ±0.44°C from 0° to 50°C. The device has IP68 certification and has a battery life of 5 years.

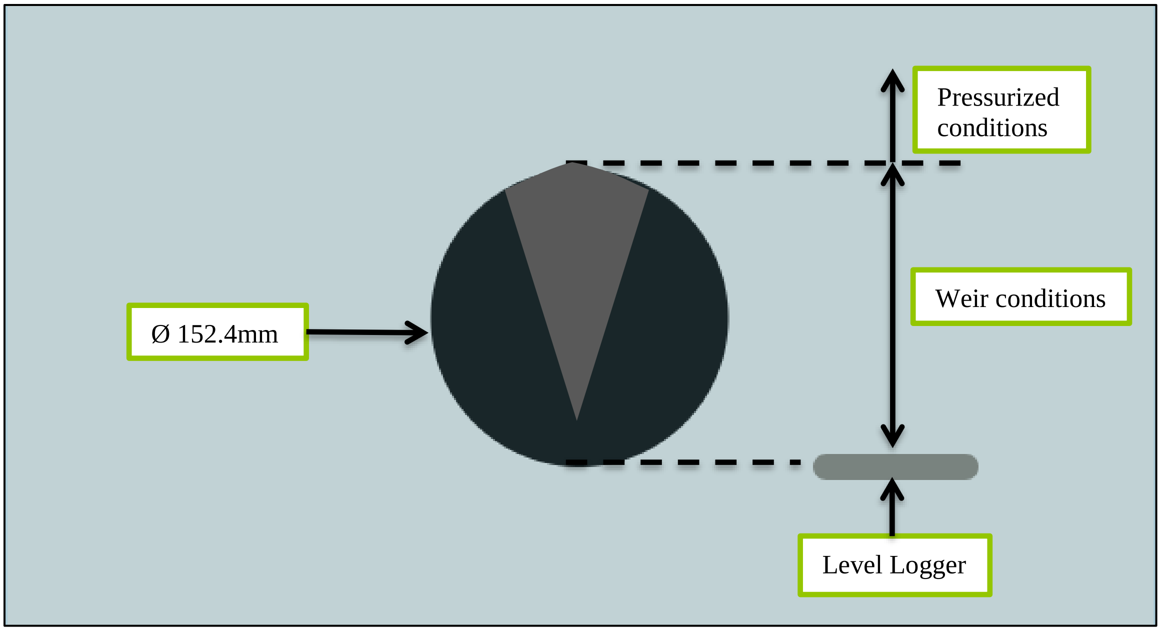

Figure 4.7: PVC weir cap and water level logger diagram

The water level is calculated using the HOBO® software which uses the recorded absolute pressure from the primary sensor and compensates it with the secondary pressure recorded by the secondary sensor (atmospheric pressure). If selected, the software can also make adjustments for the density of the liquid based on temperature and liquid type. These considerations make the water levels calculated by the software more accurate (Onset, 2019).

Figure 4.8: HOBO U20® Water Level Logger. Image source: Onset Computer Corporation (Onset, 2019)

In the odd case, the water level of the GI CB can overwhelm the PVC weir cap device. The GICB can be bypassed if water is not infiltrating at a rate of stormwater ingress to CB. In this case, the inflow can be estimated by the used of the EPA SWMM® model and corroborated by the Simple Method. The water level logger can be also used to determine at which point is the GICB bypassed and runoff estimations can be adjusted based on the time of this bypass. Due to regulations at CoV, trapping hoods are required to be installed at the mouth storm sewer connection inside a CB (City of Vancouver, 2018c). Care should be taken to ensure that the PVC weir cap has enough of a gap in front of the trapping hood. The trapping hood will protect against the inflow of floating debris.

4.2.2 Outflow Monitoring

The outflow monitoring was possible through the inclusion of a monitoring manholes connected to the underdrains of the practices. This structure also acts as a housing for the flow monitoring equipment. Figure 4.9 shows the cross-section of the typical manhole used in this study. The manhole is a PVC standpipe that has two 6” perforations to allow the installation of a 6” through pipe. The through pipe is connected to the outflow drain of the GI practices on one end and to the stormwater pipe on the other end. The grade of the through channel of each monitoring manhole is different as the construction process is not 100% accurate, which led to variances in the positioning of the monitoring manholes. The standpipe height of each manhole was adjusted after installation to be flush with the grade. The standpipe was covered by a hinged fiberglass cover for an easier access to the equipment.

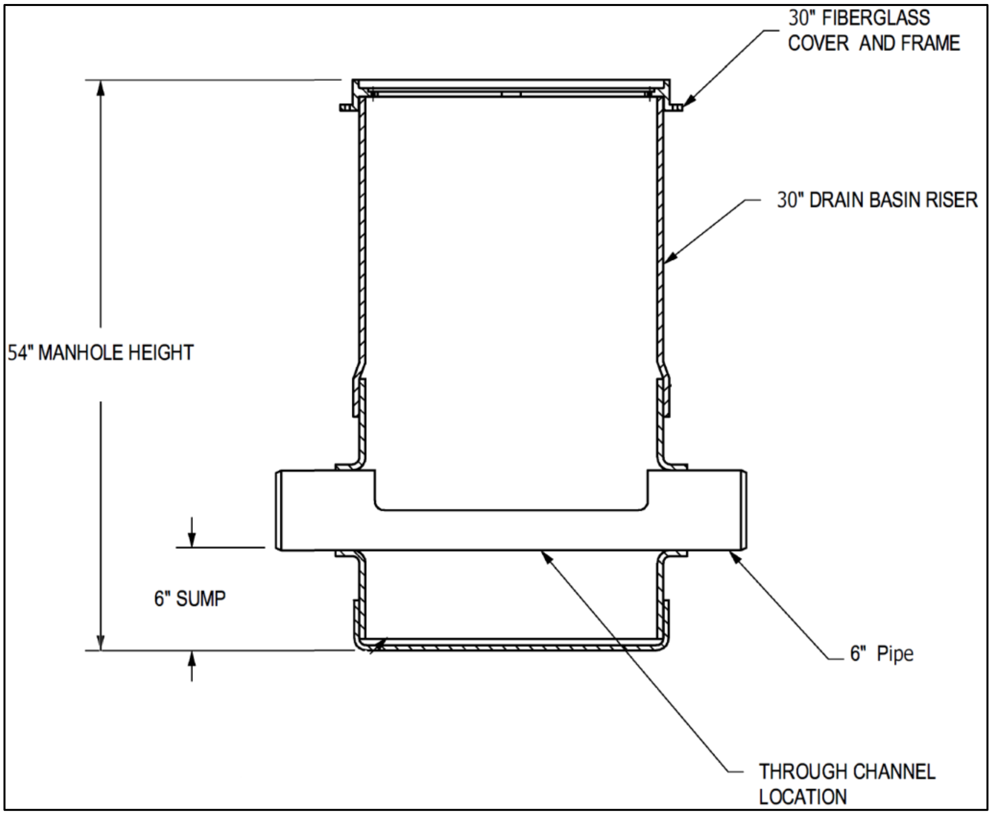

Figure 4.9: Monitoring manhole cross-section. Image source: Section drawings provided by ADS-Pipe shop drawings

4.2.2.1 Recommended Flow Measurement Method: Flumes

To monitor the outflow discharge, weir and flumes were considered. Weirs have been used as measuring devices due to extensive experimentation and the consequent development of rating curves (Te Chow, 1959). However, weirs installed in pipes have reported extensive problems. Leakages and slippage are the most common issues when using weirs in pipes (CVC, 2016a). To circumvent the latent issues surrounding weirs in pipes, the discharge should be estimated by using a flume device.

Flumes are versatile devices because they can be used in shallow canals with flat grades. Flumes have a small drop in head (water level). Under similar discharge conditions, it is estimated that flumes only require a one quarter of a drop when compare to a weir (Van Den

Bosch et al., 1993). Like weirs, flume systems make use of stage-discharge curve to provide discharge estimations. The water level upstream of the flume constriction is used to measure the discharge through the flume. The water level (head) is then converted to discharge by a diagram specific for the flume used (Kilpatrick, 1965; Van Den Bosch et al., 1993).

The Palmer-Bowlus flume was selected as the best option for a monitoring set-up as the one considered by this thesis. This particular flume is an adaptation of the Venturi flume, which is typically used in sewer discharge measurements (J. H. Ludwig & Ludwig, 1951). The Palmer-Bowlus flume design makes use of a flow rating curve based on the Bernoulli Equation in which the upstream and flume throat energies are equated. Because of this calculation method, the flume designer is able to prepare rating curves for any throat section design, making it more versatile that other flumes such as the Parshall flume (R. G. Ludwig & Parkhurst, 1974).

The Palmer-Bowlus flume does not require a drop in the downstream as other flumes do. Therefore, the flume can be installed in locations where invert elevations cannot be changed (J. H. Ludwig & Ludwig, 1951). The inflow and outflow inverts were fixed in the monitoring manhole as shown in the as-built drawings in Appendix C.

The Rational Method can be used to size the flume. The peak flow calculated by this method will determine the appropriate size of the flume. The catchment areas utilized for this analysis were provided in site description of each practice (Section 3.3.2). The flumes will be evaluated according to the standards required by the CoV for the False Creek area (City of Vancouver, 2018c). The storm intensities in Table 4.1 were used for each practice. Table 4.4 summarizes the results of the sizing calculation. A conservative GI runoff reduction performance of at least 50% was used to account for the runoff that is infiltrated to the ground.

Table 4.4: Flume sizing results

Site	Peak Outflow Discharge (m^3/s)				Peak Outflow Discharge (gpm)			
	10-Year				10-Year			
	30 min	2 hours	6 hours	24 hours	30 min	2 hours	6 hours	24 hours
Structural Soil	2.08E-03	9.86E-04	5.48E-04	2.63E-04	32.98	15.62	8.68	4.17
Bioswale 1	3.25E-03	1.54E-03	8.55E-04	4.10E-04	51.50	24.40	13.55	6.51
Bioswale 2	1.49E-03	7.05E-04	3.92E-04	1.88E-04	23.59	11.18	6.21	2.98

The sizes and capacities of the Palmer Bowlus flumes will depend on the manufacturer. For this exercise, Virtual Polymer Compounds LLC's Palmer Bowlus flumes were selected as an example. Based on the table above and the flume manufacturer's design table (VPC, 2018) it was found that the 6" flume size would be ideal for this flow application as it minimizes the constriction on the flow. In addition, the maximum capacity of the flume is well over the design requirements, guaranteeing that the flume will not overflow.

In the end, the Palmer Bowlus flume was not used to monitor the outflows due to space constraints. The monitoring manhole is 762mm in diameter, and it could not be larger due to space conflicts at the street level. The total length of the 6" Palmer Bowlus flume, including the pipe attachments was 762mm as well. This rendered the space inside the manhole insufficient for a proper installation as it is required that the flume's pipe attachments are clamped to the in-situ pipe. The manufacturer recommended a complicated, leakage prone method that was not deemed appropriate for accurately measuring outflow discharges. An alternate method will be discussed in the following section. However, the flume method is still preferred over the alternate flow measurement method employed by this thesis. Flume devices undergo several stages of calibrations by the manufacturers which makes them more accurate and reliable.

4.2.2.2 Alternate Flow Measurement Method

The method utilized in this thesis to estimate the outflows involves the development of a rating curve specific to the through pipe system shown in Figure 4.9. This must be completed for each practice included in this thesis.

The application of Manning's equation was considered to estimate the flow in the through channel. However, it was not deemed appropriate because Manning's equation was developed for steady state, uniform flow conditions (FISRWG, 1998; Margulis, 2017). This requires a uniform cross-sectional area and little to no disturbances upstream or downstream of the measurement location. In the through channel system, the stable flow conditions were not met due to the constrictions present before the through channel.

Ideally, the pipe couplings used to connect pipe ends should seamlessly connect one end of the pipe to the next to minimize leakages or disturbances to the flow. However, ensuring a proper fitting in the coupling is extremely difficult to do in the field. Consequently, gaps are left between the pipes, which in turn induce disturbances to the flow profiles because of the abrupt changes in channel width.

4.2.2.2.1 Couplings: Hydrological Investigation of Field Conditions

From a flow profile perspective, it is important to consider the pipe coupling transitions in the field and the approach conditions to the flume device. The transitions will be explained in terms of the system's specific energy diagram, where "q" stands for the discharge rate per unit width in m^2/s, "Y" is the water depth in m, and "E" is the specific energy in m.

The transition from the 4" underdrain, which collects the excess runoff from the GI practice, into the 6" outflow pipe that is connected to the monitoring manhole has two transitions hydraulically speaking. The transitions are shown in Figure 4.10.

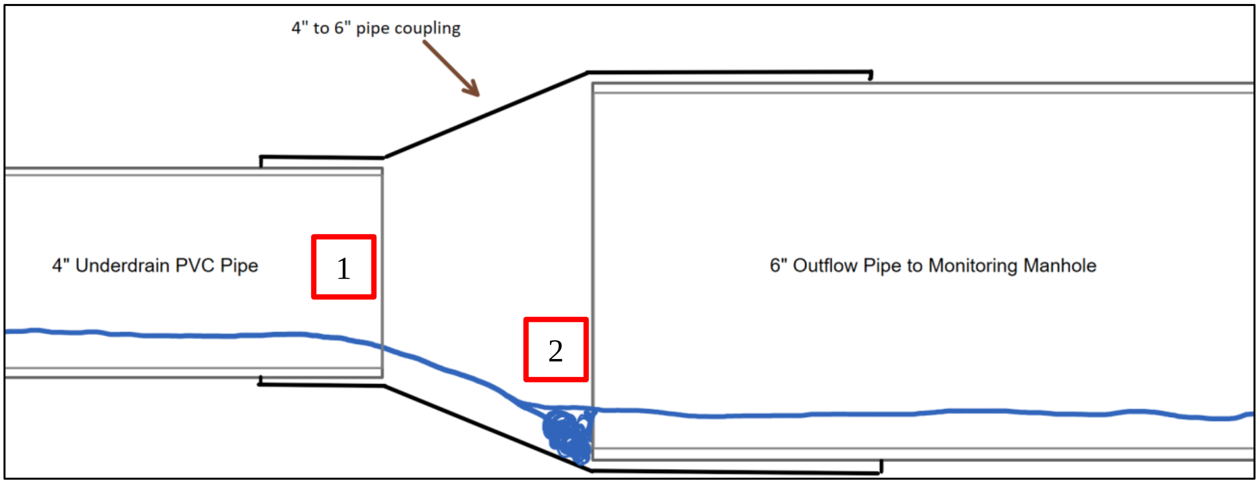

Figure 4.10: Coupling of 4" underdrain pipe to 6" lead pipe

The first transition affects the flow coming out of the 4” pipe in the way of a simultaneous downward step coupled with a channel width increase which is controlled by the coupler. The consequent change in the system’s specific energy is shown in Figure 4.11, The downward step is reflected in the rightward shift from coordinate (E1,Y1) to (E2,Y2). Simultaneously, the increase in channel width is represented by the transition from “q1” into “q2”, which is reflected in the position of (E2,Y2).

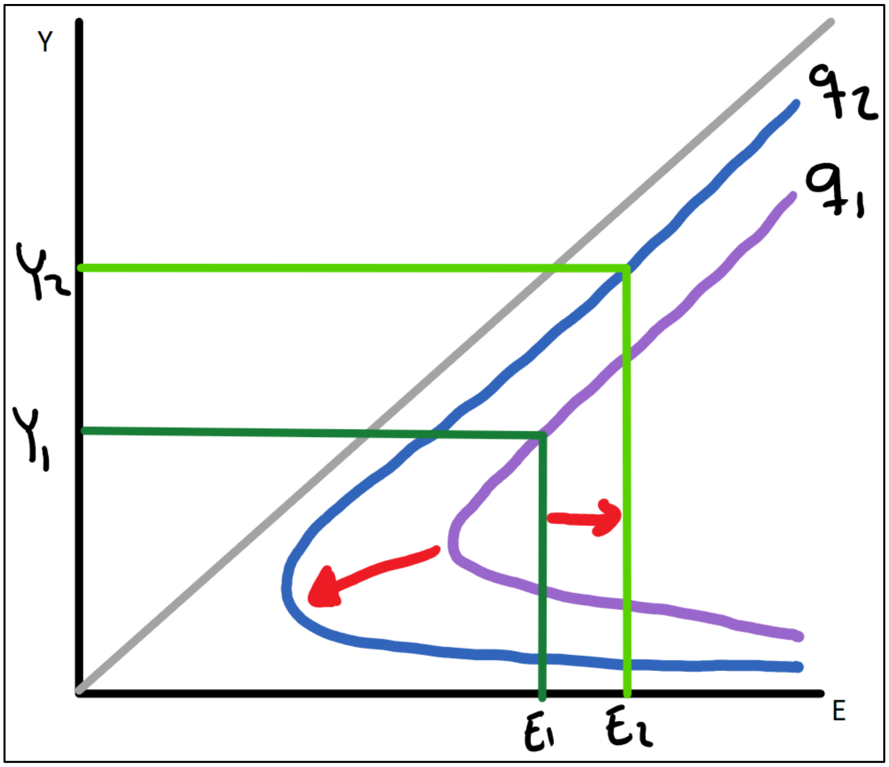

Figure 4.11: Specific energy diagram for transition between 4" underdrain pipe to coupling

The second transition occurs as soon as the flow hits the 6” pipe, there is a backwater effect that is proportional to the thickness 6” PVC pipe. This is seen by the flow as simultaneous channel width constriction and an upward step as reflected by Figure 4.12. The upward step and loss of energy due to turbulence is reflected in the leftward shift from coordinate (E2,Y2) to (E3,Y3). Simultaneously, the decrease in channel width is represented by the transition from “q2” into “q3”, which is reflected in the position of (E3,Y3).

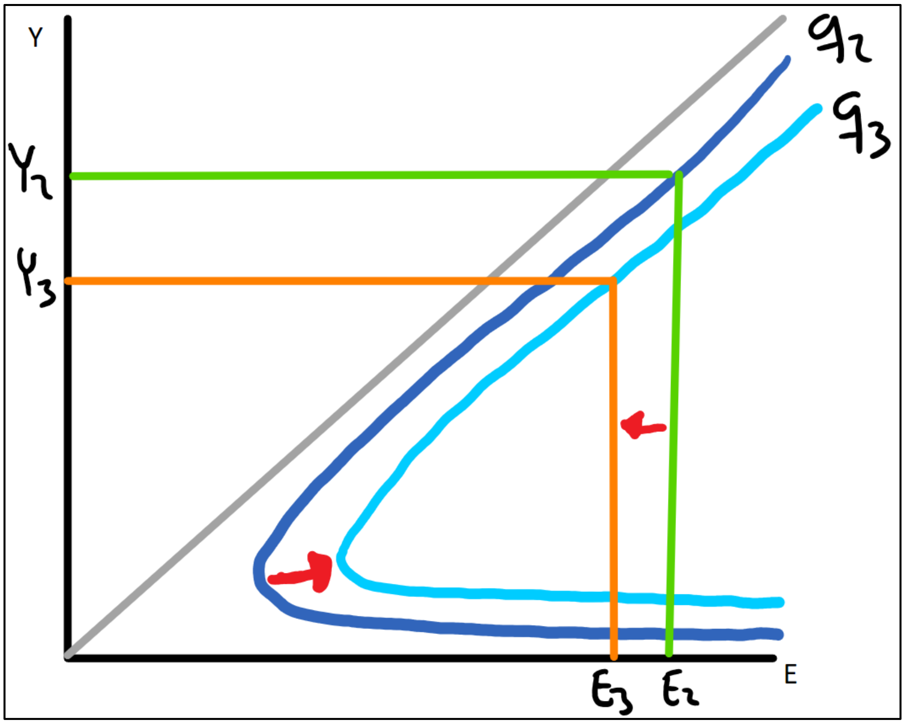

Figure 4.12: Specific energy diagram for transition between coupling and 6" outflow pipe

Before approaching the monitoring manhole, the pipe coupling transition between the 6" Outflow pipe and the 6" through channel pipe has a similar behavior to the one shown in Figure 4.13. The system has two hydraulic transitions.

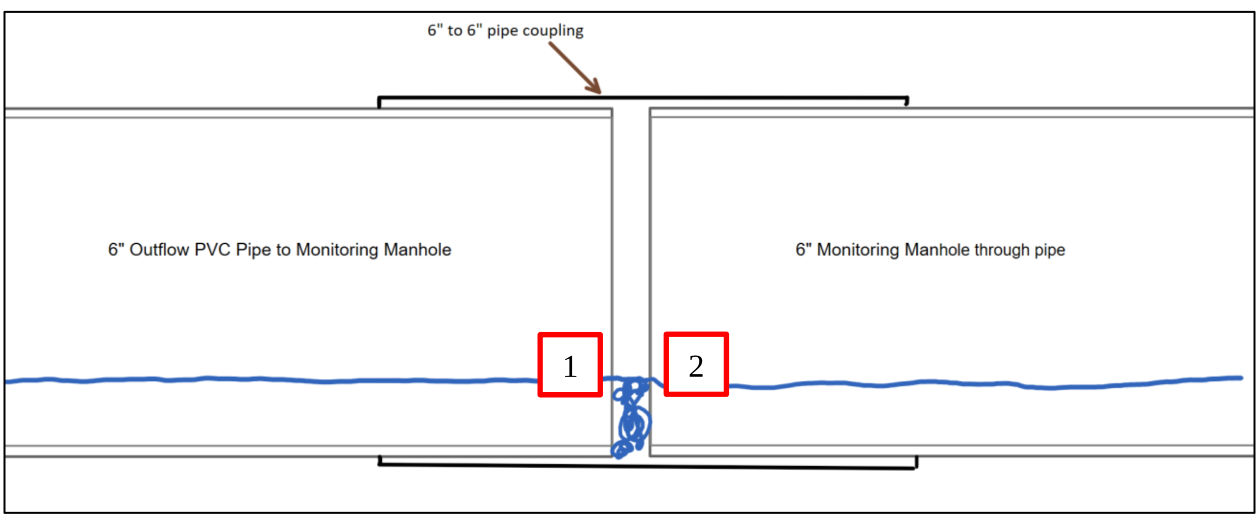

Figure 4.13: 6" Coupling of 6" Outflow pipe to 6" monitoring manhole through pipe

The first transition affects the flow coming out of the 6” Outflow pipe in the way of a simultaneous downward step coupled with a channel width increase which is controlled by the diameter of the coupler. The consequent change in the system’s specific energy is shown in

Figure 4.14. The downward step is reflected in the rightward shift from coordinate (E3,Y3) to (E4,Y4). Simultaneously, the increase in channel width is represented by the transition from “q3” into “q4”, which is reflected in the position of (E4,Y4).

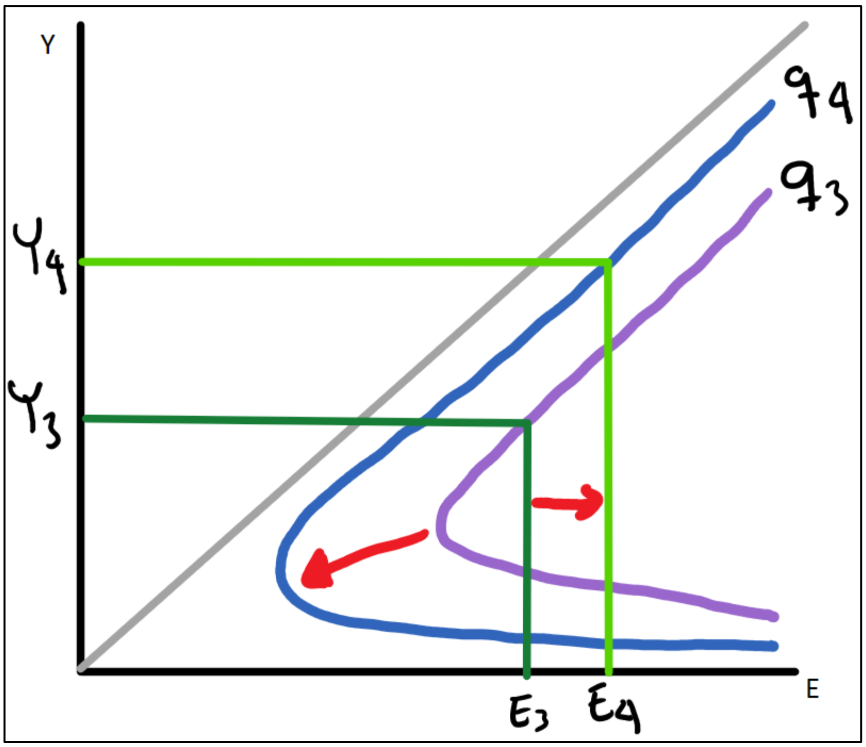

Figure 4.14: Specific energy diagram for transition between 6" Outflow pipe to coupling

The second transition occurs as soon as the flow hits the other 6” pipe. There is a backwater effect that is proportional to the thickness 6” PVC pipe. This is seen by the flow as simultaneous channel width constriction and an upward step as reflected by Figure 4.15. The upward step and loss of energy due to turbulence is reflected in the leftward shift from coordinate (E4,Y4) to (E5,Y5). Simultaneously, the decrease in channel width is represented by the transition from “q2” into “q3”, which is reflected in the position of (E5,Y5).

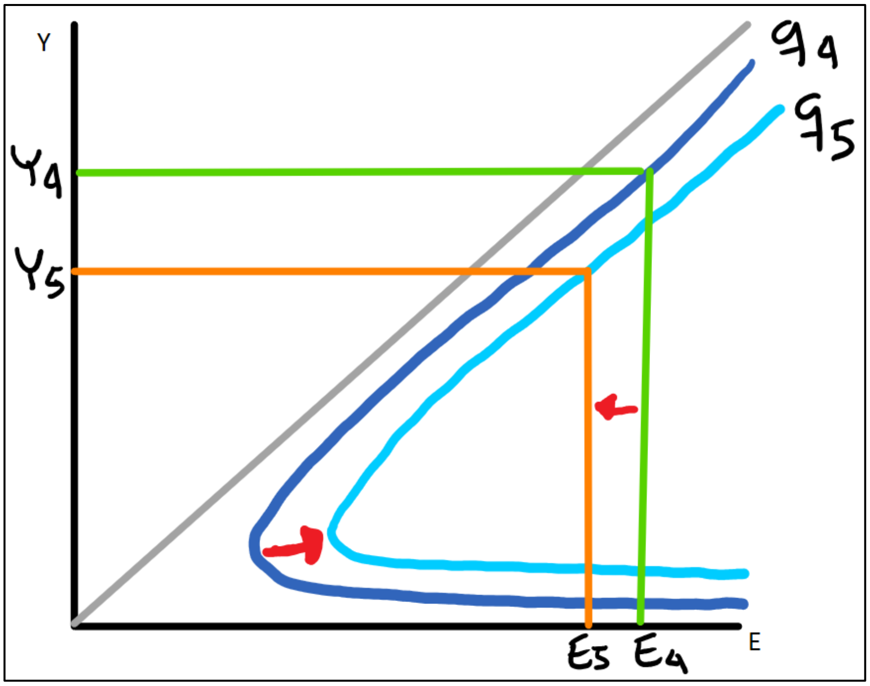

Figure 4.15: Specific energy diagram for transition between coupling and 6" monitoring manhole through pipe

4.2.2.2.2 Flow Conditions: Hydrological Investigation of Field Conditions

Each of the GI practice has differences in the approach conditions to the monitoring manhole. These can be observed in the plan view as-build drawings located in Appendix C. However, they all coincide in the approach slope which is set to 1%. The flow evaluated and the slope of the channel, will determine whether the slope is considered hydraulically mild, steep or critical (Potter, Wiggert, Ramadan, & Shih, 2012). A mild slope and subcritical flow is preferred in order to minimize the turbulence at the water level reading location.

4.2.2.2.3 Experimental Flume

To overcome the issue of properly accounting for the pipe fitting transitions and the flow approach conditions explored in the previous sections, an experimental flume device was constructed to simulate the changes in approach conditions that are encountered in the field. The conceptual design of the flume device is shown in Figure 4.16.

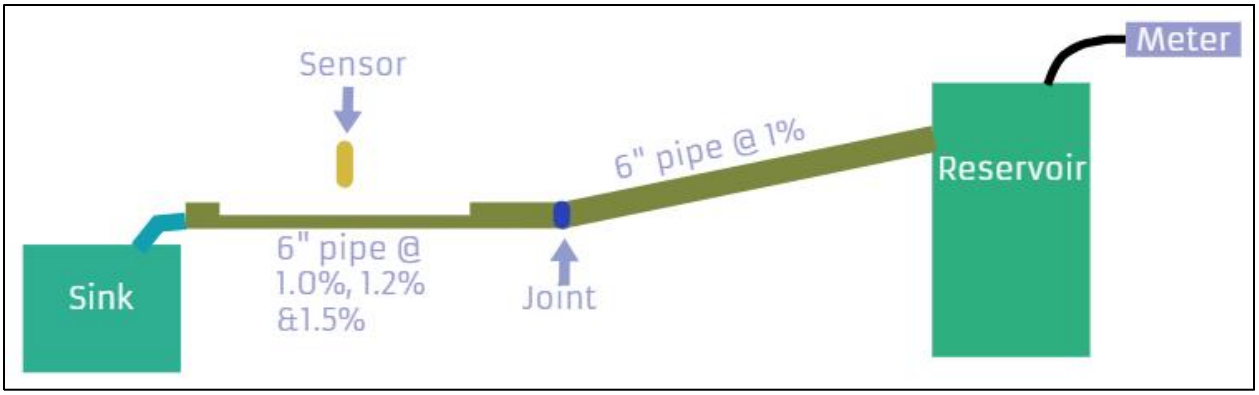

Figure 4.16: Experimental flume device conceptual design

The system will utilize a reservoir to simulate the function of the 4” underdrain pipe, which in the field collects the excess water from the practice. In the experimental flume system, the water will flow from the reservoir into the 6” solid PVC pipe. The hydrological conditions highlighted for the 4” underdrain pipe to the 6” Outflow pipe (as shown in Figure 4.10) are maintained as the constriction conditions of upward step and channel width constriction are kept in the experimental flume system. The other end of the 6” pipe is fitted into another 6” pipe that will simulate the through channel. The imperfect coupling connection in the experimental flume will simulate the channel width transitions encountered in the field as shown in Figure 4.13.

As each 6” through channel in the field has a different slope, the simulated through channel will be adjusted to match the different grades in the field. Each through channel was measured in the field to ensure that the experiment accurately recreated each flow condition. A digital level was used to measure the slopes. The three slopes tested in the experiment are summarized on Table 4.5. During each flow test, the same digital level was used to guarantee the proper slope of the experimental flume’s through pipe.

Table 4.5: Through channel slopes by practice

Practice	Slope
Structural Soil STT	1.2%
Bioswale 1	1.0%
Bioswale 2	1.5%

The flume device was devised and constructed by Paul Lightfoot, Landscape Architect of the Green Infrastructure Branch. The flume device utilizes a wooden frame which controls the slope of the 6" through pipe section where the flow sensor was placed. The sensor was carefully positioned and angled so that the sensor would capture bottom of the channel and not the sides. The sensor and its attachment device will be further discussed in Section 0. The final flume device is shown in Figure 4.17.

Figure 4.17: Experimental flume device before flow measurement experiment

4.2.2.2.4 Water Level Sensor

This study required the continuous recording of discharge data to analyze the hydrological performance of the GI practices. A non-contact sensor is recommended as outflows from the GI practices can have sediment. Over time this sediment builds-up, rendering any flow contact sensor device useless unless it is cleaned. The non-contact sensor chosen was the Toughsonic 14® (TS14) shown in Figure 4.18. This sensor is a low power consumption sensor that has IP68 certification. The resolution of this sensor is of 0.086 mm. The sensor has an optimal operating range of 3 m, a deadband of 100mm and an error of 0.2% of the target distance under stable ambient conditions (Senix Corporation, 2010, 2015).

Figure 4.18: Toughsonic 14 Sensor. Image source: The Senix Corporation®

In-house mounting attachments were designed and built by Paul Lightfoot to install the sensor, accommodate the deadband restriction, and provide a stable, consistent mounting set-up for all through channels. The attachment consists of a half PVC section, a small valve box, a rod and nuts. The attachment is shown in Figure 4.19. The vertical threaded rods accommodate the sensor's plate. This plate can be moved vertically to accommodate the sensor's deadband. The TS14 is screwed and secured to the adaptor plate by the sensor's threaded nuts as shown below.

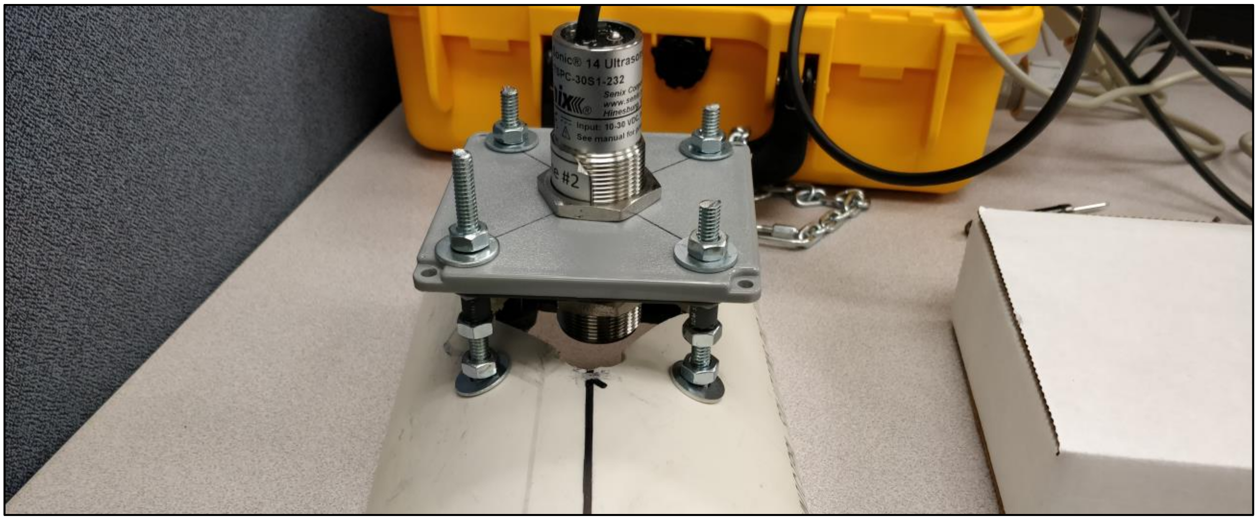

Figure 4.19: In-house built mounting attachment with TS14. Mounting attachment creation credit to Paul Lightfoot from the Green Infrastructure Implementation Branch

A data logger was used to record the readings from the TS14. A HOBO H22 Energy Data Logger® was used. A contractor (Hoskin Scientific LTD.) built the data logger box for this experiment. The box housed and powered the data logger. The final product is shown in Figure 4.20.

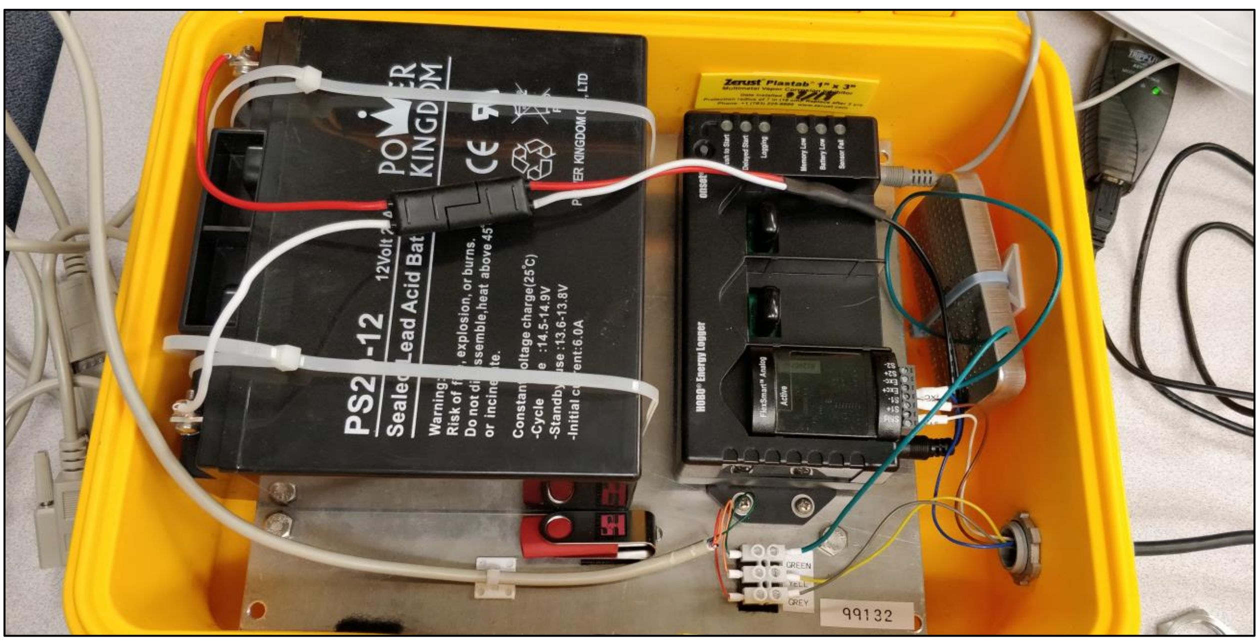

Figure 4.20: Custom-made data logger enclosure.

The mounting attachments shown in Figure 4.19 were secured in the through channels by zap straps to ensure that the attachment is held in place. The sensor top was pointed toward the lowest point of the through channel to ensure that the proper water level is recorded. The data logger box was suspended and secured by hooking the data logger box handle to a utility hook that was bolted to the PVC manhole. A zinc chain was wrapped around the handle and the utility hook as a precaution measure in case the handle falls from the utility hook. Figure 4.21 shows the sensor deployed in the field.

Figure 4.21: Flow sensor system installed in through pipe and data logger deployed in the field

4.2.2.2.5 Experimental Rating Curves

The rating curves were developed to measure predominantly low flows. For larger flows, the curves were extrapolated. The curves were developed by evaluating 16 distinct discharges. The discharges are summarized in Table 4.6 and were evaluated to understand the expected stage-discharge conditions in the system. The expected normal depths and critical depths by slope and discharge are summarized in Appendix F in Section F.1. Based on the results found, the through channel flume systems will be considered hydraulically mild slopes.

Table 4.6: Target discharges for flow experiment

Discharges	
Q (gpm)	Q (m^3/s)
0.50	3.16E-05
0.85	5.36E-05
1.00	6.31E-05
1.50	9.47E-05
2.00	1.26E-04
2.50	1.58E-04
3.00	1.89E-04
3.50	2.21E-04
4.00	2.52E-04
4.50	2.84E-04
5.00	3.16E-04
6.00	3.79E-04
7.00	4.42E-04
8.00	5.05E-04
10.00	6.31E-04
15.00	9.47E-04

The flow experiment was conducted at Manitoba Yards, one of the CoV's work yards. The flow meter used in the experiment is several years old (age unknown) and measured gallons per minute with a resolution of a single decimal place. Due to the type and age of the flow sensor device, the target flows were difficult to keep stable. This source of uncertainty will be discussed in Section 4.2.3. An industrial flexible hosepipe connected the flow meter device and the experimental flume reservoir. The hosepipe's mouth was placed at the bottom of the reservoir to avoid introducing turbulence at the mouth of the pipe as shown in Figure 4.22.

Figure 4.22: Hosepipe mouth placement in reservoir

The flow experiment was conducted based on the slope conditions of the through channel summarized in Table 4.5 and the 16 discharges shown in Table 4.6. The TS14 sensor readings were used to estimate the water level. Figure 4.23 shows a capture of the test in progress.

Figure 4.23: Flow experiment capture which shows flow width changes due to coupling transitions

In this picture, the changes in the stream width due to the coupling conditions outlined in Section 4.2.2.2.1 are noticeable, confirming the theoretical assumptions of the system. The coupling connections between the 6” pipes cause backwater conditions (possibly even hydraulic jump conditions) which are prevalent in the low flows scenarios. The transition effects from the couplings diminished as flows increased; however, the flows did become supercritical as expected which introduced turbulence. The flow sensor was placed at a distance far enough where the turbulence lessened. The sensor was also kept at a distance of at least 4x the smallest expected critical depth from the end of the pipe, where the water drops-off the experimental flume. This precaution was taken to avoid reading the drop-in water height, which is characteristic of drops. The sensor was at ~10cm from the drop. The limiting 4x critical depth distance was equal to 2cm.

The results of the stage readings and the respective flow regime based on their Froude Number are summarized in Appendix F, Section F.2. For the 1% flow scenario, the flows are predominantly subcritical until a discharge of 8gpm is reached. At this point the flow becomes supercritical. The 1.2% and 1.5% scenarios all have supercritical flow regimes.

The rating curves were based on the readings obtained in the flow scenarios tested. A power function in the form of $Y=a*(x)^b$ was fitted to all scenarios. The rating curves were optimized by minimizing the error between the measured and modelled discharges. Based on this analysis, it was determined that having a two-stage rating curve for each scenario was the best method to optimize the rating curves. The rating curve threshold for each curve was determined by trial and error utilizing the measured vs calculated discharge comparison criteria used to optimize the error. The final rating curves can be found on Appendix F in Sections F.3, F.4 and F.5.

The rating curve formula for the 1% Slope scenario, which is applicable to Bioswale 1 is shown in Equation (4.11). The error for this formula is ~4.9%.

$$\mathrm{Q}_{(h)} = \begin{cases} \mathbf{1.16E-07} * (\boldsymbol{h})^{\mathbf{2.64}}; & \boldsymbol{h} \leq \mathbf{19.7}\boldsymbol{mm} \\ \mathbf{6.22E-08} * (\boldsymbol{h})^{\mathbf{2.89}}; & \boldsymbol{h} > \mathbf{19.7}\boldsymbol{mm} \end{cases} \tag{4.8}$$

The rating curve formula for the 1.2% Slope scenario, which is applicable to the Structural Soil STT is shown in Equation (4.9). The error for this formula is ~6.7%.

$$\mathrm{Q}_{(h)} = \begin{cases} \mathbf{4.89E-06} * (\boldsymbol{h})^{\mathbf{1.75}}; & \boldsymbol{h} \leq \mathbf{14.6}\boldsymbol{mm} \\ \mathbf{1.51E-06} * (\boldsymbol{h})^{\mathbf{2.20}}, & \boldsymbol{h} > \mathbf{14.6}\boldsymbol{mm} \end{cases} \tag{4.9}$$

The rating curve formula for the 1.5% Slope scenario, which is applicable to Bioswale 2 is shown in Equation (4.9). The error for this formula is ~7.6%.

$$\mathrm{Q}_{(h)} = \begin{cases} \mathbf{8.68E-06} * (\boldsymbol{h})^{\mathbf{1.60}}, & \boldsymbol{h} \leq \mathbf{11.4}\boldsymbol{mm} \\ \mathbf{1.13E-05} * (\boldsymbol{h})^{\mathbf{1.52}}, & \boldsymbol{h} > \mathbf{11.4}\boldsymbol{mm} \end{cases} \tag{4.10}$$

4.2.3 Flow Monitoring Potential Sources of Error

There are two significant groups of potential sources of error in the flow measurement estimations that are based on the inflow and outflow estimations. The inflow estimations depend on the EPA SWMM 5.1® software and the Simple Method runoff estimations. The outflow measurements depend two constraints: the alternate flow measurement method and the TS14 sensor readings.

The inflow estimation employed for this thesis are not precise as they are estimations based on modelling. The Simple Method is known to yield fairly accurate results (CVC, 2016c, 2016b, 2016a); however, it is not an infallible tool. The EPA SWMM 5.1® is a simulation tool that uses rainfall data, and drainage properties to simulate the runoff to the GI practices. This method is a more robust tool when compared to the Simple Method formula. Nevertheless, it is an estimation tool that cannot replace field measurements.

In the outflow estimation front, the accuracy of the rating curves developed for the through channel system depend on the following factors:

- The accuracy of the flow measuring device employed during the development of the rating curve: during the tests, the readings in the flow device fluctuated, but still hovering around the target discharges. Nevertheless, a constant discharge (for each stage) was never achieved. This fluctuation means that the discharge was not steady during the state measurement readings either slightly over or under estimating the discharge.
- In hindsight, the two-stage discharge curve added two more variables to the equations without a great reduction in error. The optimization process only decreased the calculated error of each curve by a maximum of ~3% for the 1% Slope curve and under ~1% for both the 1.2% Slope and 1.5% Slope curves. This low decrease in error does not justify the inclusion of more variables that add to a process that has uncertainty already.he flow conditions in the constructed flume device are assumed to be similar to those in the field: it is impossible to confirm that each of the monitoring manholes have exactly the same pipe fitting conditions and flow behavior conditions before entering the through channel, hence, increasing the uncertainty.

The ultrasonic sensor readings are crucial to determine the stage of the flow. The manufacturer highlights the following sources of error with the device (Senix Corporation, 2010, 2015):

- Proper sensor orientation: The sensor needs to be oriented to the lowest point in the channel. Otherwise the stage recorded by the device will underestimate the real outflow in the practice.
- Recording interval. The manufacturer recommends not to set the recording interval too short. If the recording interval is too fast, the sensor may detect echoes from the previous cycle. This issue is more prevalent during cold weather, which is the condition were most of the readings will be made under. The sound absorption in cold air is lower and echoes take longer to decay.
- Temperature compensation. The sensor will not compensate for rapid temperature changes or temperature compensation between the sensor and the target. This issue is minimized if the temperature at the location of the TS14 sensor is fairly constant, which is what it is expected in the monitoring manhole system. The enclosed nature of the manhole should protect from rapid atmospheric temperature changes.
- Ultrasonic or target interference. The TS14 is an ultrasonic device that measures the distance between the tip of the sensor and the target. If obstructions are present, that is what the sensor will detect. Therefore, it is important that the sediment that builds up in the channel is cleared periodically. External sources of ultrasonic sound can change interfere with the readings of the sensor. This is a difficult aspect to control due to the location of the manhole. Quebec Street is a major arterial in Vancouver. Vehicles of all sizes transit the arterial (Vega & Lukes, 2018). The vibrations that the vehicles produce could interfere with the readings of the sensor.

4.3 Soil Monitoring

This monitoring study includes the monitoring of the soil conditions of the GI practices. One of the objectives of the monitoring program is to assess the resiliency of the GI practices to drought conditions, and the migration of salts through the cells.

The soil sensor selected to for this application is the TEROS 12®. This sensor is capable of measuring VWC, soil electrical conductivity (EC), and soil temperature (T). Figure 4.24 shows a schematic of the sensor.

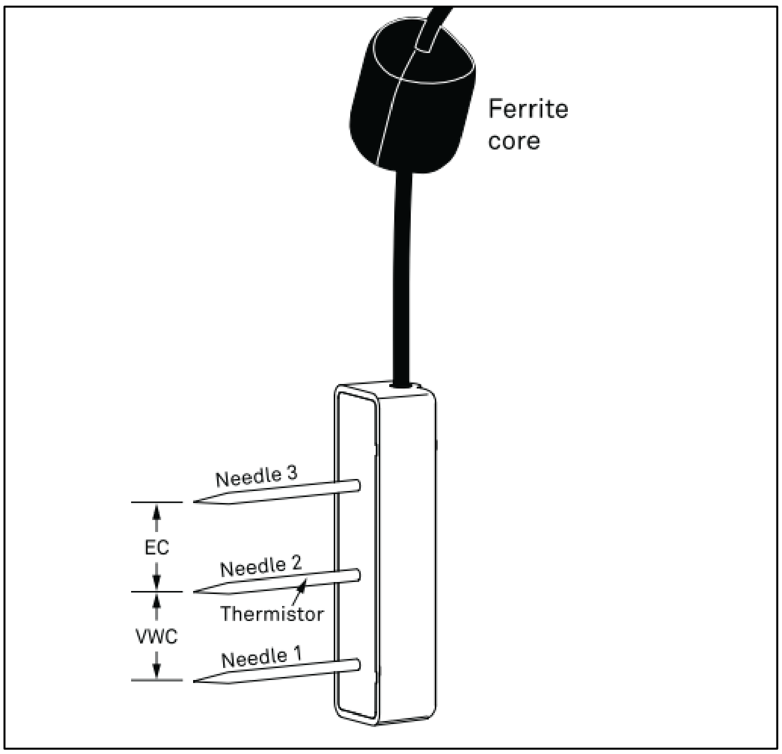

Figure 4.24: TEROS 12 schematic. Image source: TEROS 12 User Manual (Meter, 2018)

Soils have dielectric properties. The change in soil dielectric constant ε is associated with a change in soil volumetric water content (Huan, Wang, Li, & Wan, 2017). The TEROS 12® sensor measures the dielectric properties of the soil through a high frequency capacitance method. The charge time of the substrate is proportional to the dielectric properties of the material. A microprocessor inside the sensor measures the charging time and it outputs a raw value (Meter, 2018).

The volume of influence for the TEROS 12® is of 1,010 mL as shown in Figure 4.25. The soil closest to the sensor (in proximity to the probes) has the strongest influence on the readings produced. The manufacturer recommends installing the sensor in the vertical position to take advantage of the electromagnetic field of the sensor and incorporate more soil depth into the readings (Meter, 2018).

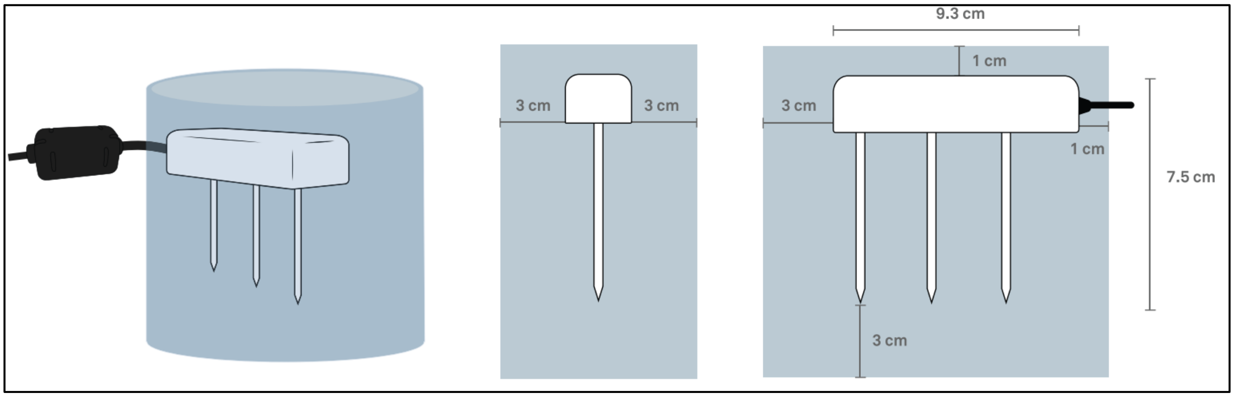

Figure 4.25: Volume of influence representation of the TEROS 12 sensor. Image source: TEROS 12 Manual (2018)

The data logger chosen for this study was the Em50®. This data logger can record up to 5 devices simultaneously and it can be deployed for several years uninterrupted. The information can be downloaded through a stereo to USB cable (Meter, 2002). The data logger was enclosed in a pelican box (model 1200) to ensure that the logger is not damaged by moisture. The pelican box was modified to connect the sensor to the data logger inside. Desiccant packs were left in each box to absorb any left-over moisture. Figure 4.26 shows the final product after being deployed in the field.

Figure 4.26: In-house made data logger box

4.3.1 Volumetric Water Content

The VWC measurements are made between needle 1 and needle 2 as shown in Figure 4.24. The raw output from the sensor is used as the input of a linear calibration equation for mineral soil, which is shown below:

$$\text{VWC} = (3.879 \text{ x } 10^{-4}\ x\ RAW) - 0.6956 \quad (4.11)$$

The TEROS 12 sensor has a mineral soil range reading of 0-70% (0.00-0.70 m^3/m^3) with an associated resolution of 0.1% (0.001 m^3/m^3) and an error of ±3% (0.03 m^3/m^3) by default calibration. It is important to highlight that the standard calibration equation is only valid for soils with EC < 8 dS/m saturation extract. The TEROS 12 sensor is not as sensitive to variations in changes in soil textures and EC because the sensor runs at a high frequency of 70M Hz (Meter, 2018). Sensors capable of producing higher resonance frequencies tend to produce more accurate volumetric water content measurements (Huan et al., 2017).

4.3.2 Electrical Conductivity

Electrical conductivity is the ability of a material to conduct electricity. In soils, EC varies by factors such as the water-holding capacity (water held by the soil pores), cation exchange capacity (CEC), porosity, temperature and salinity. Typically, sands have low conductivity and clays have high conductivity. For this study, soil salinity is of interest as an excess of dissolved salts from the stormwater runoff will affect EC of the soil. The standard units of measurement are milliSiemens per meter (mS/m). In soil, EC capable sensors measure bulk EC (EC_b) and readings are reported deciSiemens (dS/m). (Grisso, Mark Alley, Holshouser, & Thomason, 2009).

The EC_b measurements are made between needle 2 and needle 3 (shown in Figure 4.24) by applying an electrical current to the two electrodes. The EC_b measurements are later normalized to a temperature of 25 °C. The range of readings for these sensors is from 0-10dS/m, which is appropriate for most soil applications. The resolution of the sensor is of 0.001dS/m with a ±5% error of measurement (Meter, 2018). The manufacturer warns that for EC_b readings above 10dS/m, any contaminants in the needle, skin oils for example, will affect the results (Meter, 2018). Care was given to ensure that hands did not touch the needles during handling and installation of the sensors.

4.3.3 Temperature

The TEROS 12 sensor calculates the temperature in an embedded thermistor in Needle 2 (Figure 4.24). Thermistors are rugged, inexpensive sensors (Campbell & Frascarelli, 1981). The thermistor in the TEROS 12 can provide readings ranging from -40 to 60°C with an accuracy of 0.1°C and a measurement error of ±1°C (Meter, 2018)

4.3.4 Soil Sensor Installation

The soil sensors were installed at two of the three monitoring locations. The sensors were placed in a vertical orientation as shown in Figure 4.24. The sensors we placed at different depths. The spacing between the sensors was determined by using Figure 4.25 as a reference to avoid sensor interference. The final spacing was determined to be 20cm.

4.3.4.1 Structural Soil Cell

The installation soil sensors in this medium proved to be challenging. The challenges identified were:

- Damage of soil sensor needles or housing due to surrounding aggregate
- Damage of soil sensors from shovel equipment when back filling
- Sensors need to be installed in a soil pocket
- Surface compaction crushing the sensors
- Soil sensor cables damaged during installation and compaction
- Minimize alterations of structural soil medium to ensure representativeness of the rest of the structural soil conditions.

The soil sensors at this location were installed on May 31, 2018 in coordination with the CoV construction crews. The crews left a small area for the installation of the sensors (shown below). A horizontal 1” PVC pipe was left by the CoV crews to bridge the sensors cables over to the cable box located on the grass sections of the sidewalk as shown in Figure 4.27 and Figure 4.28.

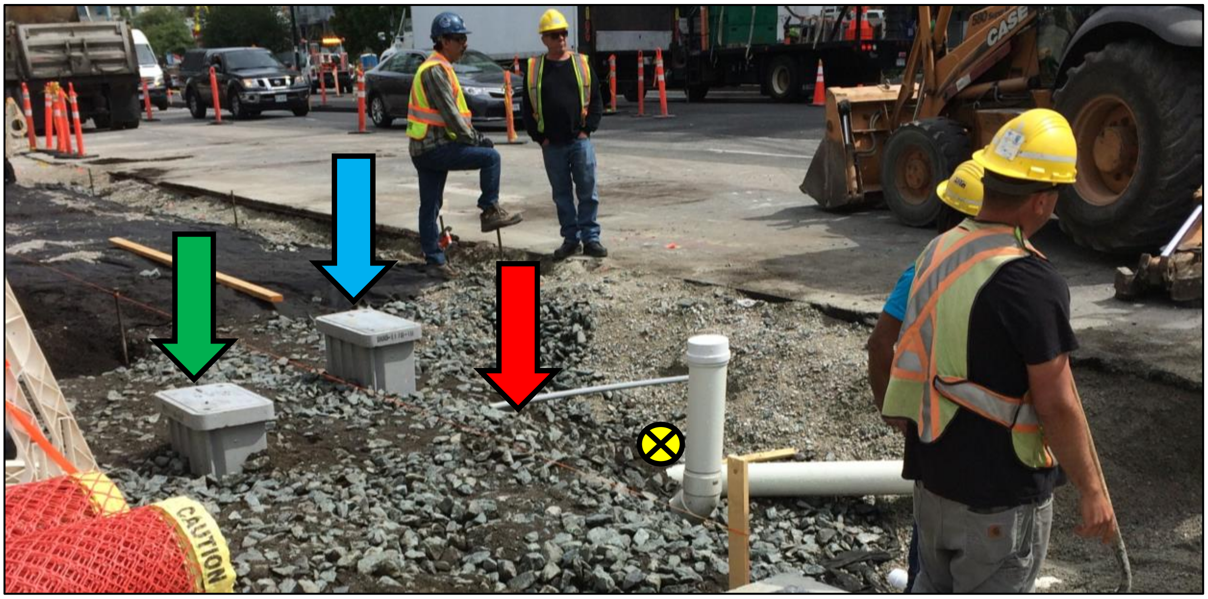

Figure 4.27: Soil sensor installation location. The yellow cross shows the approximate location where the sensors were installed. The green arrow shows the location of the valve box where the data logger was housed. The red arrow shows the 1" PVC pipe left by the CoV. Image source: GI Branch.

Figure 4.28: Assessment of the conditions for the soil sensor installation. The horizontal 1" PVC pipe in the picture was left by the CoV crews as a protection bridge to guard the soil sensors cables to the valve box.

To ensure the integrity of the sensors, it was determined that surrounding the sensor with the soil blend medium will provide enough protection from sharp edges in the surrounding aggregate and the weight column from above the sensor. A flat base was made for each sensor which consisted on utilizing flat rocks acting as a table. Soil was placed in top of the flat surface and the sensor was placed vertically as shown in Figure 4.24. Soil was packed around the sensor acting as a soil housing. Structural soil (aggregate and soil mix) was placed outside the soil housing. The ferrite core was offset by a few centimeters adjacent to the sensor, but within the soil housing.

The cables of the sensors were protected using a 40cm 3/4" PVC pipe. Holes were cut and drilled on the pipe relative to the depth location of the sensor. The stereo plug ends of the sensors were slipped into the holes during the installation of each sensor as shown in Figure 4.29.

Figure 4.29: Installation of second soil sensor at a 40cm depth. The cables of the soil sensors were slipped into the holes in the PVC pipe for protection. 1" PVC pipe left by CoV crews

All the sensors were installed using the aforementioned procedure. The soil sensor cables were later pulled through a 1” PVC elbow that was connected to the 1” PVC bridge left by the CoV crews as shown Figure 4.30. Rocks were placed under the 1” PVC bridge pipe to ensure that the surface loads will be better distributed around the circumference of the pipe. The CoV crews continued the construction of the structural soil cell, including the compaction of the 19mm clear crushed base. The sensors were tested again on June 4, 2018 using the ProCheck kit. The three sensors showed positive signs and readings that they are intact and survived the installation process.

Figure 4.30: Final product. The soil sensor cables were pulled through to the valve box where the data logger installation location.

4.3.4.2 Bioswale 1

Two soil sensors were installed at this location on July 19th, 2018. The sensors were pushed into the soil at the desired elevations. The cables were protected by utilizing the same method as the structural soil: utilizing a 1” PVC pipe to conduct the cable into the composite valve box that houses the data logger box. The sensors were installed at depths of 20cm and 40cm as shown in Figure 4.31.

Figure 4.31: Installation of soil sensors in Bioswale 1

4.4 Water Quality Monitoring

The monitoring of water quality is an important component of this thesis. Section 2.1.3 explored the level of pollutants in receiving waterbodies and their impact. The literature review on GI highlights how GI can be used as a water quality treatment unit in order to protect urban watersheds. Water is treated through the infiltration process and the pollutant uptake by the vegetation in the practice. All the practices considered in this study will be monitored for water quality.

4.4.1 Sampling Locations

Water quality samples were obtained from the inflows to the GI practices and the outflow of the practices.

The inflow samples for the structural soil STT were obtained from the GICB directly. The tubing was lowered into the CB and left at approximately the same level as the feeder pipe opening. The sampling is shown in Figure 4.32.

Figure 4.32: ISCO® 3700 sampler deployed at structural soil STT for inflow sampling

The stormwater enters the bioswale practices through the inlet curb openings. The water quality samples were taken from the water that drops directly into the sediment pad as shown in Figure 4.33. The PVC tubing was secured in place using rocks. Figure 4.34 shows a close-up of the process at the sediment pad.

Figure 4.33: ISCO® 3700 sampler deployed at Bioswale 1 for inflow sampling

Figure 4.34: PVC tubbing hose secured by rock. Rocks are also used here to pool water at the hose inlet to improve suction

The outflow system of both the structural soil STT and the bioswales is identical. They all have a monitoring manhole that is connected to the underdrain. The water quality samples were obtained directly from the through channel as shown in Figure 4.35.

Figure 4.35: PVC tubbing sapling from the through channel in the monitoring basin

4.4.2 Sampling Method

The sampling method chosen for this water quality study is a time weighted composite sampling. To collect the samples, two ISCO® automated samplers were used to pump and collect the stormwater. The samples were combined into a 10L Nalgene® bottle for compositing. A well-mixed sample of this composite were poured into a 1L pitcher in order to distribute the stormwater into the laboratory sample containers. A third-party laboratory in Richmond called CARO Labs. independently analyzed the samples. The samples were delivered within a one to two-hour window to the laboratory. The samples were transported in a cooler with cooling packs. The samples were collected in 5-minute intervals. The sampling process was held over a period of two hours, which could be at any point in time during the storm.

The automated samplers used were an ISCO® 3700 Sampler and an ISCO® 6712 Sampler. Both samplers have 24 plastic bottles in the carrousel. The ISCO® 3700 Sampler was used for inflow samples only and the ISCO® 6712 Sampler was used for outflow samples only.

All the equipment utilized per storm event (including the bottles and tubbing) was rinsed with tap water to avoid cross contamination. One blank sample of distilled water was conducted per ISCO® sampler to assess the background contamination of the samplers.

4.4.2.1 Sampling Method Collection Constraints

The time weighted composite sampling method was chosen due to space and budget constraints. The monitoring manhole chosen was small enough to fit in the boulevard spaced and large enough to house the flow monitoring equipment and allow the ingress of a single person. A larger manhole was not allowed by the CoV due to conflicting surface uses of the boulevard. To be able to perform a more academically sound method such as the flow weighted sampling, the automated samplers would have to be installed in the monitoring manhole permanently. More robust water quality studies utilize flow weighted compositing to determine Event Mean Concentrations (EMC) and total loadings. With the absence of a permanent water quality device, the water quality acquisition could only occur during business days and hours as per CoV employee policies, hence the short 2-hour collection window.

In addition to the space constraints, the flow weighted composite sampling requires the addition of a flow measuring device compatible with the automated samplers. The brand of available automated samplers, ISCO®, only allows flow samplers that are of the same brand. The budget for this monitoring study was not large enough to afford such modules.

4.4.3 Water Quality Parameters

The pollutants of interest are those that are typically found in urban stormwater runoff. This monitoring study will sample for the following parameters:

- Suspended sediment was evaluated in the form of TSS
- Nutrients
    - Nitrogen was broken down by type. Both nitrate, nitrite, total Kjeldahl nitrogen and total nitrogen (calculated based on all the forms of nitrogen)
    - Phosphorus was evaluated as total phosphorus (TP)
- Total carbon. This was evaluated in the form of total organic carbon and total inorganic carbon. Of special interest is TOC. This was used as a guide to measure the levels of hydrocarbons and other sources of organic material in the stormwater and the outflow samples. Specific hydrocarbon testing was not completed
- pH, DO and conductivity should be taken in the field, however, the equipment to perform field measurements was not available for this study
- Total Metals. The metal concentration to be reported by the laboratory is determined by the Inductively Coupled Plasma Mass Spectrometry (ICPMS) method. This method yielded the concentration of a wide array of metals. However, the metals of interest are Al, Cad, Cu, Fe, Ni, Pb, and Zn

The water quality parameters tested were compared on a concentration basis: inflow vs outflow. At the same time, the most stringent water quality guideline was used to compare against the water quality parameters of interest discussed in 2.1.3.6.

Chapter 5: Monitoring Study Results and Discussion

This chapter will present the water quantity and water quality results of the monitoring program. Each section will introduce the results by category and a small discussion will follow the presentation of the results.

5.1 Water Quantity Results

This section of the thesis will focus on the hydrological performance and soil moisture levels of the three practices of interest for this thesis.

5.1.1 Rainfall

The rain gauge became operational in August of 2018. Since that period, the rain gauge monitored 59 storm events that fell under the storm definition umbrella of this thesis: ≥2mm precipitation, ≥2-hour duration and ≥6 hours of ADP. Each storm event was identified by a unique identifier code that consisted on the year, month, date and initial hour of precipitation. On top of this, the duration, ADP and maximum 5-minute rainfall intensity (mm/h) was calculated for each storm. This thesis is aimed to provide useful information for the CoV engineers and planners, so each storm was categorized according to CoV's IRMP (City of Vancouver, 2016b) storm definitions. Table 5.1 summarizes the three event categories, which have a 24hr duration.

Table 5.1: City of Vancouver rainfall categories

Event Category	Event Rainfall
Normal	≤ 24mm
Large	>24mm & ≤ 48mm
Extreme	> 48mm

Table 5.2 summarizes all the events considered in this study. The events were classified first by the categories and later categorizes by month as shown in Table 5.1. The storm classification study found that during the months from August of 2018 to February of 2019, 86%

of the total events fall under the large category (48mm or less), which is very close to the 90% estimation made by the IRMP of the CoV. A total of 8 events were classified as extreme where 5 of those fell between the months of November and December of 2018. The average storm duration for the extreme events was 34 hours with a maximum intensity and total rainfall of 15mm/h and 75mm respectively. A total of 13 events were classified as large which were concentrated between the months of October to January. A total of 38 events were considered normal events which were mostly spread between the months of September to December.

Table 5.2: Rainfall event summary from August 2018 to February 2019 by category and by month

Category by Month	Storm Count	Storm Count (%)	Total Rainfall (mm)	Average Total Event Rainfall (mm)	Maximum Storm Intensity Average (mm/hr)	Storm Duration Average (h)
Extreme	**8**	**14%**	**600**	**75**	**15**	**34**
Jan-19	1	2%	99	99	12	43
Sep-18	1	2%	55	55	18	19
Oct-18	1	2%	52	52	18	33
Nov-18	3	5%	210	70	14	39
Dec-18	2	3%	185	92	14	29
Large	**13**	**22%**	**470**	**36**	**10**	**22**
Jan-19	3	5%	109	36	10	25
Feb-19	1	2%	45	45	6	32
Sep-18	2	3%	67	34	9	28
Oct-18	2	3%	78	39	21	11
Nov-18	1	2%	36	36	9	16
Dec-18	4	7%	135	34	8	22
Normal	**38**	**64%**	**308**	**8**	**6**	**10**
Jan-18	3	5%	41	14	7	20
Feb-19	4	7%	29	7	6	7
Aug-18	1	2%	3	3	3	6
Sep-18	7	12%	50	7	8	10
Oct-18	7	12%	65	9	8	10
Nov-18	7	12%	43	6	5	9
Dec-18	9	15%	77	9	5	11
Total	**59**	**100%**	**1,377**	**23**	**8**	**16**

5.1.2 Runoff

Section 4.2 describes the process and equations utilized to estimate the runoff for this thesis. The flow monitoring equipment was installed on November 8, 2019. All the flow data collection ceased on February 25, 2019. A total of 35 rainfall events were considered during this time interval. The month of February 2018 had snowfall events mixed rainfall precipitation. Those events were identified and excluded in the analysis as the rain gauge used for this study was not heated therefore the mass balance could not be performed accurately. Due unforeseen backwater conditions in Bioswale 1 and sensor errors in Bioswale 2, the flow data collected from these practices was not utilized. The raw data for Bioswale 1 and Bioswale 2 is shown in Appendix G and Appendix H respectively. The results discussed hereafter in this section will be for the structural soil STT.

The primary runoff estimation was completed by using the SWMM® models developed for each catchment. The models can be found in Appendix I, Section I.1. The results of each hydrograph utilized in this analysis can be found in Appendix I, Section I.2.

Figure 5.1 shows an example of the final product of the SWMM® model, the rating curve outflow estimation and the rainfall measurements. For this event in particular, the total modelled runoff equaled 2,793 liters entering the practice and 989 liters exiting the practice. The stormwater volume reduction performance was calculated utilizing Equation (4.1). The calculated performance for this event was ~65%.

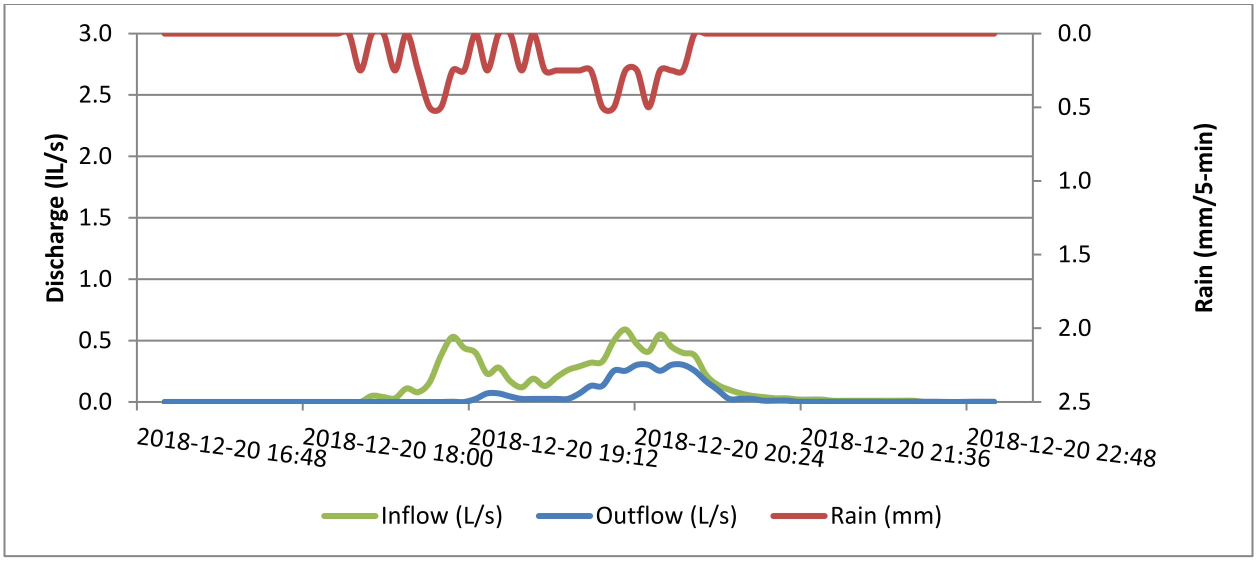

Figure 5.1: December 20, 2018 event. SMWW estimated inflow, rating curve calculated outflow and measured rainfall

Each storm event was checked with the Simple Method. All of the Simple Method checks can be found in Appendix I, Section I.3. Table 5.3 summarizes the average difference between the SWMM model for the structural soil STT and the Simple Method Calculation. The large event category has one event that has a difference of 579% in the Simple Method check. This has to do with the particular circumstances of the event, where the Simple Method is over estimating the runoff produced. For consistency, the SWMM ® model values were utilized only. This event set aside the average difference would be at 5%, similar to the other categories.

Table 5.3: Error between SWMM ® and Simple Method by event category

Event Category	Total Inflow Difference Check
Normal	5%
Large	77%
Extreme	5%
Average	29%

Figure 5.2 summarizes the total volumes treated from November of 2018 to February of 2019 by the structural soil STT. The figure also shows the average volumes treated by event category with a confidence interval (CI) of 95%. During this period, the STT practice treated a total of 35 storm events with a modelled runoff volume of 363,135 liters. A total of 116,203 liters were returned to the stormwater sewer system from the underdrain.

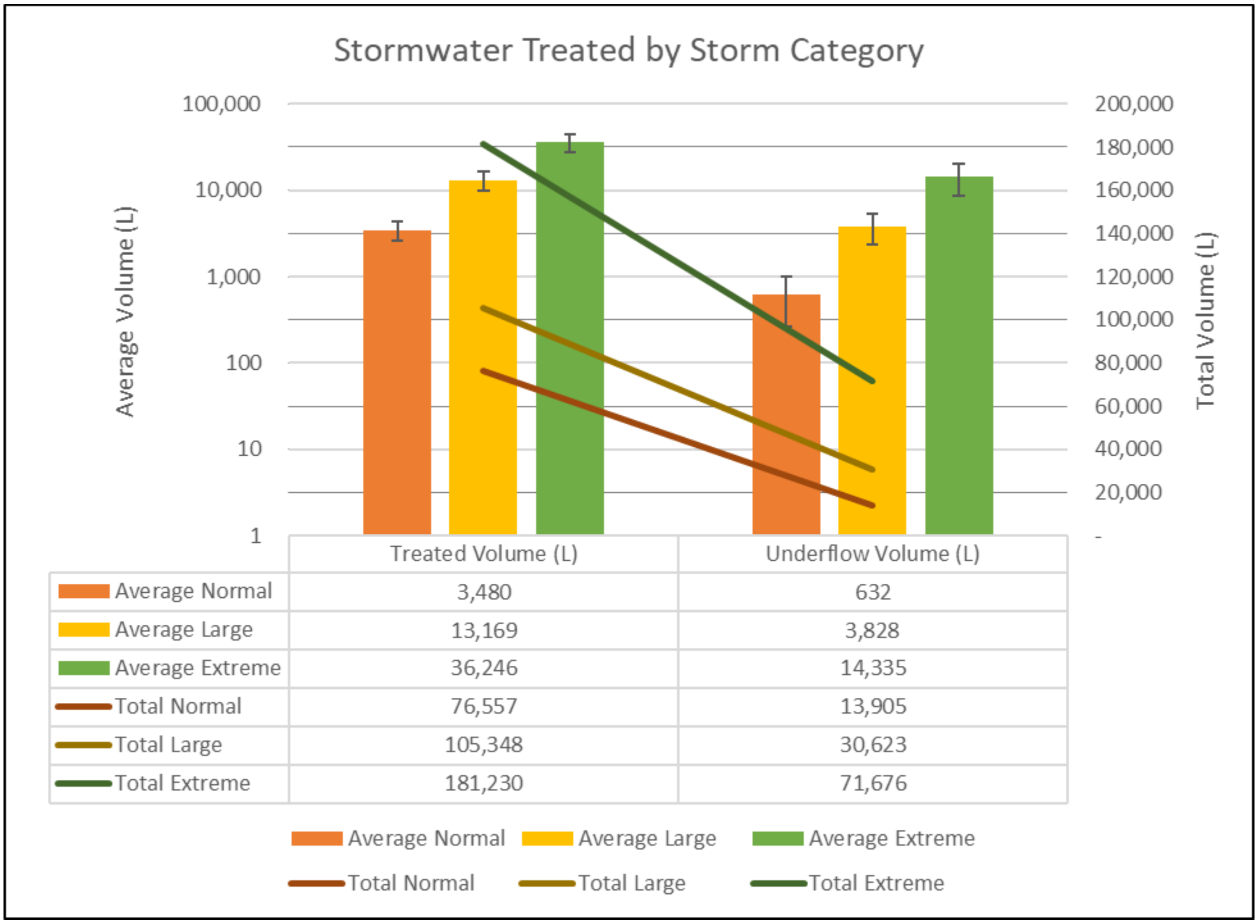

Figure 5.2: Volumes of stormwater treated by structural soil STT

The average stormwater volume reduction results can be found on Figure 5.3. On average and with all events considered, the structural soil STT has a volume reduction of 74% ± 5% (CI 95%). The normal event categories have the highest performance with a reduction of 87% ± 6% (CI 95%). The lowest performance was attributed to the extreme event category with a volume reduction of 62% ± 10% (CI 95%). The large event category has an average of 72% ± 7% (CI 95%).

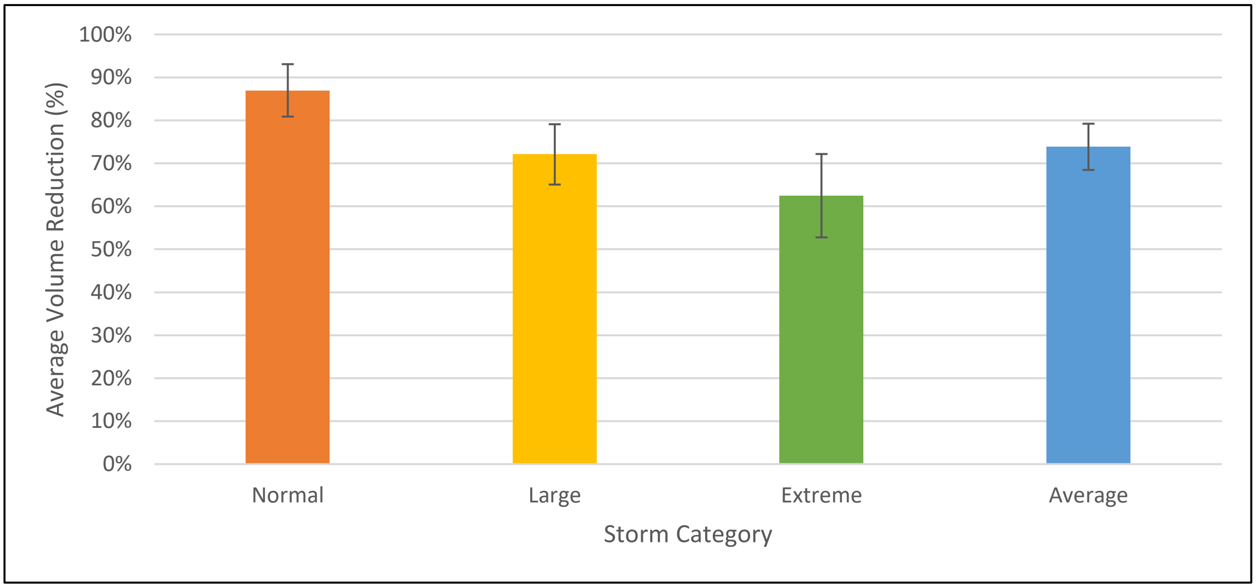

Figure 5.3: Stormwater Volume Reduction with CI of 95%

It is important to mention that the biggest caveat of this analysis is the estimation process of the inflow modelling. Under no circumstances, models can replace field measurements. Based on field observations there were instances of stormwater bypass during large events depending on the rainfall intensity and ADP. With a higher degree of certainty, there was bypass during the extreme rainfall events as the STT practice was designed for the 48mm event. The implications of this stormwater bypass on the stormwater volume reduction calculations is that the volume efficiencies shown in Figure 5.3 would be smaller for the extreme and large events as the stormwater that bypassed would be discounted from the denominator of Equation (4.1).

5.1.3 Peak Flow

Section 4.2 describes the process and equation utilized to estimate the peak flows for this thesis. The primary peak flow estimation will be done by using the SWMM® models developed for each catchment and the measured outflows. The models can be found in Appendix I, Section I.1. Similarly, to the runoff estimations, it is important to have checks hence the decision to utilize the Rational Method to corroborate the peak flow estimated by the SWMM® models. The results of each hydrograph utilized in this thesis can be found in Appendix I, Section I.2.

The peaks simulated inflow and measured outflow peaks of each hydrograph were utilized to calculate the peak flow reduction. The magnitudes were estimated directly from each hydrograph. A spreadsheet tool was developed to interactively and in real time select the peak points of interest. Only one inflow peak and one outflow peak belonging to the same rainfall cluster were utilized to perform the calculated of each storm event.

For example, Figure 5.4 shows the modelled inflow, measured outflow, measured rainfall, and utilized peak flow data points. For this event in particular, the total modelled runoff equaled 14,772 liters entering the practice and 3,314 liters where measured exiting the practice. This event has 6 distinct peak flows, however only one was utilized. In this case, the highest inflow peak flow was utilized as the reference point. The outflow peak corresponding to the inflow peak previously selected will be used. The stormwater peak flow reduction performance was calculated utilizing Equation (4.2). The calculated performance for this event was ~64%.

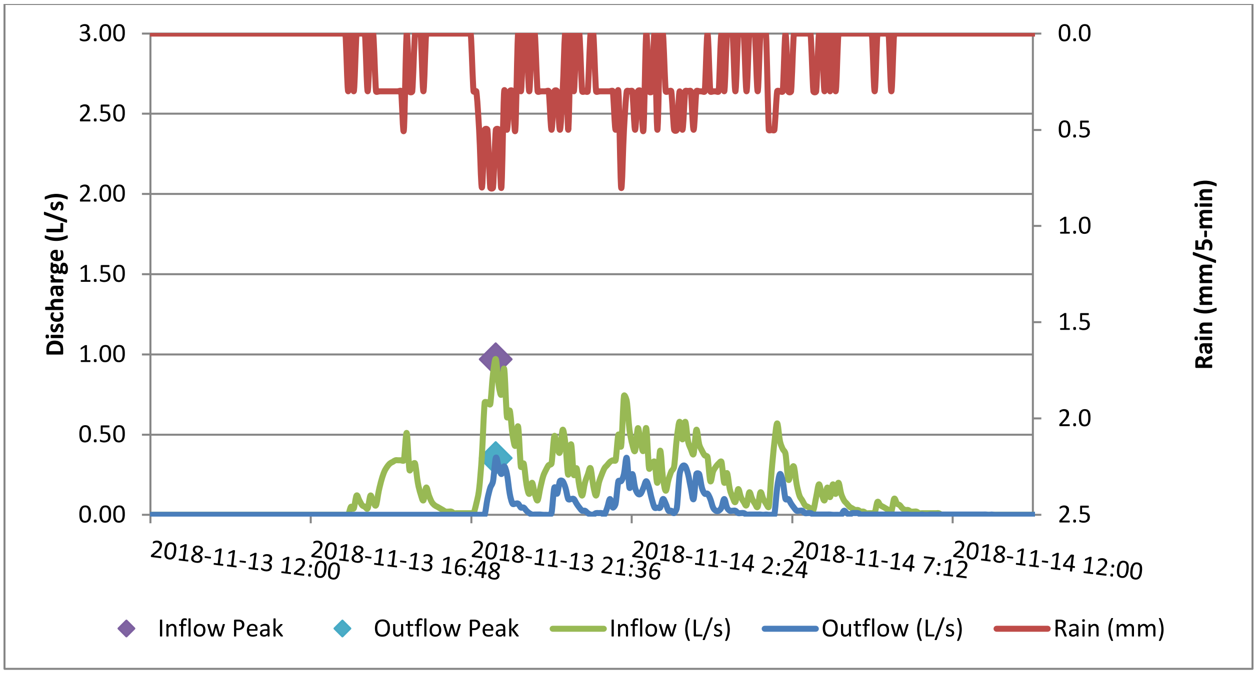

Figure 5.4: November 13, 2018 rainfall event. Only peak flow components shown.

In the case where there are multiple inflow peaks of similar magnitude the highest outflow peak will be used as a reference. In the November 21, 2018 case, there were three inflow peaks of similar magnitude, but there was one clear outflow peak higher than the others, so it was determined that the 3rd highest peak will be used in the calculation as shown in Figure 5.5. The total modelled runoff equaled 22,896 liters entering the practice and 3,799 liters were measured exiting the practice. The stormwater peak flow reduction performance for this event was ~61%.

The average error per event category was calculated, similarly to the runoff volume estimation section. Table 5.4 summarizes the average difference between the SWMM model for the structural soil STT and the Rational Method calculation.

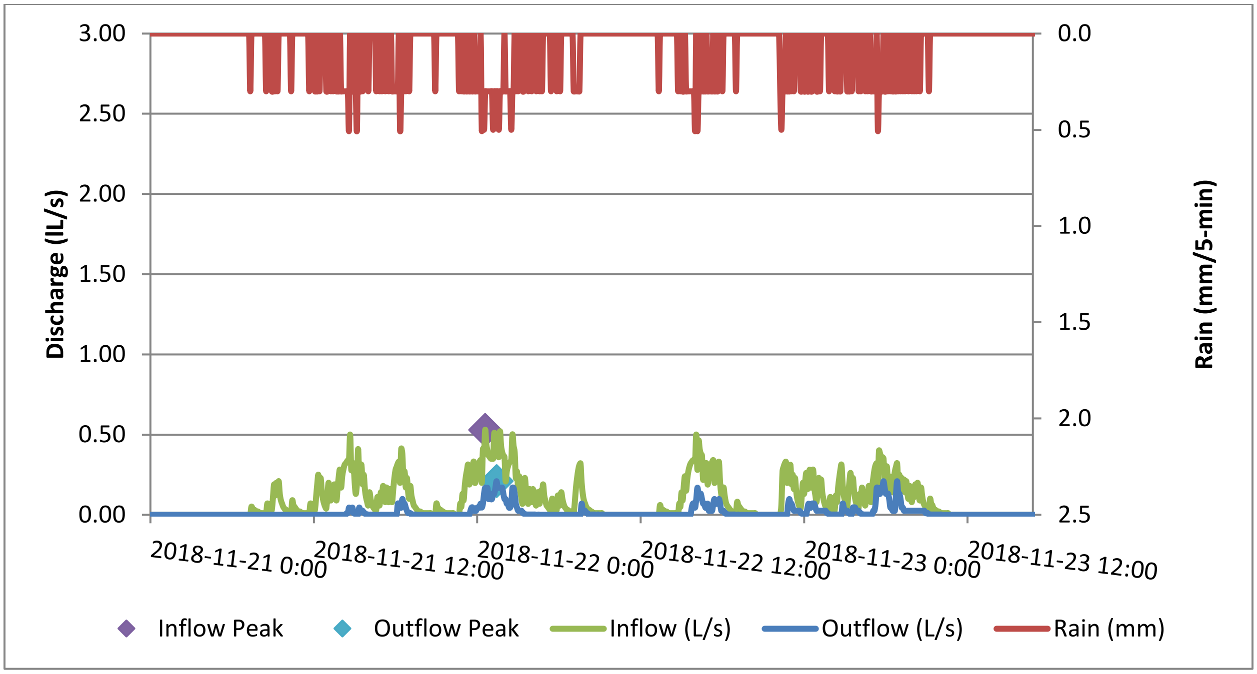

Figure 5.5: November 21, 2018 rainfall event. Only peak flow components shown.

For consistency, the SWMM ® model values were utilized in the peak flow calculations. The discrepancies between the model and the Rational Method often were because the Rational method only utilizes the peak rainfall intensity (mm/h) to estimate the peak flow. However, this method oversimplifies overall rainfall pattern of the storm and the catchment morphology. These considerations will affect the true peak of an event. Nevertheless, the SWMM ® model estimated peak flows often concurred with the Rational Method estimations. The Rational Method checks can be found on Appendix I, Section I.3.The average error of this estimation process was around 24%.

Table 5.4: Error between SWMM ® and Rational Method by event category

Event Category	Peak Flow Difference Check
Normal	35%
Large	26%
Extreme	12%
Average	24%

The average peak flow reduction results can be found on Figure 5.6. On average and with all events considered, the structural soil STT has a volume reduction of 63% ± 6% (CI 95%). The normal event categories have the highest performance with a reduction of 74% ± 9% (CI 95%). The lowest performance was attributed to the extreme event category with a volume reduction of 55% ± 4% (CI 95%). The large event category has an average of 60% ± 6% (CI 95%).

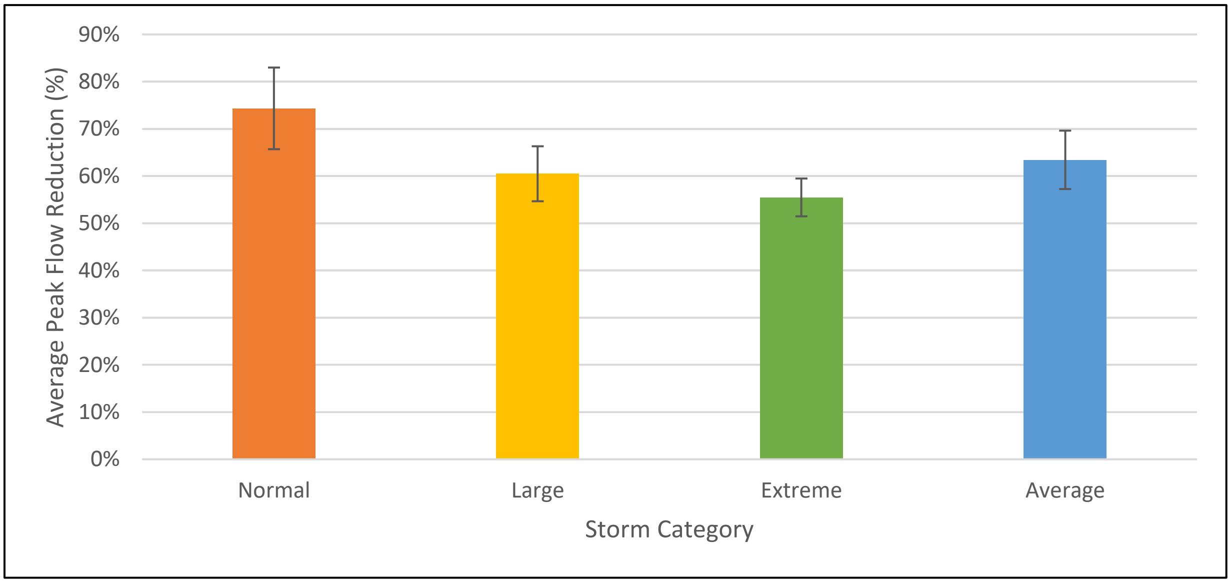

Figure 5.6: Peak flow reduction with a CI of 95%

It is important to mention that the biggest limitation of this analysis, just as with Section 5.1.2, is the estimation process of the inflow modelling. The bypass conditions observed in the field will affect the results of the peak flow reduction. The implications of this stormwater bypass on the peak flow reduction calculations is that the efficiencies calculated in Figure 5.6 would be smaller for the extreme and large events, similar to the stormwater runoff calculations. This is because the stormwater that bypassed would be discounted from the denominator of Equation (4.2). The inflow peak would be smaller, hence decrease in the efficiency.

5.1.4 Time to Peak (Lag Time)

Section 4.2 describes the process and equation utilized to estimate the lag time calculations for this thesis. Similar to the other performance calculations, the SWMM® models developed for each catchment were used, more specifically, the inflow's time stamp. The time stamp of the measured outflows will be utilized in the calculation as well. The models can be found in Appendix I, Section I.2. The spreadsheet tool mentioned in Section 5.1.2 and 5.1.3 contains a time stamp selection feature to interactively select the desired inflow and outflow time stamps based on the hydrograph.

The lag time calculation process is best exemplified with the December 12, 2018 rainfall event. Figure 5.7 shows the modelled inflow, measured outflow, measured inflow, peak flow and lag time data points for this event. This event had a total modelled runoff that equaled 49,140 liters entering the practice and 23, 339 liters where measured exiting the practice. This event had three distinct rainfall clusters. The first cluster was not accounted for as no consequential underdrain outflow was observed. However, the second cluster (the bulk of the storm) does show underdrain outflow. Therefore, this cluster was utilized in the lag time calculations. The stormwater lag time performance calculation utilized Equation (4.3). This event had a lag time of 2.7 hours before any stormwater reached the stormwater sewer network.

The lag time calculations methods did not have any checks as the SWMM® models were the only runoff estimation method that provided the necessary timestamps to perform the calculations. Therefore, the process described in this section relies completely in the accuracy of the SWMM® models.

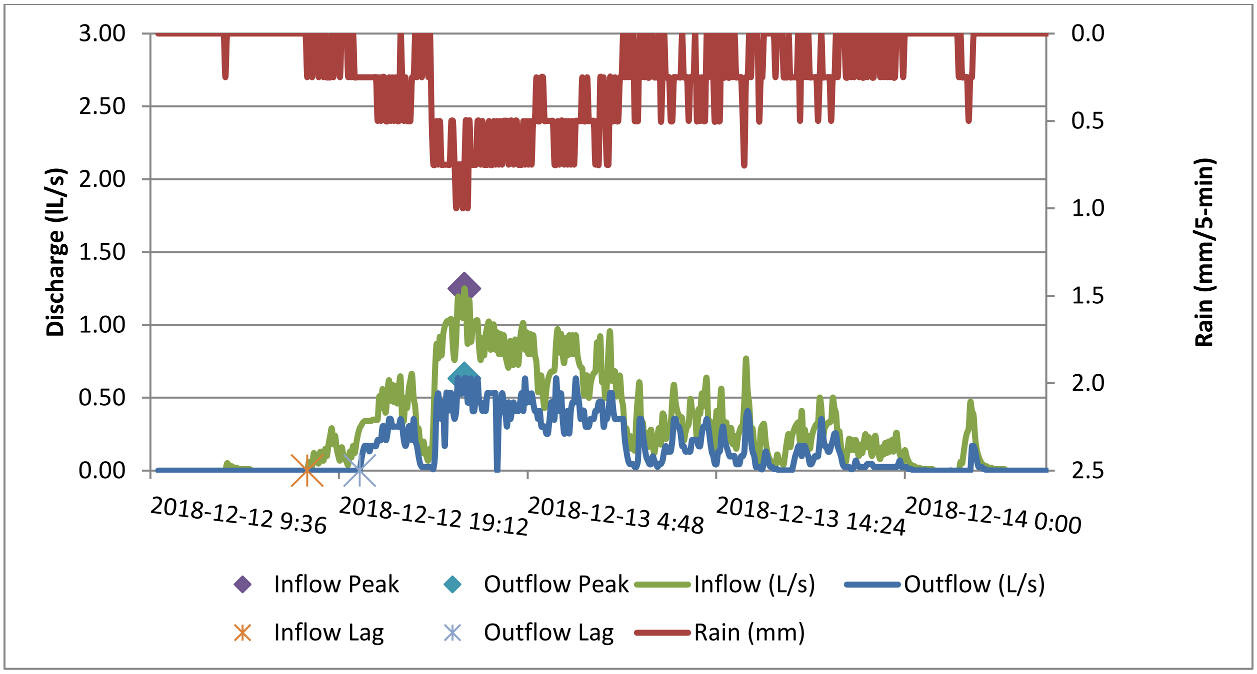

Figure 5.7: December 12, 2018 rainfall event. Inflow and outflow lag components shown along with the peak flow components.

The average storm lag time results can be found on Figure 5.8. On average and with all events considered, the structural soil STT has a lag time performance of 3.2 h ± 0.8 h (CI 95%). The extreme event category has the highest performance with a lag time of 4.4 h ± 2.8 h (CI 95%). The lowest performance was attributed to the normal event category with a lag time of 1.4 h ± 0.4 h (CI 95%). The large event category has an average of 3.8 h ± 1.8 h (CI 95%).

The lag time results mentioned are somewhat counter intuitive. One would expect the extreme events to have a lower performing lag time and a higher performance from the normal events. However, to understand these results it is important to look at the antecedent conditions of each event category (Figure 5.8.) On average, the normal events had an ADP of 1.3 days before a rainfall event. To the contrary, the extreme events had an ADP of 2.1 days. This shows that the soil moisture conditions were more saturated for the normal events, as the rainfalls were more back to back. This means that it would take less stormwater to produce underflow for the normal events. Contrary to the extreme events, the soils were drier, which means that the soils could accept more stormwater before producing any outflow to the stormwater sewer network.

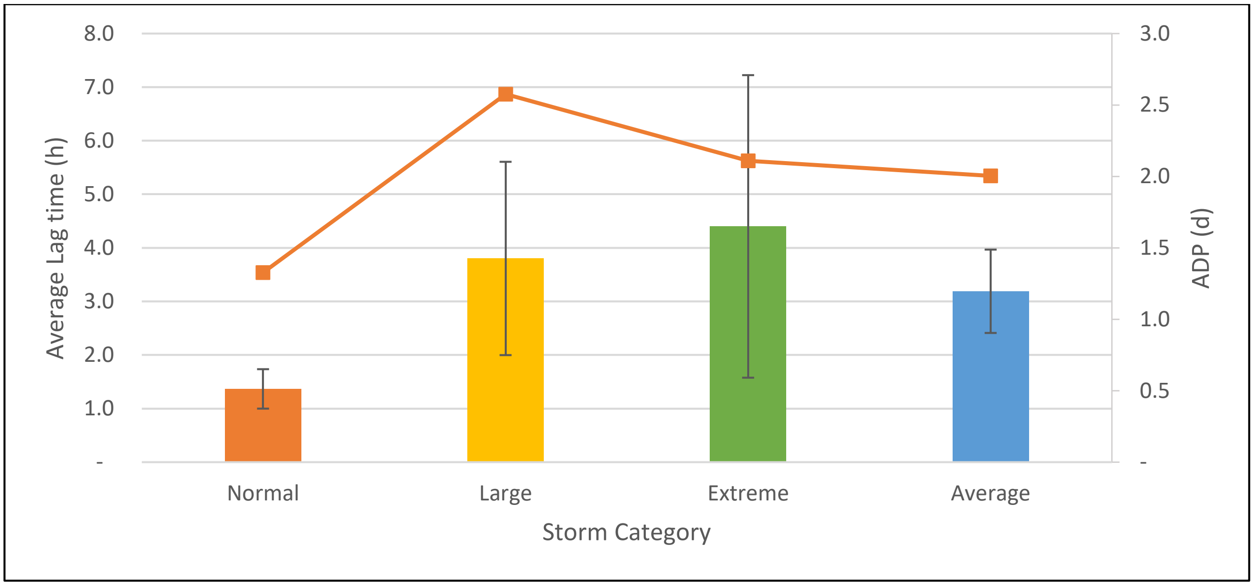

Figure 5.8: Lag time performance (CI 95%) by storm category with its corresponding average ADP days

5.1.5 Soil Moisture and Electrical Conductivity

Green Infrastructure practices aim to create a healthy and sustainable habitat for plants to grow and flourish. The conditions of the soil are important as this is the primary medium that sustains a plant's life. This section of the results will focus on two aspects of the soil monitoring that was performed:

- The first is related to the soil moisture conditions: are the moisture levels sustained above the WP?
- The second aspect of interest pertains the de-icing salts used in the winter: are they getting flushed or are they entrapped through the column?

To answer these questions, the data collected from the soil sensors installed (Section 4.3) in the STT and Bioswale 1 were analyzed. The soil moisture sensors and data loggers were deployed on September 19, 2018 and September 26, 2018 for Bioswale 1 and the structural soil

STT respectively. Bioswale 2 did not have soil sensors installed in the practice. The data collection ceased on February 25, 2019. This period of 5 months includes include a total of 55 storm events for the STT and 56 for Bioswale 1. The following sections will discuss the findings.

5.1.5.1 Soil Moisture

The soil moisture results for the entire monitoring program are shown in Figure 5.11 for the structural soil STT and Figure 5.12 for Bioswale 1. The VWC values are plotted with the theoretical WP and FC for loamy sand soil (Appendix A). Both practices follow different patterns throughout the monitoring period. The VWC in the STT does not reach the theoretical WP during the monitoring period. The consistent higher VWC values measured are attributed to the higher organic matter content of soil component of the structural soil. The proprietary soil blend provided by Veratec must adjust to the park turf blend established by the supply agreement PS20150950 held by the CoV. This guideline establishes that the organic matter content must be between 10% to 20% of total by dry weight (City of Vancouver, 2016a). This significantly differs from the 2.5% organic matter by dry weight of the water retention curve shown in Figure 2.1 of the literature review. In terms of trends, the STT seems to follow different behaviors depending on the depth. This is evident when the daily averages are plotted. The structural soil daily averages are shown in Figure 5.9.

There is a pattern of drying at the 60cm depth. This could be because during installation, significant amounts of water were used to spread the material. The high VWC values are believed to be related to the hysteresis process. Hysteresis related to soils consist on for the same VWC %, there could be two different matric suction potential. These values depend whether the system is on sorption or desorption (Dey, Sundriyal, & Sahoo, 2017; Iiyama, 2016; Sławiński, 2011). This can only be accurately determined by installing matric potential sensors in the practice. However, based on observations of the data, the STT seems to be in a desorption stage (high suction pressures) which could explain the high VWC at the beginning of the monitoring season. When the STT became active (on the sorption stage), the practice began losing the extra moisture until reaching the current equilibrium point.

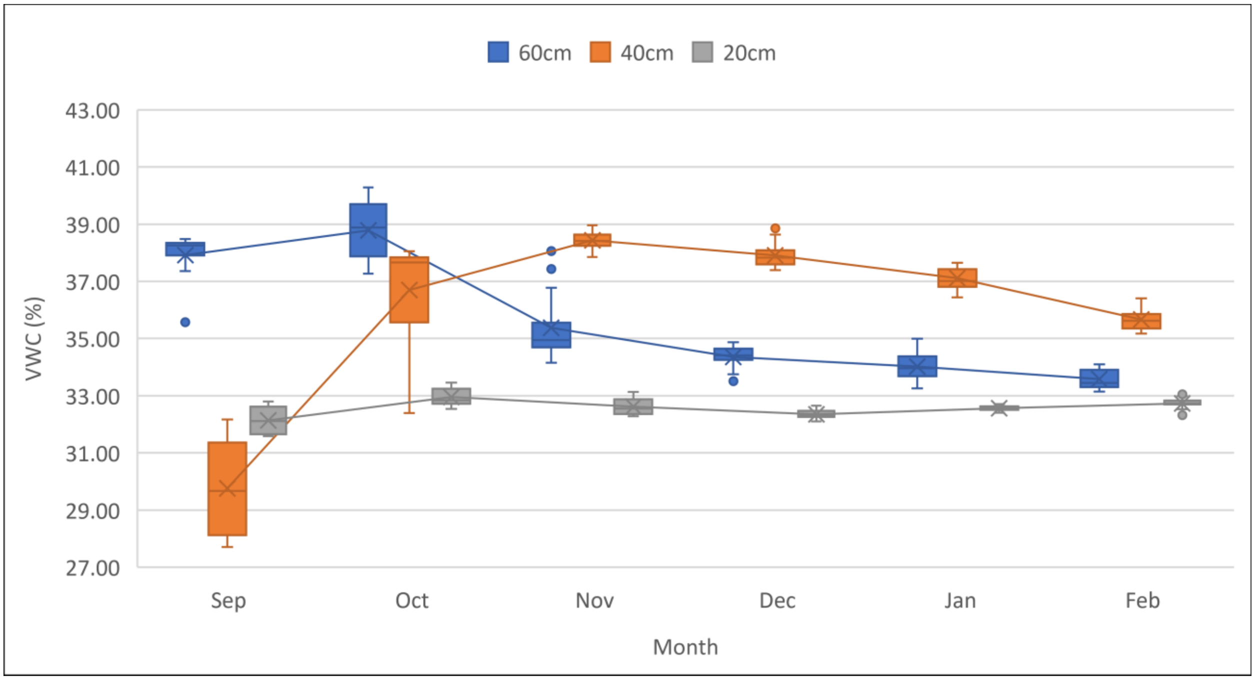

Figure 5.9: Daily averages by month for volumetric water content of the structural soil STT. Average VWC shown in connected lines

The shallowest sensor (20cm) experienced a pattern of slight increase in water content and now it is at an equilibrium point. However, the sensor located at the 40cm depth shows a pattern of increase in water content, followed by a peak and a subsequent drop. This behavior is very odd as the expected VWC at this depth should be lower than the 60cm depth readings. Nevertheless, this odd behavior could be attributed to:

- Damages of the sensor's needles after compaction of the structural soil

- Erosion of the soil pocket where the sensor was installed, leaving pockets of air (distribution pipe located at ~40cm as well)
- The practice has not reach steady state conditions related to the settlement of the soil within the practice which creates pockets of air around the sensor

Evidence of these possibilities is still inconclusive due to the short period of monitoring. It is recommended that the behavior of this sensor is maintained before ruling out its use.

To certify the trends identified, a non-parametric test known as the Mann-Kendall (MK) test was used. The daily averages were used to conduct the trend analysis. This analysis was completed in R by utilizing the Kendall package. The recommendations of Mcleod (2011) were followed to properly conduct the test in the R environment. The statistical significance hypothesis testing (modified for MK) will be completed by following the procedure recommended by Abdi (2006). For this analysis, the null hypothesis is that there is a no monotonic trend in the data.

The results of the statistical analysis for the structural soil STT are shown in Table 5.5. According to the test, the MK tau shows a downward monotonous trend for all the depths in the STT. However, only the 60cm and 40cm depth sensors are rejected as per hypothesis testing. The 20cm depth hypothesis tests was accepted which validates the null hypothesis. This means that no monotonous trends were detected in the data according to the test.

Bioswale 1 shows a trend of increase in water content, which are well above the theoretical values shown in Figure 2.1 of the literature review. This trend is clear when the daily averages are plotted (shown in Figure 5.10). The higher presence of organic matter naturally increases the moisture retention capacity of the soil mix as explained for the structural soil STT analysis due to the soil mix requirements by CoV. In addition, it is important to note that this practice has backwater issues, which also increase the saturation values. Considering all the above, the practice never reaches the theoretical values of WP during the monitoring period. To the contrary of the STT, all the sensors used in Bioswale 1 were installed safely and their reliability is not in question.

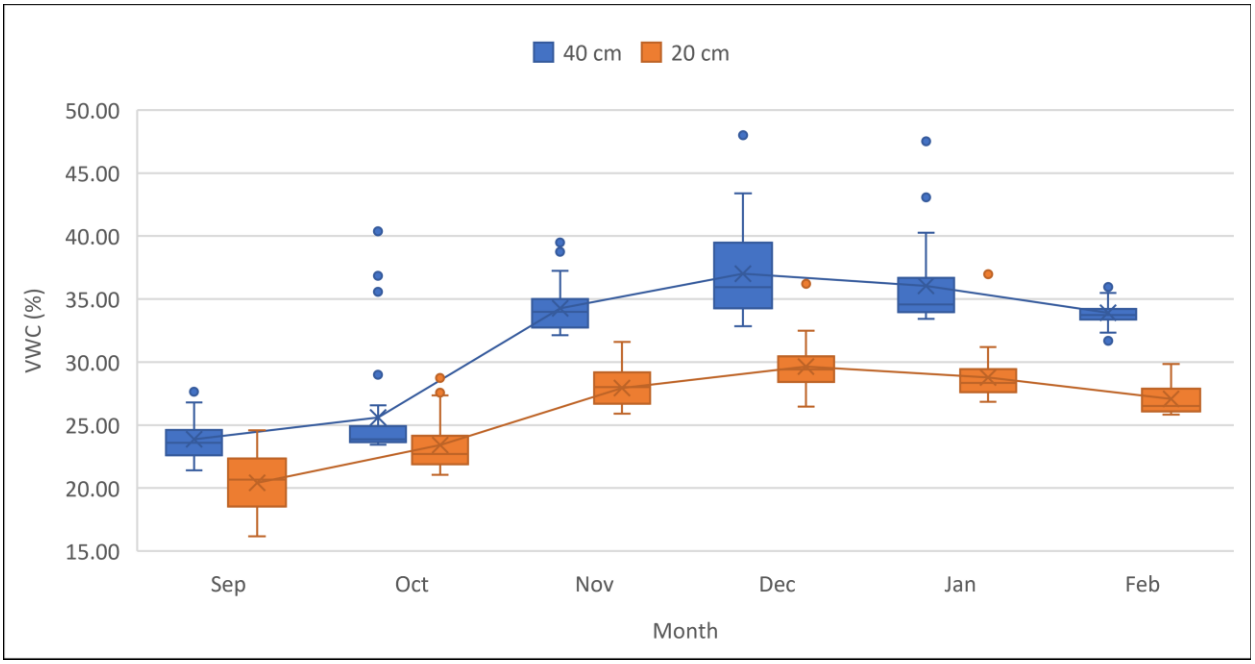

Figure 5.10: Daily averages by month for VWC of Bioswale 1. Average VWC shown in connected lines

Similar to the structural soil STT, the MK test was used to analyze trends. The same hypothesis test structure was employed in the analysis. The results of the statistical analysis are shown in Table 5.6. According the MK test, both sensors in Bioswale 1 show a monotonic upward trend. These results are backed by the hypothesis testing showing a rejection of the null hypothesis on both sensor depths, with p-values <0.0001. Hence it can be concluded that the sensors experience an increase in water content, which is expected due to the season of the year.

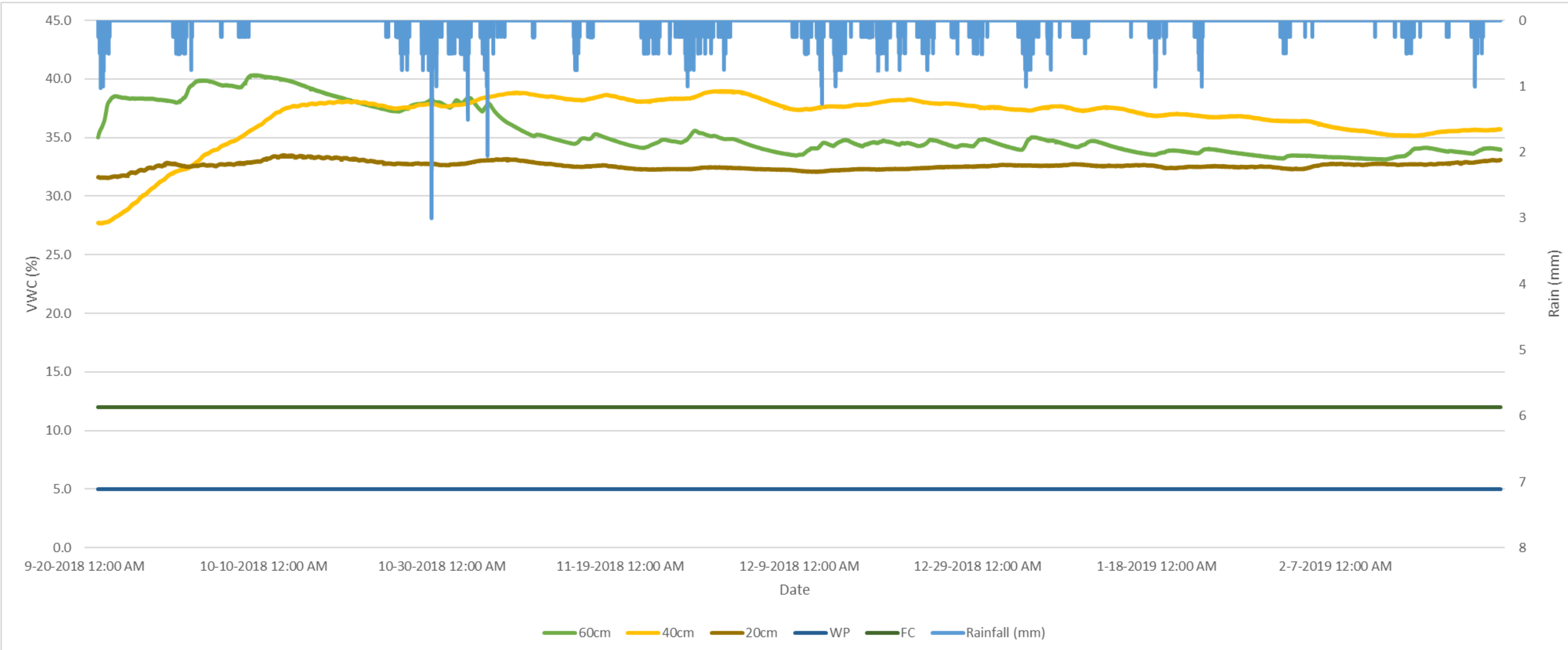

Figure 5.11: Structural soil STT VWC (%) monitoring

Table 5.5: Structural soil STT trend analysis of daily averages of volumetric water content (n=158) as recorded by soil sensors in the structural soil STT

Depth	Analysis				Analysis with Bootstrapping	
	Score	Mann-Kendall Tau	p-value	Null Hypothesis	Tau Bias	Standard Error
20cm	-205	-0.0165	0.75906	Accepted	0.0165	0.1168
40cm	-2833	-0.2280	2.06E-05	Rejected	0.2287	0.1128
60cm	-8979	-0.7240	2.22E-16	Rejected	0.7196	0.1199

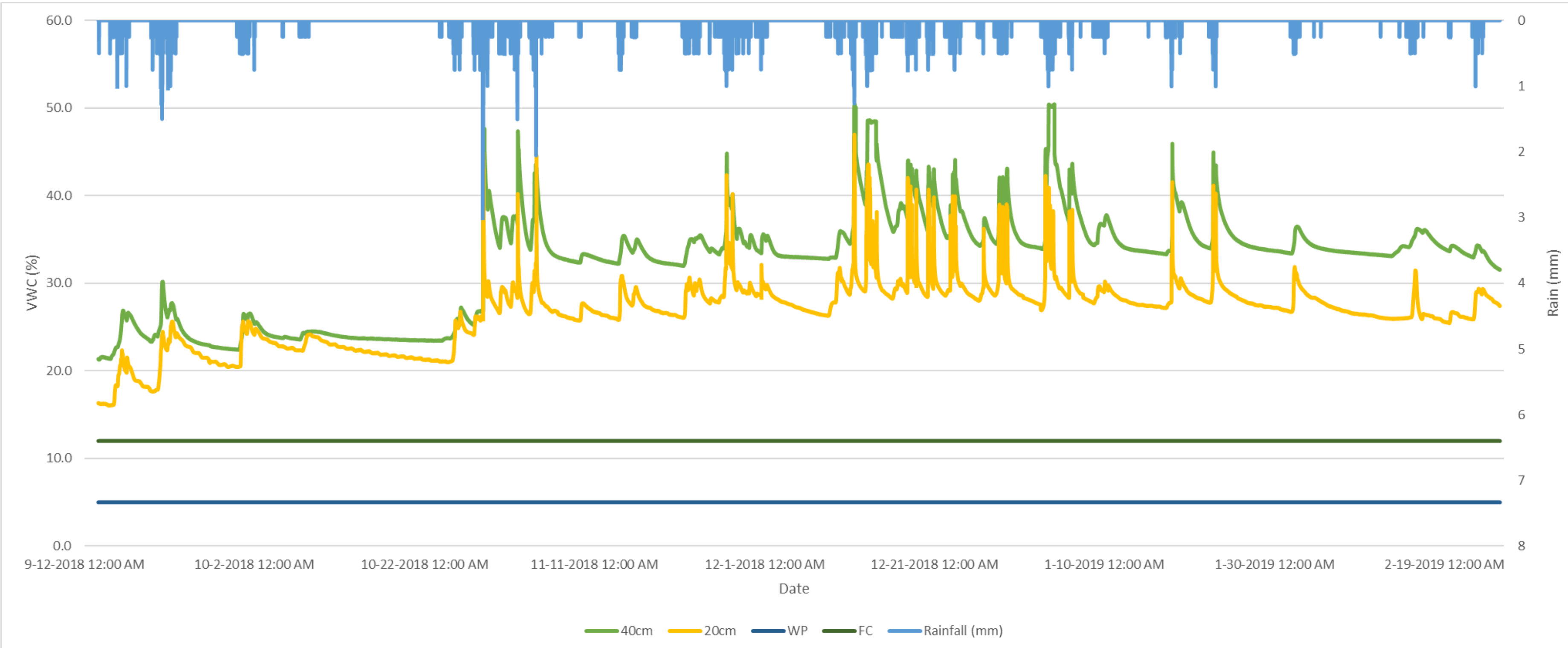

Figure 5.12: Bioswale 1 VWC (%) monitoring

Table 5.6: Bioswale 1 trend analysis of daily averages of volumetric water content (n=166) as recorded by soil sensors in Bioswale 1

Depth	Analysis				Analysis with Bootstrapping	
	Score	Mann-Kendall Tau	p-value	Null Hypothesis	Tau Bias	Standard Error
20cm	4661	0.3400	2.22E-16	Rejected	-0.3476	0.1018
40cm	5028	0.3670	2.22E-16	Rejected	-0.3748	0.1100

5.1.5.2 Electrical Conductivity

The paste extract EC (ECsol) results for the entire monitoring program are shown in Figure 5.15 for the structural soil STT and Figure 5.16 for Bioswale 1. The paste extract EC is typically used in the agriculture industry to classify the salinity of soils. The calculated ECsol values will be compared against two soil salinity classifications in this section.

The ECsol values were calculated utilizing the guidelines provided by the manufacturer of the soil sensor as the soil sensor used estimates the in-situ the bulk EC. These values were transformed to the pore water EC and subsequently transformed to the saturation extract EC. Equations 1, 2 and 4 of the user manual were utilized (Meter, 2018). Literature values were used for some of the components required by the equations. A generic offset of 4.1 was utilized for the dielectric permittivity of dry soil as recommended by researcher Hilhorst (2000) for Equation 1 of the user manual. A literature value for porosity (n) of 0.41 for loamy sand (Clapp & Hornberger, 1978) was utilized for Equation 4 of the user manual.

Similar to the VWC analysis, the daily averages for the ECsol will be utilized to analyze the behavior of the salts in the practices. The results of this process for the structural soil STT are shown in Figure 5.13. With the exception of the sensor at the 40cm depth, both the 20cm and 60cm depth sensor show a declining trend of ECsol values which progresses throughout the fall and winter. This behavior indicates that the salts in the fertilizer products used in proprietary bioretention soil mix (Veratec ®) are progressively being flushed with each storm event.

There is a point of interest related to the month of February of 2019 shown in Figure 5.15. This month experience several snow events where de-icing salts were used on the roads. The month of February in Figure 5.15 shows an increase in ECsol measurements indicating the high use of road salts. The latest readings at the 60cm depth show a downward trend, indicating that the salts that entered the practice were being flushed, however this is still inconclusive as the data ends abruptly do to the data collection cut-off. This same behavior is slightly noticed by the shallowest sensor at the 20cm depth.

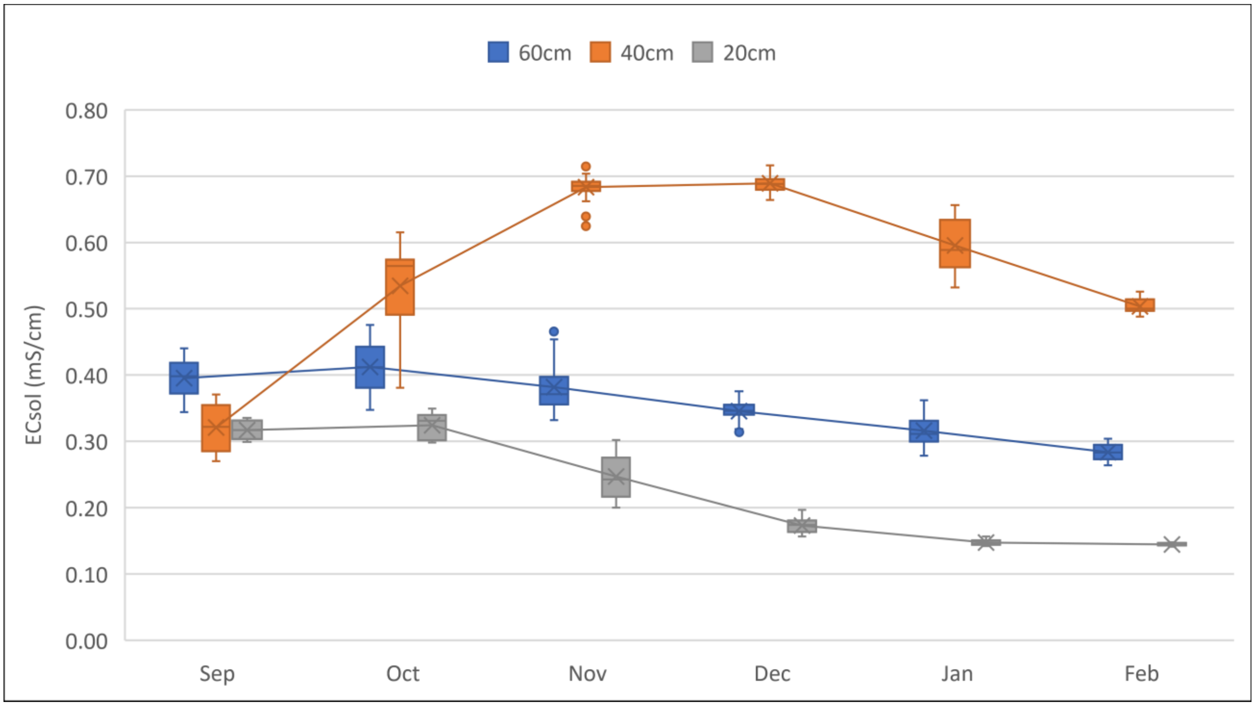

Figure 5.13: Daily averages by month for ECsol of the structural soil STT. Average ECsol shown in connected lines

The sensor located at the 40cm depth shows the same odd behavior discussed in for the VWC analysis. The readings show an increase in ECsol measurements and then a decline. This is consistent with the possibility of sensor damage, erosion of the soil pocket, or settlement in the practice (un-steady soil conditions).

The statistical analysis to analyze the monotonic trends in the data was similar to the VWC analysis. The MK test was also used. The source of information is the calculated daily average ECsol values. The results for the structural soil STT MK test are shown on Table 5.8.

The MK tau shows that for all depths, there is a monotonic trend in the data. The hypothesis testing rejected the null hypothesis with p-values <0.0001 for all depths except for the 40cm depth, where the null hypothesis was accepted with a p-value equal to 0.18. This acceptance of the null hypothesis agrees with the visual observation for the 40cm depth sensor where there is a clear downward concave shape like behavior instead of a downward monotonic trend.

The ECsol values of the structural soil practice were compared against the soil classification based on soil salinity provided the Food and Agriculture Organization (FAO) which is shown in Table 5.7. According the table, the STT would be classified under the non-saline group. The STT readings also conform to the BC government's guidelines where a non-lethal exposure is classified at 4.6mS/cm (Addison, 2002).

Table 5.7: FAO (2015) salinity guidelines

Soil Salinity Class	**Conductivity of the Saturation Extract (mS/cm)**	**Effect on Crop Plants**
Non saline	0 - 2	Negligible effects
Slightly saline	2-4	Restricted yield of sensitive crops
Moderately saline	4-8	Many crops affected
Strongly saline	8-16	Only tolerant crops produce yield satisfactorily
Very strongly saline	> 16	Only highly resistant crops produce satisfactory yield

Bioswale 1 was analyzed in a similar fashion as the structural soil STT practice. The daily average ECsol values are plotted in Figure 5.14. The bioswale data for both the 20cm and 40cm sensors shows a downward trend, which indicates a flushing of the fertilizer salts used by the manufacturer of the standard soil turf mix.

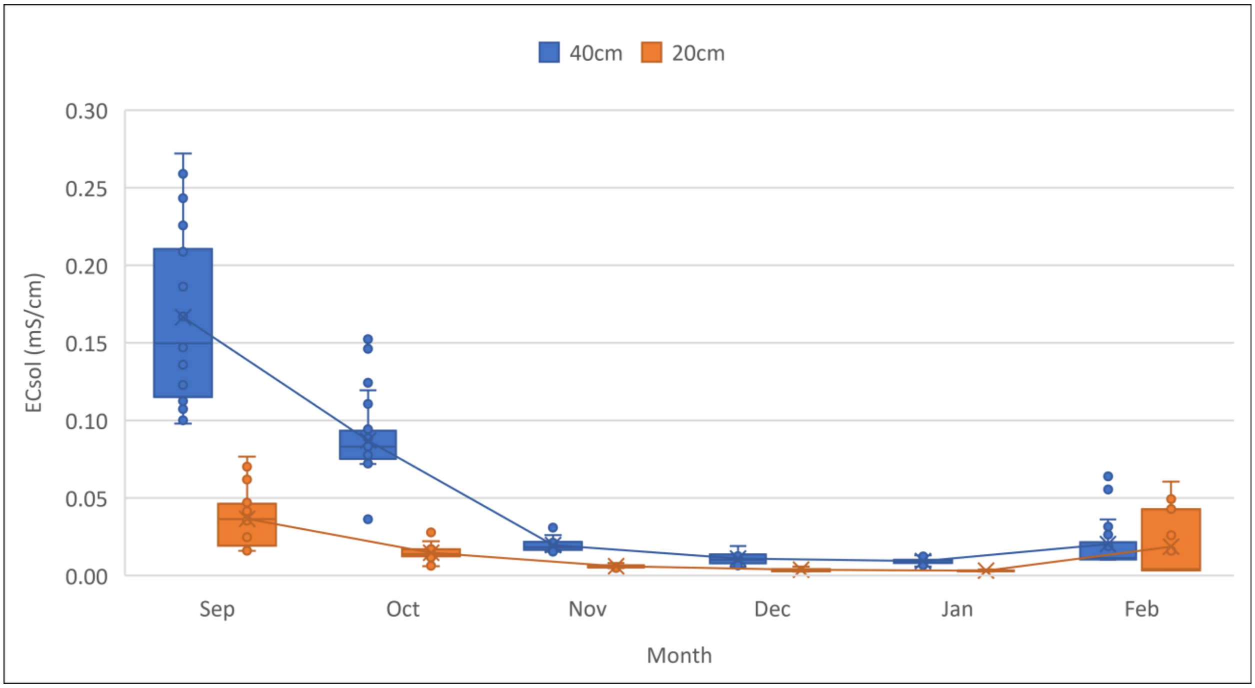

Figure 5.14: Daily averages by month for ECsol of the Bioswale 1. Average ECsol shown in connected lines

As noted for the structural soil STT, the month of February of 2019 has several snow storm events in which de-icing salts were used. There is evidence of the salts entering the system according to Figure 5.14. The plot shows an evident peak for the 20cm depth sensor and a slightly less pronounced one as well for the 40cm depth sensor.

Figure 5.16 illustrates the time series progression of the salts in the system. The peak is pronounced for the 20cm depth and it decreases shortly after as the salts migrate through the bioswale profile and the de-icing salt is no longer used (end of snow storms). This theory is backed by the more gradual rise in ECsol measurements for the 40cm depth sensor. The sensor reaches a maximum peak and subsequently begins to decline once the salts from the shallower depths continues to flush. The data was cut-off on February 25, 2019, but it shows that the ECsol measurements were still on the decline. Despite the usage of salt in the month of February, the

ECsol measurements did not exceed neither the non-saline classification from the FAO guidelines or BC government guideline during the monitoring period.

The MK trend analysis is was also performed for Bioswale 1. The MK tau values for both the 20cm and 40cm depth sensor show a downward monotonic trend in daily average ECsol values. This is confirmed by a subsequent rejection of the null hypothesis (no monotonic trend) with p-values <0.0001. The MK analysis hence confirms the theory that the salts are being flushed out of the practice with the pass of each rain event.

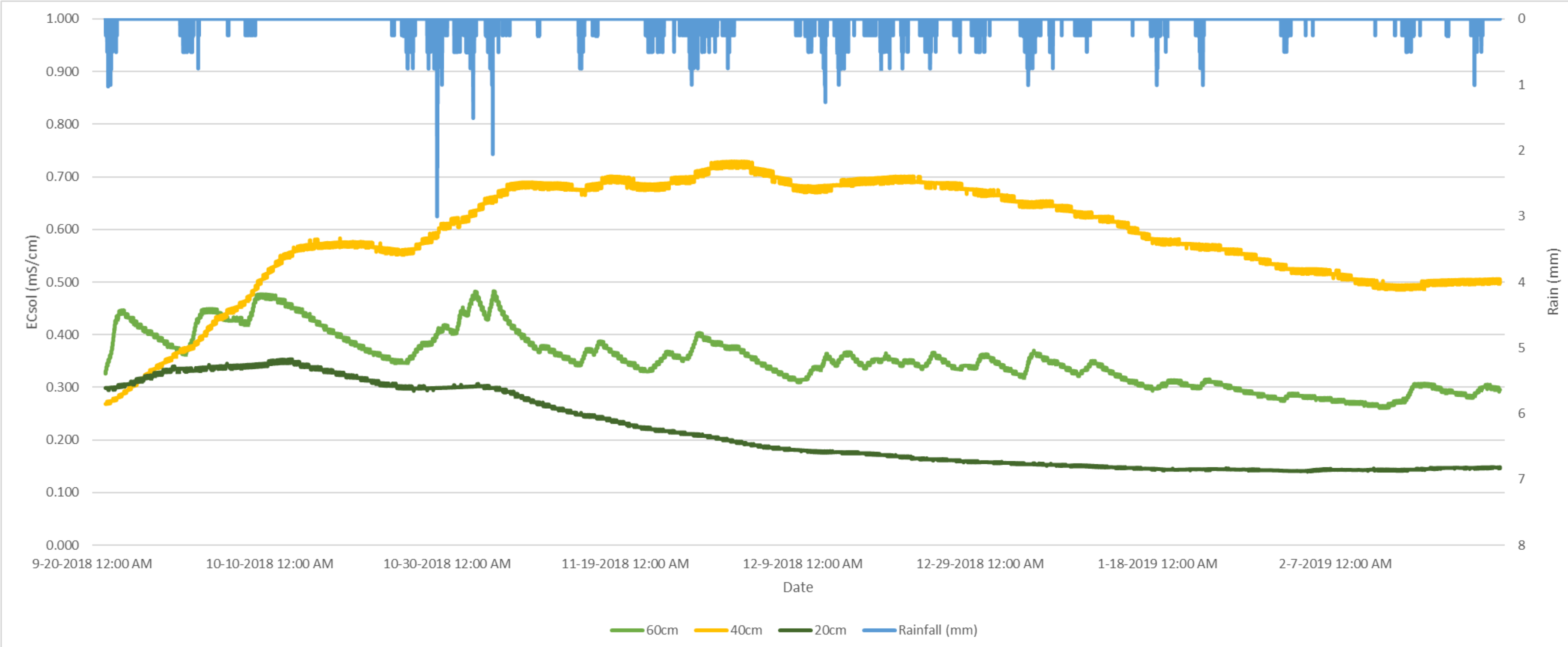

Figure 5.15: Structural soil STT paste extract EC (ECsol) monitoring values based on monitored bulk EC in (mS/cm)

Table 5.8: Structural soil STT trend analysis of daily averages of the paste extract EC (n=166), which are based on the monitored bulk EC in (mS/cm)

Depth	Analysis				Analysis with Bootstrapping	
	Score	Mann-Kendall Tau	p-value	Null Hypothesis	Tau Bias	Standard Error
20cm	-11377	-0.9180	2.22E-16	158	-1.6E-07	Rejected
40cm	-889	-0.0717	0.18184	158	-1.3E-08	Accepted
60m	-8581	-0.6920	2.22E-16	158	-1.2E-07	Rejected

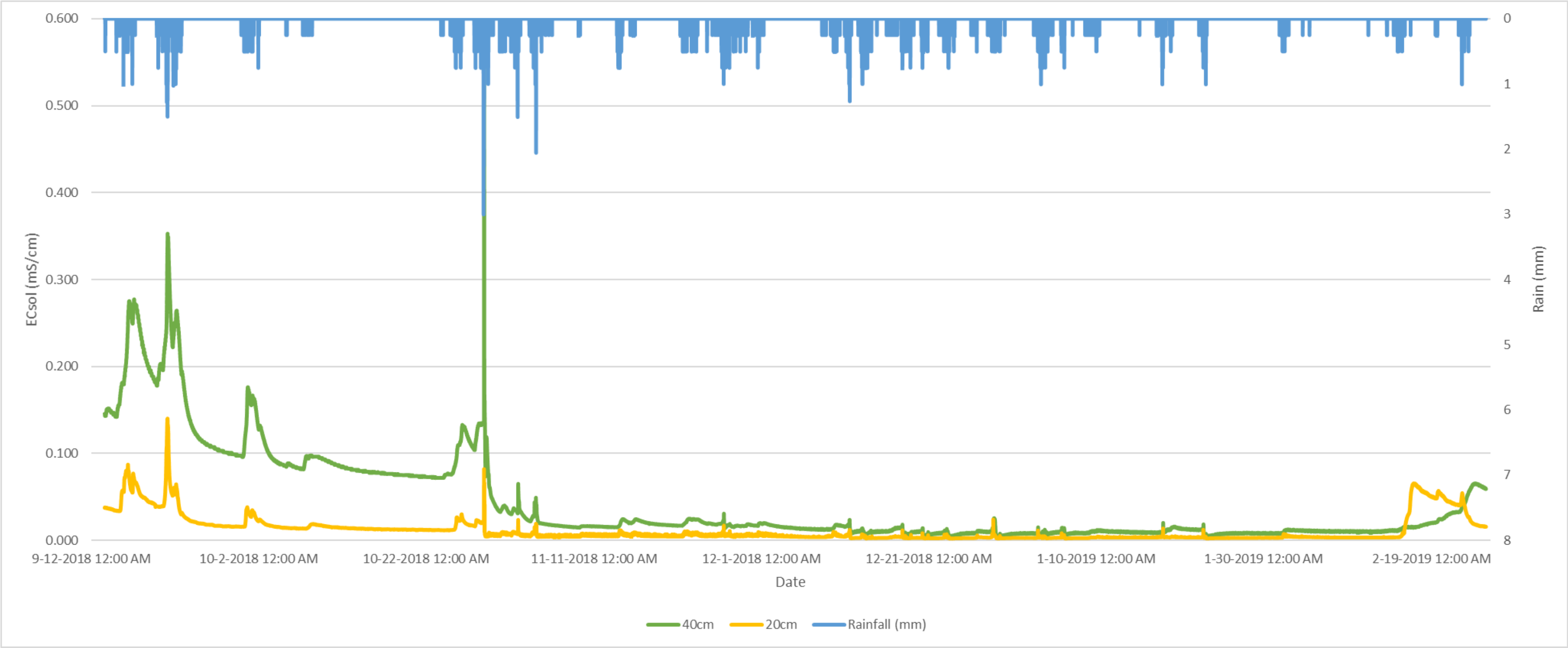

Figure 5.16: Bioswale 1 paste extract EC (ECsol) monitoring values based on monitored bulk EC in (mS/cm)

Table 5.9: Bioswale 1 trend analysis of daily averages of the paste extract EC (n=168), which are based on the monitored bulk EC in (mS/cm)

Depth	**Analysis**				**Analysis with Bootstrapping**	
	Score	**Mann-Kendall Tau**	**p-value**	**Null Hypothesis**	**Tau Bias**	**Standard Error**
20cm	-6930	-0.5120	2.22E-16	165	-8.1E-08	Rejected
40cm	-8066	-0.5960	2.22E-16	165	-9.5E-08	Rejected

5.2 Water Quality Results

This section for the thesis will show the evidence collected from the water quality monitoring program developed for this thesis.

5.2.1 Quality Control

All the samples were collected and transported according to the procedure specified in Section 4.4.2. CARO is accredited by the Canadian Association for Laboratories Accreditation (CALA) and ISO 17025:2005, for the specific tests listed in the scope of accreditation approved by CALA. The procedures followed by CARO during the analysis of the samples are shown in Table 5.10.

Table 5.10: CARO Labs. analysis methods

Analysis	Analysis Method Reference	CARO Modified Method	Technique	Analysis Location
Anions in Water	SM 4110 B (2011)	No	Ion Chromatography	Kelowna
TIC in Water	SM 5310 B (2011)	No	Combustion, Infrared CO2 Detection	Kelowna
TOC in Water	SM 5310 B (2011)	No	Combustion, Infrared CO2 Detection	Kelowna
Conductivity in Water	SM 2510 B (2011)	No	Conductivity Meter	Richmond
DO in Water	SM 4500-O G (2011)	No	Membrane Electrode	Richmond
Hardness in Water	SM 2340 B (2011)	Yes	Calculation: 2.497 [total Ca] + 4.118 [total Mg]	Estimated by formula
TKN in Water	SM 4500-H+ B (2011)	No	Electrometry	Richmond
TP	SM 4500-P B.5* (2011) / SM 4500-P F (2011)	Partially (shown in asterisk)	Persulfate Digestion / Automated Colorimetry (Ascorbic Acid)	Kelowna
TSS in Water	SM 2540 D (2011)	Yes	Gravimetry (Dried at 103-105C)	Richmond
Total Metals	EPA 200.2* / EPA 6020B	Partially (shown in asterisk)	HNO3+HCl Hot Block Digestion / Inductively Coupled Plasma-Mass Spectroscopy (ICP-MS)	Richmond

The reporting limits for these methods can be found on Table 5.11. The results were provided by CARO within a 5-business day window.

Table 5.11: CARO Labs. reporting limits by analysis

General Method	Analyte	Units	Reporting Limit
Anions	Nitrate (as N)	mg/L	0.01
Anions	Nitrite (as N)	mg/L	0.01
Calculated Parameters	Carbon, Total	mg/L	0.5
Calculated Parameters	Hardness, Total (as CaCO3)	mg/L	0.5
Calculated Parameters	Nitrate+Nitrite (as N)	mg/L	0.02
General Parameters	Carbon, Total Inorganic	mg/L	0.5
General Parameters	Carbon, Total Organic	mg/L	0.5
General Parameters	Nitrogen, Total Kjeldahl	mg/L	0.05
General Parameters	Oxygen, Dissolved	mg/L	1
General Parameters	Phosphorus, Total (as P)	mg/L	0.002
General Parameters	Solids, Total Suspended	mg/L	2
General Parameters	pH	pH units	0.1
General Parameters	Conductivity (EC)	uS/cm	2
Total Metals	Aluminum, total	mg/L	0.005
Total Metals	Cadmium, total	mg/L	0.00001
Total Metals	Copper, total	mg/L	0.0004
Total Metals	Iron, total	mg/L	0.01
Total Metals	Lead, total	mg/L	0.0002
Total Metals	Nickel, total	mg/L	0.0004
Total Metals	Zinc, total	mg/L	0.004

The tubing of the automatic samplers and plastic bottles of the samplers were rinsed using tap water. Field blanks were taken to test if the automated samplers accumulate pollutants. Distilled water was used as the sampling liquid on both automatic samplers and the samples were submitted to CARO Labs. This process was conducted at the end of the sampling program, on February 27, 2019. The results are shown on Table 5.12 .

Table 5.12: Water Quality results of field blank samples

Parameter	Units	ISCO 3700	ISCO 6712
NOx	mg/L	0.0138	<0.0050
Hardness	mg/L	<0.500	<0.500
TOC	mg/L	0.64	0.57
TKN	mg/L	<0.050	<0.050
TP	mg/L	0.0117	0.0228
TSS	mg/L	<2.0	2
EC	uS/cm	2.2	<2.0
Al	mg/L	0.0209	0.0127
Cd	mg/L	0.000033	0.000029
Cu	mg/L	0.00154	0.00137
Fe	mg/L	0.01	0.021
Pb	mg/L	<0.00020	0.00024
Ni	mg/L	<0.00040	<0.00040
Zn	mg/L	0.0092	0.0084

The results show that there is background contamination from the automated ISCO® samplers as there were parameters that were detected slightly above the detection limits (shown in red). Ideally, no metal, carbon or nutrients would have been detected. The metal exceedances (above detection limit) include Al, Cd, Cu, Fe, and Zn. These water quality results introduce uncertainty into the calculated removal performances as the background contamination in the samplers affects the quality of the data collected.

To determine if corrections need to be performed, the above exceedances will be evaluated against the measured water quality samples. However, the results of the adjustments will be discussed in each analysis (from Section 5.2.3 to Section 5.2.8). Corrections will be made if the exceedances found on Table 5.12 are less than 20 times the concentration of each sample as recommended by the sampling guidelines of the Government of British Columbia (2015).

5.2.2 Sampling Schedule and Baseline Sampling

This section will cover on the sampling schedule for the water quality program and the baseline sample collection, which includes the collection of rainwater and the characterization of the stormwater runoff of Quebec Street. The individual results of each water quality analysis provided by CARO Labs can be found in Appendix J.

5.2.2.1 Sampling Schedule

The water quality monitoring program extended from November 2018 to February of 2019. Table 5.13 shows the information of all the samples that were taken throughout the monitoring program. A total of 14 samples were collected in total. The samples were collected at diverse points of each storm event. Because of this and the time of the year, the first flush issue was not captured in this study.

Table 5.13: Sampling dates by practice type and sampling type

Practice	CARO Report ID (Project; Sample Name)	Type	Sample Number ID	Sample Date
Bioswale 1	11007; in-001	Inflow	1	2018-11-15
Bioswale 1	11007; in-002	Inflow	2	2018-11-26
Bioswale 1	11007; out-002	Outflow	2	2018-11-26
Rainwater	Rainwater; vancity-001	Baseline	1	2018-11-27
Bioswale 1	11007; in-003	Inflow	3	2018-12-11
Bioswale 1	11007; out-003	Outflow	3	2018-12-11
Bioswale 2	11006; in-001	Inflow	1	2018-12-13
Bioswale 2	11006; out-001	Outflow	1	2018-12-13
Structural Soil STT	32004; in-001	Inflow	1	2019-01-03
Structural Soil STT	32004; out-001	Outflow	1	2019-01-03
Structural Soil STT	32004; in-002	Inflow	2	2019-02-01
Structural Soil STT	32004; out-002	Outflow	2	2019-02-01
ISCO 3700	Fieldblank; in-001	Field Blank	1	2019-02-28
ISCO 6712	Fieldblank; out-001	Field Blank	1	2019-02-28

5.2.2.2 Vancouver Rainfall

Rainfall is the primary component in stormwater. To analyze the pollutants that are accumulated by the runoff process, it is important to determine what are the background pollutants that are introduced by rainwater alone. Rainwater water quality is influenced by the air pollutants that are injected to the atmosphere from natural and anthropogenic sources (Hoinaski, Franco, Haas, Martins, & Lisboa, 2014).

As specified on Table 5.13, the rainwater sample collection was done on November 27, 2018. The rainwater was collected from the roof of the West Annex Building (also known as VanCity building) located at: 515 W 10th Ave, Vancouver, BC V5Z 4A8. The sample was collected from a bucket that was clean and secured to the rooftop of the building as shown in Figure 5.17. The bucket was placed far away from any rooftop structure to avoid contamination or splashes. The bucket was exposed to three storm events: November 24, 2019 (2.5mm storm), November 25, 2019 (97.75mm storm), and November 25, 2019 (0.5mm storm). The rainwater collected directly form the bucket and it was mixed and sampled.

The results of the water quality analysis for the rainwater can be found in Appendix J. The results are limited as only three storm events were composited. However, the results show that rainwater in Vancouver for those events was acidic in nature (pH=5.24), Nitrates (0.038 mg/L), organic carbon (1.4 mg/L), and two metals of interest were detected in low concentrations: Al (0.0082 mg/L), Zn (0.0066 mg/L).

Figure 5.17: Rainwater sampling method and location

5.2.2.3 Stormwater Runoff on Quebec Street

The literature review of this study has highlighted how contaminated stormwater is. The introduction these contaminants pose the greatest threat to the survival of the aquatic creatures that live in Vancouver's adjacent waterbodies. This section of the results will focus on characterizing the stormwater runoff of a high-profile street such as Quebec Street, considered a major arterial.

The inflow samples of all the practices sampled were included in this analysis. The water quality parameters of interest were compared against the water quality guidelines shown in Table 2.4 and Table 2.5. The violations of these water quality parameters will be highlighted in the table. The results have a confidence interval of 95% and are shown in Table 5.14. The respective field blank concentrations corrections have been applied to the results.

As shown on Table 5.14 the results highlight consistent pollutant concentrations that are above the water quality standards for the three organizations considered. The high metal concentrations of Al, Cu, Fe, Pb and Zn found in the stormwater runoff of Quebec Street are consistent with the results found Section 2.1.3.2 of the literature review.

Table 5.14: Quebec Street inflow water quality results. All units in mg/L except pH (in pH units)

Parameter	Number of Samples	Average with 95% CI	Guidelines		
			CCME	BC	MV
Nitrate	5	0.12±0.13	N/A	N/A	5.00
Nitrite	4	0.01±0.005	N/A	N/A	N/A
Hardness	6	18.41±11.34	N/A	N/A	N/A
NOx	6	0.18±0.15	N/A	N/A	N/A
TOC	6	3.07±2.30	N/A	N/A	N/A
TKN	6	0.92±0.56	N/A	N/A	N/A
DO	6	9.71±0.91	8.00	8.00	6.50
TP	6	0.101±0.050	N/A	N/A	N/A
TSS	6	79.41±30.11	N/A	N/A	N/A
pH	6	6.94±0.24	7.00	7.00	6.00
Al	6	1.09±0.53	N/A	0.050	N/A
Cd	6	0.00033±0.00041	0.0010	0.0609	0.00034
Cu	6	0.033±0.012	0.0020	0.0020	0.011
Fe	6	1.35±0.69	N/A	1.00	5.00
Pb	6	0.0052±0.0025	0.0010	0.0020	0.030
Ni	6	0.0025±0.0016	N/A	N/A	N/A
Zn	6	0.10±0.05	0.025	0.010	0.040

5.2.3 Metals

This section of the results will focus on the performance analysis of both the structural soil STT and the two bioswales of interest. The prevalent theory is that bioswales are the gold standard of pollutant removal. The results of the bioswales in this study will be compared against the structural soil STT, a GI method that has not been studied for water quality as found during the literature review. Both GI methods should be effective in targeting the pollutants found on Quebec Street. The analysis has the caveat of being done on a limited number of samples and on a concentration comparison basis due to the time weighted composite method. The sampling method chosen does not allow for the calculation of EMC and total loading calculations.

All of the results will be shown by practice along with its respective removal efficiency and applicable water quality standard. Recommendations will be provided accordingly in Section 6.2 to make a future analysis such as this more robust. The respective field blank concentrations corrections have been applied to the results.

5.2.3.1 Aluminum

The results are shown in Figure 5.18. The Al samples collected are all above the most stringent water quality guideline. However, both Bioswale 1 and the structural soil STT were effective in reducing the concentrations of Al. The outlier in this result is Bioswale 2, which experienced an increase in the Al concentrations. The performance of Bioswale 1 is congruent with the efficiencies found in literature review.

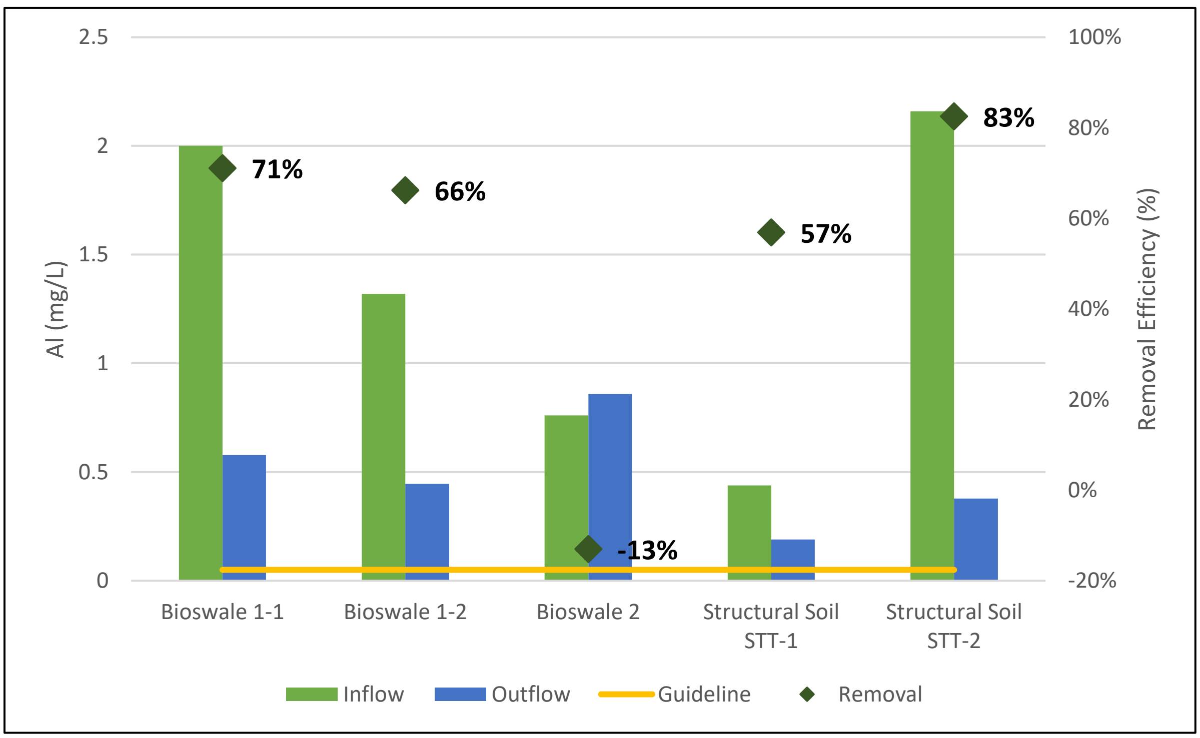

Figure 5.18: Water quality results for Al

5.2.3.2 Cadmium

The results are shown in Figure 5.19. All the samples collected are below the most stringent water quality guideline with the exception of the outflow Bioswale 2 sample, which could be an outlier. The structural soil STT was successful in almost completely removing the Cd concentrations form the street runoff. Bioswale 1 had opposite results: almost complete removal of Cd and addition of Cd to the outflow. Due to the limited number of samples, the incongruency in the results, and sampling method, it is difficult conclude if the bioswale practices are effective in removing Cd as claimed by literature.

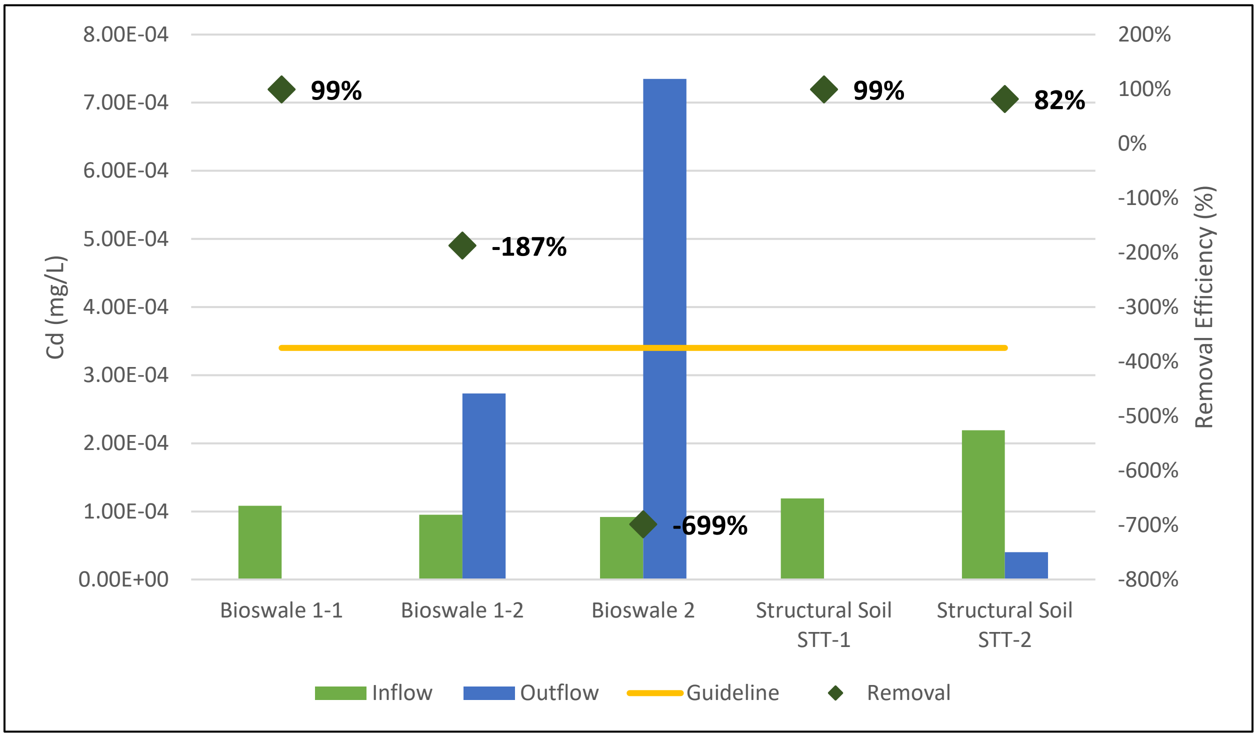

Figure 5.19: Water quality results for Cd

5.2.3.3 Copper

The results are shown in Figure 5.20. All of the samples are above the most stringent water quality guideline for Cu. All practices consistently performed in removing Cu from the stormwater runoff. The performance for the bioswales ranged from 21% to 81%. These results are congruent with the bioswale literature performance values. The structural soil STT performance varied from 57% to 82%.

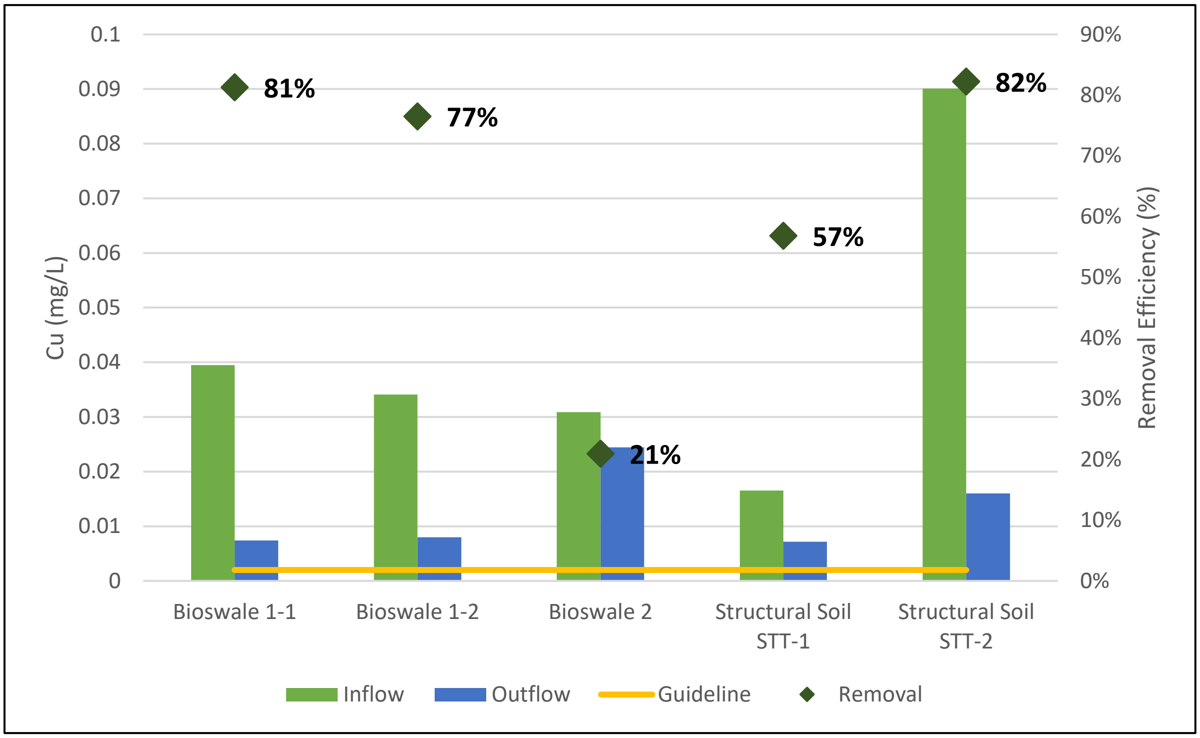

Figure 5.20 Water quality results for Cu

5.2.3.4 Iron

The results are shown in Figure 5.21. The inflow samples consistently exceed the most stringent water quality standard. All the practices were effective in removing Fe from the street runoff except for Bioswale 2. The removal efficiencies of Bioswale 1 ranged between 68% and 74% which agrees with the literature performance. The structural soil practice had a better performance than Bioswale 1 with efficiencies between 66% and 89%. All of the outflow samples are below the water quality guideline except for the Bioswale 2 sample.

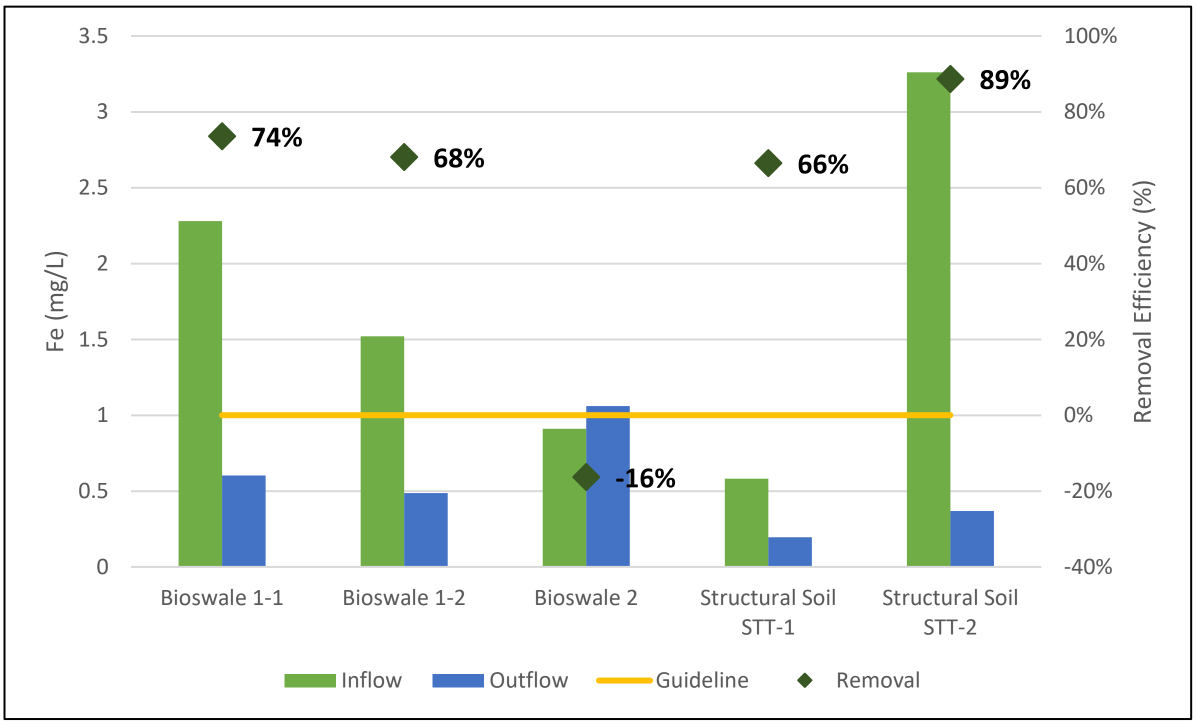

Figure 5.21 Water quality results for Fe

5.2.3.5 Lead

The results are shown in Figure 5.22. All the inflow samples consistently exceed the most stringent water quality standard. All of the outflow samples are below the water quality guideline except for the second STT sample (from left to right). Both bioswale practices showed consistent results, which indicate an effective removal of Pb. The efficiencies range from 66% to 91% which is consistent with the literature. The STT shows positive performance, even comparable to the bioswale practices. The STT performance ranges between 66% to 86%.

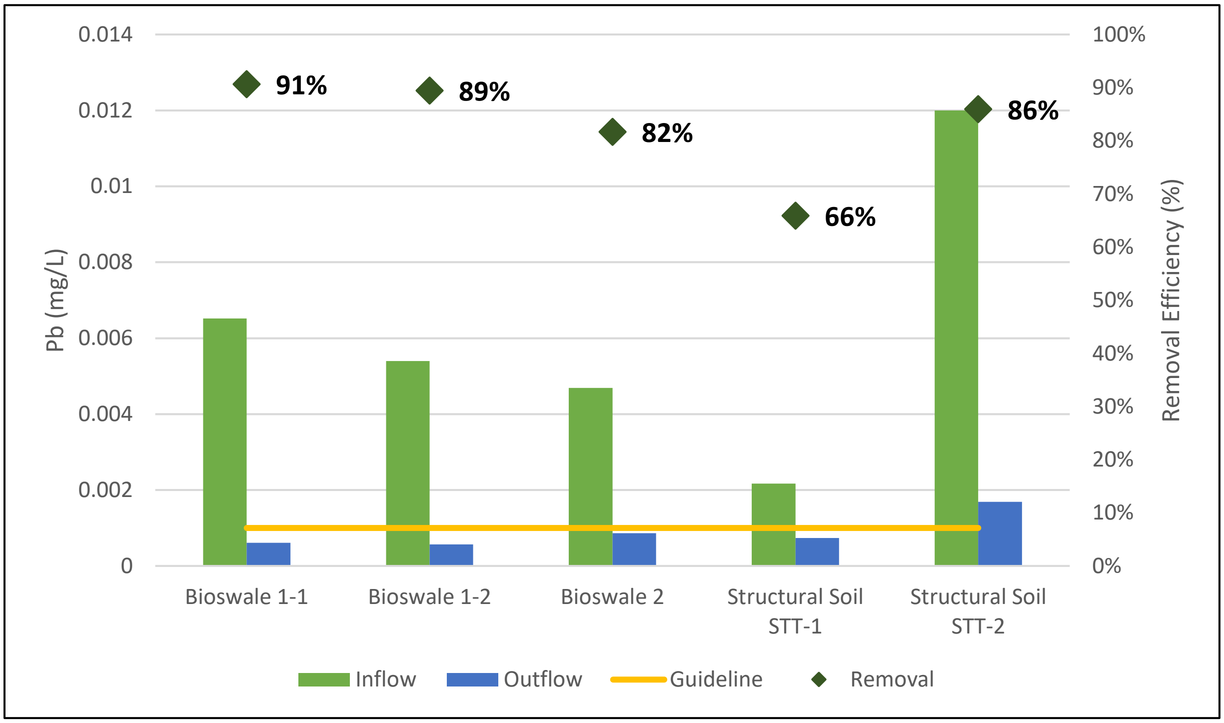

Figure 5.22 Water quality results for Pb

5.2.3.6 Nickel

The results are shown in Figure 5.23. There are no applicable water quality guidelines for Ni. All the practices show positive removal efficiencies apart from Bioswale 2. The removal efficiencies for Bioswale 1 range from 12% to 29%. This performance is poor when compared to the structural soil STT, where the removal performance ranges from 49% to 84%. This shows that the STT could be a more effective tool in removing Ni.

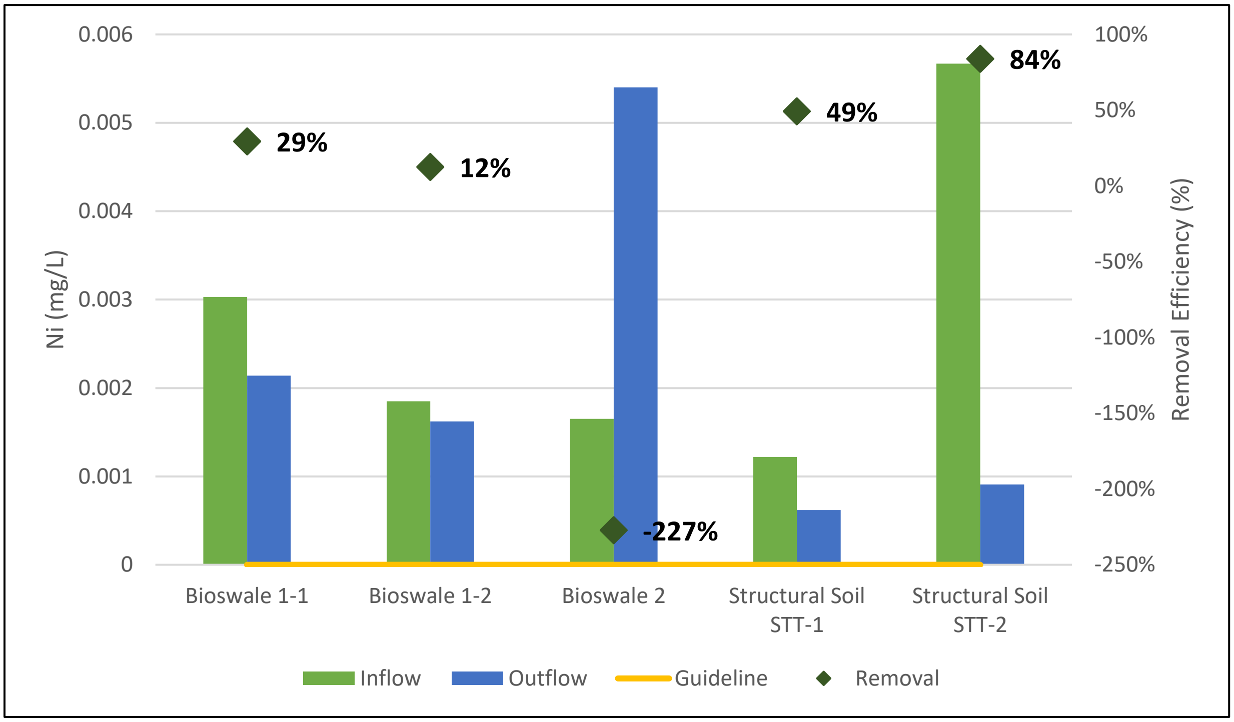

Figure 5.23: Water quality results for Ni

5.2.3.7 Zinc

The results are shown in Figure 5.24. All the inflow samples are above the most stringent water quality guideline for Zn. The majority of the outflow samples barely exceed the water quality guideline with the exception of the first Bioswale 1 sample (from left to right) which is under the guideline. Both bioswale practices show a high performance on Zn removal with efficiencies ranging from 80% to 93% which agrees with he performances found in literature. The structural soil practice also shows satisfactory performance with efficiencies that range between 69% to 86%.

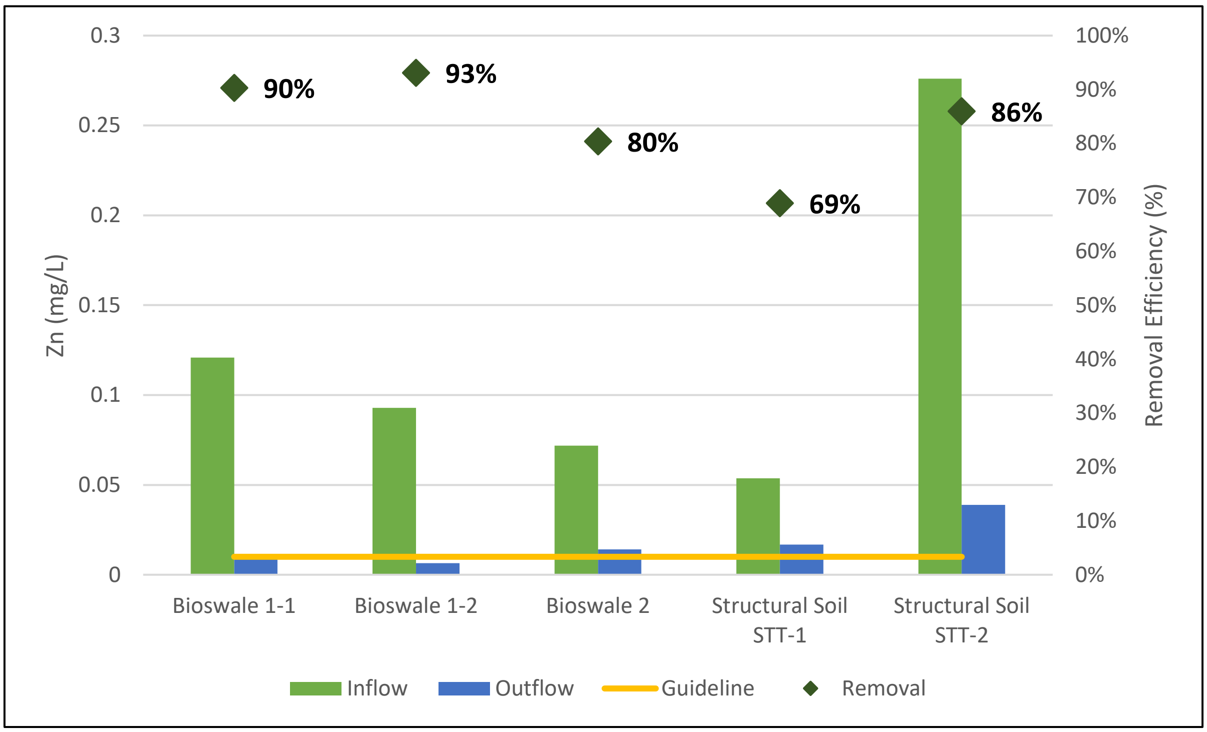

Figure 5.24: Water quality results for Zn

5.2.4 Nutrients and Oxygen

This section will be devoted to evaluating the performance on nutrient removal (or leaching) and the DO increase (or decrease) for all the water quality samples.

5.2.4.1 Nitrogen

Nitrogen will be evaluated from the perspective of NOx (which is the combination of the nitrate and nitrite) and the TKN removal.

The NOx results are shown in Figure 5.25. all the practices consistently show a significant increase in the concentrations of NOx leaving the practices through the underdrain These results do not agree with the literature review performances. An explanation for this is that the nutrient leaching results are consistent with the ECsol results (Section 5.1.5.1), which indicated that the fertilizers used by the manufacturer were leaching out through the practices. It is important to note that the all the practices remained unvegetated throughout the monitoring season until the end of January. The introduction of plants can minimize the nutrient leaching in the future as they will be utilized by the plants. In addition, the bioswale practices were recently built. The nutrient leaching could be explained by a settling period in which the excess nutrients would be leached until reaching an equilibrium. The structural soil STT had lower nutrient leaching than the bioswale practices, however the structural soil has far less soil than the bioswale practices.

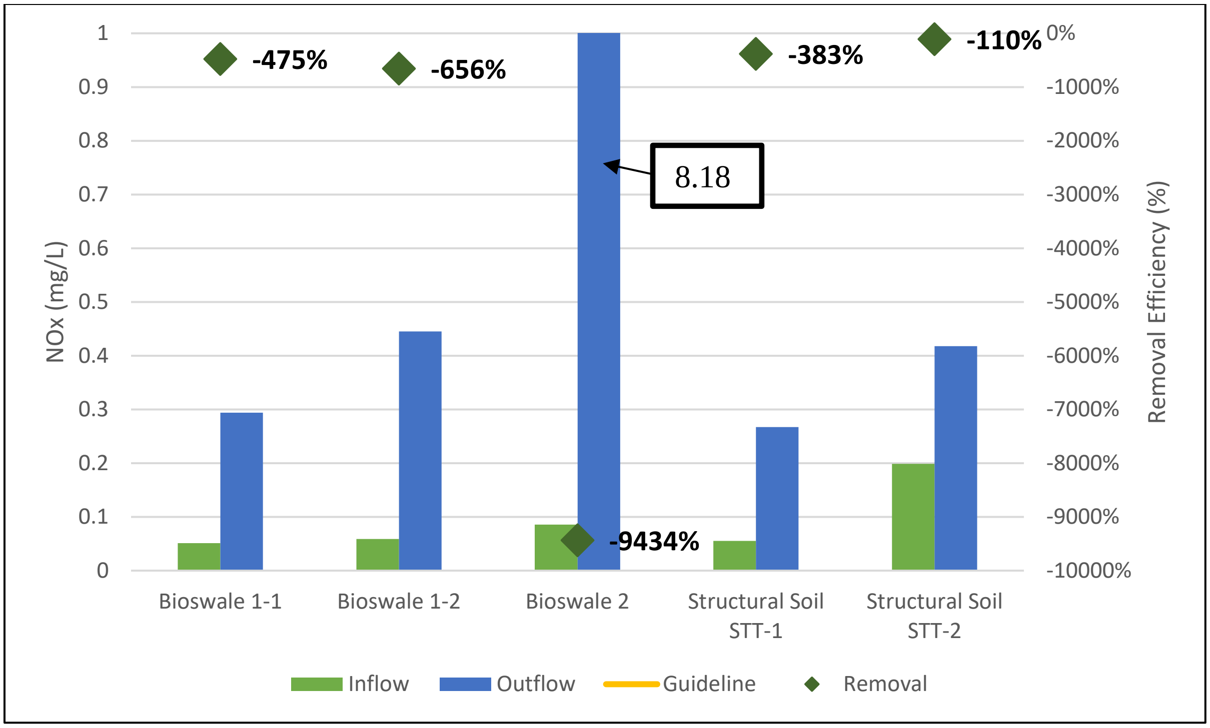

Figure 5.25: Water quality results for NOx

The TKN results are shown in Figure 5.26. Similar to the NOx results, the bioswale practices leach ammonia-based nitrogen into the underdrain. This contradicts the performances found in the literature review. The explanation for this phenomenon is the same as for the NOx leaching. On the other hand, the structural soil practices effectively remove ammonia-based nitrogen with efficiencies between 53% to 73%.

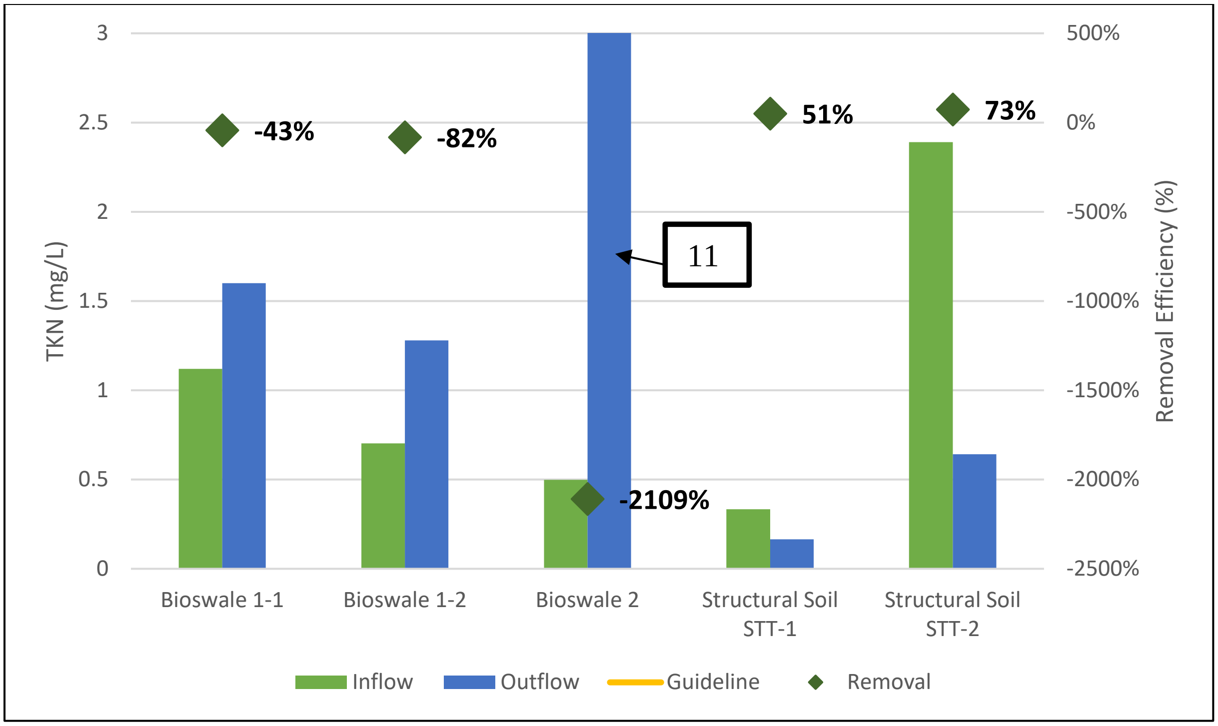

Figure 5.26: Water quality results for TKN

5.2.4.2 Phosphorus

The TP results are shown in Figure 5.27. Similar to the Nitrogen analysis, the bioswale practices consistently leach P to the underdrain of the practice. The nutrient leaching explanation of the nitrogen section apply for the phosphorus analysis.

Contrary to the bioswale practices, the structural soil STT shows to be an effective tool in the removal of P. The removal efficiencies range between 74% to 85%. These results are comparable to the performance literature review of bioswale practices.

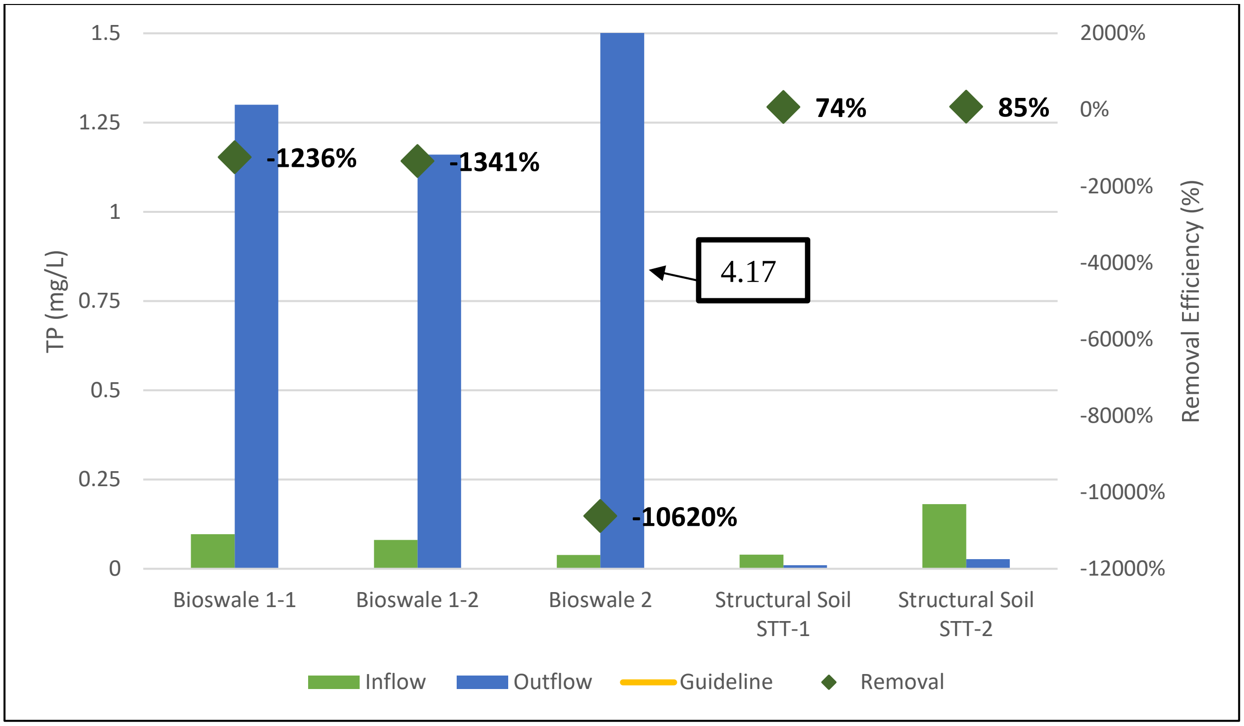

Figure 5.27: Water quality results for TP

5.2.4.3 Oxygen

The DO results are shown in Figure 5.28. All the samples evaluated are above the most stringent water quality guideline. With the exception of Bioswale 2, all the practices show to increase the DO in the outflows. This is important as GI should increase the amount of DO and not decrease it.

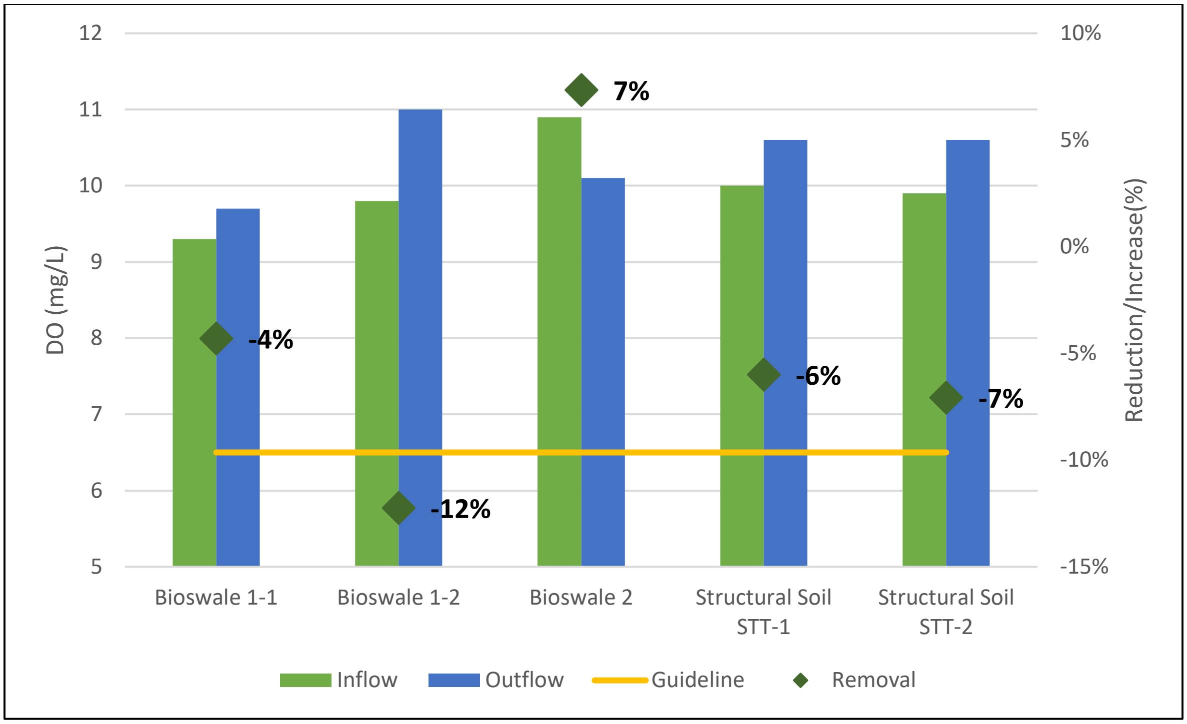

Figure 5.28: Water quality results for DO

5.2.5 pH

The pH results are shown in Figure 5.29. The water quality guidelines are not shown in the figure below however they state that pH should be between 7 and 8.7 for the protection of marine life. The results indicate that all the bioswale practices increase the pH slightly when compared to the inflow results. This result is contrary to the literature review finding where a 10 year bioswale increased on average the pH values (Stime, 2014). It could be that once the practice finishes leaching the fertilizer salts, the bioswale will begin to maintain or increase the pH once the stormwater is filtered through the practice. Contrary to the bioswales, the STT consistently decreases (acidifying) the pH out of the practice.

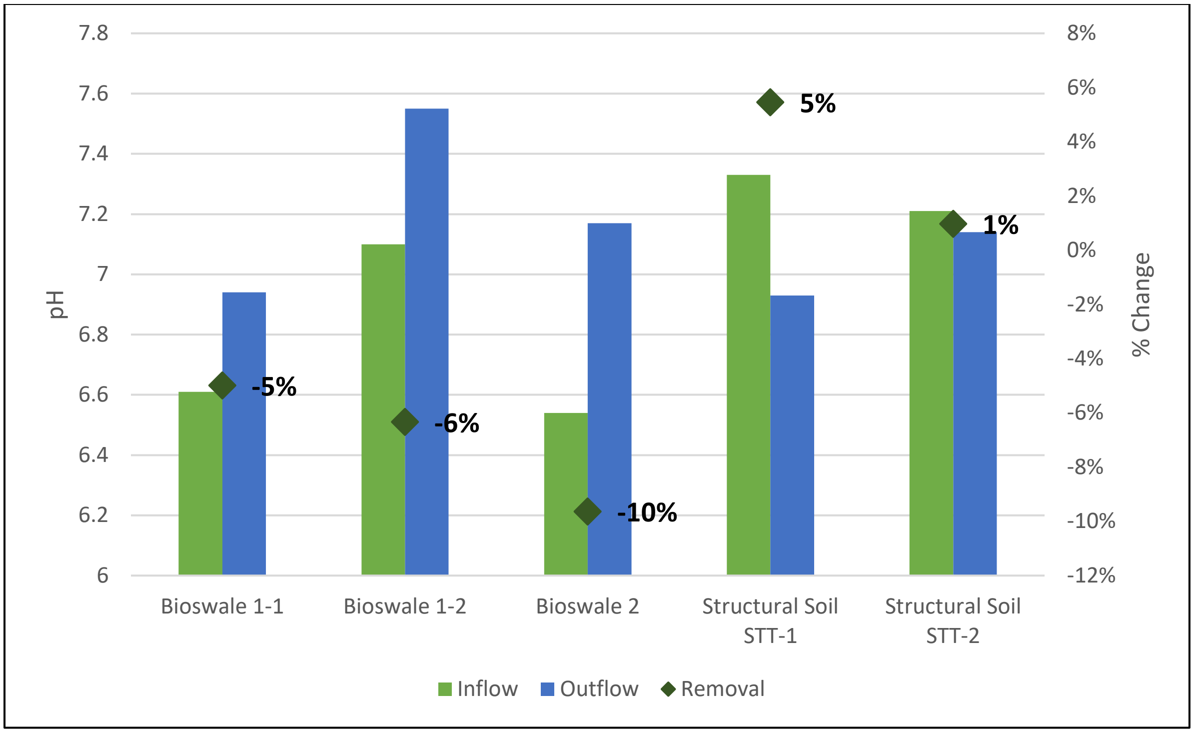

Figure 5.29: Water quality results for pH

5.2.6 Hardness

The Hardness as $CaCO_3$ results are shown in Figure 5.30. The results show that on average all practices increase the water hardness of the outflow. The outlier in this analysis is the second sample of the structural soil STT (from left to right). This sample shows a decrease in hardness. The wide range of results on the STT make it hard to draw conclusions based on the short sampling. The bioswales on the other hand are consistent on the increase and this increase matches the found in literature.

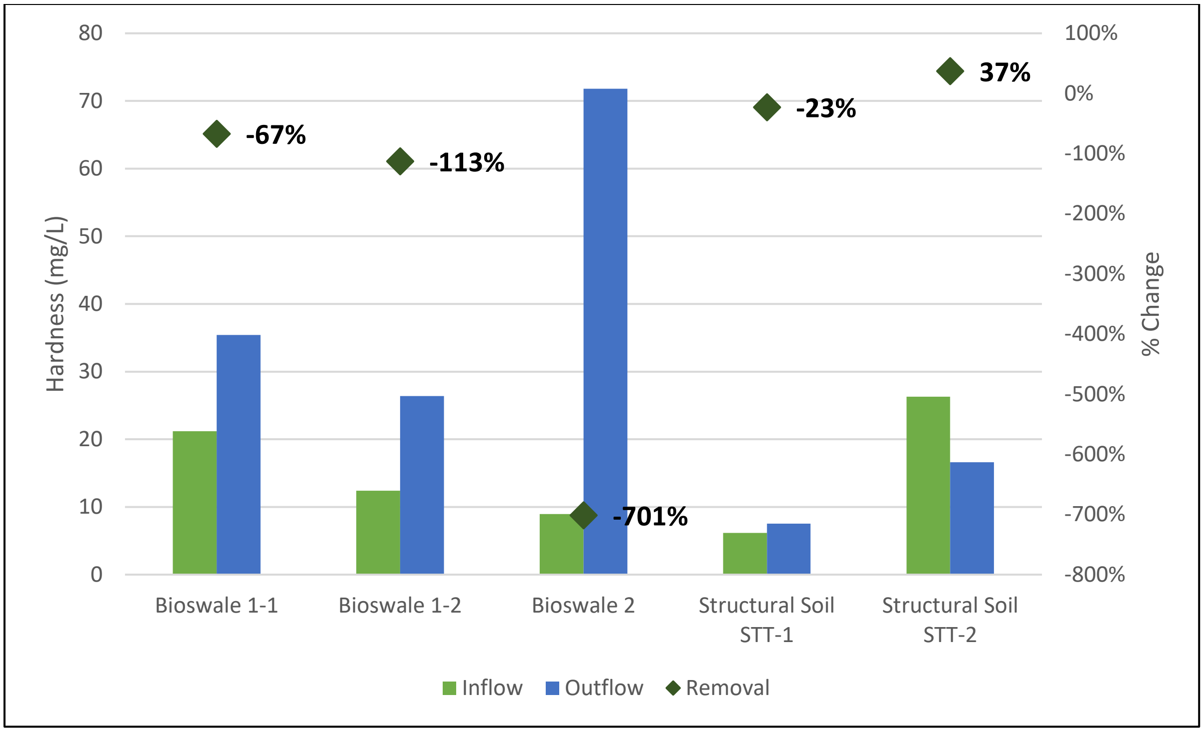

Figure 5.30: Water quality results for Hardness (as $CaCO_3$)

5.2.7 Organic Matter

Organic matter will be evaluated form the perspective of TOC. This parameter is important as it characterizes the hydrocarbons present in the inflow and outflow samples. However, direct sampling of hydrocarbons is the best tool determine its presence. The TOC results are shown in Figure 5.31.

The results show that there is significant increase in the concentrations of organic carbon across all methods. The increase in TOC found in these results do not agree with the literature values, which indicated decrease in TOC concentrations. This increase is attributed to the intrusion of fine sediment into the underdrain, which would be the main source of carbon in the practice as the soil is composed of compost, soil, biochar (for Bioswale 2 and STT) and fertilizers. Hence it cannot be concluded that it is the hydrocarbons component of the TOC that leaches out of the practices.

Based on visual observations, there were no oil sheens in any of the outflow samples that could indicate hydrocarbons in the samples. However, the yellow-orange tint of the samples further validates the soil leach into the underdrain. This sediment leaching is expected to decrease with the pass of time as the soil in the practice settles.

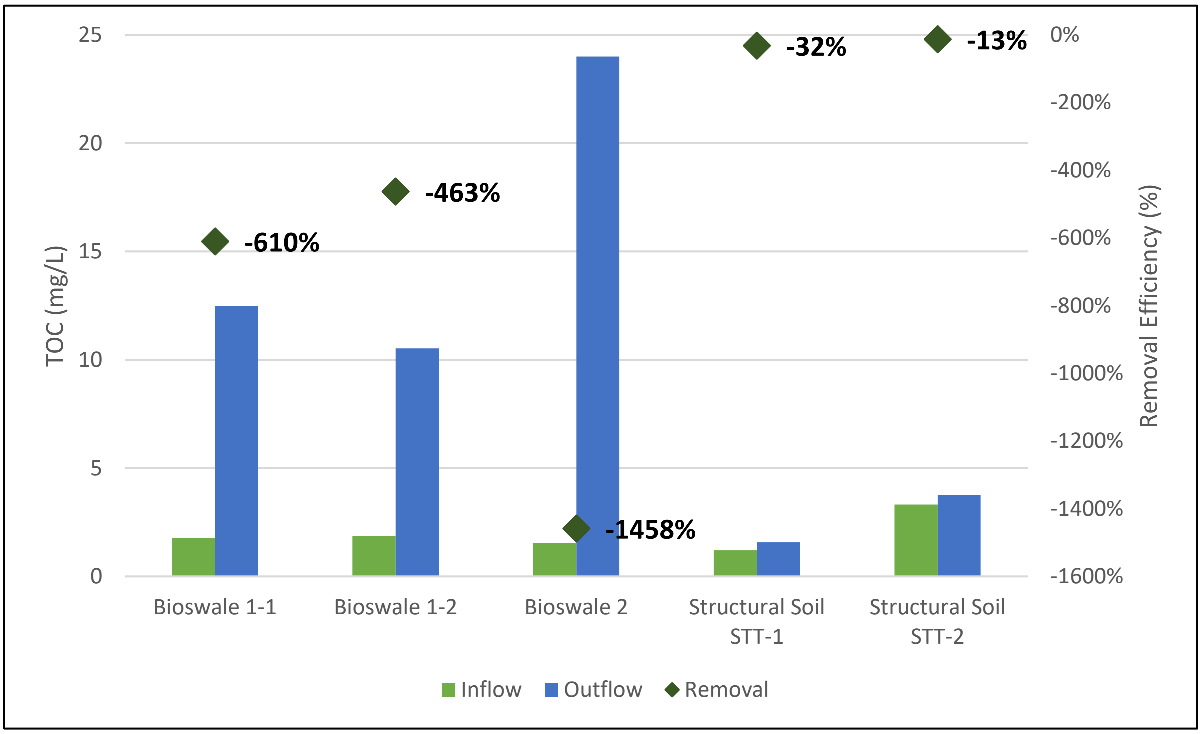

Figure 5.31: Water quality results for TOC

5.2.8 Sediments

The results of TSS are shown in Figure 5.32. All of the practices show a significant decrease in the TSS concentrations. The bioswale performance ranges from 49% to 90%, with the highest performance being attributed to Bioswale 1. These performance results concur with the values found in the literature review. The structural soil STT is also an effective tool in reducing the TSS concentration in the stormwater with efficiencies comparable to the bioswale practices. The efficiencies for the STT ranged from 68% to 88%.

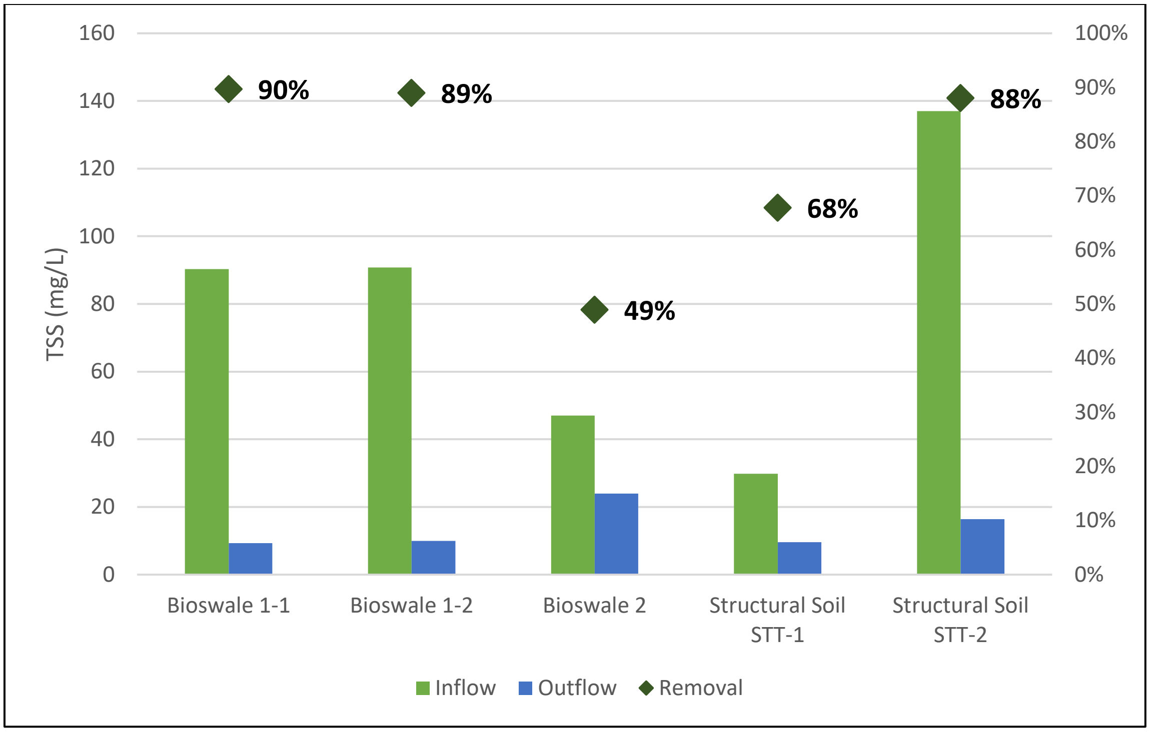

Figure 5.32: Water quality results for TSS

Chapter 6: Conclusion and Recommendation

This thesis aimed to assess the hydrological and water quality performance of three green infrastructure practices in the CoV. This thesis is the first of its kind with direct, applicable results for the CoV. The following sections will further provide the conclusion of the analysis completed and it will make recommendations for future researchers on what can be done to continue the endeavor of studying GI.

6.1 Conclusions

Overall, GI has demonstrated to be an effective tool that can be used by engineers and landscape architects to protect watersheds. This section will provide the conclusions of the analysis completed in Chapter 5 of this thesis. Chapter 5 was categorized by two main sections which group the water quantity related analysis (Section 5.1) and the water quality analysis (Section 5.2). The conclusions are organized in the same fashion.

6.1.1 Water Quantity

Green infrastructure is advertised as a tool that can effectively alter the hydrological regime of the catchments where they are installed. The literature review of this thesis found performance results for both bioswale and STT practices that show this impact. This thesis aimed to put those efficiencies to the test by monitoring the hydrological behavior of the three GI practices in the SEFC in a climate such as the Pacific Northwest.

6.1.1.1 Hydrological

The hydrological impacts were monitored from the month of November 2018 to the month of February 2019. The inflow to the practices were monitored by utilizing the rainfall information provided by the rain gauge installed at the Creekside Community Centre (<300m from site) and developing three SWMM® models for each catchment that utilized the rainfall data of the rain gauge. The outflow of the practices was monitored by using a non-contact ultrasonic sensor that permanently measured the underdrain outflows of a through channel that was installed in a monitoring manhole. The water level provided by the sensors was later transformed to a discharge based on the individual rating curves developed for each through channel of the monitoring manholes. The volume reduction, peak flow reduction and lag time were calculated by utilizing the modelled inflow and measured outflow. Due to backwater and sensor issues, the outflow flow data collected from the bioswale practices was not utilized. Nevertheless, the structural soil STT outflow data was evaluated and showed no signs of error therefore it was deemed appropriate for analysis.

The structural soil STT showed positive hydrological performance overall. The performance was categorized based on the storm event definitions utilized by the municipality of the CoV: normal event (≤24mm, 24hr), large event (>24mm & ≤ 48mm, 24hr) and extreme event (>48mm, 24hr). Based on these categories the structural soil STT had the following performance:

- Volume reduction performance of 87% for normal events, 72% for large events and 62% for extreme events with an overall average volume reduction of 74%
- Peak flow reduction of 74% for normal events, 60% for large events and 55% for extreme events with an overall average volume reduction of 63%
- Flow was effectively delayed on average by 1.4 hours for normal events, 3.8 hours for large events and 4.4 hours for extreme events with an overall average lag time of 3.2 hours

These results show that GI can be effectively utilized to positively impact the hydrological regime of Vancouver's urbanized watershed. Water was effectively captured and infiltrated into the native soils, which mimics the behavior of undisturbed watersheds. Only a small fraction of the stormwater runoff eventually reached the stormwater sewer network. The positive aspect of this water reaching the stormwater sewer network is that the water was effectively delayed from entering the network during the rain events, including at the peak intensity. This means that the stormwater sewer network had extra capacity during the peak of the storm as the runoff was detained in the GI practice. This effectively decreases the flashiness that characterizes urban watersheds.

There are three caveats in the hydrological analysis:

- Inflow measurements: During large and extreme storm events, there GICB would be overwhelmed and the stormwater runoff would bypass to the next CB. The peak flow and volume reduction efficiencies assume that all the runoff generated entered the practice. The implication of this assumption would be: 1) decrease in volume reduction efficiencies for the large and extreme storm events and 2) decrease in the peak flow reduction efficiencies for the large and extreme events.
- Outflow measurements: A flume device was the preferred method of those to estimate the inflow and outflows of the practice bioswale practices, and the PVC weir cap method was the desired method for the structural soil STT. Utilizing modelling methods and developing specific rating curves bring a level of uncertainty which is not present with flume devices which have been more carefully studied.
- Lag time accuracy: The lag time calculations rely on the accuracy of the SWMM® models made for each GI practice. Any issues with the models and their inputs, will translate to a misestimation in the inflow's time stamp.

6.1.1.2 Soil Moisture

The soil monitoring program began in September 2018 and concluded on February 2019. Two practices were monitored for this study: Bioswale 1 and the structural soil STT. Two sensors were installed at a depth of 20cm and 40cm below ground for Bioswale 1. Three sensors were installed at a depth of 20cm, 40cm and 60cm below grade at the structural soil STT. All of the sensors utilized were of the same model: TEROS 12®. This sensor is capable of monitoring bulk EC, temperature and VWC. The bulk EC measurements were converted to paste extract EC (ECsol) values based on the procedure provided by the manufacturer and literature values.

The data collected by all the sensors was analyzed. Though, the information provided by the sensor located at 40cm in the structural soil STT showed evidence of 1) malfunction due to damage, 2) erosion in the soil pocket where it was installed, or 3) soil migration through the practice as steady-state had not been reached as of the time of the analysis. Nevertheless, these theories cannot be confirmed with the small period of data.

6.1.1.2.1 Water content

On the water content front, the Bioswale 1 shows a different behavior to the STT. Bioswale 1 experiences an increase in water content which is tied to the rainy season, amount of organic matter in the soil and the backwater issues of the practice. The structural soil experiences a slight drying which is attributed to draining towards FC.

All in all, both practices never cross the theoretical WP or even the FC curve. An explanation to this is that the organic matter (by weight) in the soil used in the GI practices evaluated have higher organic matter content than the theoretical water retention curves. Organic matter is known to retain moisture. The elevated VWC values indicated that both practices contain enough moisture in the soil to successfully sustain vegetation. However, this should be furthered studied during the driest months (May to September) when evapotranspiration is the highest and precipitation is the lowest in the Lower Mainland.

6.1.1.2.2 Electrical Conductivity

The ECsol values showed that neither Bioswale 1 or the structural soil STT would be considered saline soils under the FAO guidelines and the BC government guidelines. This is true even during the month of February of 2019 where high amounts of de-icing salts were used due to the numerous snow storm events during the month. The peaks are evident in the times series plots for Bioswale 1 and the STT. The flush of fertilizer salts was evident for both Bioswale 1 and the structural soil STT. This visual observation was further corroborated by the statistical analysis utilized in the analysis.

6.1.2 Water Quality

Green infrastructure is typically researched only on the hydrological aspect. This was evident during the literature review as there are far more sources pertaining hydrological research of GI than there is for water quality. This partial analysis approach does not do justice when analyzing the performance of GI. Green infrastructure is a highly complex form of softscape infrastructure that allows the achievement of multiple objectives which include water quality treatment. This thesis aimed to provide a more complete assessment on the performance of the three GI practices evaluated by including a water quality analysis.

Water quality samples were taken at the inflow and outflow of the practices by utilizing two automated samplers. The pollutants on Quebec Street were characterized from the inflow samples in order to understand the typical pollutants that are found in this busy arterial. This analysis showed exceedances of Al, Cu, Pb and Zn. A baseline rainwater sample was also collected from a rooftop in order to understand the background pollutants that fall from the atmosphere through the rainwater.

The water quality analysis performed on this thesis is limited by the sampling method. Ideally, the first flush would be captured in the sampling during the summer and winter, storms of different intensities and sizes should be sampled and compared, and the EMC and total loadings would be calculated per storm event to assess the removal efficiency. However, due to the limitations mentioned in Section 4.4, time weighted sampling during the winter months of 2018 and 2019 was the only feasible option. Nevertheless, the results show promising application of bioswale practices in Vancouver and break ground on the water quality treatment capabilities of structural soil STT. A quality control analysis of the samplers revealed that there was existing background contamination in the samplers, so adjustments were made where necessary. The sampling guide provided by the BC Government (2015) was utilized as a reference to conduct the adjustment.

The bioswale practices and structural soil STT were effective in targeting the heavy metal pollutants present on Quebec Street. Particularly the structural soil was effective in removing Al, Cd, Cu, Fe, Pb, Ni and Zn with performances comparable to the bioswale practices, or even better in the case of Cd, Fe and Ni.

On the nutrient front, all the practices showed signs of nutrient leaching. This was evident in the high concentrations of Nox and TP. However, both the bioswale practices and the structural soil practices were effective in reducing the TKN. The nutrient leaching results corroborate the behavior noted in the Ecsol measurements in which there is a clear trend in declining EC measurements. Dissolved oxygen was increased by all the GI methods.

Organic matter was monitored in this study thought TOC measurements. There is evidence of organic carbon leaching happening at all the GI practices in this study. This is believed to be associated with the soil sediment that leaches into the underdrain, which is corroborated by the visual observations made in the field during sampling. However, the results on this are still inconclusive and VOC sampling is required to corroborate the observations.

On the pH side, both bioswale practices increased the pH of the outflow. The opposite effect was observed in the structural soil STT where the pH was either almost maintained or reduced (more acidic). The hardness results of the bioswale practices are congruent with the pH results. Both bioswale practices effectively increase the water hardness in the outflows. The structural soil STT on the other hand showed mixed results on the water hardness front which does not allow this research to draw any conclusions regarding the water hardness effect.

The sediment reduction efficiencies are congruent among all three GI practices: both the bioswales and structural soil STT are effective tools to target TSS. The efficiencies ranged from 49% to 90% on the bioswale practices and from 68% to 88% on the structural soil STT.

All in all, these results shed light on the water quality effects of bioswales and structural soil STT. All method positively affects the stormwater runoff by treating it at its source. This will ensure that our watersheds are protected downstream.

6.2 Recommendations and Future Work

This research broke ground on the monitoring efforts for structural soil STT and bioswale practices. It is recommended that future research should be devoted to more accurately quantify the water quantity and water quality performance of bioswales and STT. Based on this thesis, the recommendations to achieve this are the following:

- **Hydrological study**: It is recommended that flumes and weirs are utilized to measure inflows and outflows depending on the GI method as explained in Section 4.2.1. To measure inflows in bioswales, flumes should be installed at a strategic location in the inlet. For STT, the PVC weir cap method can be used to measure the inflows coming from the dedicated CB. To measure the outflows, flumes should be utilized. The installation of these flumes can be made through the installation of monitoring manholes that allow the permanent installation of monitoring equipment. Modelling cannot replace on-site measurements.
- **Water Quality Analysis:** This analysis should be made on a flow weighed basis and the sampling period should include the summer time to account for the first flush issue. To be able to perform this, the automated samplers need to be permanently deployed. The samplers should also follow laboratory grade maintenance in order to improve the accuracy of the results.
- **Soil moisture and EC study:** Among the many objectives of GI, the ability of sustaining plants is among the most important. GI practices are exposed to detrimental conditions all year round and it is necessary to understand the implications of these conditions to plants. Monitoring for soil moisture and EC soil be conducted for at least an entire year. This will allow the researches to identify if the practices are able to sustain acceptable levels of moisture (above the WP) and if the salts that enter the practices during the winter months are flushed.
- **Pollutant accumulation:** Although not attempted by this thesis, the practices should be studied for the pollutant behavior in the GI practice's soils: Will the

practices ever reach a pollutant saturation limit and begin to allow their migration into the native soils or into outflow water? Some locations around the world rely on groundwater as a source of drinking water and introducing contaminants to these sources of potable water would be detrimental to the population.

Based on the results found on this thesis, this author recommends the municipality of the CoV and other municipalities to continue to develop their GI installation programs. This study has shed light on the multiple benefits that the use of GI can have on the protection of urbanized watersheds. Green infrastructure effectively unseals the impervious dominated landscape by capturing, treating and infiltrating stormwater at its source. This successfully mimics what a natural watershed, in which very little water leaves the site as runoff. The infiltration component is one of the most important facets for municipalities located in regions where, before urbanization, infiltration dominated the watersheds. Examples of an infiltration dominated watersheds are the cities located in the Pacific Northwest. The stormwater problem will very likely only get worse with climate change; alternatives to greywater infrastructure are warranted to safely mitigate the increasing amount of stormwater that will fall in our cities.

Bibliography

Abdi, H. (2006). The Kendall Rank Correlation Coefficient, 1–7. Retrieved from http://www.utd.edu/

Addison, J. A. (2002). *Derivation of Matrix Soil Standards for Salt under the British Columbia Contaminated Sites Regulation, Addendum C: Soil Invertebrate Toxicity Tests: Lessons and Recommendations*. Retrieved from https://www2.gov.bc.ca/assets/gov/environment/air-land-water/site-remediation/docs/requests-for-comments-archive/rev_prov_saltmatrix.pdf

Alamdari, N., Sample, D. J., Steinberg, P., Ross, A. C., & Easton, Z. M. (2017). Assessing the effects of climate change on water quantity and quality in an urban watershed using a calibrated stormwater model. *Water (Switzerland)*, *9*(7), 464. https://doi.org/10.3390/w9070464

Angelakis, A. N., Koutsoyiannis, D., & Tchobanoglous, G. (2005). Urban wastewater and stormwater technologies in ancient Greece. *Water Research*, *39*(1), 210–220. https://doi.org/10.1016/j.watres.2004.08.033

Asadian, Y. (2010). *Rainfall interception in an urban environment*. University of British Columbia. https://doi.org/10.14288/1.0069783

ASTM. (2013). Standard Test Method for Open-Channel Flow Measurement of Water with Thin-Plate Weirs. *ASTM International*, *92*(Reapproved 2013), 1–8. https://doi.org/10.1520/D5242-92R13.2

ASTM. (2014). Standard Guide for Selection of Weirs and Flumes for Open-Channel Flow Measurement of Water 1. *ASTM International*, 1–7. https://doi.org/10.1520/D5640-95R14

Bach, P. M., McCarthy, D. T., & Deletic, A. (2010). Redefining the stormwater first flush phenomenon. *Water Research*, *44*(8), 2487–2498.

https://doi.org/10.1016/j.watres.2010.01.022

Balter, M. (2005). The Seeds of Civilization. *Smithsonian Magazine*. Retrieved from https://www.smithsonianmag.com/history/the-seeds-of-civilization-78015429/

Bartens, J., Wiseman, P. E., & Smiley, E. T. (2010). Stability of landscape trees in engineered and conventional urban soil mixes. *Urban Forestry and Urban Greening*, *9*(4), 333–338. https://doi.org/10.1016/j.ufug.2010.06.005

Bassuk, N. (2013). Two Different Approaches to Improve Growing Conditions for Trees Comparing Silva Cells and Structural Soil. *American Society of Consulting Arborists*, *46*(2), 4–14. Retrieved from https://static1.squarespace.com/static/52ec31b2e4b04eb0bbd9c075/t/533b63c8e4b07f69c06bb3b0/1396401096862/asca_newsletter.pdf

Bassuk, N., Grabosky, J., & Trowbridge, P. (2005). Using CU-Structural Soil ™ in the Urban Environment. Retrieved from www.hort.cornell.edu/UHI

BC Government. (2015). *Section A: LABORATORY QUALITY ASSURANCE/QUALITY CONTROL*. Victoria. Retrieved from https://www2.gov.bc.ca/assets/gov/environment/research-monitoring-and-reporting/monitoring/emre/lab-manual/section-a.pdf

BC Ministry of Environment. (2016). *Indicators of Climate Change for British Columbia: 2016 Update*. *BC Ministry of Environment*. Victoria: Ministry of Environment. Retrieved from http://www.llbc.leg.bc.ca/public/pubdocs/bcdocs2016_2/603258/climatechangeindicators-13sept2016_final.pdf

Bertrand-Krajewski, J., Chebbo, G., & Saget A. (1998). DISTRIBUTION OF POLLUTANT MASS VS VOLUME IN STORMWATER DISCHARGES AND THE FIRST FLUSH

PHENOMENON. *ILAR Journal*, *49*(2), 145–156. https://doi.org/10.1093/ilar.49.2.145

Blight, G. E. (2003). The vadose zone soil-water balance and transpiration rates of vegetation. *Géotechnique*, *53*(1), 55–64. https://doi.org/10.1680/geot.2003.53.1.55

Booth, D. (1991). Urbanization and the Natural Drainage System -- Impacts, Solutions, and Prognoses. *The Northwest Environmental Journal*, *7*(1), 93–118. Retrieved from http://hdl.handle.net/1773/17032

Booth, D. B., & Jackson, C. R. (1997). URBANIZATION OF AQUATIC SYSTEMS: DEGRADATION THRESHOLDS, STORMWATER DETECTION, AND THE LIMITS OF MITIGATION. *Journal of the American Water Resources Association*, *33*(5), 1077–1090. https://doi.org/10.1111/j.1752-1688.1997.tb04126.x

Bradford, A. (2016). *LAKEVIEW DRIVE, CITY OF MISSISSAUGA LOW IMPACT: DEVELOPMENT INFRASTRUCTURE PERFORMANCE AND RISK ASSESSMENT*. Mississagua. https://doi.org/10.1097/01.AOG.0000239105.39149.d8

Caltrans. (2011). *Biofiltration Swale Design Guidance*. Sacramento. Retrieved from http://www.dot.ca.gov/hq/env/stormwater/index.htm

Campbell, J., & Frascarelli, L. (1981). INEXPENSIVE THERMISTOR SENSORS FOR TEMPERATURE MEASUREMENTS IN ORGANIC SOILS. *Can. J. Soil. Sci.*, *61*(3), 521–524.

CCME. (2007). *A Protocol for the Derivation of Water Quality Guidelines for the Protection of Aquatic Life 2007*. Hull. Retrieved from http://ceqg-rcqe.ccme.ca/download/en/220

CCME. (2014). Canadian Environmental Quality Guidelines. Retrieved February 20, 2019, from https://www.ccme.ca/en/resources/canadian_environmental_quality_guidelines/

Cheung, P., & Anderton, R. (2016). The Queensway Sustainable Sidewalk Pilot Project. In

TRIECA. Toronto: TRIECA. Retrieved from https://trieca.com/app/uploads/2016/07/4-A-1-Patrick-Cheung-and-Rod-Anderton-The-Queensway-Sustainable-SW-Pilot-Project.pdf

City of Trees. (2016). Howard Street, Salford. Retrieved February 18, 2019, from http://www.cityoftrees.org.uk/project/howard-street-salford

City of Vancouver. (n.d.). VanMap. Retrieved June 2, 2018, from http://vancouver.ca/your-government/vanmap.aspx

City of Vancouver. (2015). *The Flats Area Profile: An Overview of Your False Creek Flats*. Vancouver. Retrieved from https://vancouver.ca/files/cov/false-creek-flats-area-profile.pdf

City of Vancouver. (2016a). *PS20150950 Supply Agreement Between Harvest Fraser Richmond Organics Ltd. and the City of Vancouver - related to the supply and delivery of soil*. Vancouver.

City of Vancouver. (2016b). *Rainwater Management Plan and Green Infrastructure Strategy*. Vancouver.

City of Vancouver. (2017). *2017-2021 Budget Outlook*. Vancouver. Retrieved from https://vancouver.ca/files/cov/2017-2021-budget-outlook.pdf

City of Vancouver. (2018a). *Budget Outlook 2019-2023*. Vancouver. Retrieved from https://vancouver.ca/files/cov/budget-outlook-2019-2023.pdf

City of Vancouver. (2018b). *City of Vancouver Planning By-law Administration Bulletins Rainwater Management Bulletin*. Retrieved from https://vancouver.ca/docs/bulletins/Rainwater-Management-Bulletin.pdf

City of Vancouver. (2018c). *Engineering Design Manual*. Vancouver.

City of Vancouver. (2018d). *Report - 2019 Annual Review of Sewer Rates and Environmental Updates Under the Sewer & Watercourse By-law: 2018 Dec 11*. Vancouver. Retrieved from https://council.vancouver.ca/20181211/documents/spec1b.pdf

Clapp, R. B., & Hornberger, G. M. (1978). Empirical equations for some soil hydraulic properties. *Water Resources Research*, *14*(4), 601–604. https://doi.org/10.1029/WR014i004p00601

Conly, F. M., Crosley, R. W., & Headley, J. V. (2002). Characterizing sediment sources and natural hydrocarbon inputs in the lower Athabasca River, Canada. *Journal of Environmental Engineering and Science*, *1*(3), 187–199. https://doi.org/10.1139/s02-013

CVC. (2015). *LESSONS LEARNED : CVC Stormwater Management and Low Impact Development Monitoring and Performance Assessment Guide*.

CVC. (2016a). *Central Parkway Road Right-of-Way Retrofit Monitoring Plan CVC LID Demonstration Monitoring Projects: Central Parkway Monitoring Plan*.

CVC. (2016b). Central Parkway Road Right-of-Way Retrofit Technical Report.

CVC. (2016c). Elm Drive Road Right-of-Way Retrofit Technical Report.

CVC. (2016d). *TECHNICAL REPORT MONITORING RESULTS (2010-2012) RIVERWOOD BIOSWALE, CITY OF MISSISSAUGA*. MISSISSAUGA. Retrieved from https://cvc.ca/wp-content/uploads/2016/06/TechReport_Riverwood_Final.pdf

CVC. (2016e). *TECHNICAL REPORT MONITORING RESULTS (2013 –2015) IMAX, CITY OF MISSISSAUGA*. MISSISSAUGA. Retrieved from https://cvc.ca/wp-content/uploads/2016/06/TechReport_IMAX_Final.pdf

CVC. (2016f). *TECHNICAL REPORT MONITORING RESULTS (2015) CENTRAL PARKWAY, CITY OF MISSISSAUGA*. MISSISSAUGA. Retrieved from https://cvc.ca/wp-content/uploads/2016/06/TechReport_CPW_Final.pdf

Dane, J. H., Topp, C. G., Romano, N., & Santini, A. (2002). 3.3.3 Field. In *Methods of Soil*

Analysis: Part 4 Physical Methods (SSSA Book). Soil Science Society of America. https://doi.org/10.2136/sssabookser5.4.c26

Davis, A. P., Stagge, J. H., Jamil, E., & Kim, H. (2012). Hydraulic performance of grass swales for managing highway runoff. *Water Research*, *46*(20), 6775–6786. https://doi.org/10.1016/J.WATRES.2011.10.017

DeepRoot. (2016). CENTRAL PARKWAY CASE STUDY. Retrieved February 18, 2019, from https://www.deeproot.com/products/silva-cell/case-studies/central-boulevard.html

Deletic, A. (1998). The first flush load of urban surface runoff. *Water Research*, *32*(8), 2462–2470. https://doi.org/10.1016/S0043-1354(97)00470-3

Delleur, J. W. (2003). The Evolution of Urban Hydrology : Past , Present , and Future, *129*(8), 563–573.

Dey, P., Sundriyal, P., & Sahoo, S. K. (2017). Science of Lagging Behind- Hysteresis in Soil Moisture Characteristic Curve - A Review. *International Journal of Current Microbiology and Applied Sciences*, *6*(10), 151–156. https://doi.org/10.20546/ijcmas.2017.610.019

Dunne, T. (1975). Field studies of hillslope flow processes, in: M.J. Kirkby. *Wiley Intersience, Hillslope*, 227–293.

Dunne, T., & Leopold, L. B. (Luna B. (1978). *Water in environmental planning*. W.H. Freeman. Retrieved from http://webcat2.library.ubc.ca/vwebv/holdingsInfo?bibId=7093

Dutta, T., Kwon, E., Bhattacharya, S. S., Jeon, B. H., Deep, A., Uchimiya, M., & Kim, K. H. (2017). Polycyclic aromatic hydrocarbons and volatile organic compounds in biochar and biochar-amended soil: a review. *GCB Bioenergy*. https://doi.org/10.1111/gcbb.12363

Ebrahimian, A., Gulliver, J. S., & Wilson, B. N. (2016). Effective impervious area for runoff in urban watersheds. *Hydrological Processes*, *30*(20), 3717–3729.

https://doi.org/10.1002/hyp.10839

Ebrahimian, A., Wilson, B. N., & Gulliver, J. S. (2016). Improved methods to estimate the effective impervious area in urban catchments using rainfall-runoff data. *Journal of Hydrology*, *536*, 109–118. https://doi.org/10.1016/j.jhydrol.2016.02.023

Environment Canada. (2018). Historical Data - Climate - Environment and Climate Change Canada 2008-2018. Retrieved February 3, 2019, from http://climate.weather.gc.ca/historical_data/search_historic_data_e.html

Erickson, A. J., Weiss, P. T., & Gulliver, J. S. (2013). *Optimizing stormwater treatment practices: A handbook of assessment and maintenance*. *Optimizing Stormwater Treatment Practices: A Handbook of Assessment and Maintenance*. https://doi.org/10.1007/978-1-4614-4624-8

Espelund, M., & Klaveness, D. (2014). Botulism outbreaks in natural environments - an update. *Frontiers in Microbiology*, *5*, 287. https://doi.org/10.3389/fmicb.2014.00287

FAO. (2015). SALINE SOILS AND THEIR MANAGEMENT. Retrieved March 9, 2019, from http://www.fao.org/3/x5871e/x5871e04.htm

Fatahi, B., Khabbaz, H., & Indraratna, B. (2014). Modelling of unsaturated ground behaviour influenced by vegetation transpiration. *Geomechanics and Geoengineering*, *9*(3), 187–207. https://doi.org/10.1080/17486025.2014.880520

Ferré, T. P. A., & Warrick, A. W. (2005). Infiltration. *Encyclopedia of Soils in the Environment*, *1*(1977), 254–260. https://doi.org/10.1016/B0-12-348530-4/00382-9

Finkenbine, J. (1998). The Impact of Urbanization on Stream Habitat In Lower Mainland British Columba, (June).

FISRWG. (1998). *Stream Corridor Restoration: Principles, Processes, and Practices*. *Bridges*.

https://doi.org/-0-934213-59-3

Franzluebbers, A. J. (2002). Water infiltration and soil structure related to organic matter and its stratification with depth. *Soil and Tillage Research*, *66*(2), 197–205. https://doi.org/10.1016/S0167-1987(02)00027-2

Fundenburg, E. (2001). What Does Organic Matter Do In Soil? Retrieved April 7, 2019, from https://www.noble.org/news/publications/ag-news-and-views/2001/august/what-does-organic-matter-do-in-soil/

Gilman, Edward F.;Partin, T. (2007). Urban Design for a Wind Resistant Urban Forest. In *The Institute of Food and Agricultural Sciences* (Vol. ENH 1056, pp. 1–8). Retrieved from https://edis.ifas.ufl.edu/pdffiles/EP/EP30900.pdf

Grimmond, C. S. B., & Oke, T. R. (1986). Urban Water Balance 2. Results From a Suburb of Vancouver, British Columbia. https://doi.org/10.14288/1.0041948

Grisso, R., Mark Alley, W. G., Holshouser, D., & Thomason, W. (2009). Two Sensor Types Can Measure Soil EC. *Virginia Cooperative Extension*, *442–508*.

Hall, K. J. ;, & Schreier, H. ; (1996). Urbanization and agricultural intensification in the Lower Fraser River valley: Impacts on water use and quality. *GeoJournal*, *40*(2), 135–146. Retrieved from https://link-springer-com.ezproxy.library.ubc.ca/content/pdf/10.1007%2FBF00222539.pdf

Han, Y. M., Bandowe, B. A. M., Wei, C., Cao, J. J., Wilcke, W., Wang, G. H., … Yan, B. Z. (2015). Stronger association of polycyclic aromatic hydrocarbons with soot than with char in soils and sediments. *Chemosphere*, *119*, 1335–1345. https://doi.org/10.1016/j.chemosphere.2014.02.021

He, B., Dai, M., Huang, W., Liu, Q., Chen, H., & Xu, L. (2010). Sources and accumulation of organic carbon in the Pearl River Estuary surface sediment as indicated by elemental, stable carbon isotopic, and carbohydrate compositions. *Biogeosciences*, *7*(10), 3343–3362. https://doi.org/10.5194/bg-7-3343-2010

Henshaw, P. C., & Booth, D. B. (2000). Natural restabilization of stream channels in urban watersheds. *Journal of the American Water Resources Association*, *36*(6), 1219–1236. https://doi.org/10.1111/j.1752-1688.2000.tb05722.x

Hilhorst, M. A. (2000). A Pore Water Conductivity Sensor. *Soil Science Society of America Journal*, *64*(6), 1922. https://doi.org/10.2136/sssaj2000.6461922x

Hodge, A., Berta, G., Doussan, C., Merchan, F., & Crespi, M. (2009). Plant root growth, architecture and function. *Plant and Soil*. https://doi.org/10.1007/s11104-009-9929-9

Hoinaski, L., Franco, D., Haas, R., Martins, R. F., & Lisboa, H. de M. (2014). Investigation of rainwater contamination sources in the southern part of Brazil. *Environmental Technology*, *35*(7), 868–881. https://doi.org/10.1080/09593330.2013.854412

Hollis, G. E. (1975). The effect of urbanization on floods of different recurrence interval. *Water Resources Research*, *11*(3), 431–435. https://doi.org/10.1029/WR011i003p00431

Holthusen, D., Brandt, A. A., Reichert, J. M., & Horn, R. (2018). Soil porosity, permeability and static and dynamic strength parameters under native forest/grassland compared to no-tillage cropping. *Soil and Tillage Research*, *177*, 113–124. https://doi.org/10.1016/J.STILL.2017.12.003

Hopton, M., Simon, M., Michael Borst Ahjond Garmestani, P., Scott Jacobs Dennis Lye, J., William Shuster, P., & Jarnagin, T. (2015). *Green Infrastructure for Stormwater Control: Gauging Its Effectiveness with Community Partners*.

Horton, R. E. (1933). The Role of infiltration in the hydrologic cycle. *Transactions, American*

Geophysical Union, *14*(1), 446. https://doi.org/10.1029/TR014i001p00446

Huan, Z., Wang, H., Li, C., & Wan, C. (2017). The soil moisture sensor based on soil dielectric property. *Personal and Ubiquitous Computing*, *21*(1), 67–74. https://doi.org/10.1007/s00779-016-0975-z

Huber, M., Welker, A., & Helmreich, B. (2016). Critical review of heavy metal pollution of traffic area runoff: Occurrence, influencing factors, and partitioning. *Science of the Total Environment*. https://doi.org/10.1016/j.scitotenv.2015.09.033

IARC. (1983). *Polynuclear aromatic compounds, Part 1, Chemical, environmental and experimental data. IARC monographs on the evaluation of the carcinogenic risk of chemicals to humans* (Vol. 32). Retrieved from http://www.ncbi.nlm.nih.gov/pubmed/6586639

Iiyama, I. (2016). Differences between field-monitored and laboratory-measured soil moisture characteristics. *Soil Science and Plant Nutrition*, *62*(5–6), 416–422. https://doi.org/10.1080/00380768.2016.1242367

Jaishankar, M., Tseten, T., Anbalagan, N., Mathew, B. B., & Beeregowda, K. N. (2014, June). Toxicity, mechanism and health effects of some heavy metals. *Interdisciplinary Toxicology*. Slovak Toxicology Society. https://doi.org/10.2478/intox-2014-0009

Jiang, C., Li, J., Li, H., Li, Y., & Chen, L. (2017). Field Performance of Bioretention Systems for Runoff Quantity Regulation and Pollutant Removal. *Water, Air, and Soil Pollution*, *228*(12). https://doi.org/10.1007/s11270-017-3636-6

Jin, J. (2016). *Green Stormwater Infrastructure on City Streets*. *The University of British Columbia*.

Kilpatrick, F. A. (1965). Hydraulic Measurments and Computations. In *Surface Water*

Techniques (1st ed., Vol. 1, pp. 1–27). United States Department of the Interior Geological Survey. Retrieved from https://pubs.usgs.gov/unnumbered/70039153/report.pdf

Kimbrough, D. R. (2006). Salting Roads. *ChemMatters*, (February), 14–16. Retrieved from http://chemistry.org/education/chemmatters.html

Klein, R. D. (1979). Urbanization and Stream Quality Impairment. *Journal of the American Water Resources Association (JAWRA)*, *15*(4), 948–963. https://doi.org/10.1111/j.1752-1688.1979.tb01074.x

Kokkonen, T. V., Grimmond, C. S. B., Christen, A., Oke, T. R., & Järvi, L. (2018, September 1). Changes to the Water Balance Over a Century of Urban Development in Two Neighborhoods: Vancouver, Canada. *Water Resources Research*, pp. 6625–6642. https://doi.org/10.1029/2017WR022445

Kuichling, E. (1889). The Relation Between the Rainfall and the Discharge of Sewers in Populous Districts. *Transactions of the American Society of Civil Engineers*, *XX*(1), 1–56.

Lee, J. G., & Heaney, J. P. (2003). Estimation of Urban Imperviousness and its Impacts on Storm Water Systems. *Journal of Water Resources Planning and Management*, *129*(5), 419–426. https://doi.org/10.1061/(ASCE)0733-9496(2003)129:5(419)

Leopold, L. B. (1968). *Hydrology for Urban land Planning - A Guidebook on the Hydrologic Effects of Urban Land Use* (GEOLOGICAL). U.S. Department of the Interior. Retrieved from https://pubs.usgs.gov/circ/1968/0554/report.pdf

Li, M.-H., & Barrett, M. E. (2008). Relationship Between Antecedent Dry Period and Highway Pollutant: Conceptual Models of Buildup and Removal Processes. *Water Environment Research*, *80*(8), 740–747. https://doi.org/10.2175/106143008X296451

Li, T. (2007). *Trace Metals in Urban Stormwater Runoff and their Management*. The University of British Columbia.

Ligtenberg, J. (2017). *Runoff changes due to urbanization: A review*. Umeå. Retrieved from https://www.diva-portal.org/smash/get/diva2:1067287/FULLTEXT01.pdf

Liu, Y., Ahiablame, L. M., Bralts, V. F., & Engel, B. A. (2015). Enhancing a rainfall-runoff model to assess the impacts of BMPs and LID practices on storm runoff. *Journal of Environmental Management*. https://doi.org/10.1016/j.jenvman.2014.09.005

Liu, Y., Bralts, V. F., & Engel, B. A. (2015). Evaluating the effectiveness of management practices on hydrology and water quality at watershed scale with a rainfall-runoff model. *Science of the Total Environment*. https://doi.org/10.1016/j.scitotenv.2014.12.077

Lloyd, S. D., Wong, T. H. F., & Chesterfield, C. J. (2002). *WATER SENSITIVE URBAN DESIGN-A STORMWATER MANAGEMENT PERSPECTIVE by*. Retrieved from www.catchment.crc.org.au/publications

Ludwig, J. H., & Ludwig, R. G. (1951). Design of Palmer-Bowlus Flumes. *Source: Sewage and Industrial Wastes*. Retrieved from http://www.jstor.org/stable/25031687

Ludwig, R. G., & Parkhurst, J. D. (1974). Simplified Application of Palmer-Bowlus Flow Meters. *Source Journal (Water Pollution Control Federation)*, *46*(12), 2764–2769. https://doi.org/10.1177/2325967116679640

Margulis, S. (2017). *Introduction to Hydrology* (2017A ed.). California: University of California Los Angeles. Retrieved from https://ucla.app.box.com/v/Intro-to-Hydrology-pdf

Marosz, A., & Nowak, J. S. (2008). Effect of salinity stress on growth and macroelements uptake of four tree species. *Dendrobiology*, *59*(January 2008), 23–29.

Mccallum, D. W. (1995). *AN EXAMINATION OF TRACE METAL CONTAMINATION AND LAND USE IN AN URBAN WATERSHED*. The University of British Columbia.

McKenzie, E. R., Money, J. E., Green, P. G., & Young, T. M. (2009). Metals associated with stormwater-relevant brake and tire samples. *Science of the Total Environment*, *407*(22), 5855–5860. https://doi.org/10.1016/j.scitotenv.2009.07.018

McLeod, A. I. (2011). Kendall: Kendall rank correlation and Mann-Kendall trend test. R package version 2.2. Retrieved March 5, 2019, from http://www.stats.uwo.ca/faculty/aim

Mesner, N., & Geiger, J. (2010). *What is phosphorus?* Logan. Retrieved from https://extension.usu.edu/waterquality/files-ou/Watershed-information/NR_WQ_2005-Phosphorus.pdf

Meter. (2002). *Em50 User Manual*.

Meter. (2018). *Teros 12 User Manual*.

Metro Vancouver. (2010). *Integrated Liquid Waste and Resource Management - A Liquid Waste Management Plan*. Burnaby. Retrieved from http://www.metrovancouver.org/services/liquid-waste/LiquidWastePublications/IntegratedLiquidWasteResourceManagementPlan.pdf

Metro Vancouver. (2014). *Monitoring and Adaptive Management Framework for Stormwater*. Burnaby. Retrieved from http://www.metrovancouver.org/services/liquid-waste/LiquidWastePublications/Monitoring_Adaptive_Management_Framework_for_Stormwater.pdf

Metro Vancouver. (2018). About Us: Metro Vancouver. Retrieved January 26, 2019, from http://www.metrovancouver.org/about/Pages/default.aspx

Miller, J. D., Kim, H., Kjeldsen, T. R., Packman, J., Grebby, S., & Dearden, R. (2014). Assessing the impact of urbanization on storm runoff in a peri-urban catchment using historical change in impervious cover. *Journal of Hydrology*, *515*, 59–70.

https://doi.org/10.1016/J.JHYDROL.2014.04.011

Munck, I. A., Bennett, C. M., Camilli, K. S., & Nowak, R. S. (2010). Long-term impact of de-icing salts on tree health in the Lake Tahoe Basin: Environmental influences and interactions with insects and diseases. *Forest Ecology and Management*, *260*(7), 1218–1229. https://doi.org/10.1016/j.foreco.2010.07.015

NH DES. (2008). *NH DES Stormwater Manual Volume 1: Stormwater and Antidegradation* (Vol. 1).

Novotny, V., & Olem, H. (1994). *Water Quality: Prevention, Identification and Management of Diffuse Pollution*. *Wiley* (Vol. 162). New York. https://doi.org/0442005598

Oke, T., & Hay, J. (1994). *The Climate of Vancouver* (2nd ed., Vol. 38). Vancouver: University of British Columbia. Retrieved from http://webcat1.library.ubc.ca/vwebv/holdingsInfo?bibId=985733

Oke, T. R., Mills, G., Christen, A., & Voogt, J. A. (2017). *Urban climates*. *Urban Climates*. Cambridge: Cambridge University Press. https://doi.org/10.1017/9781139016476

Onset. (2019). HOBO U20 Water Level Data Logger 13 feet. Retrieved February 17, 2019, from https://www.onsetcomp.com/products/data-loggers/u20-001-04

Ordóñez-Barona, C., Sabetski, V., Millward, A. A., & Steenberg, J. (2018). De-icing salt contamination reduces urban tree performance in structural soil cells. *Environmental Pollution*, *234*, 562–571. https://doi.org/10.1016/j.envpol.2017.11.101

Page, J. L., Winston, R. J., Mayes, D. B., Perrin, C., & Hunt, W. F. (2015). Retrofitting with innovative stormwater control measures: Hydrologic mitigation of impervious cover in the municipal right-of-way. *Journal of Hydrology*. https://doi.org/10.1016/j.jhydrol.2015.04.046

PCIC. (2012). Plan2Adapt - Notes. Retrieved April 4, 2019, from https://www.pacificclimate.org/analysis-tools/plan2adapt

Potter, M., Wiggert, D., Ramadan, B., & Shih, T. (2012). *Mechanics of Fluids 4th Edition* (4th ed.). Stamford: Cengage Learning.

Pour, S. (2013). *Implementing a neighbourhood scale stormwater retrofit : effect of self-draining rain barrels on an urban stream*. THE UNIVERSITY OF BRITISH COLUMBIA.

Precision Identification Biological Consultants. (1997). *Wild, Threatened, Endangered, and Lost streams of the Lower Fraser Valley Summary Report*. Vancouver.

Province of British Columbia. (2018). Welcome to the Lower Mainland Region. Retrieved May 27, 2018, from http://www.env.gov.bc.ca/lower-mainland/

PWD. (2016). *Appendix A Completed Green Stormwater Infrastructure Projects*. Philadelphia. Retrieved from http://phillywatersheds.org/doc/Year5_EAPCombinedAppendices_website.pdf

Radcliffe, D., Hayden, T., Walson, K., Crowley, P., & Phillips, R. E. (1980). Simulation of soil water within the root zone of a corn crop. *Agron. J.*, *72*(1), 19–24.

Rinderer, M., & Seibert, J. (2012). Soil Information in Hydrologic Models : Hard Data , Soft Data , and the Dialog between Experimentalists and Modelers. In *Hydropedology*. (First, pp. 515–536). 16: Academic Press, Inc. https://doi.org/10.1016/B978-0-12-386941-8.00016-0

Rindosh, S. E. (2016). *An Analysis of Hydraulic Monitoring Equipment for Inflow and Outflow Structures in Urban SCMs*. Villanova University.

Saget, A., Chebbo, G., & Bertrand-Krajewski, J.-L. (1996). The first flush in sewer systems. *Water Science and Technology*, *33*(9), 101–108. https://doi.org/10.1016/0273-

1223(96)00375-7

Saxton, K. E., & Rawls, W. J. (2006). Soil Water Characteristic Estimates by Texture and Organic Matter for Hydrologic Solutions. *Soil Science Society of America Journal*, *70*(5), 1569. https://doi.org/10.2136/sssaj2005.0117

Scanes, C. G. (2018). *Animal Domestication , and Early Forms of Animal Agriculture*. *Animals and Human Society*. Elsevier Inc. https://doi.org/10.1016/B978-0-12-805247-1/00006-X

Schifman, L. A., Herrmann, D. L., Shuster, W. D., Ossola, A., Garmestani, A., & Hopton, M. E. (2017). Situating Green Infrastructure in Context: A Framework for Adaptive Socio-Hydrology in Cities. *Water Resources Research*, *53*(12), 10139–10154. https://doi.org/10.1002/2017WR020926

Schmidt, N. (2017). *BIOSWALE MODELING IN A TRANSITIVE URBAN TRANSPORTATION SETTING: Green Infrastructure Instrumentation, Challenges, and Lessons Learned*. *Villanova University*. Villanova University.

Scholz, N. L., Myers, M. S., McCarthy, S. G., Labenia, J. S., McIntyre, J. K., Ylitalo, G. M., … Collier, T. K. (2011). Recurrent die-offs of adult coho salmon returning to spawn in Puget Sound lowland urban streams. *PLoS ONE*, *6*(12), e28013. https://doi.org/10.1371/journal.pone.0028013

Schueler, T. R. (1987). *Controlling Urban Runoff: a practical manual for planning and designing BMPs*. Washington, D.C.

Senix Corporation. (2010). ToughSonic® 14 Level & Distance Sensor, 1–2.

Senix Corporation. (2015). ToughSonic ® Series Product Manual.

Sickman, J. O., Zanoli, M. J., & Mann, H. L. (2007). Effects of urbanization on organic carbon loads in the Sacramento River, California. *Water Resources Research*, *43*(11), 11422.

https://doi.org/10.1029/2007WR005954

Sławiński, C. (2011). Hysteresis in soil. In *Encyclopedia of Earth Sciences Series* (Vol. Part 4, pp. 385–387). Springer, Dordrecht. https://doi.org/10.1007/978-90-481-3585-1_72

Smith, S. A., & Bella, D. A. (1973). Dissolved Oxygen and Temperature in a Stratified Lake. *Journal (Water Pollution Control Federation)*. https://doi.org/10.2307/25037715

Spinello, A., & Simmons, D. (1992). Base flow of 10 south-shore streams, Long Island, New York, 1976-85, and the effects of urbanization on base flow and flow duration. *USGS Water Resources Investigations Report 90-4205*, 1–39.

Spromberg, J. A., Baldwin, D. H., Damm, S. E., Mcintyre, J. K., Huff, M., Sloan, C. A., … Scholz, N. L. (2016). Coho salmon spawner mortality in western US urban watersheds: Bioinfiltration prevents lethal storm water impacts. *Journal of Applied Ecology*, *53*(2), 398–407. https://doi.org/10.1111/1365-2664.12534

Statistics Canada. (2017). Focus on Geography Series, 2016 Census: City of Vancouver. Retrieved February 1, 2019, from https://www12.statcan.gc.ca/census-recensement/2016/as-sa/fogs-spg/Facts-csd-eng.cfm?LANG=Eng&GK=CSD&GC=5915022&TOPIC=1

Stephens, K. A. (2002). *Stormwater Planning: A Guidebook for British Columbia*.

Stime, S. E. (2014). *Source Controls for Runoff Treatment: Hydrologic Response and Water Quality Attenuation*. University of British Columbia.

Straus, D. L., & Tucker, C. s. (1993). Acute Toxicity of Copper Sulfate and Chelated Copper to Channel Catfish Ictalurus punctatus. *Journal of the World Aquaculture Society*, *24*(3), 390–395. https://doi.org/10.1111/j.1749-7345.1993.tb00170.x

Susdrain. (2018). *Case study Howard Street, Salford, Manchester*. Retrieved from www.susdrain.org

Sussmann, C. G. (2012). *Toward the Sustainable City: Vancouver's Southeast False Creek*. University of British Columbia. https://doi.org/10.14288/1.0073098

Te Chow, V. (1959). Open channel hydraulics., 1–26.

Thompson, D. B. (2006). The Rational Method. *Engineering Hydrology*, (January), 21. https://doi.org/http://drdbthompson.net/writings/rational.pdf

Timoney, K. P., & Lee, P. (2011). Polycyclic aromatic hydrocarbons increase in athabasca river delta sediment: Temporal trends and environmental correlates. *Environmental Science and Technology*, *45*(10), 4278–4284. https://doi.org/10.1021/es104375d

UN. (2017). World Population Prospects: The 2017 Revision. Retrieved September 25, 2018, from https://www.un.org/development/desa/publications/world-population-prospects-the-2017-revision.html

UN. (2018). 68% of the world population projected to live in urban areas by 2050, says UN. Retrieved September 25, 2018, from https://www.un.org/development/desa/en/news/population/2018-revision-of-world-urbanization-prospects.html

University of the West of England. (2012). *The Multifunctionality of Green Infrastructure*. *Science for Environment Policy*.

Urban, J. (2013). Two Different Approaches to Improve Growing Conditions for Trees Comparing Silva Cells and Structural Soil. *American Society of Consulting Arborists*, *46*(2), 5–14. Retrieved from https://static1.squarespace.com/static/52ec31b2e4b04eb0bbd9c075/t/533b63c8e4b07f69c06bb3b0/1396401096862/asca_newsletter.pdf

US EPA. (1999a). Combined Sewer Overflow Management Fact Sheet Sewer Separation.

Environmental Protection Agency, *EPA 832-F-*. Retrieved from https://www3.epa.gov/npdes/pubs/sepa.pdf

US EPA. (1999b). *Combined Sewer Overflows Guidance for Monitoring and Modeling*. Washington, D.C.: United States Environmental Protection Agency. Retrieved from https://nepis.epa.gov/Exe/ZyNET.exe/20004344.TXT?ZyActionD=ZyDocument&Client=EPA&Index=1995+Thru+1999&Docs=&Query=&Time=&EndTime=&SearchMethod=1&TocRestrict=n&Toc=&TocEntry=&QField=&QFieldYear=&QFieldMonth=&QFieldDay=&IntQFieldOp=0&ExtQFieldOp=0&XmlQuery=

US EPA. (2004). *SEWER SEDIMENT AND CONTROL: A MANAGEMENT PRACTICES REFERENCES GUIDE*. Washington DC. Retrieved from https://cfpub.epa.gov/si/si_public_record_report.cfm?Lab=NRMRL&dirEntryId=84068

US EPA. (2005). *National Management Measures to Control Nonpoint Source Office of Water* (EPA-841-B-). Washington, DC: US EPA.

US EPA. (2018). What is Green Infrastructure? Retrieved October 7, 2018, from https://www.epa.gov/green-infrastructure/what-green-infrastructure

US EPA. (2019). Storm Water Management Model (SWMM). Retrieved February 17, 2019, from https://www.epa.gov/water-research/storm-water-management-model-swmm

Van Den Bosch, B. E., Snellen, W. B., Brouwer, C., & Hatcho, N. (1993). Flow Measurement. In *Structures for water control and distribution* (pp. 29–37). Food and Agriculture Organization of the United Nations.

Vega, O., & Lukes, R. (2018). *Application of Stormwater Tree Trenches in the City of Vancouver*. *University of British Columbia Sustainability*. Vancouver.

VPC. (2018). Palmer Bowlus Flumes - VPC Fiberglass - Virtual Polymer Compounds. Retrieved

February 17, 2019, from http://www.vpcfiberglass.com/palmer_bowlus_flume.shtml

Walsh, C. J. (2004). Protection of in-stream biota from urban impacts: minimise catchment imperviousness or improve drainage design?, *55*, 317–326. https://doi.org/10.1071/MF03206

Water Protection & Sustainability Branch. (2018). Approved Water Quality Guidelines - Province of British Columbia. Retrieved February 20, 2019, from https://www2.gov.bc.ca/gov/content/environment/air-land-water/water/water-quality/water-quality-guidelines/approved-water-quality-guidelines

Welker, a L., Mandarano, L., Greising, K., & Mastrocola, K. (2013). Application of a Monitoring Plan for Storm-Water Control Measures in the Philadelphia Region. *Journal of Environmental Engineering*, *139*(August), 1108–1118. https://doi.org/10.1061/(asce)ee.1943-7870.0000714

White, M. D., & Greer, K. A. (2006). The effects of watershed urbanization on the stream hydrology and riparian vegetation of Los Peñasquitos Creek, California. *Landscape and Urban Planning*, *74*(2), 125–138. https://doi.org/10.1016/j.landurbplan.2004.11.015

Winston, R. J., Dorsey, J. D., & Hunt, W. F. (2016). Quantifying volume reduction and peak flow mitigation for three bioretention cells in clay soils in northeast Ohio. *Science of the Total Environment*, *553*, 83–95. https://doi.org/10.1016/j.scitotenv.2016.02.081

Wojtenko, I., Minamyer, S., Tafuri, A. N., Field, R., & Lai, F. (2004). CSO Considerations. In *Management of Combined Sewer Overflows* (1st ed., p. 272). CRC Press.

Wurtsbaugh, W. A. (n.d.). *Relationships between eutrophication, cyanobacteria blooms and avian botulism mortalities in the Great Salt Lake*. *Watershed Sciences Faculty Publications Watershed Sciences*. Retrieved from https://digitalcommons.usu.edu/wats_facpub/880

Xiao, Q., & Mcpherson, E. G. (2011). Urban Water Journal Performance of engineered soil and trees in a parking lot bioswale. https://doi.org/10.1080/1573062X.2011.596213

Yang, B., & Li, S. (2013). Green Infrastructure Design for Stormwater Runoff and Water Quality: Empirical Evidence from Large Watershed-Scale Community Developments. *Water*, *5*(4), 2038–2057. https://doi.org/10.3390/w5042038

Young, A., Kochenkov, V., McIntyre, J. K., Stark, J. D., & Coffin, A. B. (2018). Urban stormwater runoff negatively impacts lateral line development in larval zebrafish and salmon embryos. *Scientific Reports*, *8*(1), 2830. https://doi.org/10.1038/s41598-018-21209-z

Zimmer, C. (2016). How the First Farmers Changed History. *New York Times*. Retrieved from https://www.nytimes.com/2016/10/18/science/ancient-farmers-archaeology-dna.html

Appendices

Left blank intentionally

Appendix A: **Wilting point and field capacity by soil texture summary table**

This table was adapted from Saxton and Rawls (2006). The VWC contain 2.5% organic matter. The results were not adjusted for gravel content, density, or salinity changes. These values were utilized to produce Figure 2.1.

Texture	**Composition (%w)**		**Wilting Point (VWC%)**	**Field Capacity (VWC%)**	**Available Water in (VWC%)**	**Saturation in VWC%**	**K_{sat}**	**Matric Density**
	Sand	**Clay**	**@ 1,500 kPa**	**@ 33 kPa**		**@ 0kPa**	**mm/h**	**g/cm**
Sand	88	5	5	10	5	46	108.10	1.43
Loamy Sand	80	5	5	12	7	46	96.70	1.43
Sandy Loam	65	10	8	18	10	45	50.30	1.46
Loam	40	20	14	28	14	46	15.50	1.43
Silty Loam	20	15	11	31	20	48	16.10	1.38
Silt	10	5	6	30	24	48	22.00	1.38
Sandy Clay Loam	60	25	17	27	10	43	11.30	1.50
Clay Loam	30	35	22	36	14	48	4.30	1.39
Silty Clay Loam	10	35	22	38	16	51	5.70	1.30
Silty Clay	10	45	27	41	14	52	3.70	1.26
Sandy Clay	50	40	25	36	11	44	1.40	1.47
Clay	25	50	30	42	12	50	1.10	1.33

Appendix B: Water quality performance results

B.1 Bioswales

Location	Site	Average Pollutant Removal Efficiencies															Source
		Heavy Metals							Nutrients		TSS	DO	TOC	Hardness	pH	EC	
		Al	Cd	Cu	Fe	Ni	Pb	Zn	N	P							
Maple Ridge, BC (CA)	Silver Valley	79%	N/A	N/A	84%	29%	N/A	N/A	TKN 38-63%, NOx -81%	TP 63-70%	92%	N/A	53%	-170%	Decrease	N/A	(Stime, 2014)
Mississagua, ON (CA)	Lakeview Drive (LV-2)	N/A	72%	65%	73%	78%	70%	98%	TKN 68.3%, NOx 14.5%	TP 69.1%	72%	N/A	N/A	N/A	N/A	N/A	(Bradford, 2016)
	Lakeview Drive (LV-4)	N/A	91%	90%	95%	39%	96%	75%	TKN 86.2%, NOx 67.3%	TP 82.5%	93%	N/A	N/A	N/A	N/A	N/A	
	Elm Drive	N/A	90%	89%	N/A	96%	95%	95%	TKN 91.1%, NOx 60%	TP 91%, Ortho 85.6%	88%	N/A	N/A	N/A	N/A	N/A	(CVC, 2016c)
	IX-2	N/A	N/A	91%	N/A	N/A	N/A	98%	TKN 85%, NOx 84%	TP 85%	97%	N/A	N/A	N/A	N/A	N/A	(CVC, 2016e)
	IX-3	N/A	N/A	89%	N/A	N/A	N/A	98%	TKN 79%, NOx 67%	TP 60%	98%	N/A	N/A	N/A	N/A	N/A	
	IX-4	N/A	N/A	86%	N/A	N/A	N/A	97%	TKN 74%, NOx 66%	TP 60%	97%	N/A	N/A	N/A	N/A	N/A	
	Riverwood (<25mm rain)	N/A	N/A	90%	N/A	N/A	N/A	96%	TKN 79%, NOx 86%	TP 70%	91%	N/A	N/A	N/A	N/A	N/A	(CVC, 2016d)
	Riverwood (>25mm rain)	N/A	N/A	89%	N/A	N/A	N/A	95%	TKN 74%, NOx 85%	TP 55%	86%	N/A	N/A	N/A	N/A	N/A	
Davis, SA (USA)	UCLA Davis	N/A	N/A	N/A	86%	N/A	N/A	87%	TN 97%	TP 95%	95%	N/A	95%	N/A	N/A	N/A	(Xiao & Mcpherson, 2011)
Melbourne (AUS)	Lynbrook	N/A	N/A	N/A	N/A	N/A	N/A	N/A	TN 70%, TKN N/A	TP 47%	60%	N/A	N/A	N/A	N/A	N/A	(Lloyd et al., 2002)
Tongde Jiayuan, Xi'an (CH)	Bioswale A	N/A	N/A	N/A	N/A	N/A	N/A	N/A	TN 61.37%; NOx 61.59%	TP 61.06%	73%	N/A	N/A	N/A	N/A	N/A	(Jiang et al., 2017)
	Bioswale A	N/A	N/A	N/A	N/A	N/A	N/A	N/A	TN 76.67%; NOx 85.53%	TP 78.54%	88%	N/A	N/A	N/A	N/A	N/A	

B2 Stormwater Tree Trenches

Location	Site	STT Type	Average Pollutant Removal Efficiencies															Source
			Heavy Metals							Nutrients		TSS	DO	TOC	Hardness	pH	EC	
			Al	Cd	Cu	Fe	Ni	Pb	Zn	N	P							
Toronto, ON (CA)	Queensway	Soil Cell	45-88.6%	N/A	44.02-62.54%	84.84-88.57%	57.77-78.59%	80.57-91.94%	57.34-71.15%	Nitrate -1.32-53.33%	TP 52.64-61.7%	76.92-95%	N/A	N/A	N/A	N/A	N/A	(Cheung & Anderton, 2016)
Toronto, ON (CA)	Mississagua, ON (CA)	Soil Cell	N/A	N/A	>88%	~70-88%	71%	N/A	>88%	NOx ~40%	TP >88%	~80-98%	N/A	N/A	N/A	N/A	N/A	(DeepRoot, 2016; Vega & Lukes, 2018)
Raleigh, NC (USA)	Orange St and Anne St	Soil Cell	N/A	N/A	>86%	N/A	N/A	>86%	>86%	TKN 72-84%, NOx 35-70%	TP >72%, Ortho 72-82%	N/A	N/A	N/A	N/A	N/A	N/A	(Page et al., 2015)

Appendix C: **As-build drawing of the three GI practices investigated**

Quebec & 1st Ave Precinct Improvements

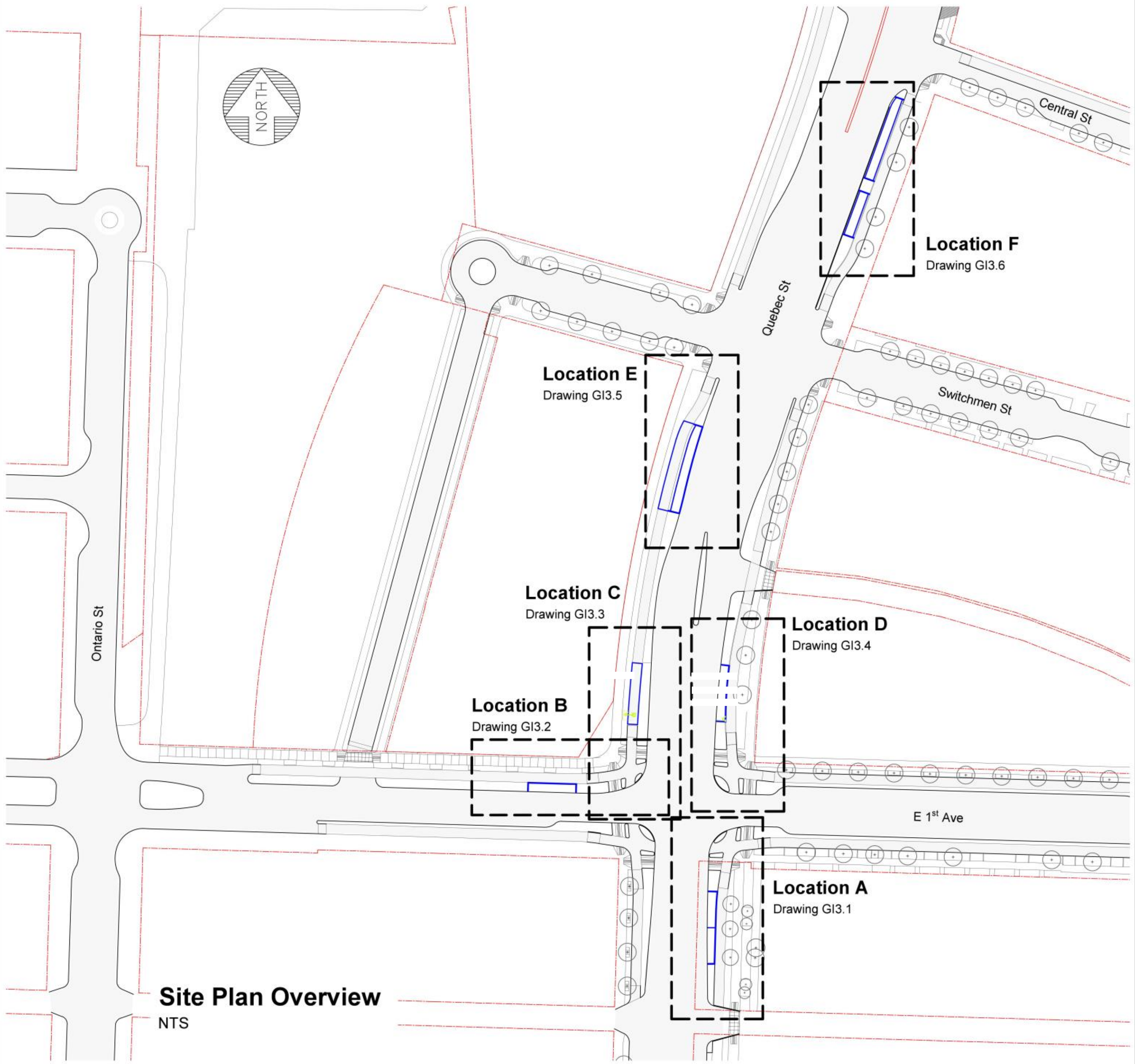

As-Built Drawings

Drawing List:

Protection of Green Infrastructure Practices

Any construction activity that would impact the condition, infiltration capabilities, or general plant health of Green Infrastructure (GI) practices shall require the below protective measures:

- Flow control at inlet/outlet - sandbags shall be placed at each inlet and outlet of the GI practice. A sufficient number of sandbags shall be placed to completely block flow from entering the GI practice.
- Debris and dust control - plastic tarps shall be placed and secured over the GI practice to prevent debris and excessive dust resulting from construction from settling into the engineered soil and obstructing infiltration and harming vegetation.
- Storage of construction materials, disposing of construction waste or effluent, or illegal dumping within the GI practice is strictly prohibited.

Common contaminants include, but are not limited to, runoff from wet saw-cutting of sidewalks or roadways, runoff seeping from stockpiled soils or materials, debris from street milling activities, dust and other fine particles, general construction litter and debris. Excessive damage may result in loss of functionality and will require reconstruction of the GI practice.

Maintenance and Removal

GI practices shall remain protected, closed, and all protection measures will remain in place and maintained until the construction activity is complete and the GI Branch has accepted the GI for being opened up to rainwater runoff.

CITY OF VANCOUVER

APPROVALS	INITIALS	CONTACT
LANDSCAPE ARCHITECT		
PROJECT ENGINEER		
CONSTRUCTION COORDINATOR		

REVISIONS / DESCRIPTION	INITIALS
Rev 0. Final Drawing issued for Construction	
ACCOUNT #:	
DIRECTORY: H:\GREEN INFRASTRUCTURE\13-8100-40 - Green Infrastructure Case Files\ENG - GI - Quebec and 1st Precinct Upgrades\11 - Design\	

ENGINEERING SERVICES – CITY OF VANCOUVER – GREEN INFRASTRUCTURE

DESIGNED BY:	Quebec and 1st Ave Precinct Improvements	SCALE: As shown
DRAFTED BY:	Green Infrastructure	DATE: March 2018
CHECKED BY:	Cover Sheet and Drawing Index	DWG. NO. 2008-63-D-GI2 AB
FILE NAME: ENG - GI - Quebec St Reconstruction_AS-BUILT.dwg		REV. NO. 0
		SHEET: 1 OF 7

FILE: H:\GREEN INFRASTRUCTURE\13-8100-40 - Green Infrastructure Case Files\ENG - GI - Quebec and 1st Precinct Upgrades\11 - Design\ENG - GI - Quebec St Reconstruction_AS-BUILT.dwg DATE Oct 16, 2018 - 2:00pm USER:emapi

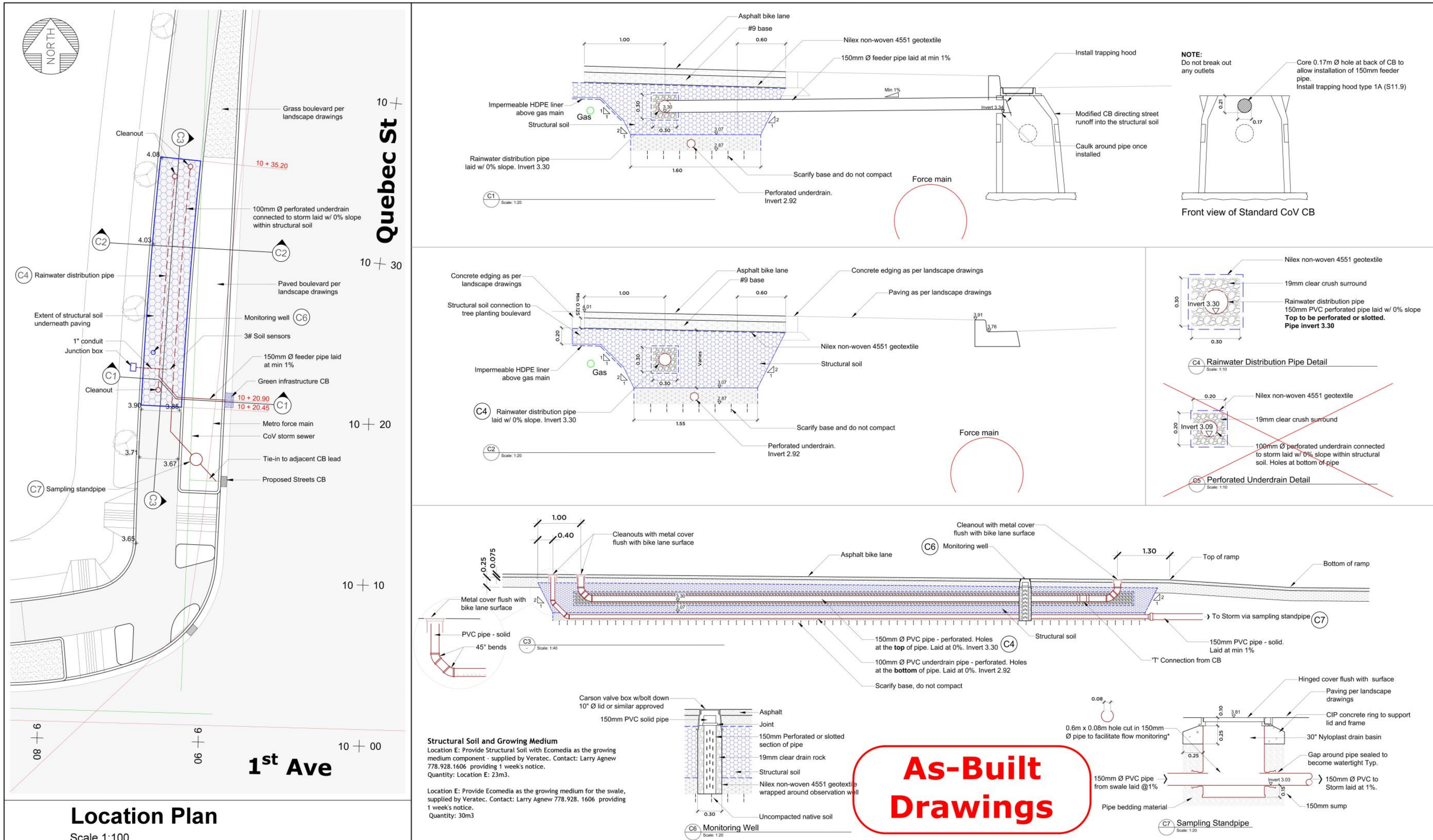

APPROVALS	INITIALS	CONTACT
LANDSCAPE ARCHITECT		
PROJECT ENGINEER		
CONSTRUCTION COORDINATOR		

CITY OF VANCOUVER

REVISIONS / DESCRIPTION	INITIALS
Rev 2 Standpipe invert and cover elevation amended April 2018	
Rev 3 Standpipe installation amended. Additional JB and conduit for monitoring May 2018	
ACCOUNT #:	
DIRECTORY: H:\GREEN INFRASTRUCTURE\13-8100-40 - Green Infrastructure Case Files\ENG - GI - Quebec and 1st Precinct Upgrades\11 - Design\	

ENGINEERING SERVICES – CITY OF VANCOUVER – GREEN INFRASTRUCTURE

DESIGNED BY:
DRAFTED BY:
CHECKED BY:
FILE NAME: ENG - GI - Quebec St Reconstruction_AS-BUILT.dwg

Quebec and 1st Ave Precinct Improvements
Green Infrastructure
Location C - Plan and Sections

SCALE:	As shown
DATE:	March 2018
DWG. NO.	2008-63-D-GI3.3 AB
REV. NO.	3
SHEET:	4 OF 7

FILE: H:\GREEN INFRASTRUCTURE\13-8100-40 - Green Infrastructure Case Files\ENG - GI - Quebec and 1st Precinct Upgrades\11 - Design\ENG - GI - Quebec St Reconstruction_AS-BUILT.dwg DATE Oct 16, 2018 - 3:27pm USER:enapi

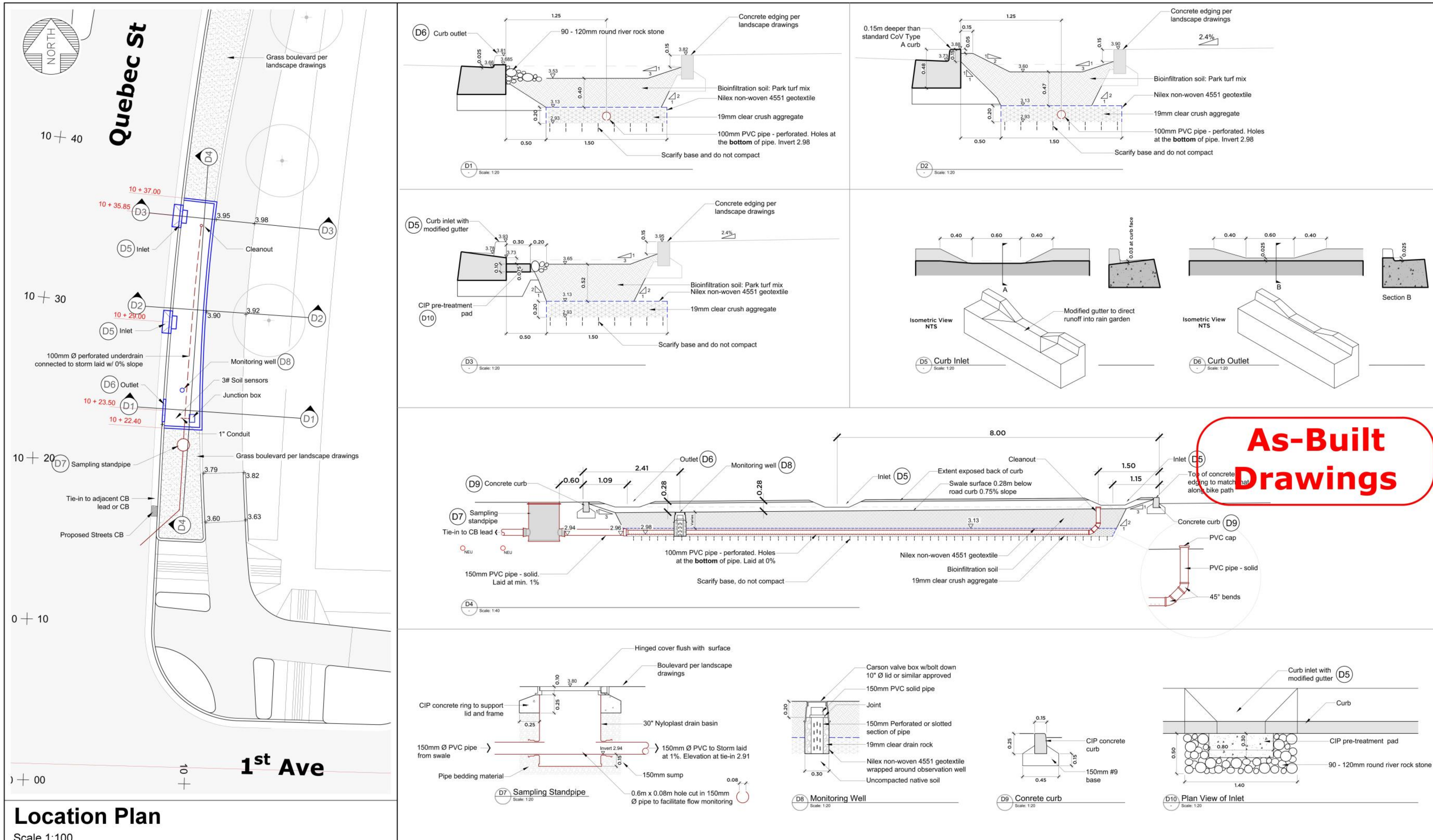

APPROVALS	INITIALS	CONTACT
LANDSCAPE ARCHITECT		
PROJECT ENGINEER		
CONSTRUCTION COORDINATOR		

CITY OF VANCOUVER

REVISIONS / DESCRIPTION	INITIALS
Rev 0 Final Drawing Issued for Construction	
Rev 1 Elevation of underdrain raised May 15 2018	
ACCOUNT #:	
DIRECTORY: H:\GREEN INFRASTRUCTURE\13-8100-40 - Green Infrastructure Case Files\ENG - GI - Quebec and 1st Precinct Upgrades\11 - Design	

ENGINEERING SERVICES – CITY OF VANCOUVER – GREEN INFRASTRUCTURE

DESIGNED BY:
DRAFTED BY:
CHECKED BY:
FILE NAME: ENG - GI - Quebec St Reconstruction_AS-BUILT.dwg

Quebec and 1st Ave Precinct Improvements
Green Infrastructure
Location D - Plan and Sections

SCALE: As shown
DATE: March 2018
DWG. NO. 2008-63-D-GI3.4 AB
REV. NO. 1
SHEET: 5 OF 7

FILE: H:\GREEN INFRASTRUCTURE\13-8100-40 - Green Infrastructure Case Files\ENG - GI - Quebec and 1st Precinct Upgrades\11 - Design\ENG - GI - Quebec St Reconstruction_AS-BUILT.dwg DATE:Oct 16, 2018 - 3:29pm USER:enapl

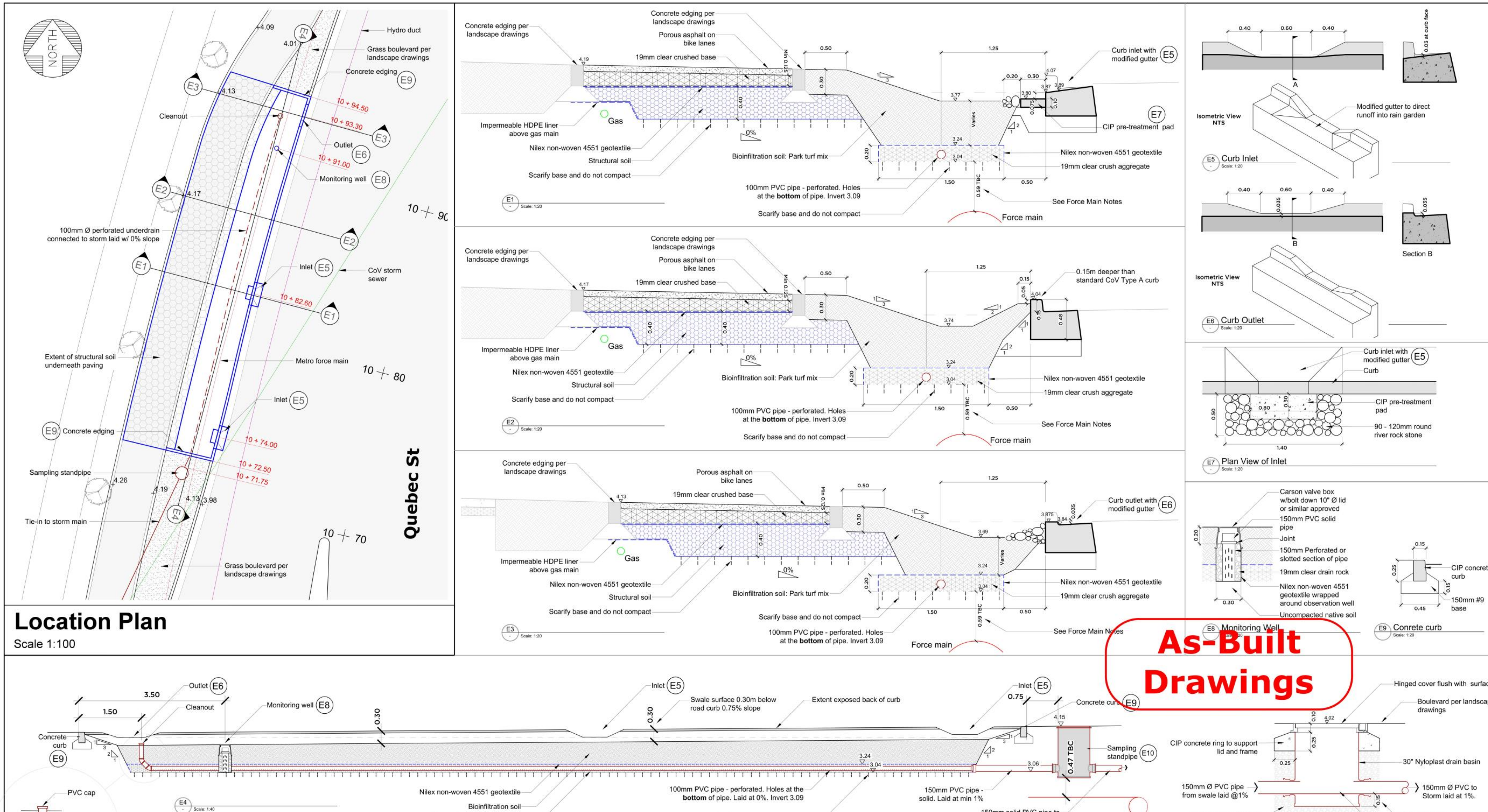

Structural Soil and Growing Medium

Location E: Provide Structural Soil with Ecomedia as the growing medium component - supplied by Veratec. Contact: Larry Agnew 778.928.1606 providing 1 week's notice.
Quantity: 23m3.

Location E: Provide Ecomedia as the growing medium for the swale, supplied by Veratec. Contact: Larry Agnew 778.928. 1606 providing 1 week's notice.
Quantity: 30m3

Force Main Notes:

1. Daylight Force Main (using hydroexcavator) to confirm pipe depth at two locations. Please provide 48 hours advance notice so that Metro Vancouver staff can be on site to inspect.

CITY OF VANCOUVER

APPROVALS	INITIALS	CONTACT
LANDSCAPE ARCHITECT		
PROJECT ENGINEER		
CONSTRUCTION COORDINATOR		

REVISIONS / DESCRIPTION	INITIALS
Rev 3 Tie-in to storm main moved to south end of practice April 2018	
Rev 4 Structural soil/growing medium supply details/Sampling standpipe amended May 2018	
ACCOUNT #:	
DIRECTORY: H:\GREEN INFRASTRUCTURE\13-8100-40 - Green Infrastructure Case Files\ENG - GI - Quebec and 1st Precinct Upgrades\11 - Design\	

ENGINEERING SERVICES – CITY OF VANCOUVER – GREEN INFRASTRUCTURE

DESIGNED BY:
DRAFTED BY:
CHECKED BY:
FILE NAME: ENG - GI - Quebec St Reconstruction_AS-BUILT.dwg

Quebec and 1st Ave Precinct Improvements
Green Infrastructure
Location E - Plan and Sections

SCALE: As shown
DATE: March 2018
DWG. NO. 2008-63-D-GI3.5 AB
REV. NO. 4
SHEET: 6 OF 7

FILE: H:\GREEN INFRASTRUCTURE\13-8100-40 - Green Infrastructure Case Files\ENG - GI - Quebec and 1st Precinct Upgrades\11 - Design\ENG - GI - Quebec St Reconstruction_AS-BUILT.dwg DATE:Oct 16, 2018 - 3:32pm USER:enapl

Appendix D**: City of Vancouver Precast Concrete Catch Basin Standard Detail**

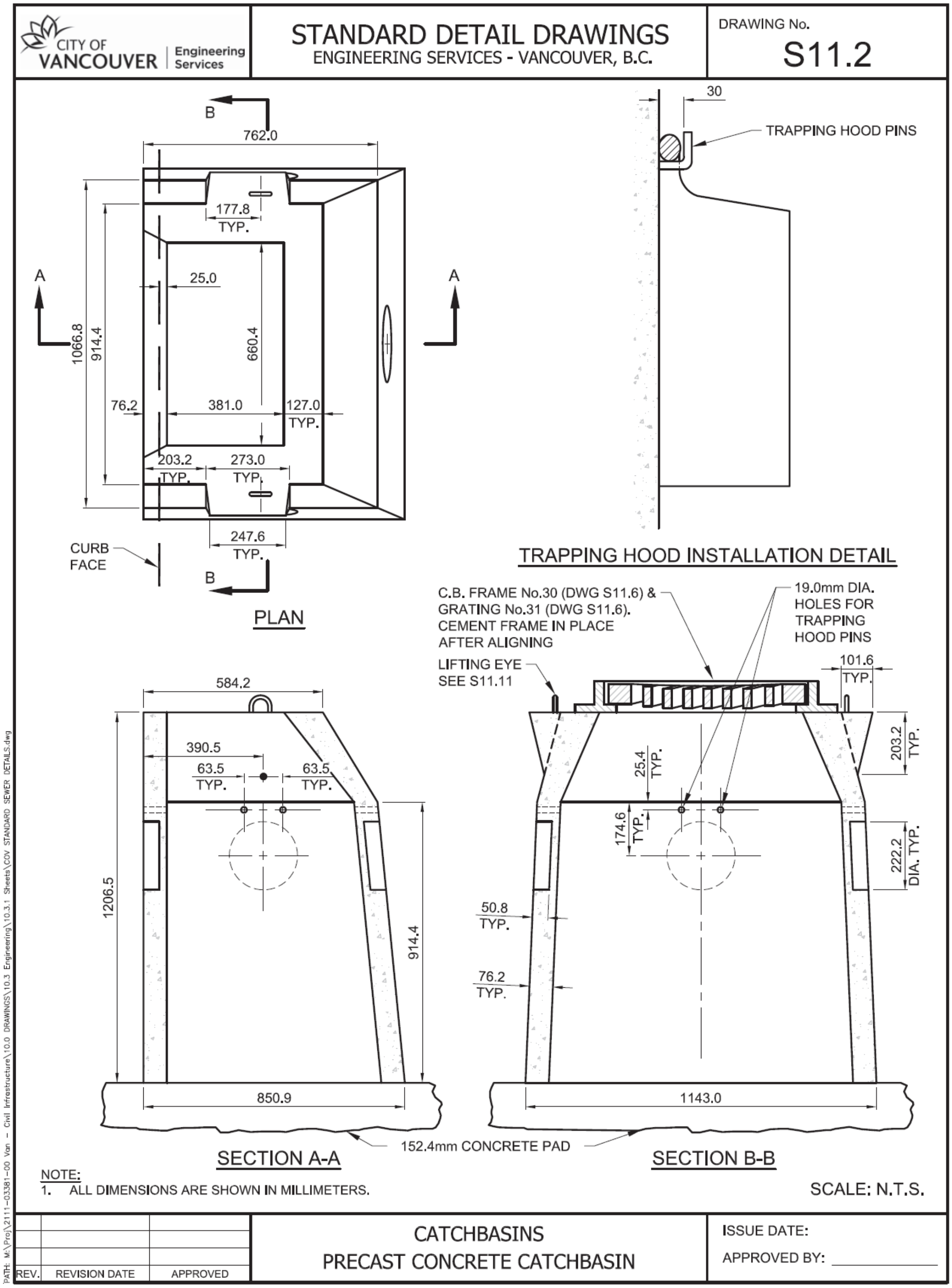

Appendix E**: PVC Weir Cap Sizing**

Assessment of two V-notch angles within the context of the CB. This process checked if approach condition of the V-notch angles are satisfied inside the CB.

Vnotch (Theta)	**Parameters**			**Operations**		**Parameter Conditions for each V-Notch from ASTM D5242 − 92 (2013)**						**Checks**				
	H (mm)	**B (mm)**	**P (mm)**	**H/P**	**H/B**	**H/P**	**H/B**	**P (m)**	**B (m)**	**H_Low (m)**	**H_High (m)**	**H/P**	**H/B**	**P (m)**	**B (m)**	**H_Low_High (m)**
53.13	117.00	914.40	663.60	0.18	0.13	0.40	0.20	0.45	0.90	0.05	0.38	Pass	Pass	Pass	Pass	Pass
90	81.00	914.40	663.60	0.12	0.09	1.20	0.40	0.10	0.60	0.05	0.60	Pass	Pass	Pass	Pass	Pass

B

H

P

Appendix F**: Hydraulic Study of Experimental Flume Device**

F.1 Expected flow conditions for the different slope conditions in the through channel flume

Discharges		Normal Depth Calculation			Critical Depth Calculation			Hydraulic Slope		
Q (gpm)	Q (m^3/s)	1% (mm)	1.2% (mm)	1.5% (mm)	1% (mm)	1.2% (mm)	1.5% (mm)	1%	1.2%	1.5%
0.50	3.16E-05	12.51	11.98	11.37	4.89	4.89	4.89	Mild Slope	Mild Slope	Mild Slope
0.85	5.36E-05	16.08	15.39	14.60	6.37	6.37	6.37	Mild Slope	Mild Slope	Mild Slope
1.00	6.31E-05	17.38	16.64	15.78	6.92	6.92	6.92	Mild Slope	Mild Slope	Mild Slope
1.50	9.47E-05	21.12	20.21	19.16	8.48	8.48	8.48	Mild Slope	Mild Slope	Mild Slope
2.00	1.26E-04	24.25	23.20	21.98	9.79	9.79	9.79	Mild Slope	Mild Slope	Mild Slope
2.50	1.58E-04	27.08	25.90	24.53	10.97	10.97	10.97	Mild Slope	Mild Slope	Mild Slope
3.00	1.89E-04	29.57	28.27	26.77	12.01	12.01	12.01	Mild Slope	Mild Slope	Mild Slope
3.50	2.21E-04	31.95	30.54	28.90	13.00	13.00	13.00	Mild Slope	Mild Slope	Mild Slope
4.00	2.52E-04	34.10	32.59	30.84	13.89	13.89	13.89	Mild Slope	Mild Slope	Mild Slope
4.50	2.84E-04	36.20	34.59	32.72	14.75	14.75	14.75	Mild Slope	Mild Slope	Mild Slope
5.00	3.16E-04	38.20	36.49	34.50	15.57	15.57	15.57	Mild Slope	Mild Slope	Mild Slope
6.00	3.79E-04	41.89	39.99	37.80	17.07	17.07	17.07	Mild Slope	Mild Slope	Mild Slope
7.00	4.42E-04	45.33	43.25	40.86	18.45	18.45	18.45	Mild Slope	Mild Slope	Mild Slope
8.00	5.05E-04	48.57	46.33	43.74	19.73	19.73	19.73	Mild Slope	Mild Slope	Mild Slope
10.00	6.31E-04	54.62	52.04	49.08	22.09	22.09	22.09	Mild Slope	Mild Slope	Mild Slope
15.00	9.47E-04	68.22	64.82	60.95	27.16	27.16	27.16	Mild Slope	Mild Slope	Mild Slope

F.2 Experimental Stage-Discharge Measurements

The TS14 sensor was located at a distance of 180mm. This distance is from the tip of the sensor to the bottom of the through channel.

Discharges		Raw Measurements			Processed Measurements			Froude Number			Flow		
Q (gpm)	Q (m^3/s)	1% (mm)	1.2% (mm)	1.5% (mm)	1% (mm)	1.2% (mm)	1.5% (mm)	1%	1.2%	1.5%	1%	1.2%	1.5%
0.50	3.16E-05	173.50	177.20	178.10	6.50	2.80	1.90	0.46	2.49	5.39	Subcritical	Supercritical	Supercritical
0.85	5.36E-05	171.20	177.20	177.80	8.80	2.80	2.20	0.43	4.22	6.82	Subcritical	Supercritical	Supercritical
1.00	6.31E-05	170.50	176.80	177.50	9.50	3.20	2.50	0.44	3.80	6.22	Subcritical	Supercritical	Supercritical
1.50	9.47E-05	169.20	175.90	177.10	10.80	4.10	2.90	0.51	3.48	6.95	Subcritical	Supercritical	Supercritical
2.00	1.26E-04	169.20	175.80	176.40	10.80	4.20	3.60	0.68	4.42	6.01	Subcritical	Supercritical	Supercritical
2.50	1.58E-04	167.20	174.60	175.30	12.80	5.40	4.70	0.61	3.36	4.43	Subcritical	Supercritical	Supercritical
3.00	1.89E-04	166.00	173.80	175.10	14.00	6.20	4.90	0.61	3.05	4.88	Subcritical	Supercritical	Supercritical
3.50	2.21E-04	164.20	173.70	174.10	15.80	6.30	5.90	0.56	3.46	3.94	Subcritical	Supercritical	Supercritical
4.00	2.52E-04	163.80	172.60	172.30	16.20	7.40	7.70	0.61	2.86	2.65	Subcritical	Supercritical	Supercritical
4.50	2.84E-04	163.10	170.90	172.50	16.90	9.10	7.50	0.63	2.14	3.14	Subcritical	Supercritical	Supercritical
5.00	3.16E-04	161.50	170.40	172.20	18.50	9.60	7.80	0.59	2.14	3.24	Subcritical	Supercritical	Supercritical
6.00	3.79E-04	161.00	169.70	171.40	19.00	10.30	8.60	0.67	2.24	3.20	Subcritical	Supercritical	Supercritical
7.00	4.42E-04	160.30	169.00	170.60	19.70	11.00	9.40	0.73	2.29	3.13	Subcritical	Supercritical	Supercritical
8.00	5.05E-04	159.70	167.00	169.10	20.30	13.00	10.90	0.78	1.88	2.67	Supercritical	Supercritical	Supercritical
10.00	6.31E-04	158.70	166.60	168.60	21.30	13.40	11.40	0.89	2.21	3.05	Supercritical	Supercritical	Supercritical
15.00	9.47E-04	157.40	165.40	168.30	22.60	14.60	11.70	1.19	2.81	4.34	Supercritical	Supercritical	Supercritical
20.00	1.26E-03	156.90	165.30	166.70	23.10	14.70	13.30	1.52	3.69	4.49	Supercritical	Supercritical	Supercritical
25.00	1.58E-03	155.00	165.10	166.00	25.00	14.90	14.00	1.63	4.50	5.09	Supercritical	Supercritical	Supercritical
30.00	1.89E-03	151.90	161.30	161.70	28.10	18.70	18.30	1.56	3.44	3.59	Supercritical	Supercritical	Supercritical

F.3 Rating Curve: 1% Slope

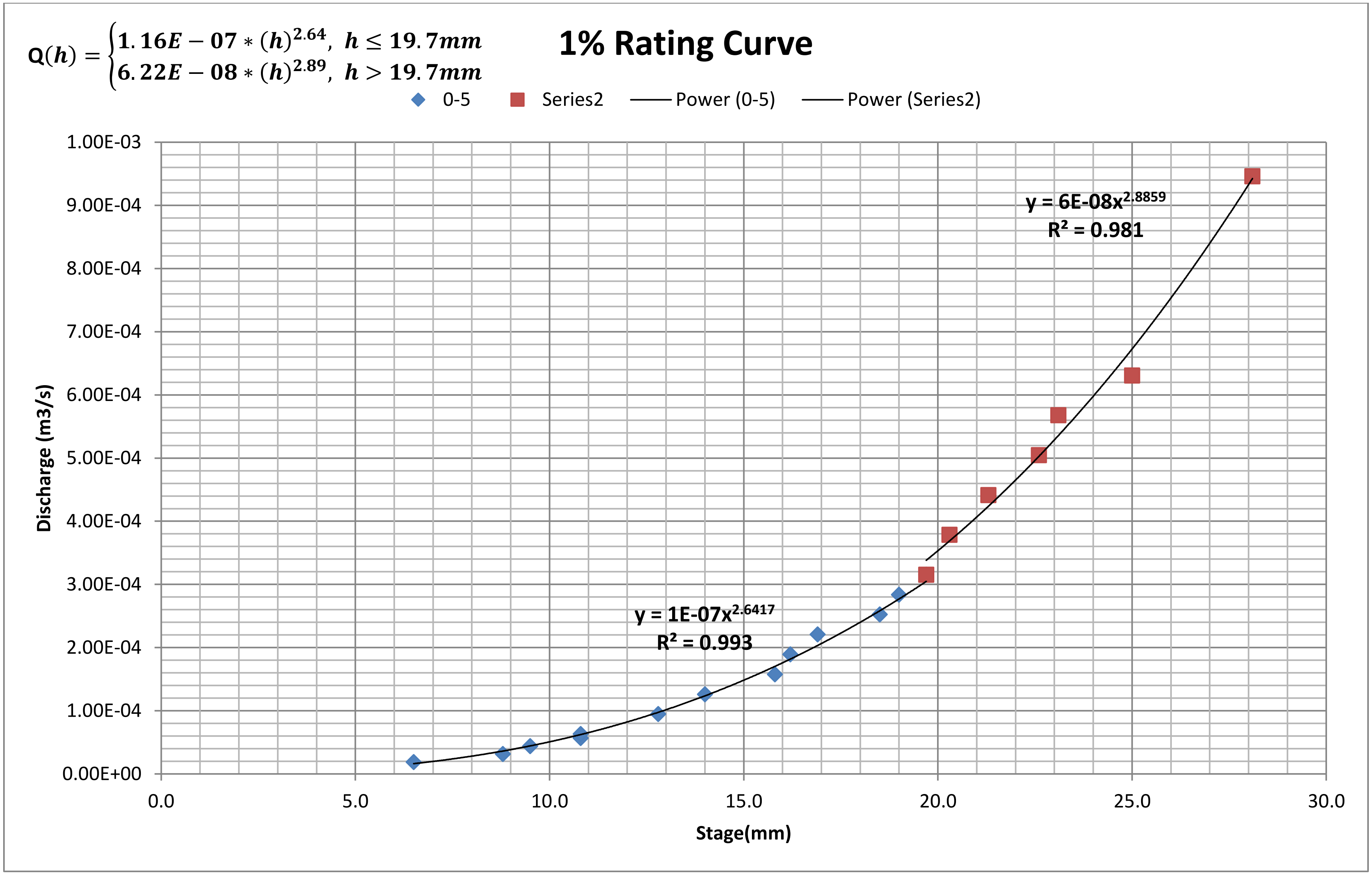

F.4 Rating Curve: 1.2% Slope

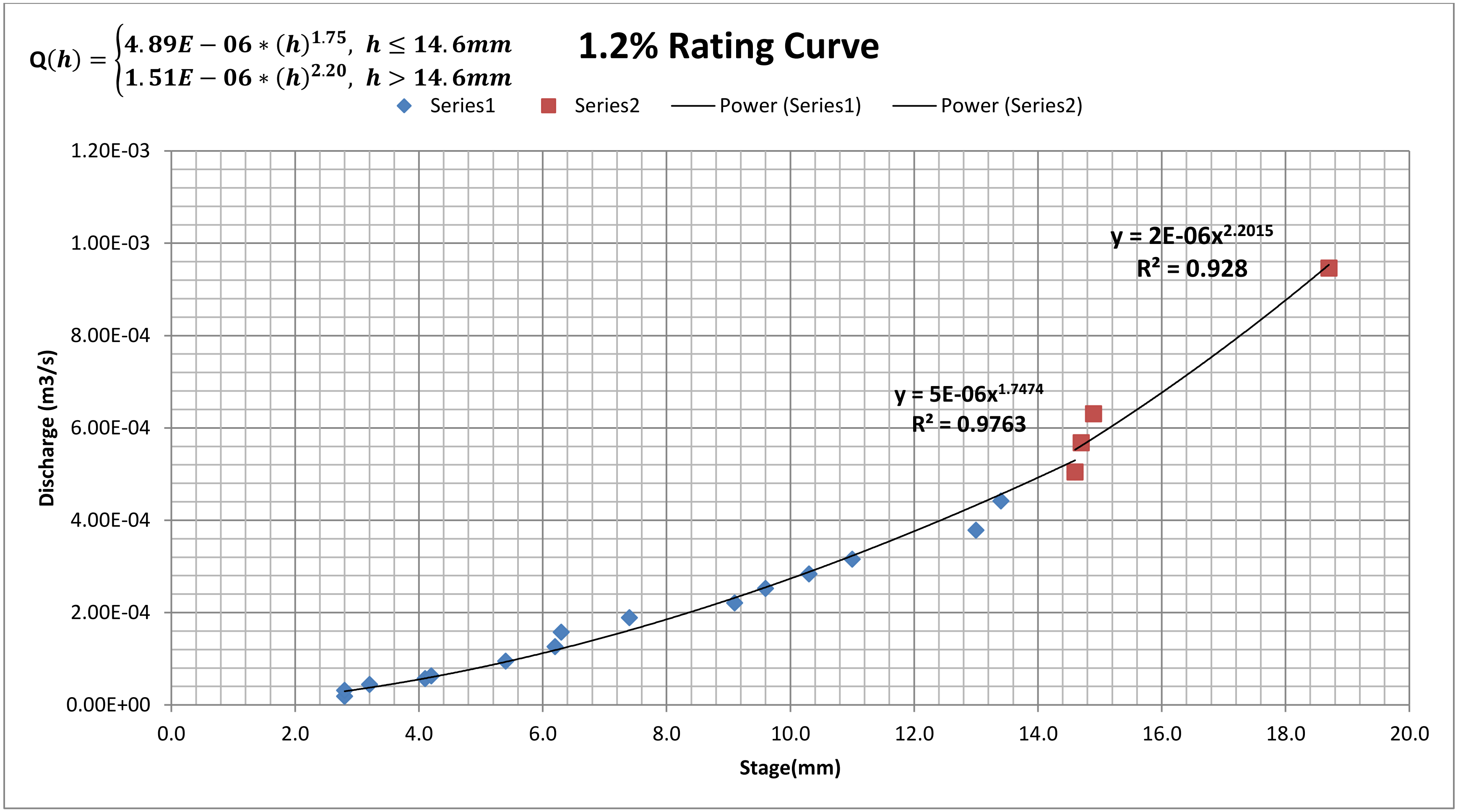

F.5 Rating Curve: 1.5% Slope

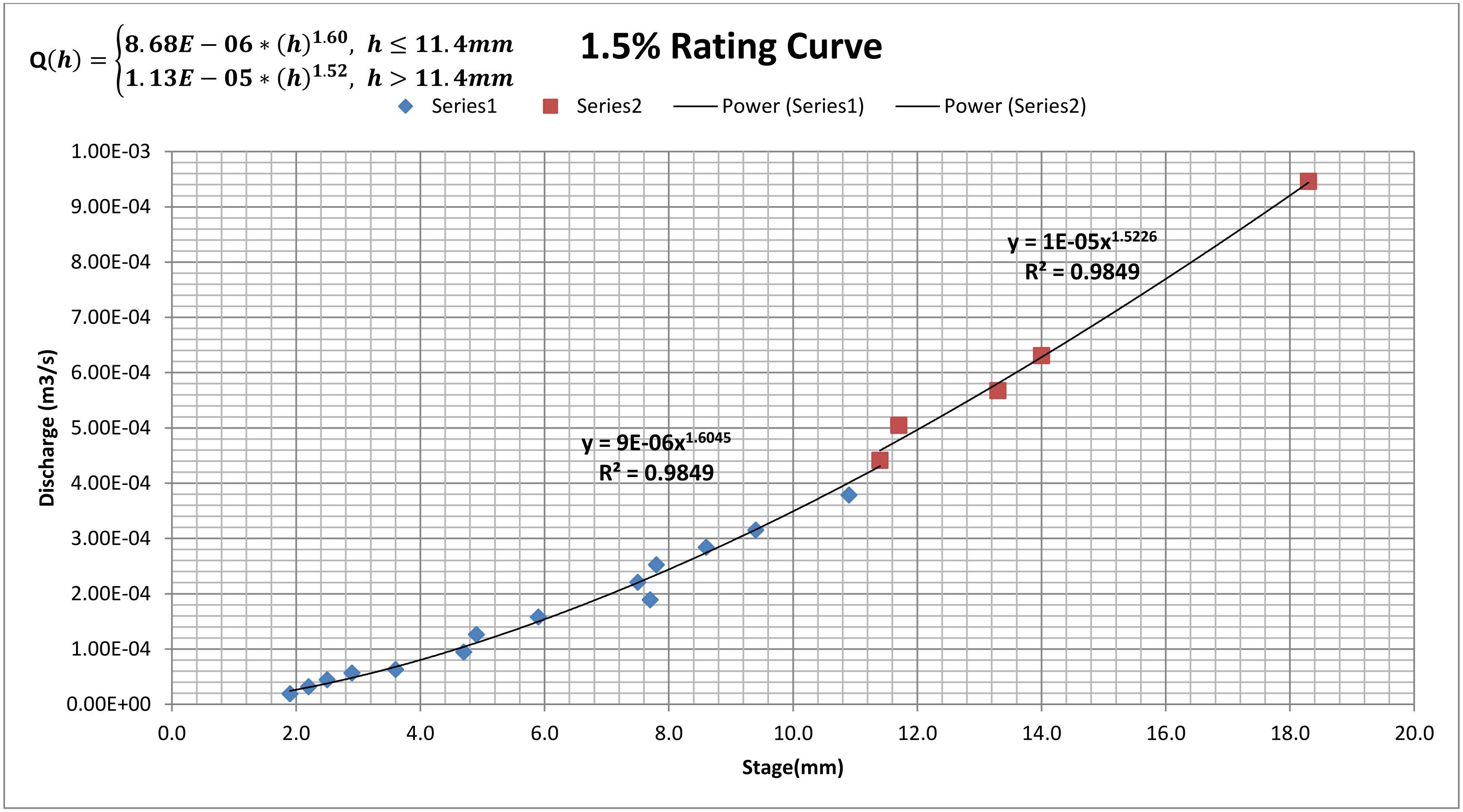

Appendix G**: Bioswale 1 raw data**

Backwater error evidence shown in red below.

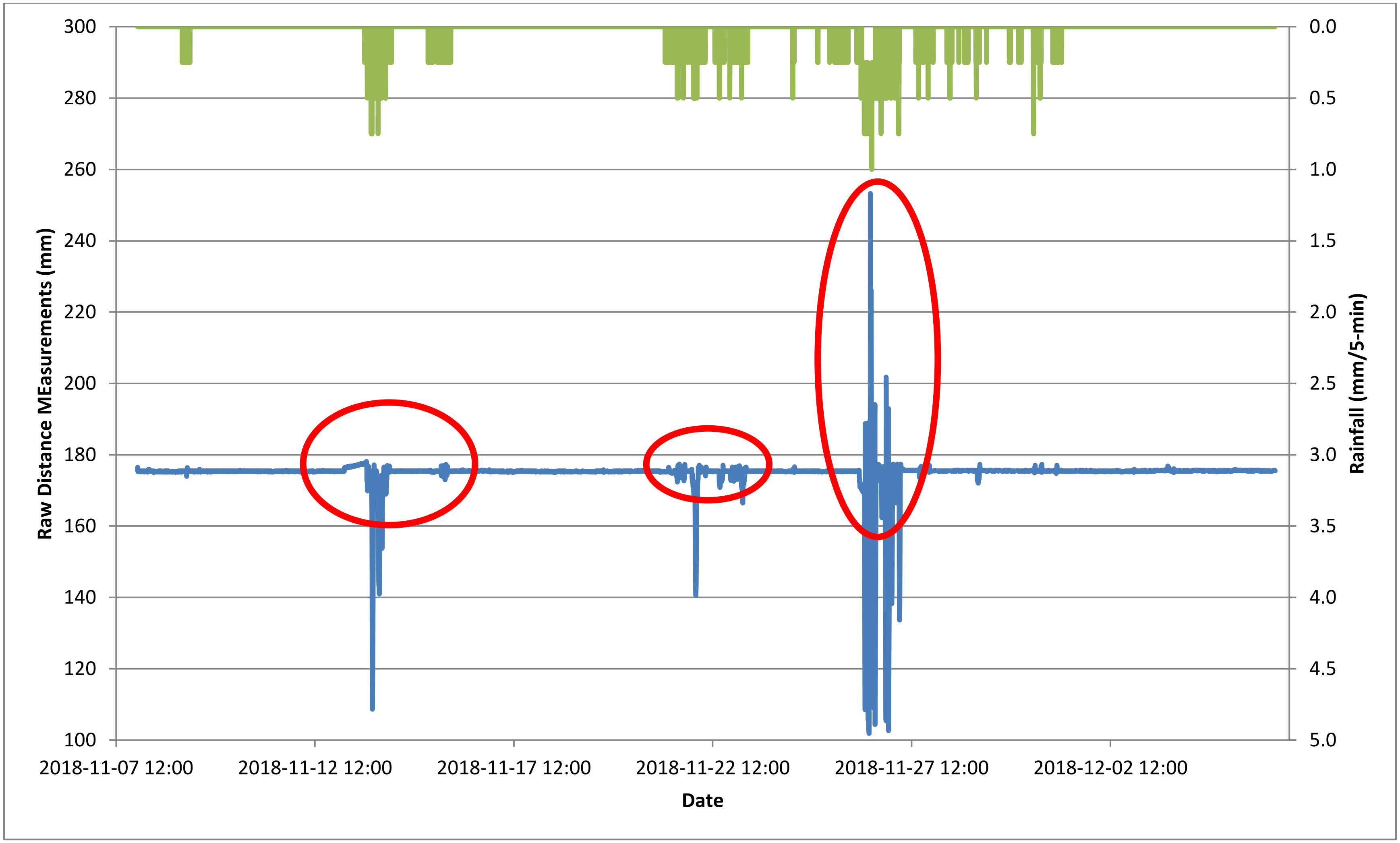

Appendix H**: Bioswale 2 raw data**

Sensor error evidence shown in red below.

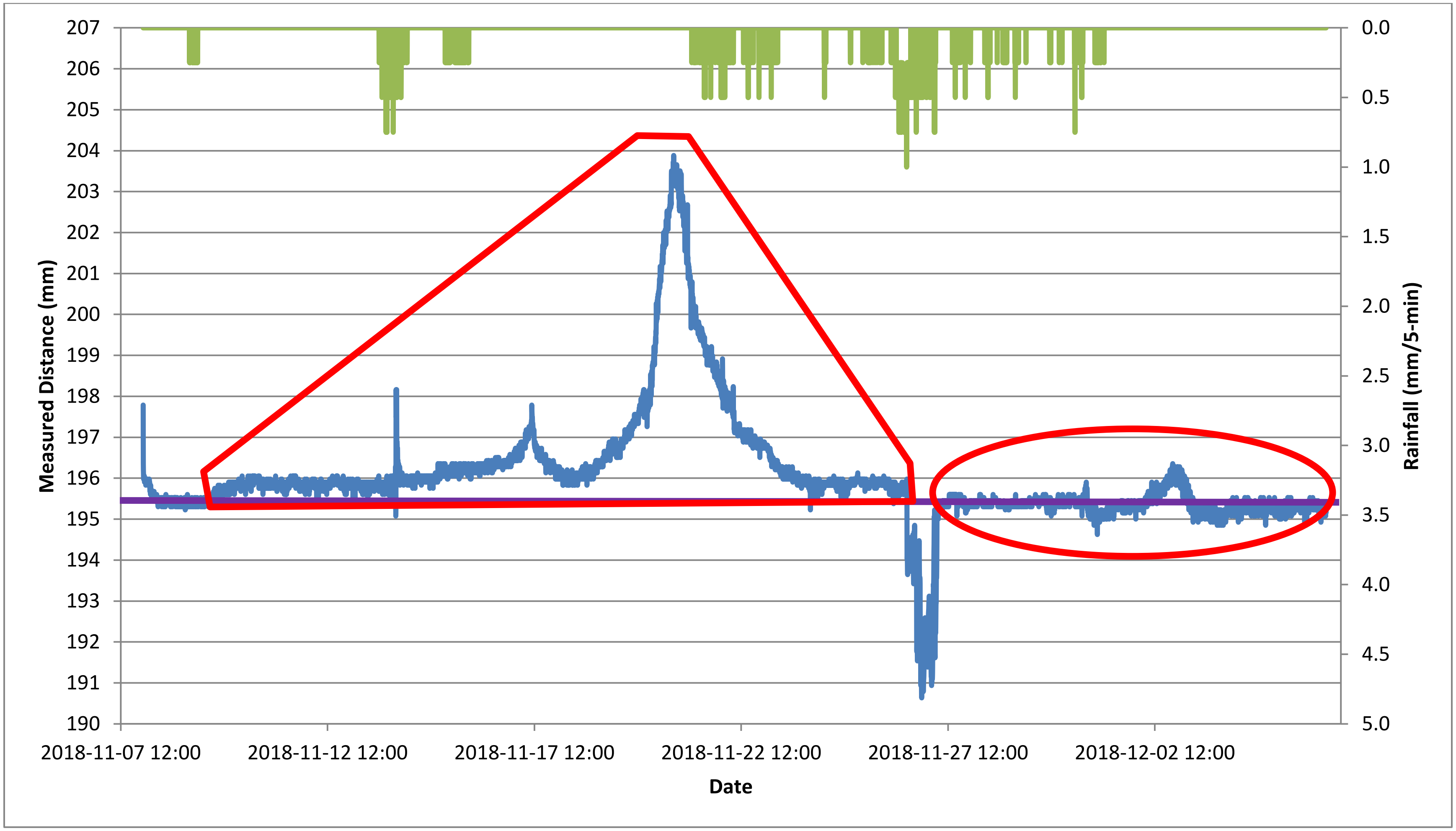

Appendix I: Water quantity analysis

I.1 SWMM® Models

Left blank intentionally

Structural Soil STT SWMM® Model

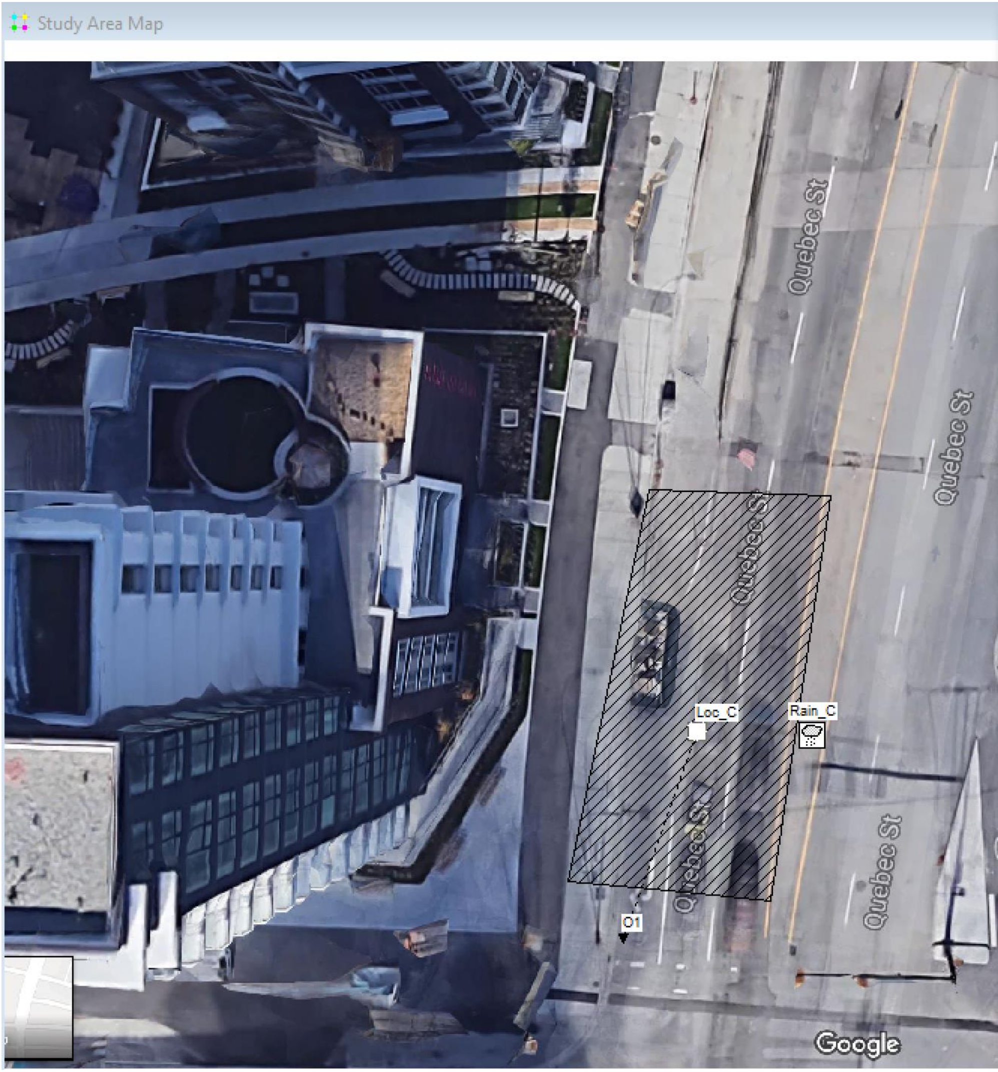

Subcatchment Loc_C

Property	Value
Name	Loc_C
X-Coordinate	3329.041
Y-Coordinate	3416.309
Description	
Tag	
Rain Gage	Rain_C
Outlet	O1
Area	0.0415
Width	8
% Slope	0.9
% Imperv	100
N-Imperv	0.013
N-Perv	0.24
Dstore-Imperv	1
Dstore-Perv	5
%Zero-Imperv	25
Subarea Routing	OUTLET
Percent Routed	100
Infiltration	HORTON
Groundwater	NO
Snow Pack	
LID Controls	0
Land Uses	0
Initial Buildup	NONE
Curb Length	0

User-assigned name of subcatchment

Bioswale 1 SWMM® Model

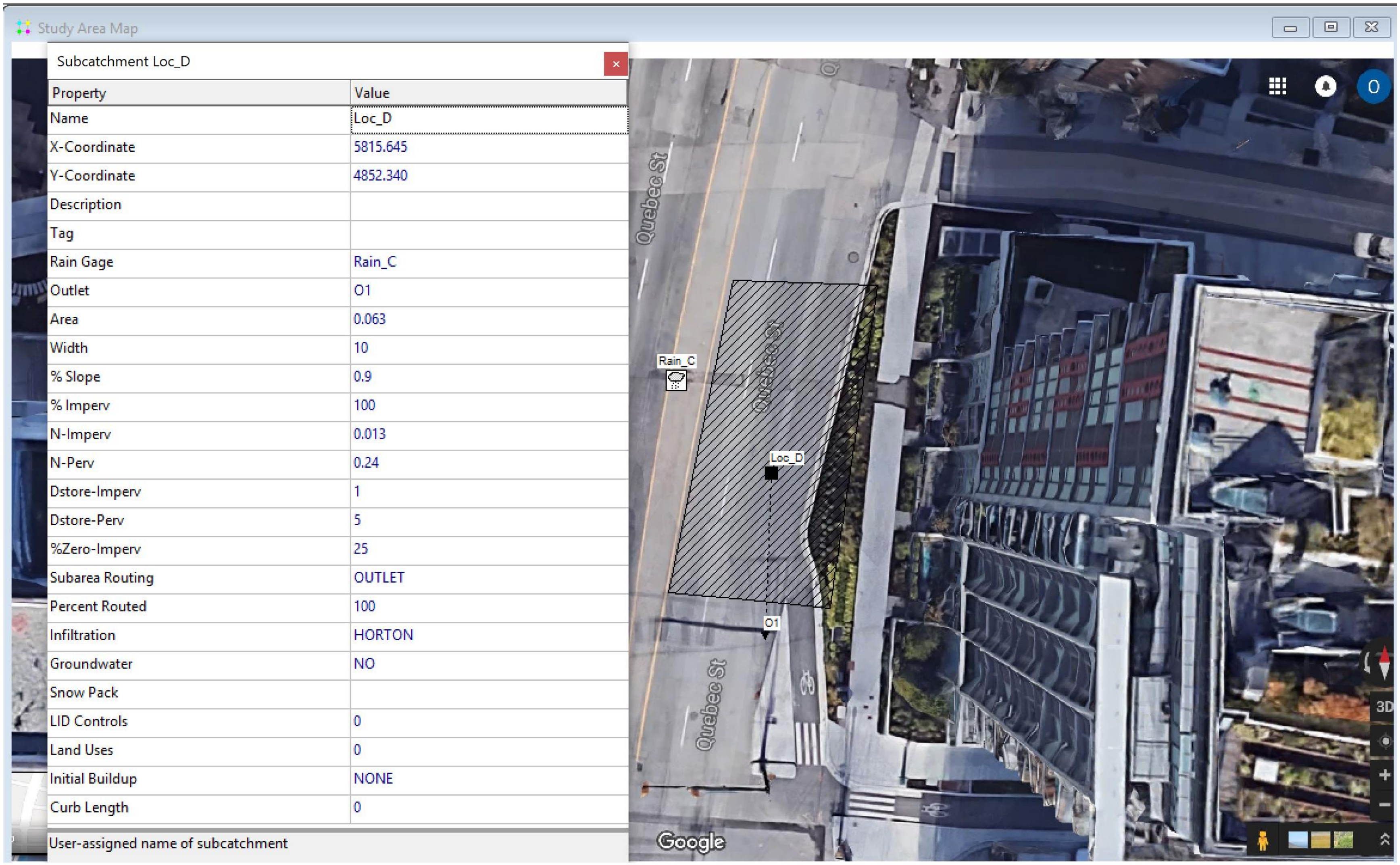

Bioswale 2 SWMM® Model

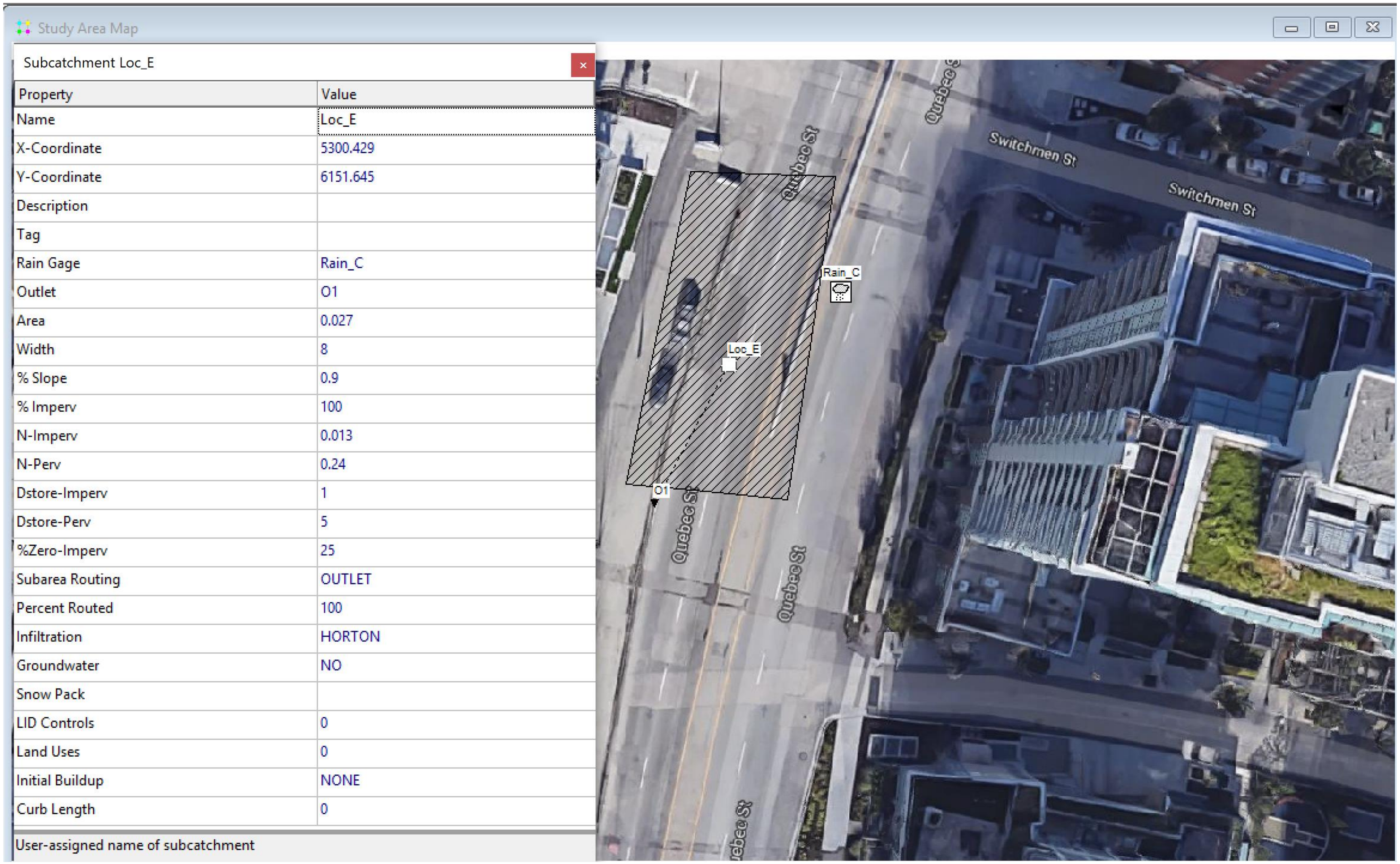
Subcatchment Loc_E

Property	Value
Name	Loc_E
X-Coordinate	5300.429
Y-Coordinate	6151.645
Description	
Tag	
Rain Gage	Rain_C
Outlet	O1
Area	0.027
Width	8
% Slope	0.9
% Imperv	100
N-Imperv	0.013
N-Perv	0.24
Dstore-Imperv	1
Dstore-Perv	5
%Zero-Imperv	25
Subarea Routing	OUTLET
Percent Routed	100
Infiltration	HORTON
Groundwater	NO
Snow Pack	
LID Controls	0
Land Uses	0
Initial Buildup	NONE
Curb Length	0

User-assigned name of subcatchment

I.2 Storm events, modelled inflow and measured outflow graphs

Left blank intentionally

Storm ID: 2018-11-09-3

Performance		
Total Inflow (m^3|L)	2.1	2,076
Total Outflow (m^3|L)	-	-
Volume Reduction	100.0%	100.0%
Peak Flow Reduction	100.0%	100.0%
Lag Time (min|hours)	No Outflow	No Outflow
Total Rainfall (mm)	5.8	5.8
Storm Duration (hours|days)	4.8	0.2
ADP (hours|days)	75.5	3.1
Max Rain Intensity (mm/hr)	3.0	3.0

Dates for Graph	
Beginning	2018-11-08 3:00
End	2018-11-09 23:55
Inflow Peak	2018-11-09 6:35
Outflow Peak	2018-11-09 6:35
Inflow Lag	2018-11-09 4:05
Outflow Lag	2018-11-09 4:05

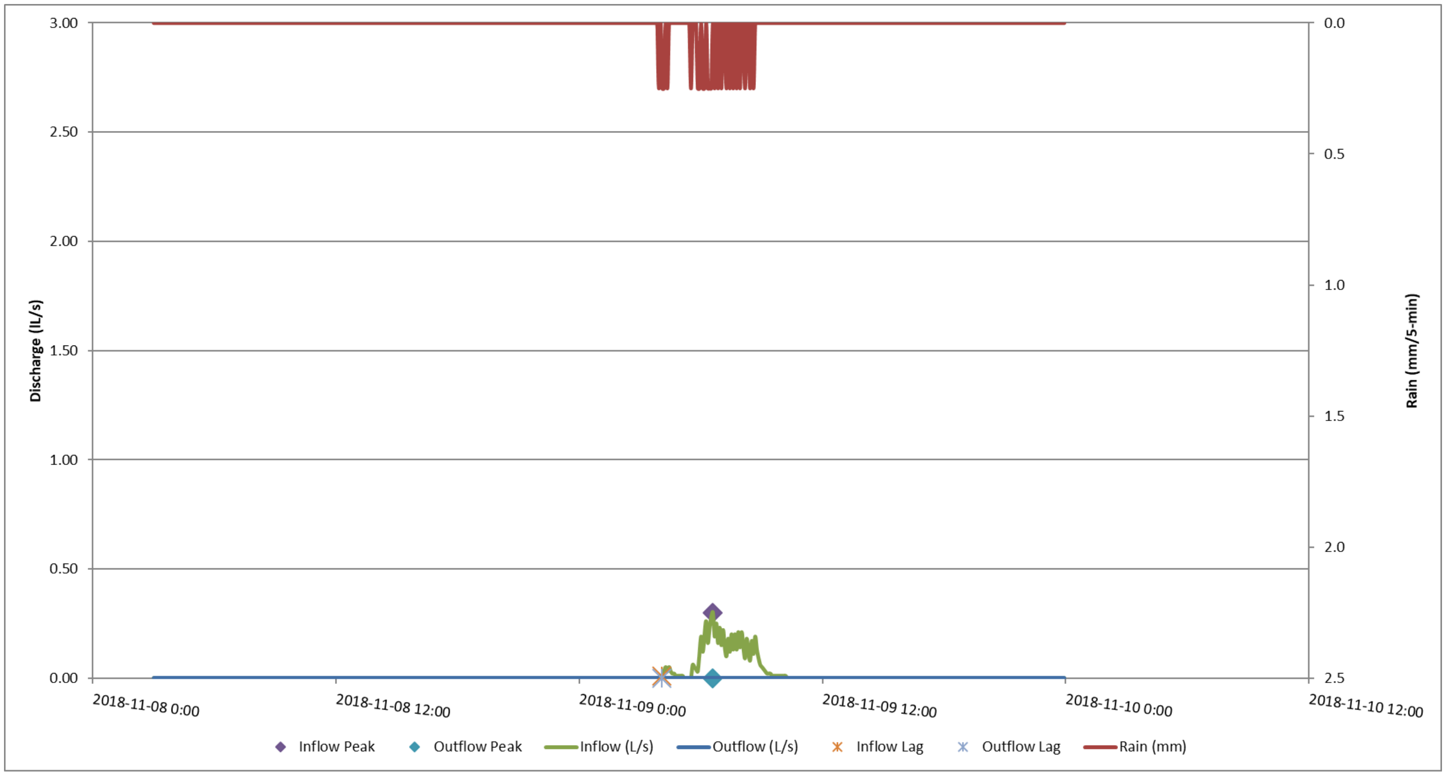

Storm ID: 2018-11-13-5

Dates for Graph	
Beginning	2018-11-12 17:40
End	2018-11-15 4:20
Inflow Peak	2018-11-13 22:20
Outflow Peak	2018-11-13 22:20
Inflow Lag	2018-11-13 17:55
Outflow Lag	2018-11-13 22:00

Performance		
Total Inflow (m^3|L)	14.8	14,772
Total Outflow (m^3|L)	3.3	3,314
Volume Reduction	77.6%	77.6%
Peak Flow Reduction	63.5%	63.5%
Lag Time (min|hours)	245.00	4.1
Total Rainfall (mm)	35.5	35.5
Storm Duration (hours|days)	16.3	0.7
ADP (hours|days)	105.3	4.4
Max Rain Intensity (mm/hr)	9.0	9.0

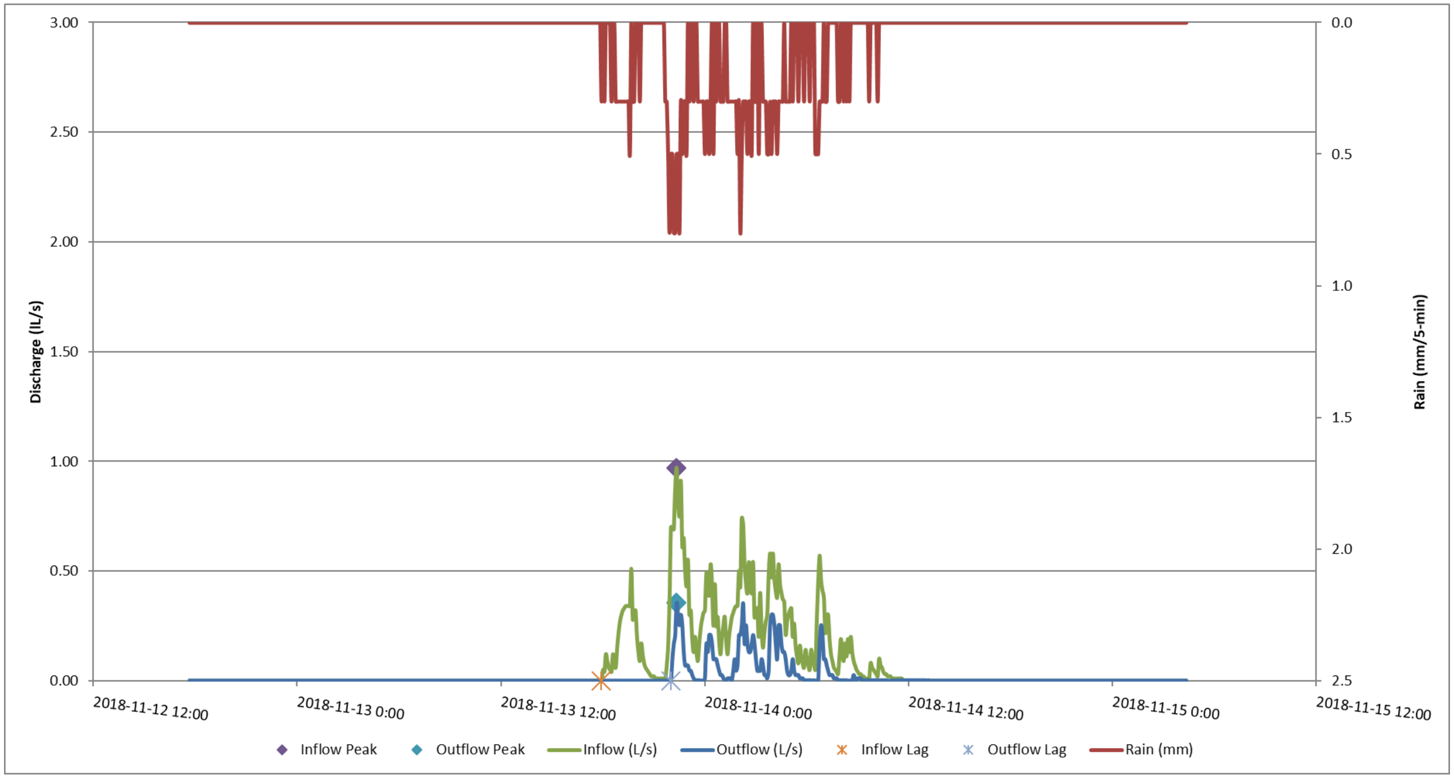

Storm ID: 2018-11-15-8

Dates for Graph	
Beginning	2018-11-15 0:00
End	2018-11-16 5:55
Inflow Peak	2018-11-15 18:25
Outflow Peak	2018-11-15 18:25
Inflow Lag	2018-11-15 13:50
Outflow Lag	2018-11-15 15:55

Performance		
Total Inflow (m^3|L)	4.9	4,887
Total Outflow (m^3|L)	0.3	343
Volume Reduction	93.0%	93.0%
Peak Flow Reduction	58.9%	58.9%
Lag Time (min|hours)	125.00	2.1
Total Rainfall (mm)	11.8	11.8
Storm Duration (hours|days)	13.8	0.6
ADP (hours|days)	22.1	0.9
Max Rain Intensity (mm/hr)	3.0	3.0

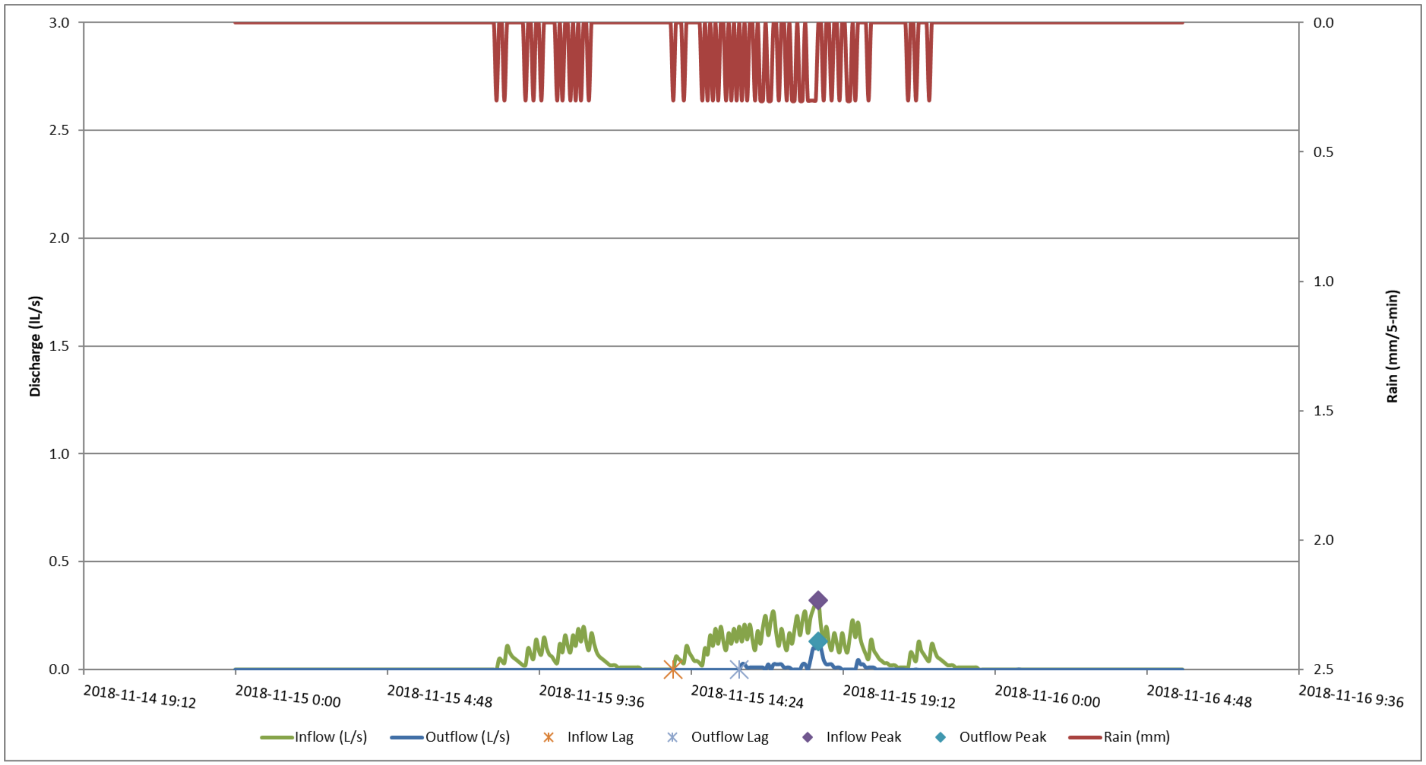

Storm ID: 2018-11-21-7

Performance		
Total Inflow (m^3|L)	22.9	22,896
Total Outflow (m^3|L)	3.8	3,799
Volume Reduction	83.4%	83.4%
Peak Flow Reduction	60.5%	60.5%
Lag Time (min|hours)	425.00	7.1
Total Rainfall (mm)	55.0	55.0
Storm Duration (hours|days)	49.9	2.1
ADP (hours|days)	129.4	5.4
Max Rain Intensity (mm/hr)	6.0	6.0

Dates for Graph	
Beginning	2018-11-21 0:00
End	2018-11-23 19:55
Inflow Peak	2018-11-22 0:35
Outflow Peak	2018-11-22 1:25
Inflow Lag	2018-11-21 7:20
Outflow Lag	2018-11-21 14:25

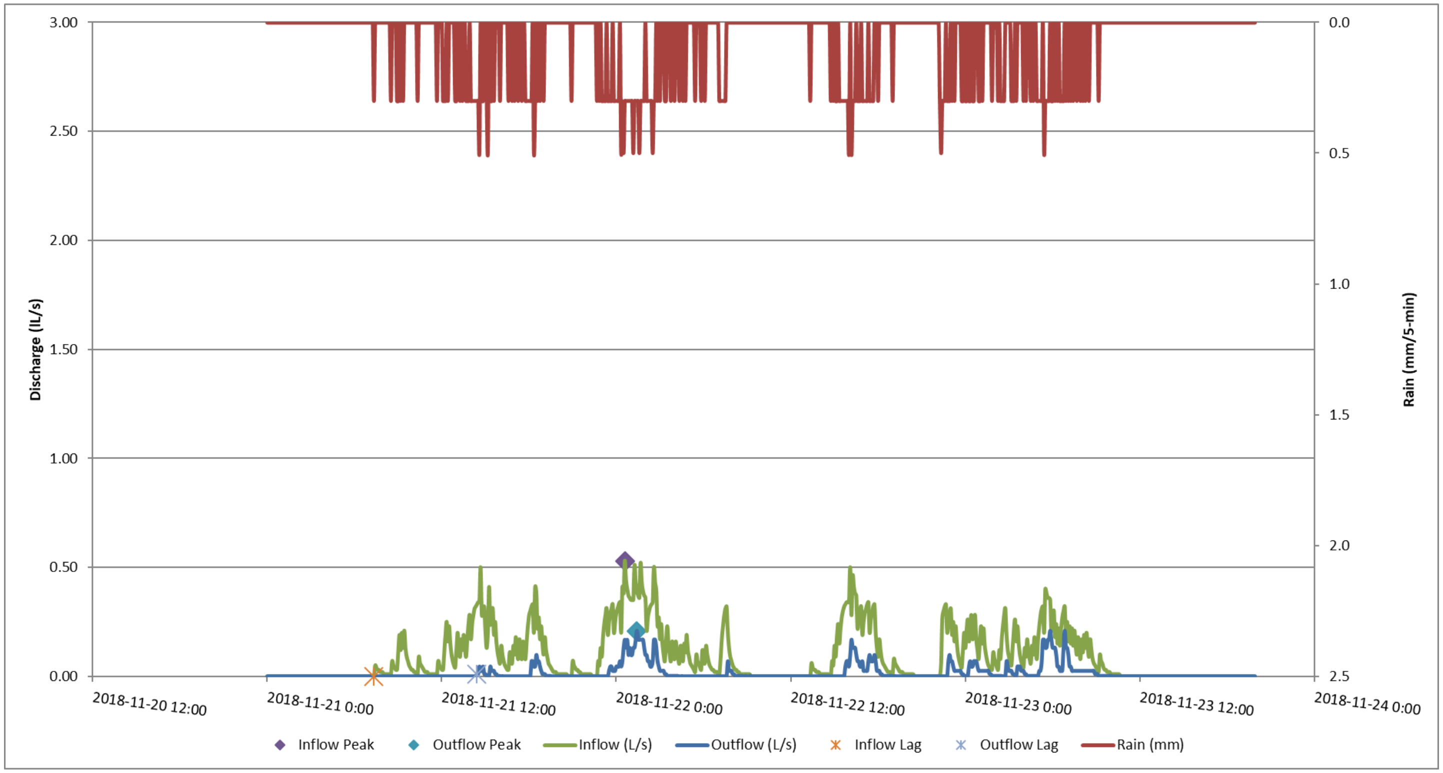

Storm ID: 2018-11-24-12

Dates for Graph	
Beginning	2018-11-24 0:00
End	2018-11-24 22:00
Inflow Peak	2018-11-24 12:25
Outflow Peak	2018-11-24 12:25
Inflow Lag	2018-11-24 12:10
Outflow Lag	2018-11-24 12:25

Performance		
Total Inflow (m^3|L)	1.0	1,026
Total Outflow (m^3|L)	-	-
Volume Reduction	100.0%	100.0%
Peak Flow Reduction	100.0%	100.0%
Lag Time (min|hours)	No Outflow	No Outflow
Total Rainfall (mm)	2.5	2.5
Storm Duration (hours|days)	1.1	0.0
ADP (hours|days)	27.0	1.1
Max Rain Intensity (mm/hr)	6.0	6.0

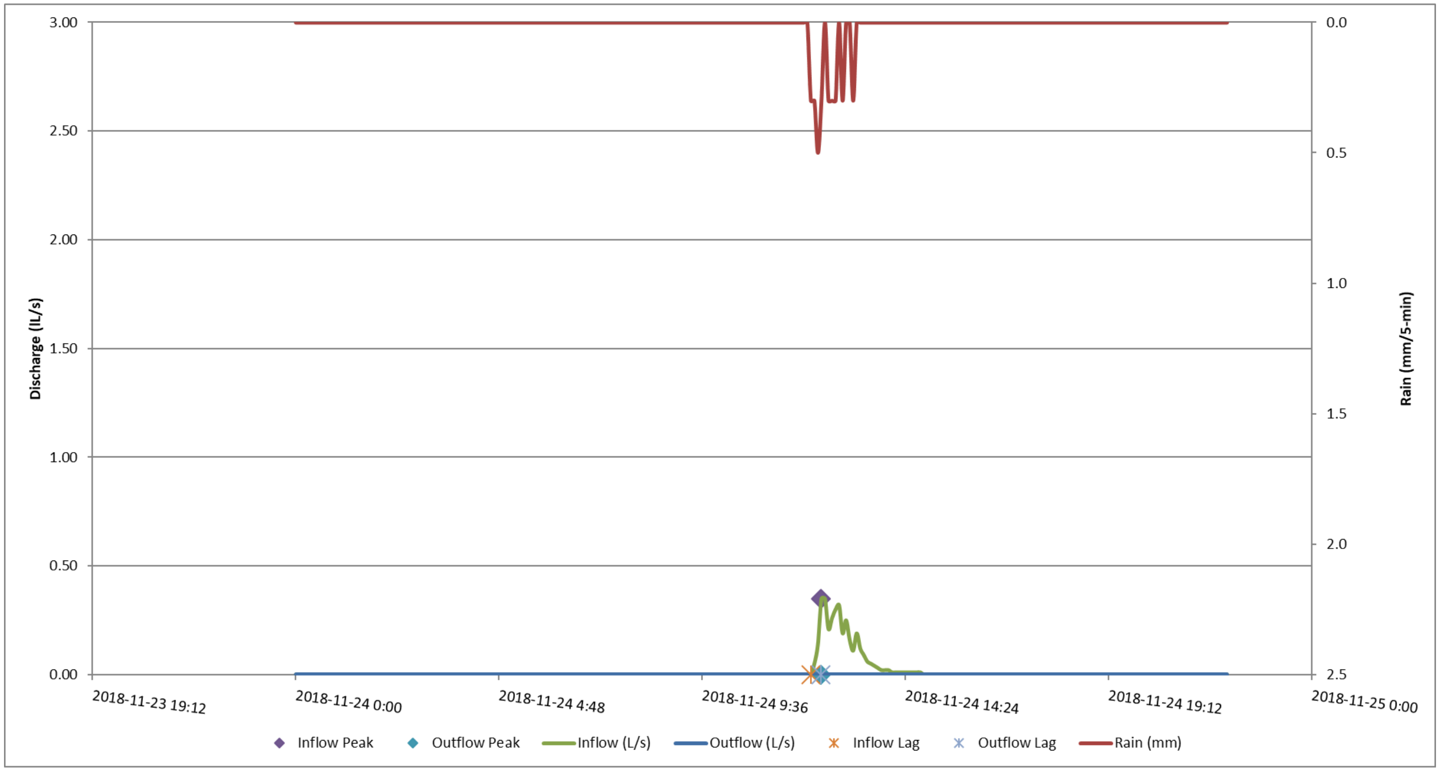

Storm ID: 2018-11-25-10

Dates for Graph	
Beginning	2018-11-25 6:00
End	2018-11-27 8:55
Inflow Peak	2018-11-26 12:05
Outflow Peak	2018-11-26 12:10
Inflow Lag	2018-11-26 3:00
Outflow Lag	2018-11-26 4:20

Performance		
Total Inflow (m^3|L)	40.6	40,632
Total Outflow (m^3|L)	14.8	14,832
Volume Reduction	63.5%	63.5%
Peak Flow Reduction	52.2%	52.2%
Lag Time (min|hours)	80.00	1.3
Total Rainfall (mm)	97.8	97.8
Storm Duration (hours|days)	42.3	1.8
ADP (hours|days)	7.0	0.3
Max Rain Intensity (mm/hr)	12.0	12.0

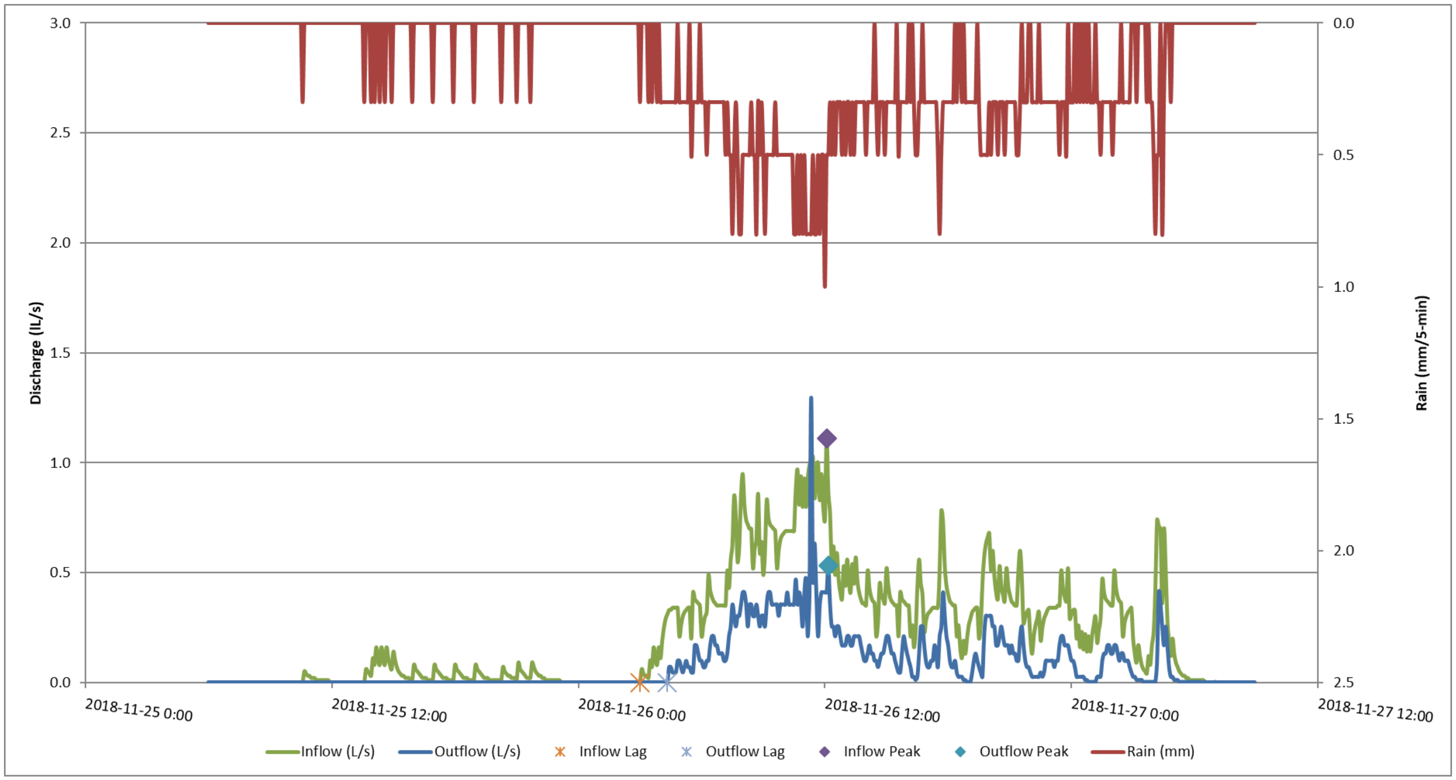

Storm ID: 2018-11-27-14

Dates for Graph	
Beginning	2018-11-27 9:00
End	2018-11-28 4:55
Inflow Peak	2018-11-27 16:20
Outflow Peak	2018-11-27 16:45
Inflow Lag	2018-11-27 14:35
Outflow Lag	2018-11-27 16:35

Performance		
Total Inflow (m^3|L)	2.8	2,796
Total Outflow (m^3|L)	0.2	201
Volume Reduction	92.8%	92.8%
Peak Flow Reduction	75.4%	75.4%
Lag Time (min|hours)	120.00	2.0
Total Rainfall (mm)	6.8	6.8
Storm Duration (hours|days)	10.6	0.4
ADP (hours|days)	9.8	0.4
Max Rain Intensity (mm/hr)	6.0	6.0

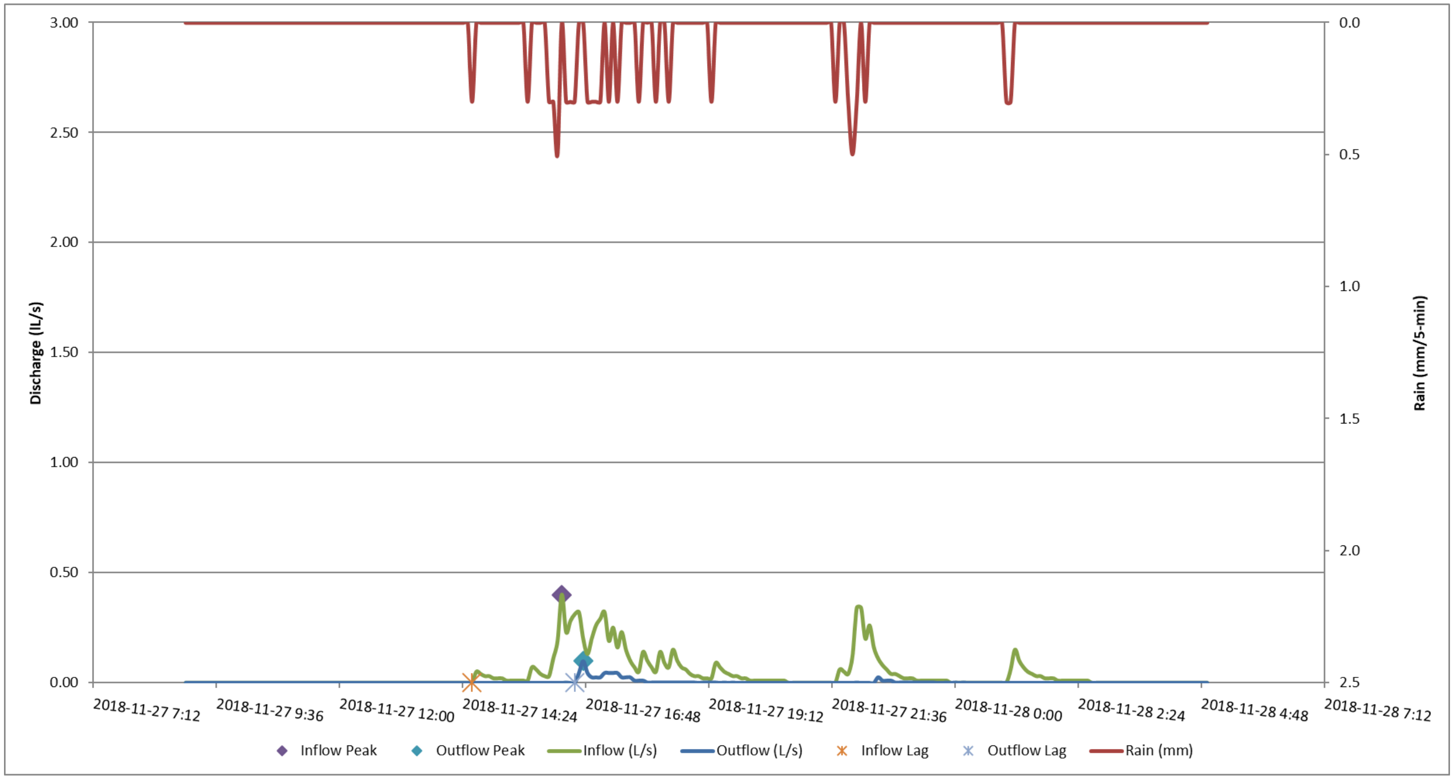

Storm ID: 2018-11-27-14

Dates for Graph	
Beginning	2018-11-28 5:00
End	2018-11-29 14:55
Inflow Peak	2018-11-29 3:10
Outflow Peak	2018-11-29 3:45
Inflow Lag	2018-11-29 2:50
Outflow Lag	2018-11-29 3:30

Performance		
Total Inflow (m^3|L)	3.6	3,600
Total Outflow (m^3|L)	0.2	223
Volume Reduction	93.8%	-
Peak Flow Reduction	79.5%	-
Lag Time (min|hours)	40.00	0.7
Total Rainfall (mm)	8.8	-
Storm Duration (hours|days)	24.0	1.0
ADP (hours|days)	8.3	0.3
Max Rain Intensity (mm/hr)	6.0	-

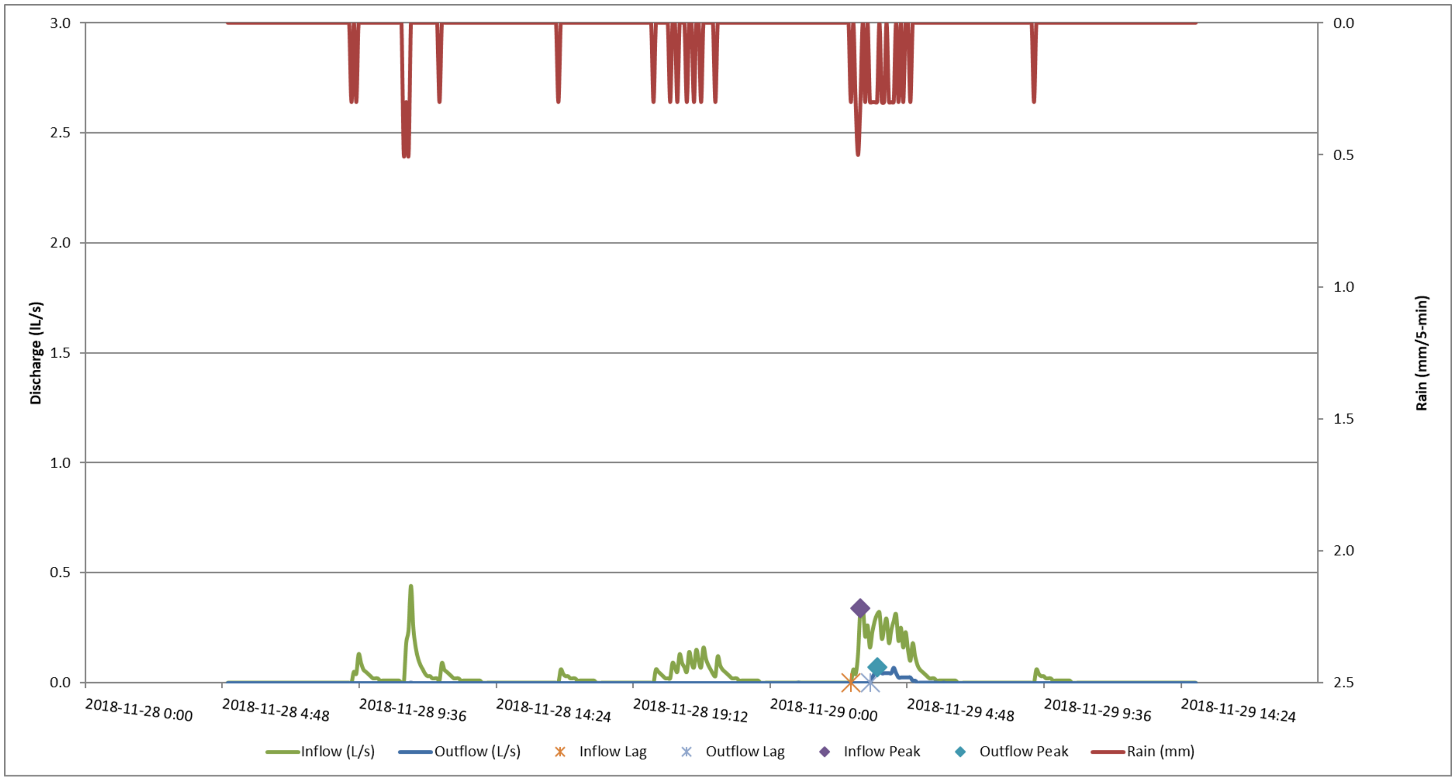

Storm ID: 2018-11-28-9

Dates for Graph	
Beginning	2018-11-28 5:00
End	2018-11-29 14:55
Inflow Peak	2018-11-29 3:10
Outflow Peak	2018-11-29 3:45
Inflow Lag	2018-11-29 2:50
Outflow Lag	2018-11-29 3:30

Performance		
Total Inflow (m^3|L)	3.6	3,600
Total Outflow (m^3|L)	0.2	223
Volume Reduction	93.8%	-
Peak Flow Reduction	79.5%	-
Lag Time (min|hours)	40.00	0.7
Total Rainfall (mm)	8.8	-
Storm Duration (hours|days)	24.0	1.0
ADP (hours|days)	8.3	0.3
Max Rain Intensity (mm/hr)	6.0	-

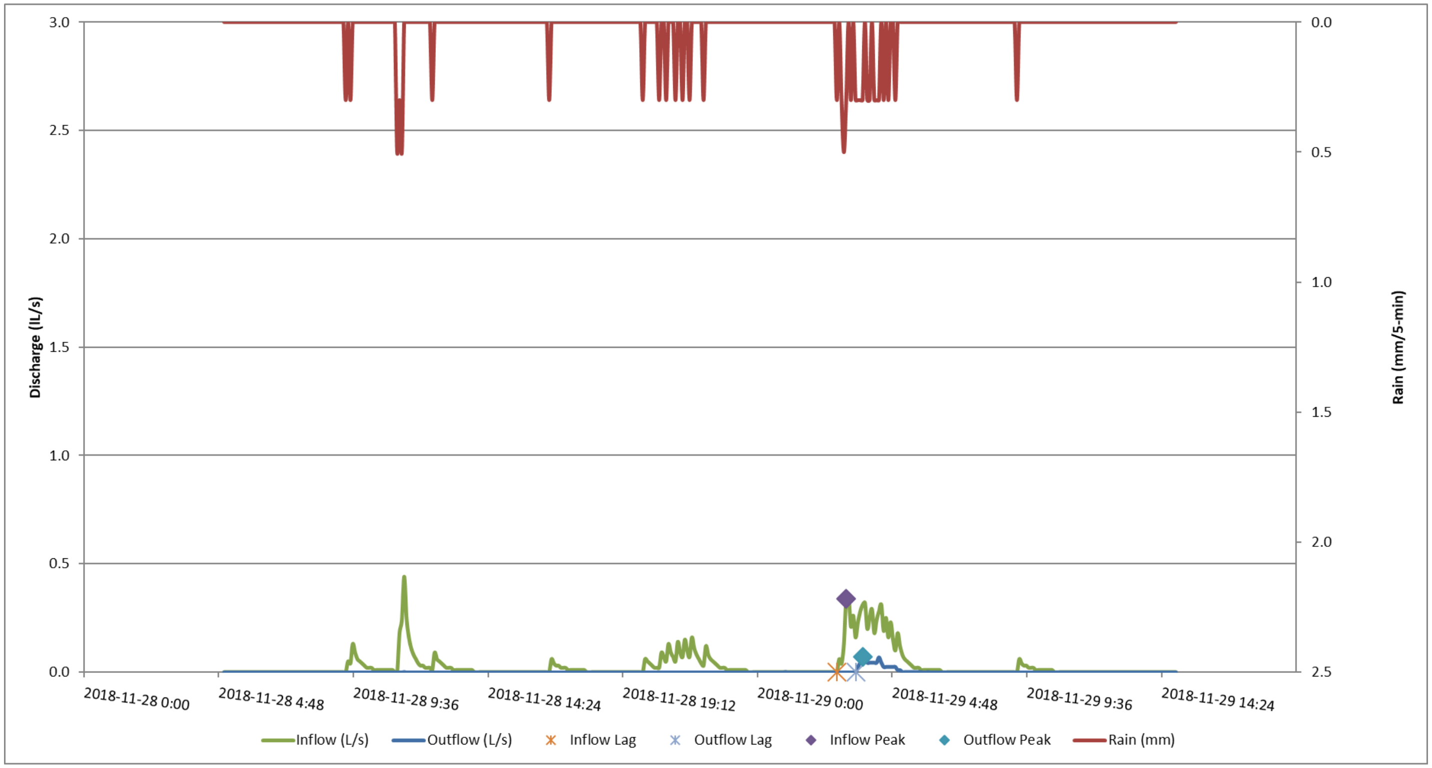

Storm ID: 2018-11-29-23

Performance		
Total Inflow (m^3|L)	0.9	906
Total Outflow (m^3|L)	0.0	1
Volume Reduction	99.9%	99.9%
Peak Flow Reduction	99.4%	99.4%
Lag Time (min|hours)	175.00	2.9
Total Rainfall (mm)	2.3	2.3
Storm Duration (hours|days)	7.3	0.3
ADP (hours|days)	13.8	0.6
Max Rain Intensity (mm/hr)	3.0	3.0

Dates for Graph	
Beginning	2018-11-29 15:00
End	2018-11-30 8:55
Inflow Peak	2018-11-29 23:35
Outflow Peak	2018-11-30 1:55
Inflow Lag	2018-11-29 23:00
Outflow Lag	2018-11-30 1:55

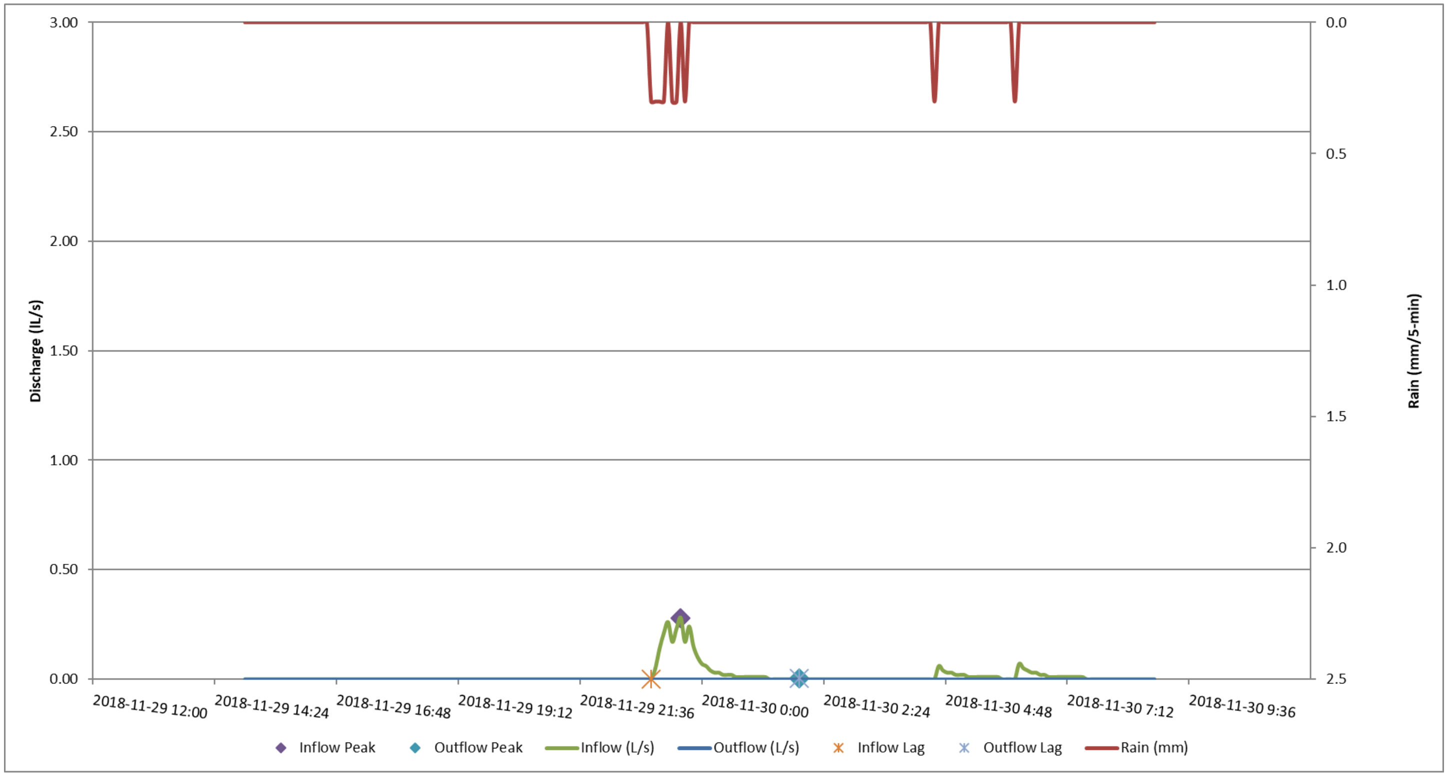

Storm ID: 2018-11-30-13

Dates for Graph	
Beginning	2018-11-30 9:00
End	2018-11-30 20:55
Inflow Peak	2018-11-30 13:50
Outflow Peak	2018-11-30 13:55
Inflow Lag	2018-11-30 13:25
Outflow Lag	2018-11-30 13:50

Performance		
Total Inflow (m^3|L)	2.3	2,292
Total Outflow (m^3|L)	0.1	108
Volume Reduction	95.3%	95.3%
Peak Flow Reduction	94.9%	94.9%
Lag Time (min|hours)	25.00	0.4
Total Rainfall (mm)	5.5	5.5
Storm Duration (hours|days)	4.9	0.2
ADP (hours|days)	7.3	0.3
Max Rain Intensity (mm/hr)	9.0	9.0

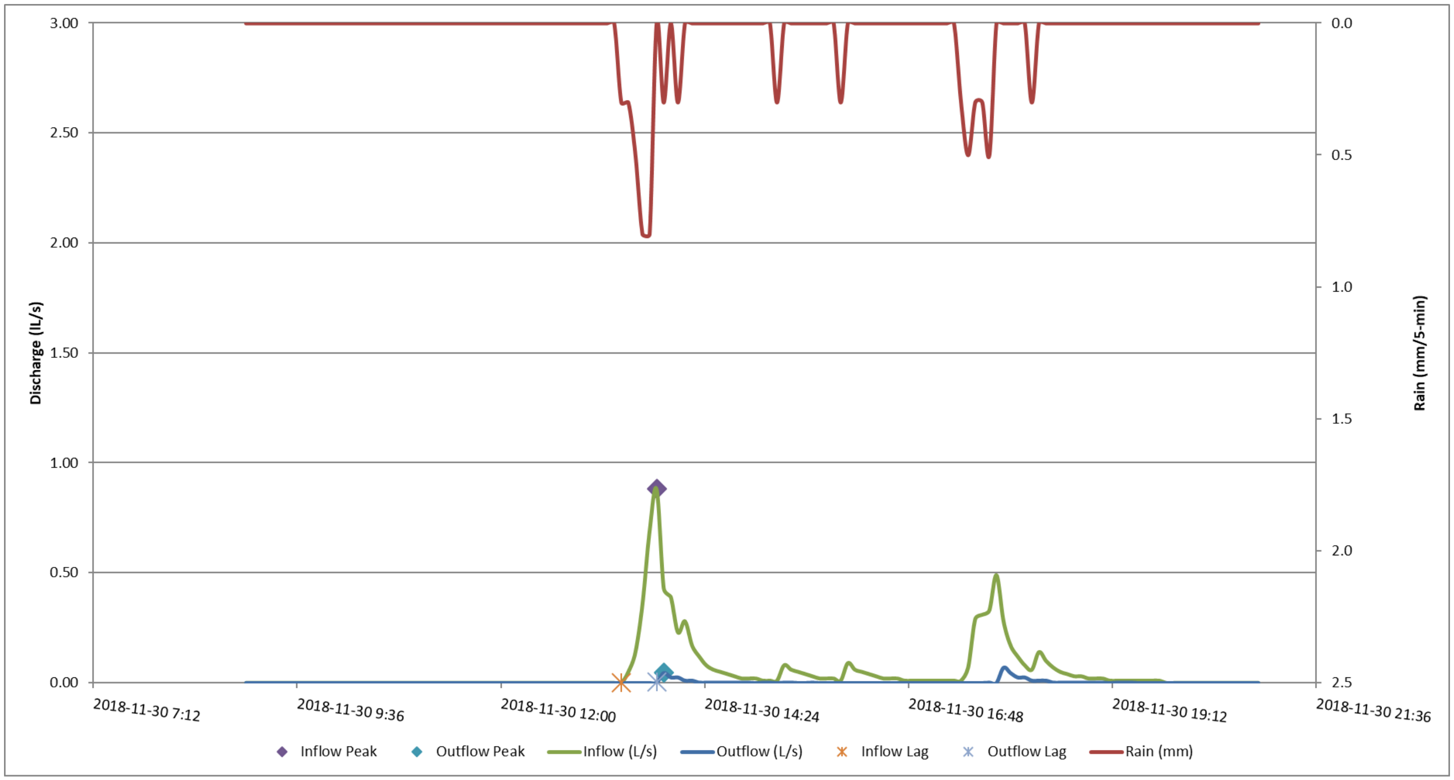

Storm ID: 2018-12-1-1

Dates for Graph	
Beginning	2018-11-30 23:00
End	2018-12-01 5:55
Inflow Peak	2018-12-01 2:50
Outflow Peak	2018-12-01 3:00
Inflow Lag	2018-12-01 1:15
Outflow Lag	2018-12-01 2:55

Performance		
Total Inflow (m^3|L)	1.3	1,329
Total Outflow (m^3|L)	0.0	33
Volume Reduction	97.5%	97.5%
Peak Flow Reduction	92.3%	92.3%
Lag Time (min|hours)	100.00	1.7
Total Rainfall (mm)	3.5	3.5
Storm Duration (hours|days)	5.4	0.2
ADP (hours|days)	7.0	0.3
Max Rain Intensity (mm/hr)	3.0	3.0

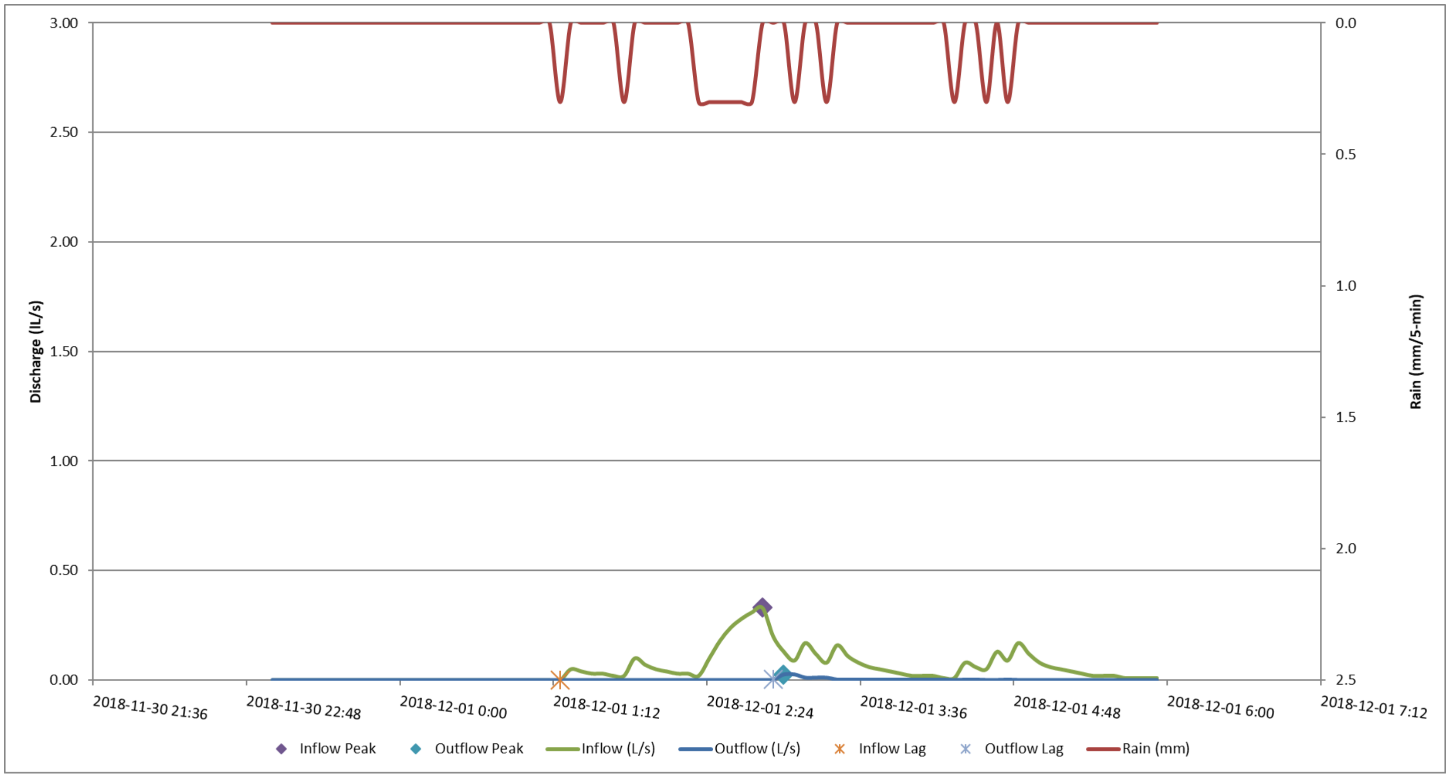

Storm ID: 2018-12-8-5

Dates for Graph	
Beginning	2018-12-07 23:00
End	2018-12-08 22:20
Inflow Peak	2018-12-08 10:50
Outflow Peak	2018-12-01 3:00
Inflow Lag	2018-12-01 1:15
Outflow Lag	2018-12-01 2:55

Performance		
Total Inflow (m^3|L)	1.0	1,008
Total Outflow (m^3|L)	-	-
Volume Reduction	100.0%	100.0%
Peak Flow Reduction	100.0%	100.0%
Lag Time (min|hours)	100.00	1.7
Total Rainfall (mm)	2.5	2.5
Storm Duration (hours|days)	11.6	0.5
ADP (hours|days)	167.1	7.0
Max Rain Intensity (mm/hr)	3.0	3.0

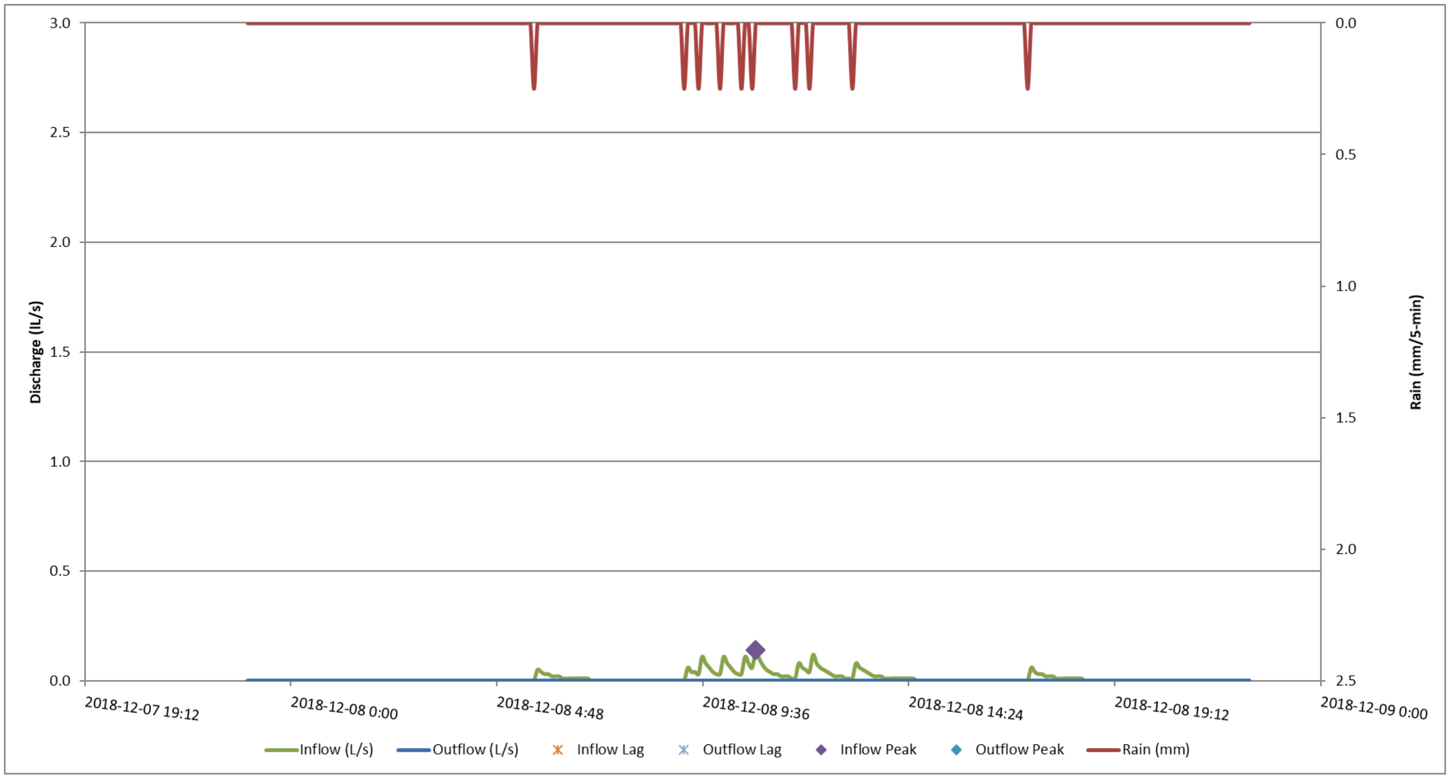

Storm ID: 2018-12-9-6

Dates for Graph	
Beginning	2018-12-09 4:00
End	2018-12-10 18:00
Inflow Peak	2018-12-09 18:15
Outflow Peak	2018-12-09 18:20
Inflow Lag	2018-12-09 6:30
Outflow Lag	2018-12-09 11:00

Performance		
Total Inflow (m^3|L)	15.1	15,084
Total Outflow (m^3|L)	2.3	2,318
Volume Reduction	84.6%	84.6%
Peak Flow Reduction	52.0%	52.0%
Lag Time (min|hours)	270.00	4.5
Total Rainfall (mm)	36.3	36.3
Storm Duration (hours|days)	26.2	1.1
ADP (hours|days)	13.3	0.6
Max Rain Intensity (mm/hr)	6.0	6.0

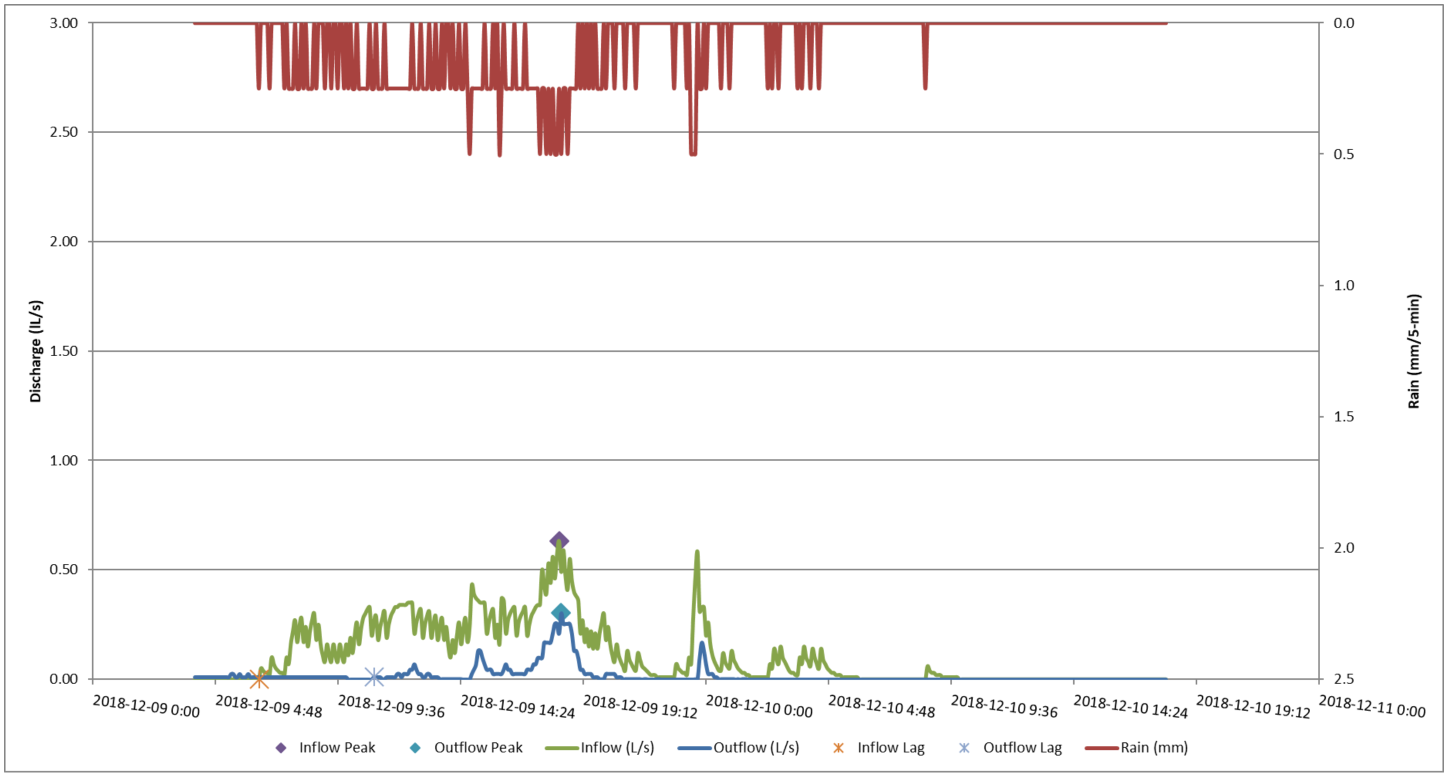

Storm ID: 2018-12-10-22

Dates for Graph	
Beginning	2018-12-10 16:00
End	2018-12-12 9:55
Inflow Peak	2018-12-11 13:20
Outflow Peak	2018-12-11 13:15
Inflow Lag	2018-12-10 22:30
Outflow Lag	2018-12-11 0:05

Performance		
Total Inflow (m^3|L)	27.6	27,597
Total Outflow (m^3|L)	12.3	12,297
Volume Reduction	55.4%	55.4%
Peak Flow Reduction	54.3%	54.3%
Lag Time (min|hours)	95.00	1.6
Total Rainfall (mm)	66.5	66.5
Storm Duration (hours|days)	19.3	0.8
ADP (hours|days)	13.9	0.6
Max Rain Intensity (mm/hr)	15.0	15.0

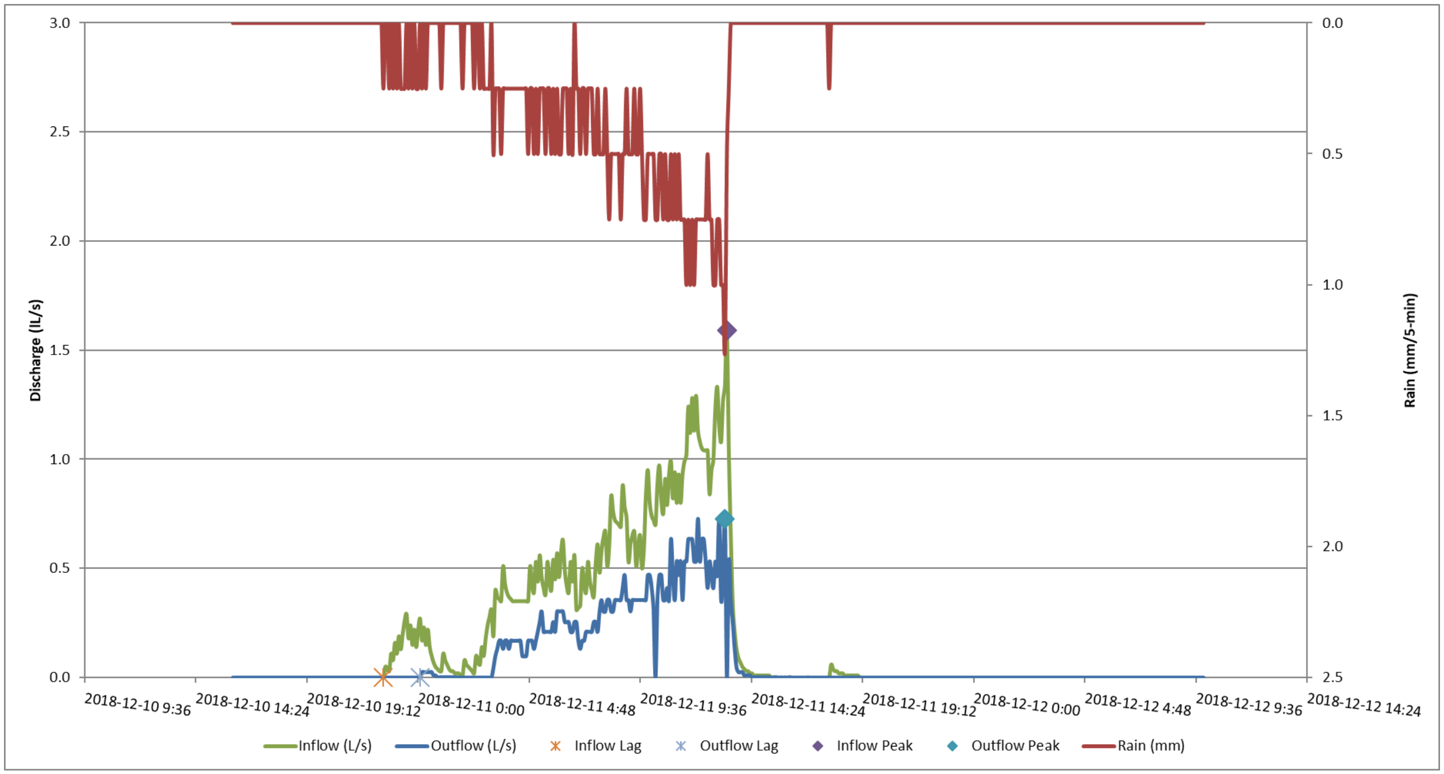

Storm ID: 2018-12-12-13

Dates for Graph	
Beginning	2018-12-12 10:00
End	2018-12-14 9:30
Inflow Peak	2018-12-13 1:35
Outflow Peak	2018-12-13 1:35
Inflow Lag	2018-12-12 17:35
Outflow Lag	2018-12-12 20:15

Performance		
Total Inflow (m^3|L)	49.1	49,140
Total Outflow (m^3|L)	23.3	23,339
Volume Reduction	52.5%	52.5%
Peak Flow Reduction	49.4%	49.4%
Lag Time (min|hours)	160.00	2.7
Total Rainfall (mm)	118.3	118.3
Storm Duration (hours|days)	38.1	1.6
ADP (hours|days)	19.7	0.8
Max Rain Intensity (mm/hr)	12.0	12.0

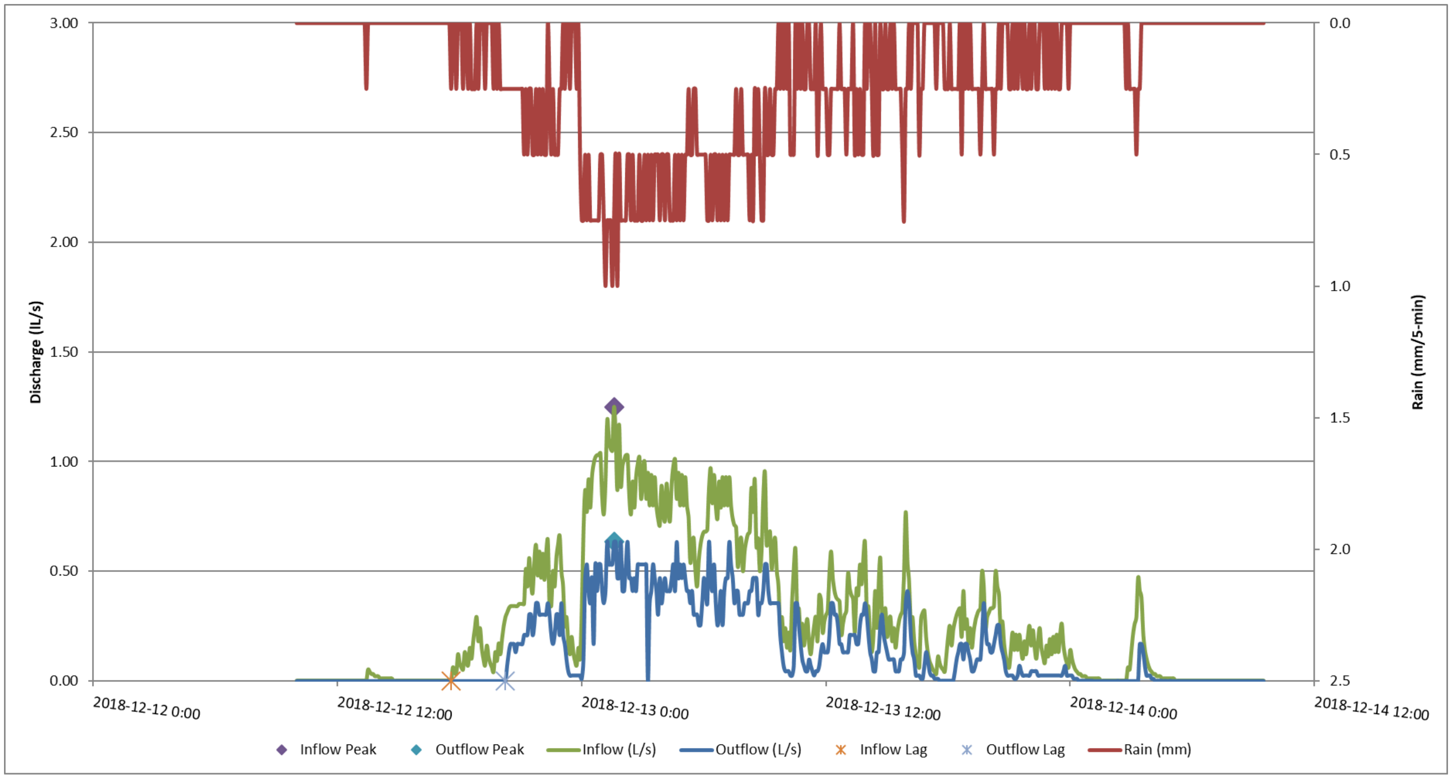

Storm ID: 2018-12-15-22

Dates for Graph	
Beginning	2018-12-15 12:00
End	2018-12-17 11:55
Inflow Peak	2018-12-16 14:45
Outflow Peak	2018-12-16 14:45
Inflow Lag	2018-12-16 11:25
Outflow Lag	2018-12-16 13:20

Performance		
Total Inflow (m^3|L)	7.3	7,272
Total Outflow (m^3|L)	1.0	1,047
Volume Reduction	85.6%	85.6%
Peak Flow Reduction	70.2%	70.2%
Lag Time (min|hours)	115.00	1.9
Total Rainfall (mm)	17.5	17.5
Storm Duration (hours|days)	30.5	1.3
ADP (hours|days)	27.6	1.1
Max Rain Intensity (mm/hr)	3.0	3.0

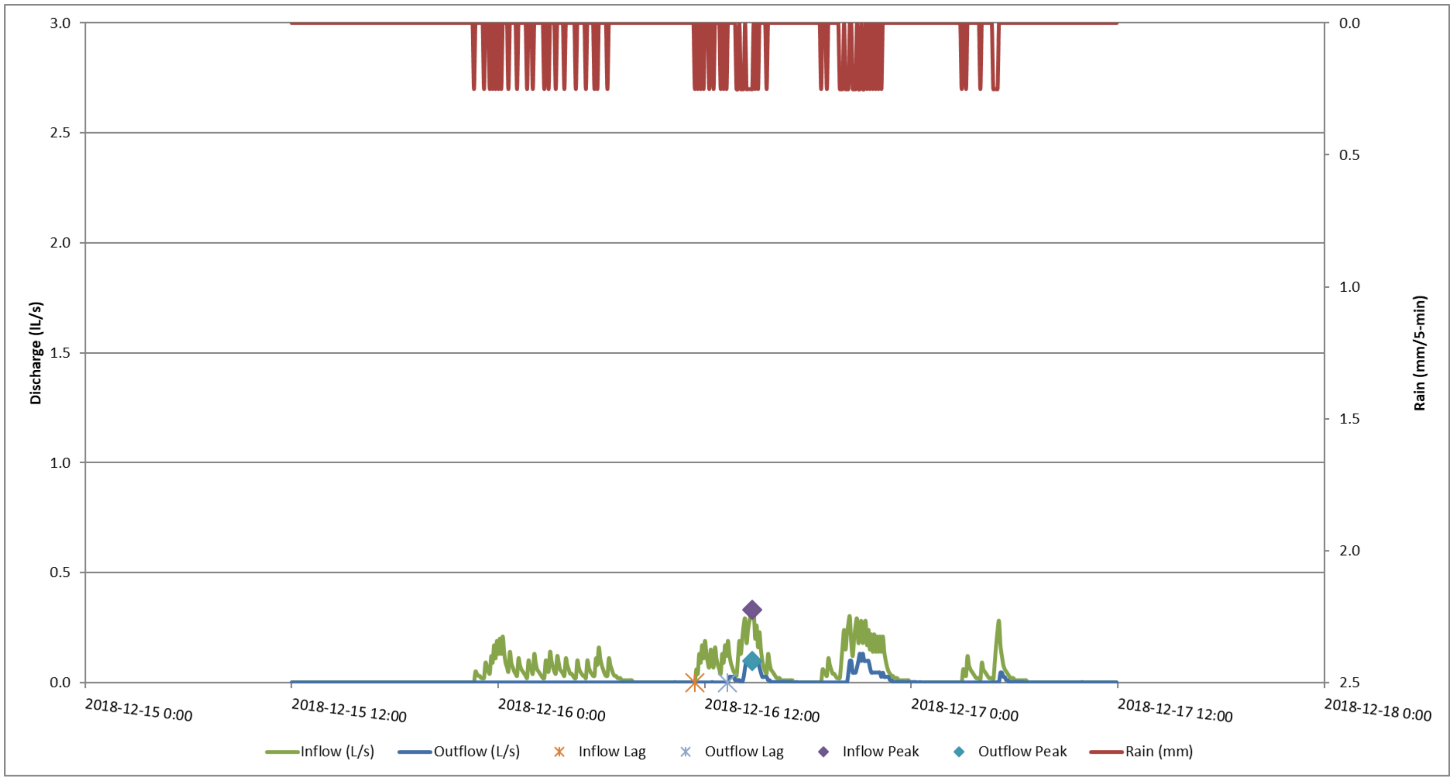

Storm ID: 2018-12-17-16

Dates for Graph	
Beginning	2018-12-17 7:00
End	2018-12-18 11:55
Inflow Peak	2018-12-17 20:10
Outflow Peak	2018-12-17 20:10
Inflow Lag	2018-12-17 16:40
Outflow Lag	2018-12-17 17:55

Performance		
Total Inflow (m^3|L)	12.1	12,060
Total Outflow (m^3|L)	4.9	4,904
Volume Reduction	59.3%	59.3%
Peak Flow Reduction	52.4%	52.4%
Lag Time (min|hours)	75.00	1.3
Total Rainfall (mm)	29.0	29.0
Storm Duration (hours|days)	15.0	0.6
ADP (hours|days)	11.7	0.5
Max Rain Intensity (mm/hr)	9.0	9.0

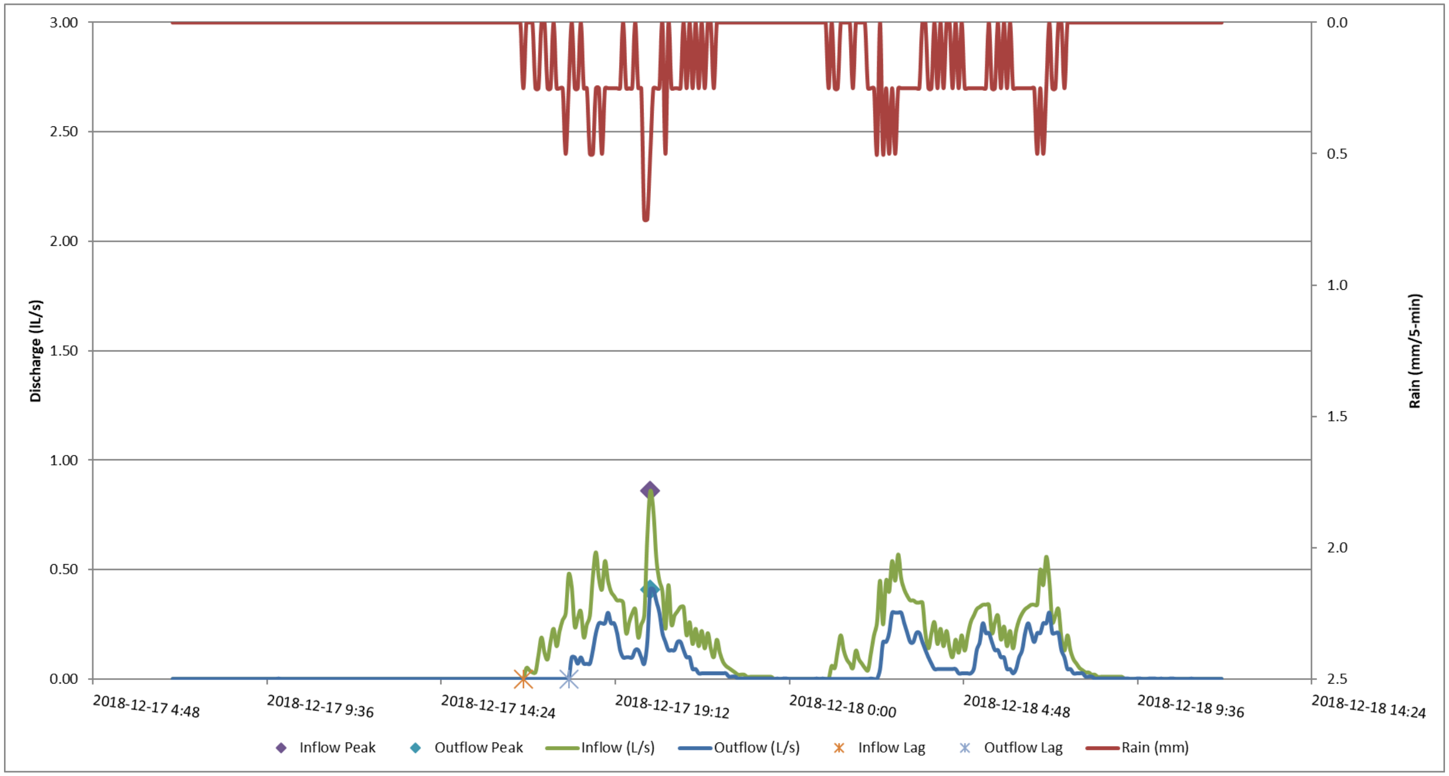

Storm ID: 2018-12-18-14

Dates for Graph	
Beginning	2018-12-18 12:00
End	2018-12-19 11:00
Inflow Peak	2018-12-18 19:05
Outflow Peak	2018-12-18 19:15
Inflow Lag	2018-12-18 18:50
Outflow Lag	2018-12-18 19:05

Performance		
Total Inflow (m^3|L)	2.2	2,163
Total Outflow (m^3|L)	0.2	170
Volume Reduction	92.2%	92.2%
Peak Flow Reduction	70.5%	70.5%
Lag Time (min|hours)	15.00	0.3
Total Rainfall (mm)	5.3	5.3
Storm Duration (hours|days)	14.5	0.6
ADP (hours|days)	6.4	0.3
Max Rain Intensity (mm/hr)	9.0	9.0

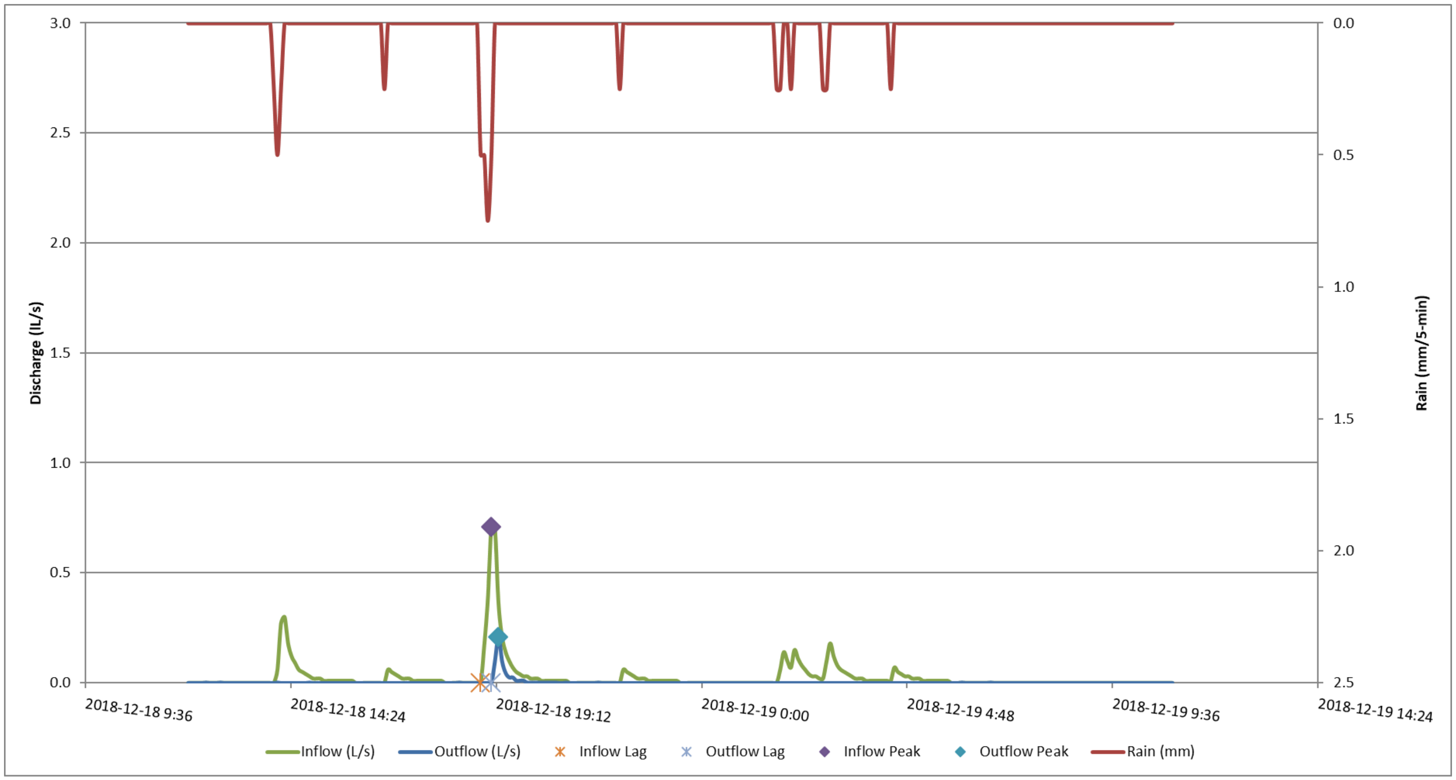

Storm ID: 2018-12-20-1

Dates for Graph	
Beginning	2018-12-19 16:00
End	2018-12-20 17:00
Inflow Peak	2018-12-20 5:30
Outflow Peak	2018-12-20 5:35
Inflow Lag	2018-12-20 1:40
Outflow Lag	2018-12-20 3:45

Performance		
Total Inflow (m^3|L)	7.6	7,590
Total Outflow (m^3|L)	3.0	3,046
Volume Reduction	59.9%	59.9%
Peak Flow Reduction	41.5%	41.5%
Lag Time (min|hours)	125.00	2.1
Total Rainfall (mm)	18.3	18.3
Storm Duration (hours|days)	7.1	0.3
ADP (hours|days)	21.3	0.9
Max Rain Intensity (mm/hr)	9.0	9.0

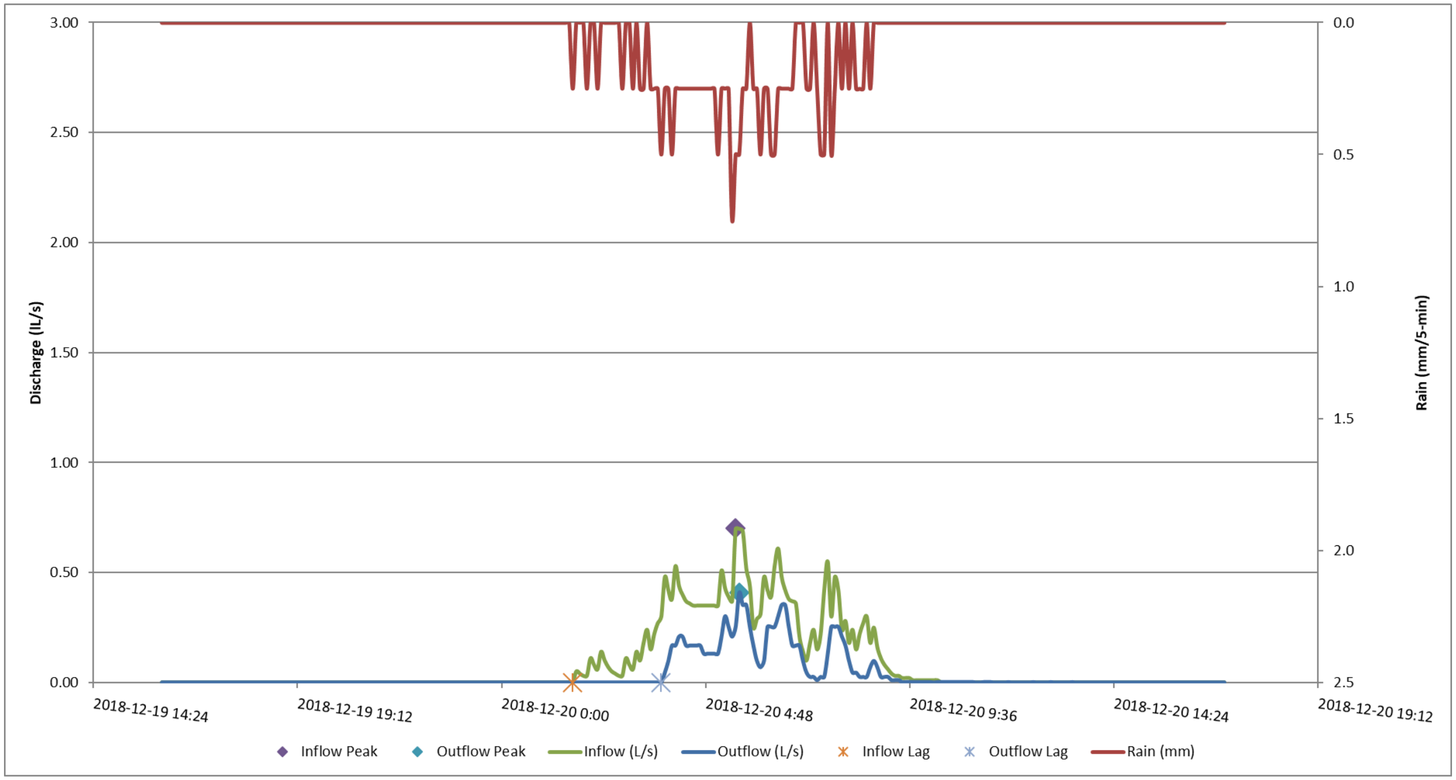

Storm ID: 2018-12-20-18

Dates for Graph	
Beginning	2018-12-20 17:00
End	2018-12-20 23:00
Inflow Peak	2018-12-20 20:20
Outflow Peak	2018-12-20 20:25
Inflow Lag	2018-12-20 18:25
Outflow Lag	2018-12-20 19:10

Performance		
Total Inflow (m^3|L)	2.8	2,793
Total Outflow (m^3|L)	1.0	989
Volume Reduction	64.6%	64.6%
Peak Flow Reduction	48.7%	48.7%
Lag Time (min|hours)	45.00	0.8
Total Rainfall (mm)	6.8	6.8
Storm Duration (hours|days)	2.4	0.1
ADP (hours|days)	9.8	0.4
Max Rain Intensity (mm/hr)	6.0	6.0

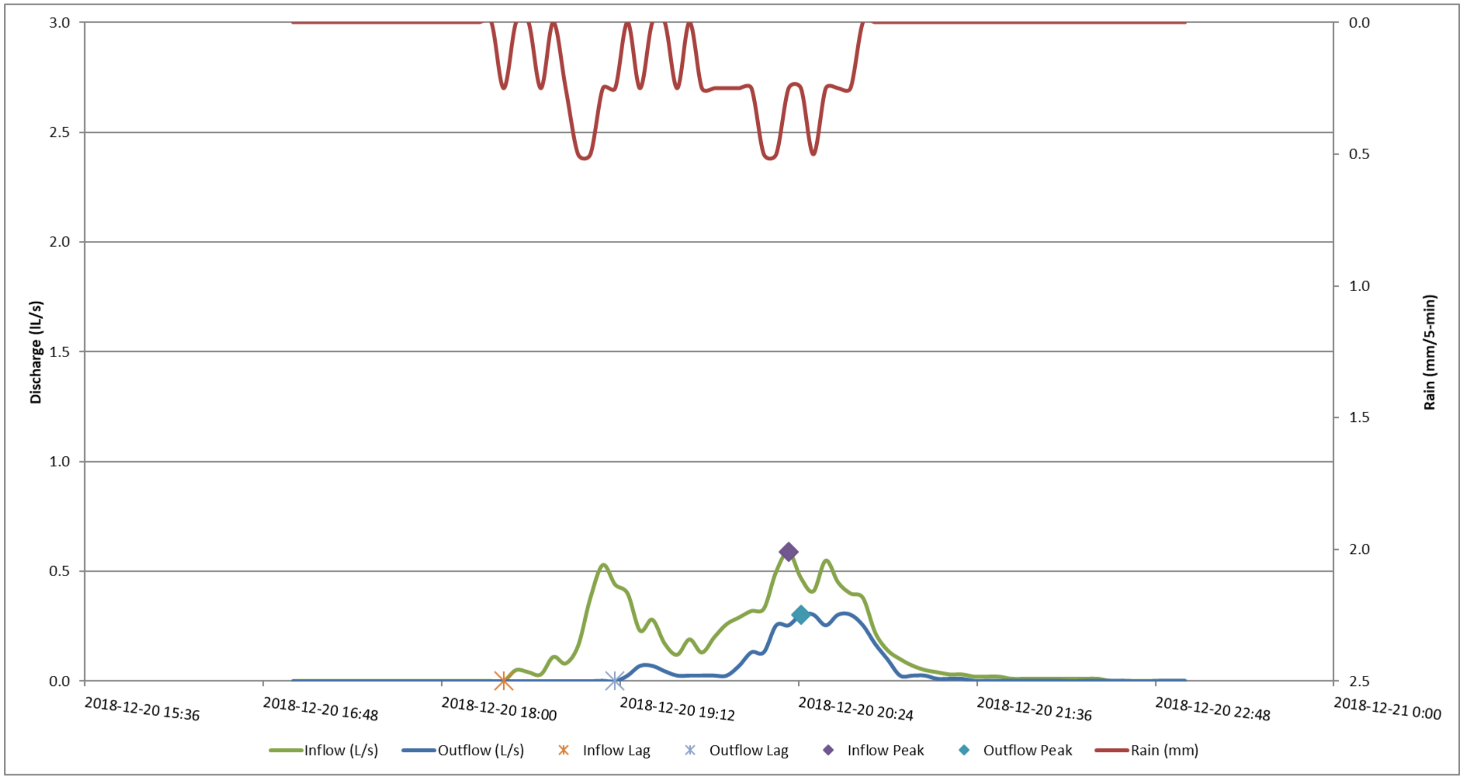

Storm ID: 2018-12-22-4

Dates for Graph	
Beginning	2018-12-22 1:00
End	2018-12-22 15:10
Inflow Peak	2018-12-22 5:25
Outflow Peak	2018-12-22 5:30
Inflow Lag	2018-12-22 4:40
Outflow Lag	2018-12-22 5:25

Performance		
Total Inflow (m^3|L)	1.2	1,239
Total Outflow (m^3|L)	0.0	5
Volume Reduction	99.6%	99.6%
Peak Flow Reduction	99.1%	99.1%
Lag Time (min|hours)	45.00	0.8
Total Rainfall (mm)	3.0	3.0
Storm Duration (hours|days)	6.6	0.3
ADP (hours|days)	31.9	1.3
Max Rain Intensity (mm/hr)	3.0	3.0

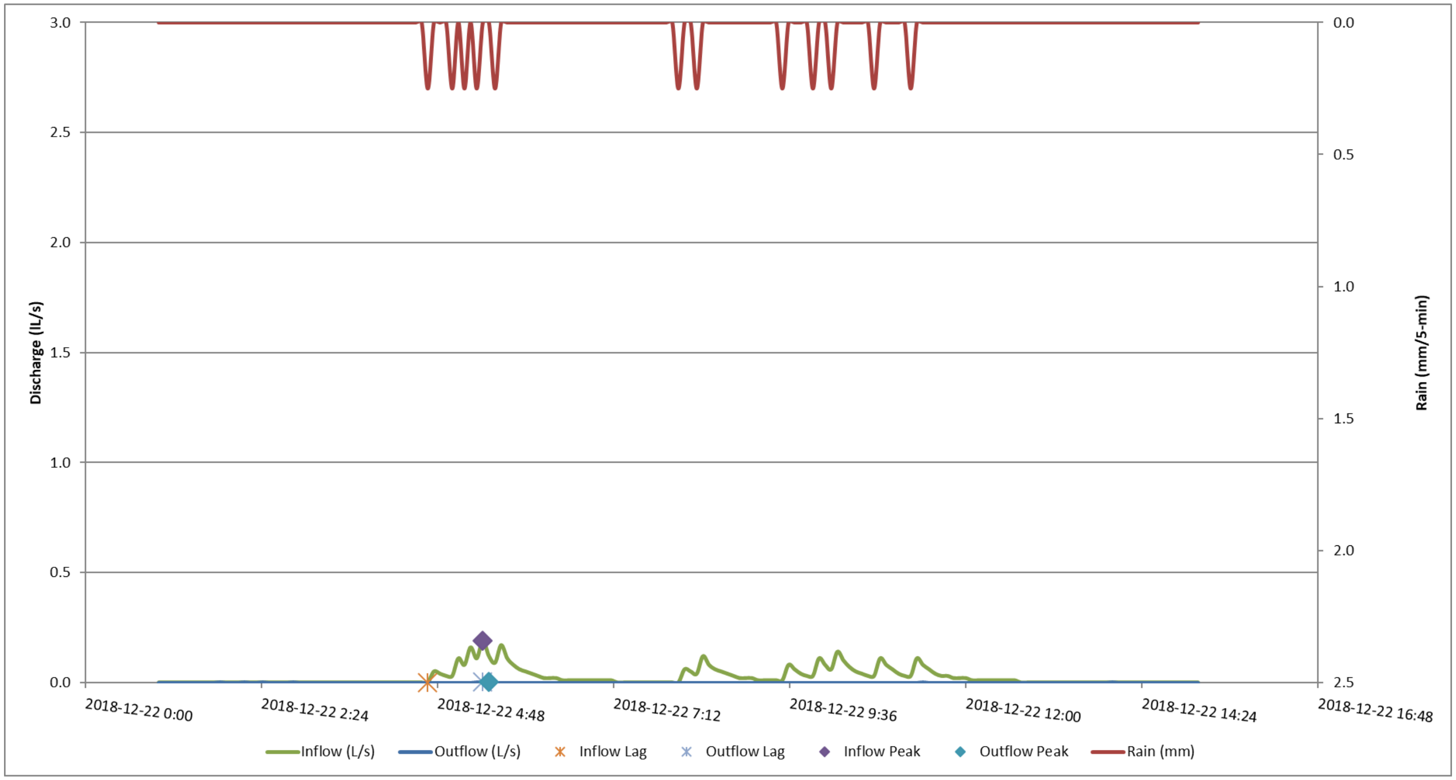

Storm ID: 2018-12-22-17

Dates for Graph	
Beginning	2018-12-22 15:00
End	2018-12-22 23:00
Inflow Peak	2018-12-22 19:00
Outflow Peak	2018-12-22 19:20
Inflow Lag	2018-12-22 18:15
Outflow Lag	2018-12-22 19:00

Performance		
Total Inflow (m^3|L)	1.8	1,770
Total Outflow (m^3|L)	0.4	352
Volume Reduction	80.1%	80.1%
Peak Flow Reduction	70.8%	70.8%
Lag Time (min|hours)	45.00	0.8
Total Rainfall (mm)	30.5	30.5
Storm Duration (hours|days)	21.2	0.9
ADP (hours|days)	0.0	0.0
Max Rain Intensity (mm/hr)	9.0	9.0

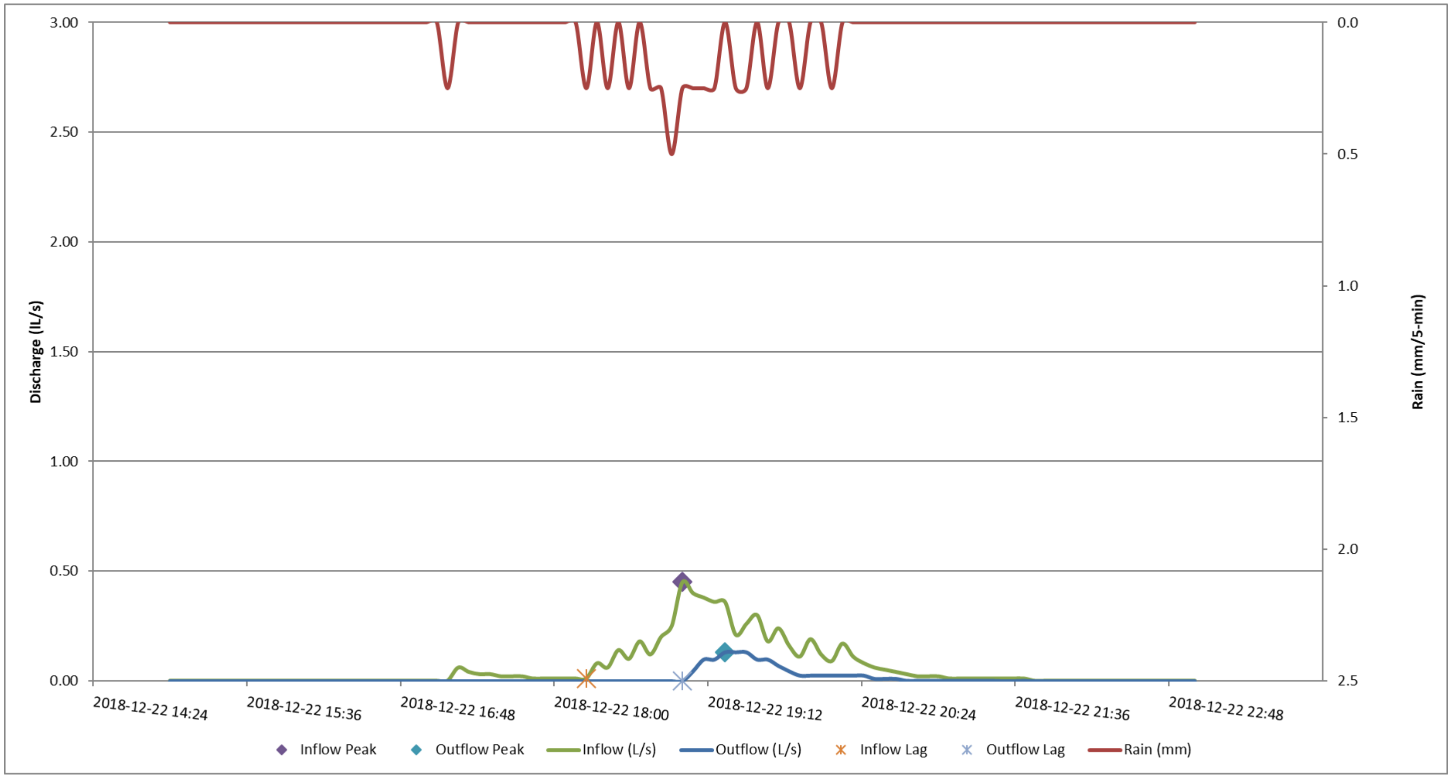

Storm ID: 2018-12-26-0

Dates for Graph	
Beginning	2018-12-25 0:00
End	2018-12-27 15:55
Inflow Peak	2018-12-26 17:10
Outflow Peak	2018-12-26 17:20
Inflow Lag	2018-12-26 12:10
Outflow Lag	2018-12-26 14:30

Performance		
Total Inflow (m^3|L)	3.2	3,210
Total Outflow (m^3|L)	0.1	125
Volume Reduction	96.1%	96.1%
Peak Flow Reduction	67.9%	67.9%
Lag Time (min|hours)	140.00	2.3
Total Rainfall (mm)	7.8	7.8
Storm Duration (hours|days)	16.5	0.7
ADP (hours|days)	47.1	2.0
Max Rain Intensity (mm/hr)	6.0	6.0

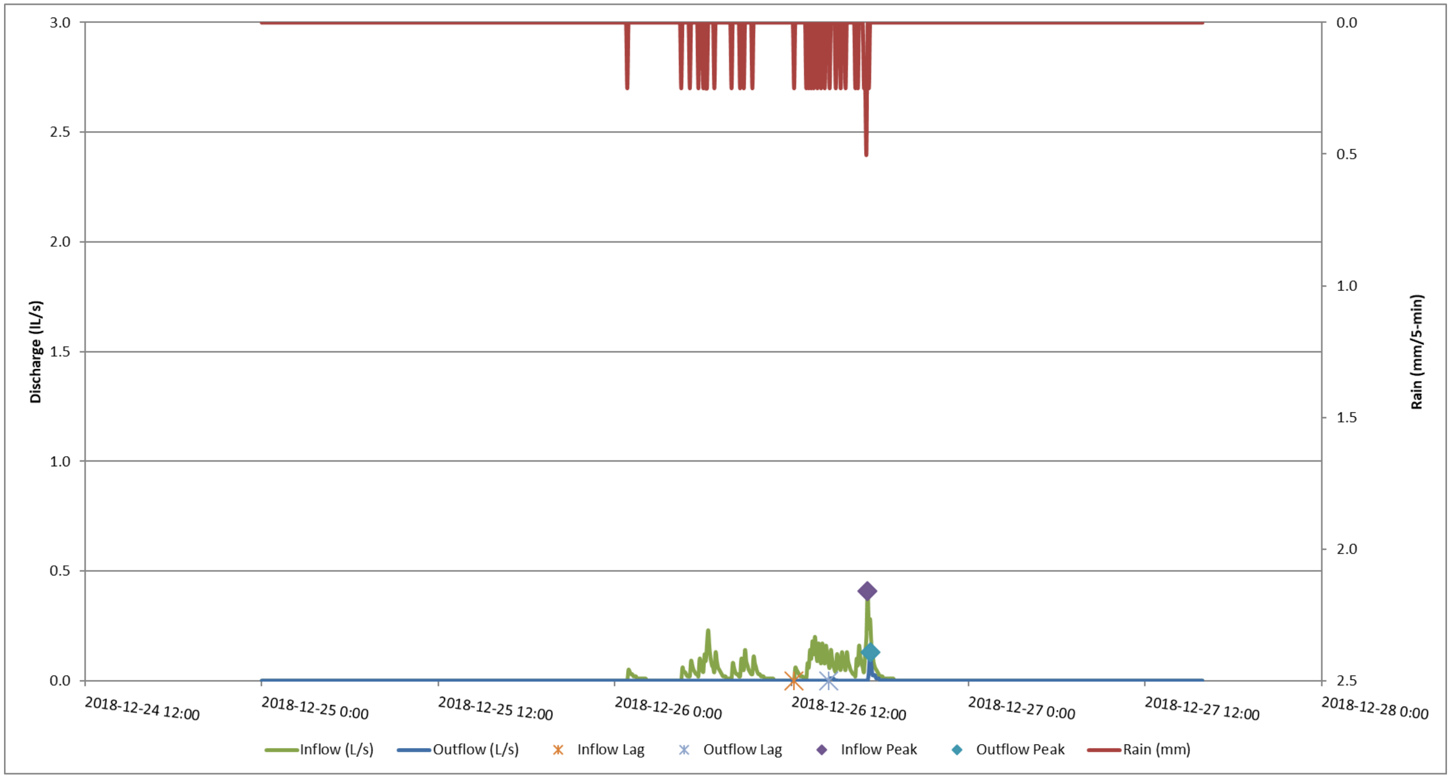

Storm ID: 2018-12-28-0

Dates for Graph	
Beginning	2018-12-27 21:00
End	2018-12-29 7:00
Inflow Peak	2018-12-28 13:25
Outflow Peak	2018-12-28 13:25
Inflow Lag	2018-12-28 4:10
Outflow Lag	2018-12-28 8:45

Performance		
Total Inflow (m^3|L)	16.4	16,359
Total Outflow (m^3|L)	6.9	6,937
Volume Reduction	57.6%	57.6%
Peak Flow Reduction	50.2%	50.2%
Lag Time (min|hours)	275.00	4.6
Total Rainfall (mm)	39.3	39.3
Storm Duration (hours|days)	24.2	1.0
ADP (hours|days)	31.1	1.3
Max Rain Intensity (mm/hr)	6.0	6.0

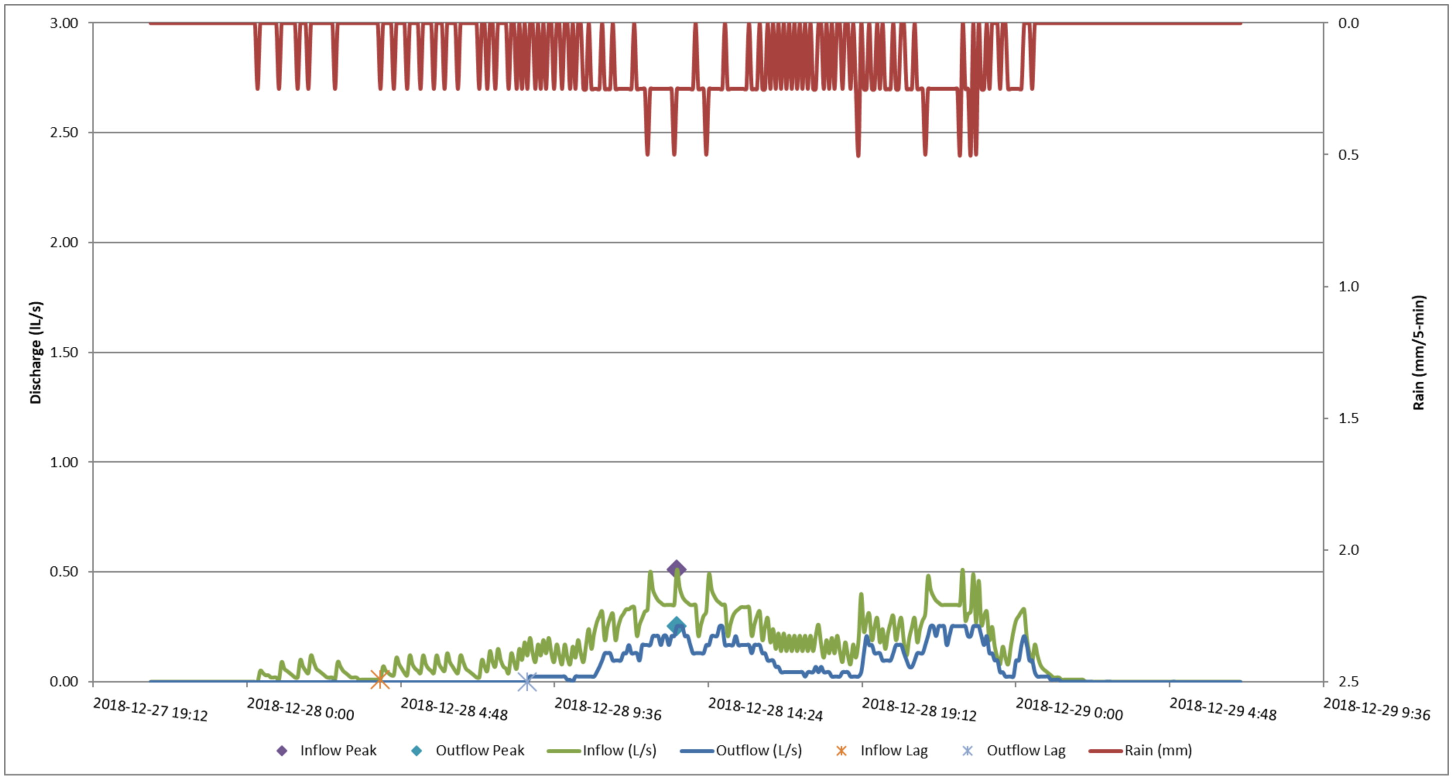

Storm ID: 2018-12-29-7

Dates for Graph	
Beginning	2018-12-29 2:30
End	2018-12-29 20:00
Inflow Peak	2018-12-29 10:55
Outflow Peak	2018-12-29 11:05
Inflow Lag	2018-12-29 7:45
Outflow Lag	2018-12-29 9:20

Performance		
Total Inflow (m^3|L)	5.2	5,187
Total Outflow (m^3|L)	2.7	2,744
Volume Reduction	47.1%	47.1%
Peak Flow Reduction	40.9%	40.9%
Lag Time (min|hours)	95.00	1.6
Total Rainfall (mm)	12.5	12.5
Storm Duration (hours|days)	5.1	0.2
ADP (hours|days)	7.3	0.3
Max Rain Intensity (mm/hr)	6.0	6.0

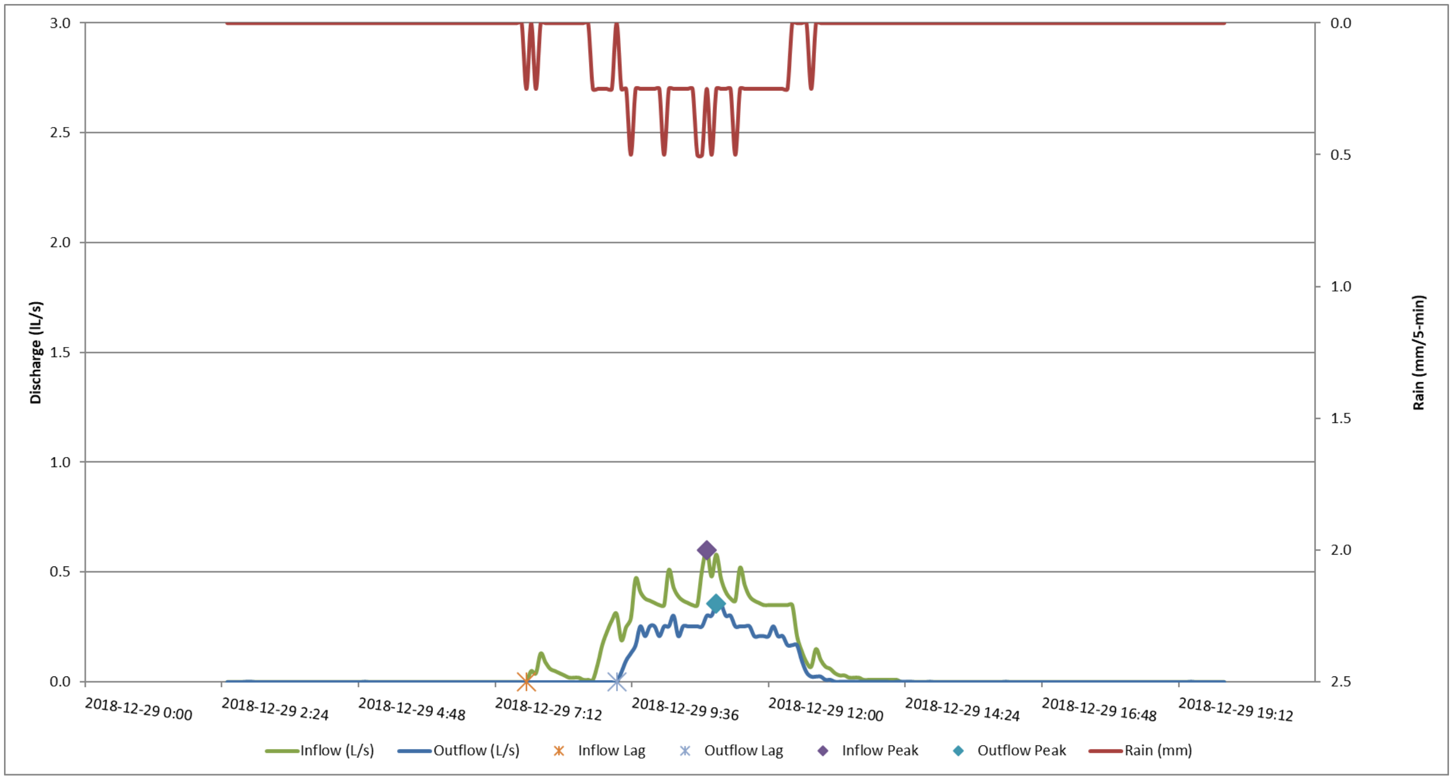

Storm ID: 2019-1-2-12

Dates for Graph	
Beginning	2019-01-02 0:00
End	2019-01-04 16:00
Inflow Peak	2019-01-03 9:15
Outflow Peak	2019-01-03 9:00
Inflow Lag	2019-01-02 12:15
Outflow Lag	2019-01-02 21:35

Performance		
Total Inflow (m^3|L)	41.0	40,965
Total Outflow (m^3|L)	17.4	17,409
Volume Reduction	57.5%	57.5%
Peak Flow Reduction	61.0%	61.0%
Lag Time (min|hours)	560.00	9.3
Total Rainfall (mm)	98.5	98.5
Storm Duration (hours|days)	43.4	1.8
ADP (hours|days)	83.0	3.5
Max Rain Intensity (mm/hr)	12.0	12.0

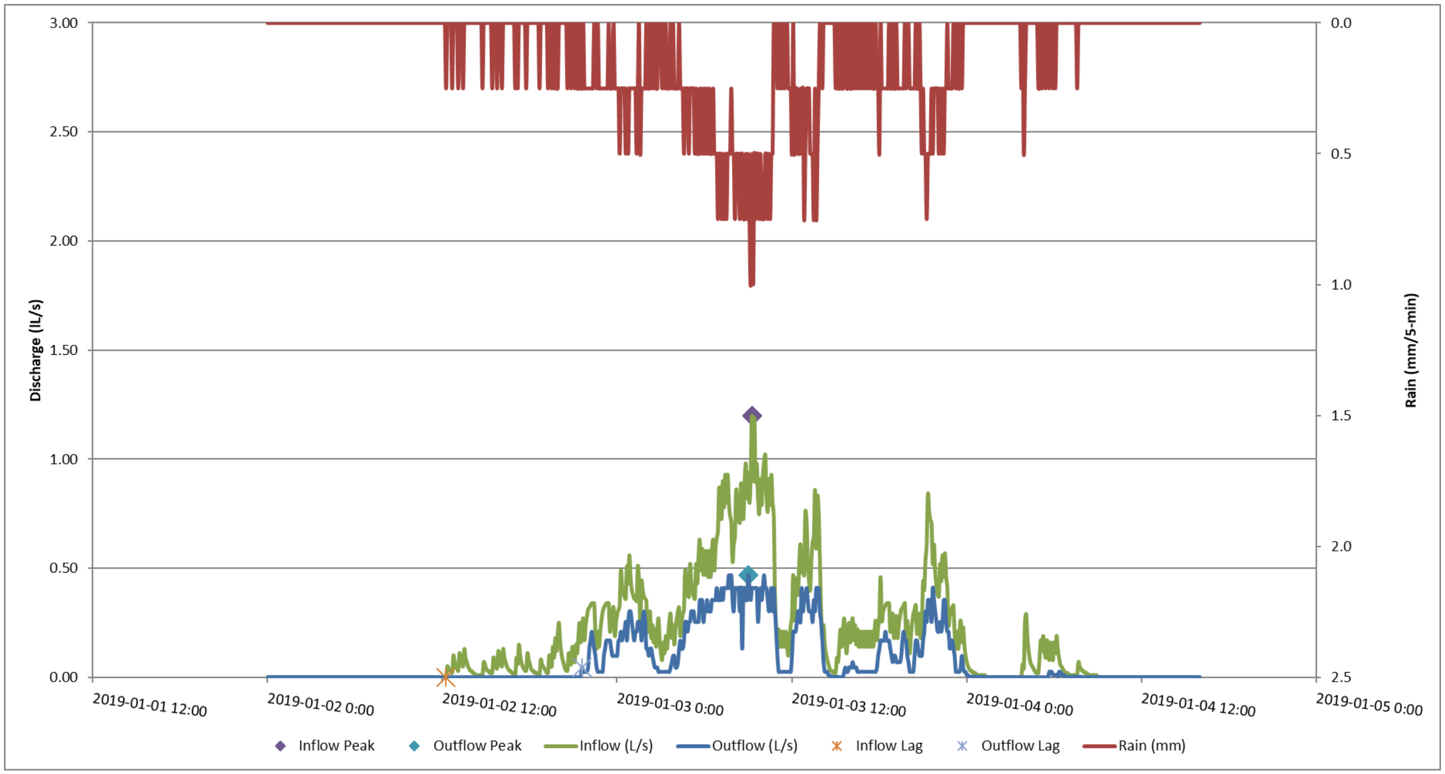

Storm ID: 2019-1-5-18

Dates for Graph	
Beginning	2019-01-05 0:00
End	2019-01-06 23:55
Inflow Peak	2019-01-06 3:55
Outflow Peak	2019-01-06 3:55
Inflow Lag	2019-01-06 0:00
Outflow Lag	2019-01-06 3:00

Performance		
Total Inflow (m^3|L)	6.1	6,123
Total Outflow (m^3|L)	2.1	2,062
Volume Reduction	66.3%	66.3%
Peak Flow Reduction	52.4%	52.4%
Lag Time (min|hours)	180.00	3.0
Total Rainfall (mm)	14.8	14.8
Storm Duration (hours|days)	10.5	0.4
ADP (hours|days)	23.5	1.0
Max Rain Intensity (mm/hr)	9.0	9.0

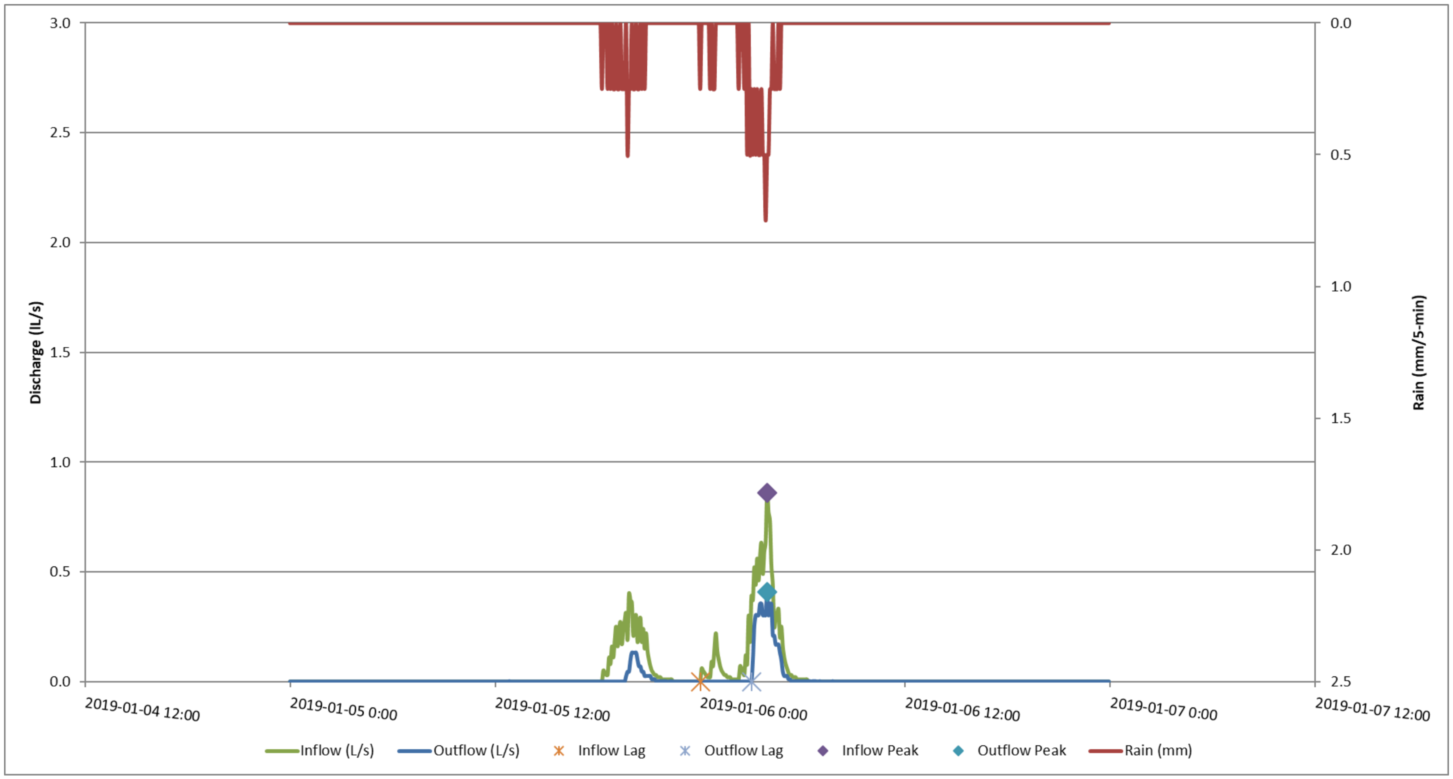

Storm ID: 2019-1-8-15

Dates for Graph	
Beginning	2019-01-07 6:00
End	2019-01-11 11:55
Inflow Peak	2019-01-10 0:20
Outflow Peak	2019-01-10 0:30
Inflow Lag	2019-01-09 21:55
Outflow Lag	2019-01-09 22:35

Performance		
Total Inflow (m^3|L)	7.5	7,464
Total Outflow (m^3|L)	1.2	1,166
Volume Reduction	84.4%	84.4%
Peak Flow Reduction	52.1%	52.1%
Lag Time (min|hours)	40.00	0.7
Total Rainfall (mm)	18.0	18.0
Storm Duration (hours|days)	41.0	1.7
ADP (hours|days)	35.8	1.5
Max Rain Intensity (mm/hr)	6.0	6.0

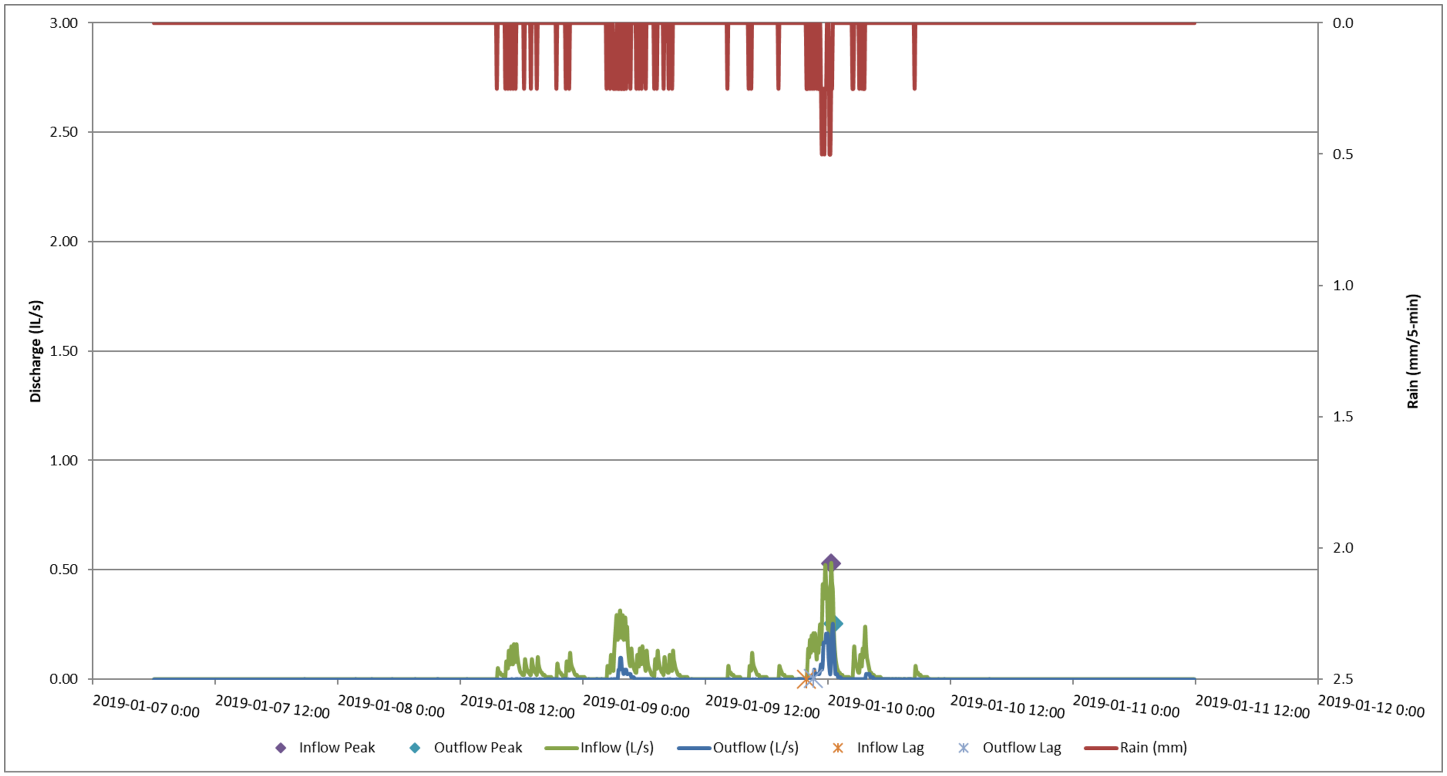

Storm ID: 2019-1-17-4

Dates for Graph	
Beginning	2019-01-16 18:00
End	2019-01-18 18:00
Inflow Peak	2019-01-17 20:45
Outflow Peak	2019-01-17 20:45
Inflow Lag	2019-01-17 19:35
Outflow Lag	2019-01-17 20:05

Performance		
Total Inflow (m^3|L)	12.7	12,657
Total Outflow (m^3|L)	3.0	3,030
Volume Reduction	76.1%	76.1%
Peak Flow Reduction	74.8%	74.8%
Lag Time (min|hours)	30.00	0.5
Total Rainfall (mm)	30.5	30.5
Storm Duration (hours|days)	27.1	1.1
ADP (hours|days)	48.8	2.0
Max Rain Intensity (mm/hr)	12.0	12.0

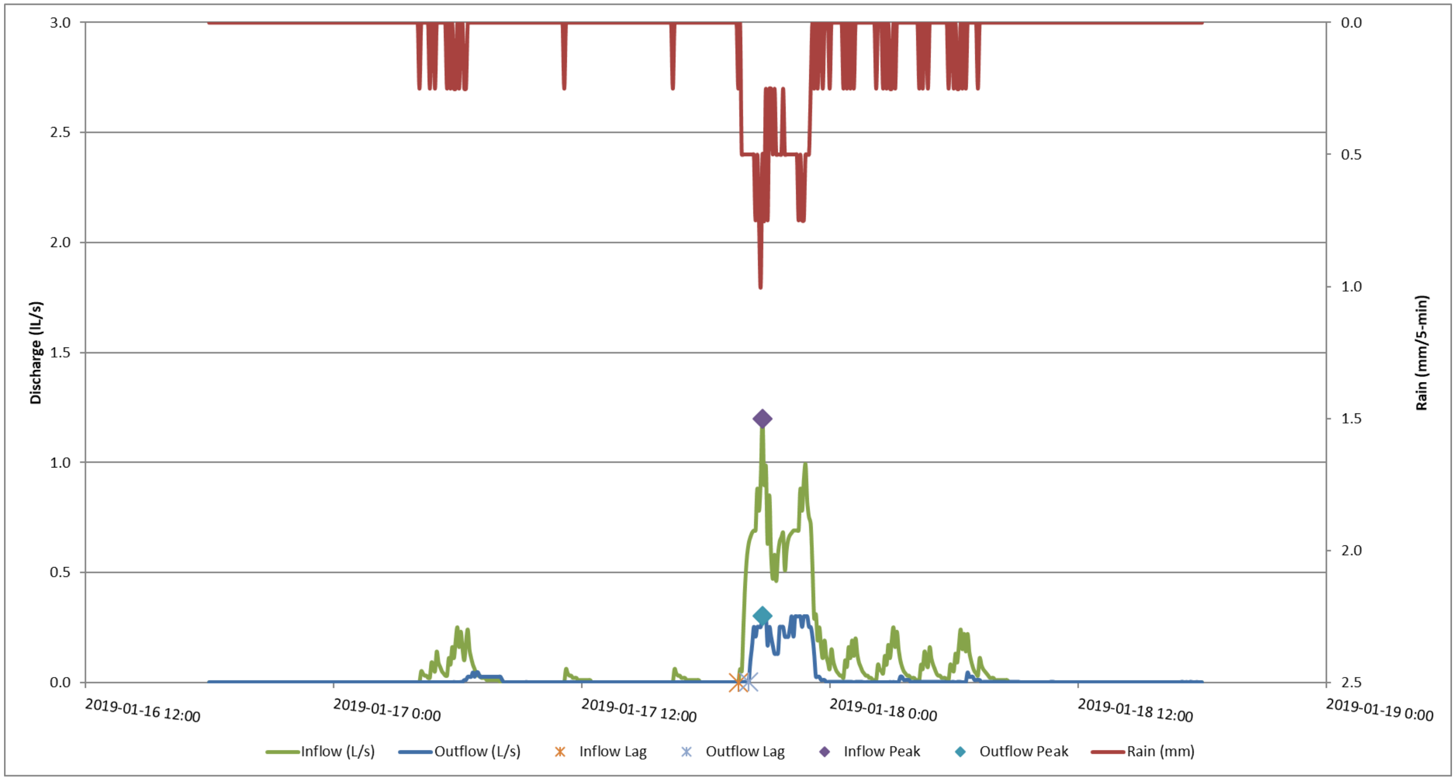

Storm ID: 2019-1-18-18

Dates for Graph	
Beginning	2019-01-18 12:00
End	2019-01-19 12:00
Inflow Peak	2019-01-18 21:10
Outflow Peak	2019-01-18 21:20
Inflow Lag	2019-01-18 18:25
Outflow Lag	2019-01-18 19:35

Performance		
Total Inflow (m^3|L)	3.2	3,225
Total Outflow (m^3|L)	0.6	569
Volume Reduction	82.4%	82.4%
Peak Flow Reduction	52.4%	52.4%
Lag Time (min|hours)	70.00	1.2
Total Rainfall (mm)	7.8	7.8
Storm Duration (hours|days)	7.2	0.3
ADP (hours|days)	11.3	0.5
Max Rain Intensity (mm/hr)	6.0	6.0

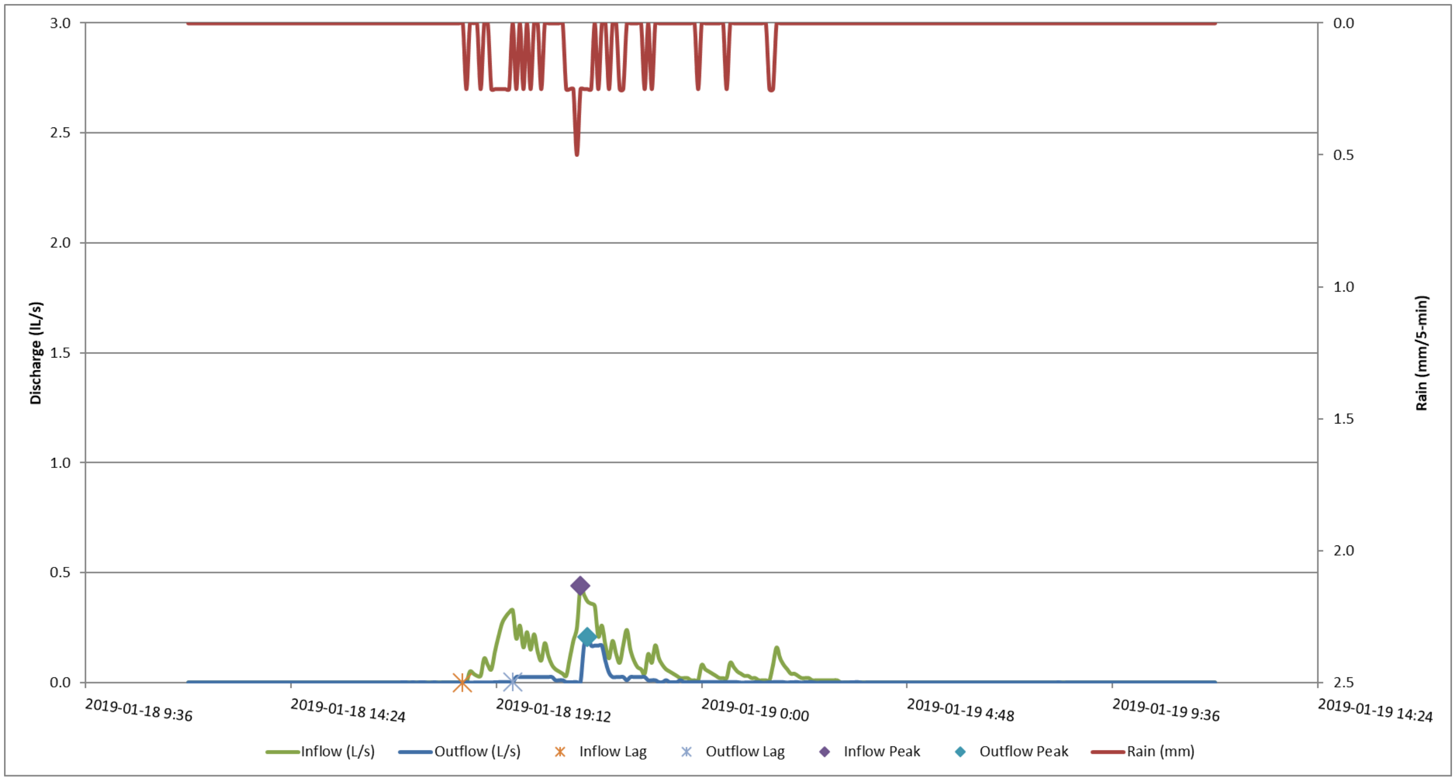

Storm ID: 2019-1-22-5

Dates for Graph	
Beginning	2019-01-21 12:00
End	2019-01-23 23:55
Inflow Peak	2019-01-23 1:30
Outflow Peak	2019-01-23 1:30
Inflow Lag	2019-01-22 8:50
Outflow Lag	2019-01-22 15:35

Performance		
Total Inflow (m^3|L)	17.4	17,364
Total Outflow (m^3|L)	6.7	6,724
Volume Reduction	61.3%	61.3%
Peak Flow Reduction	60.6%	60.6%
Lag Time (min|hours)	405.00	6.8
Total Rainfall (mm)	41.8	41.8
Storm Duration (hours|days)	22.3	0.9
ADP (hours|days)	76.3	3.2
Max Rain Intensity (mm/hr)	12.0	12.0

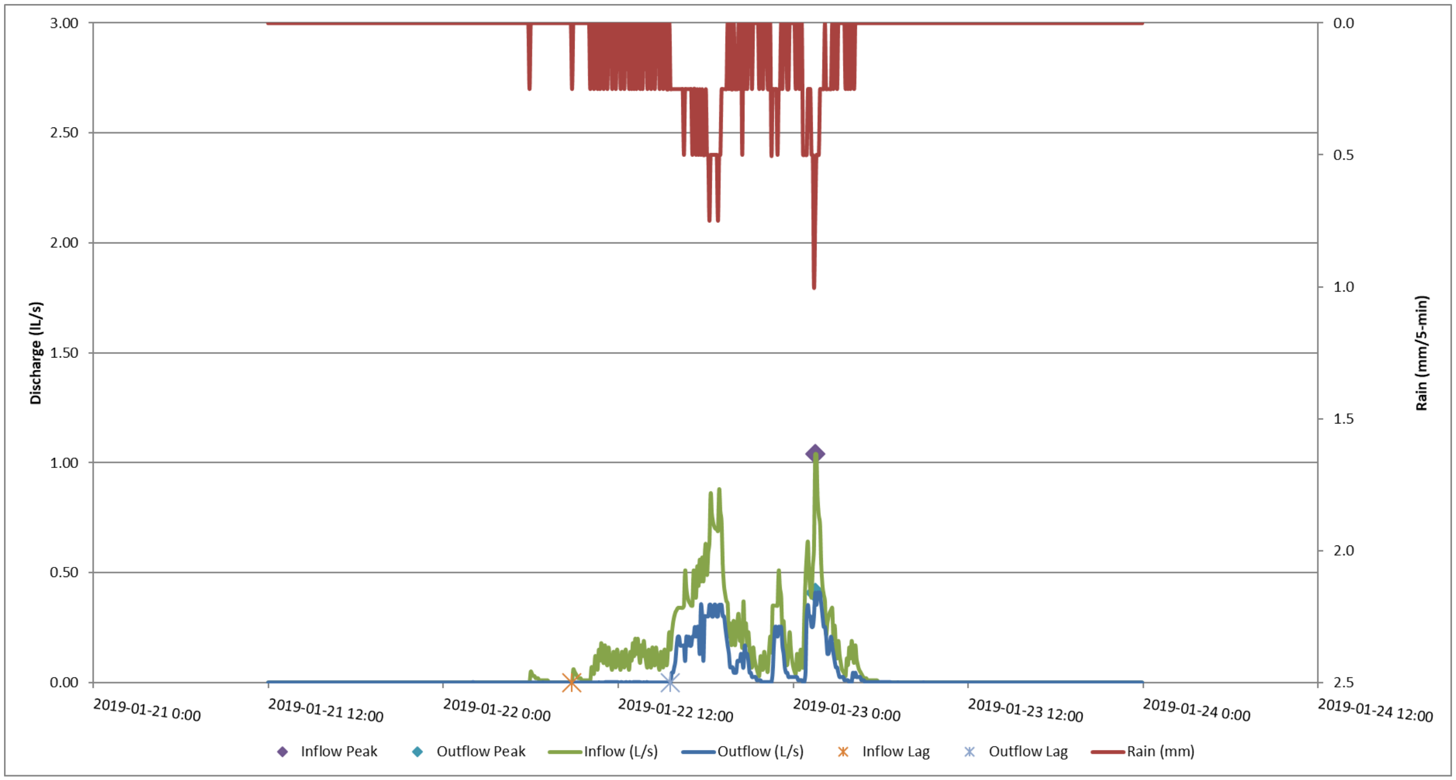

Storm ID: 2019-1-31-20

Performance		
Total Inflow (m^3|L)	15.3	15,282
Total Outflow (m^3|L)	3.0	3,044
Volume Reduction	80.1%	80.1%
Peak Flow Reduction	59.7%	59.7%
Lag Time (min|hours)	480.00	8.0
Total Rainfall (mm)	36.8	36.8
Storm Duration (hours|days)	26.6	1.1
ADP (hours|days)	208.2	8.7
Max Rain Intensity (mm/hr)	6.0	6.0

Dates for Graph	
Beginning	2019-01-31 12:00
End	2019-02-02 11:55
Inflow Peak	2019-02-01 8:25
Outflow Peak	2019-02-01 11:30
Inflow Lag	2019-01-31 20:20
Outflow Lag	2019-02-01 4:20

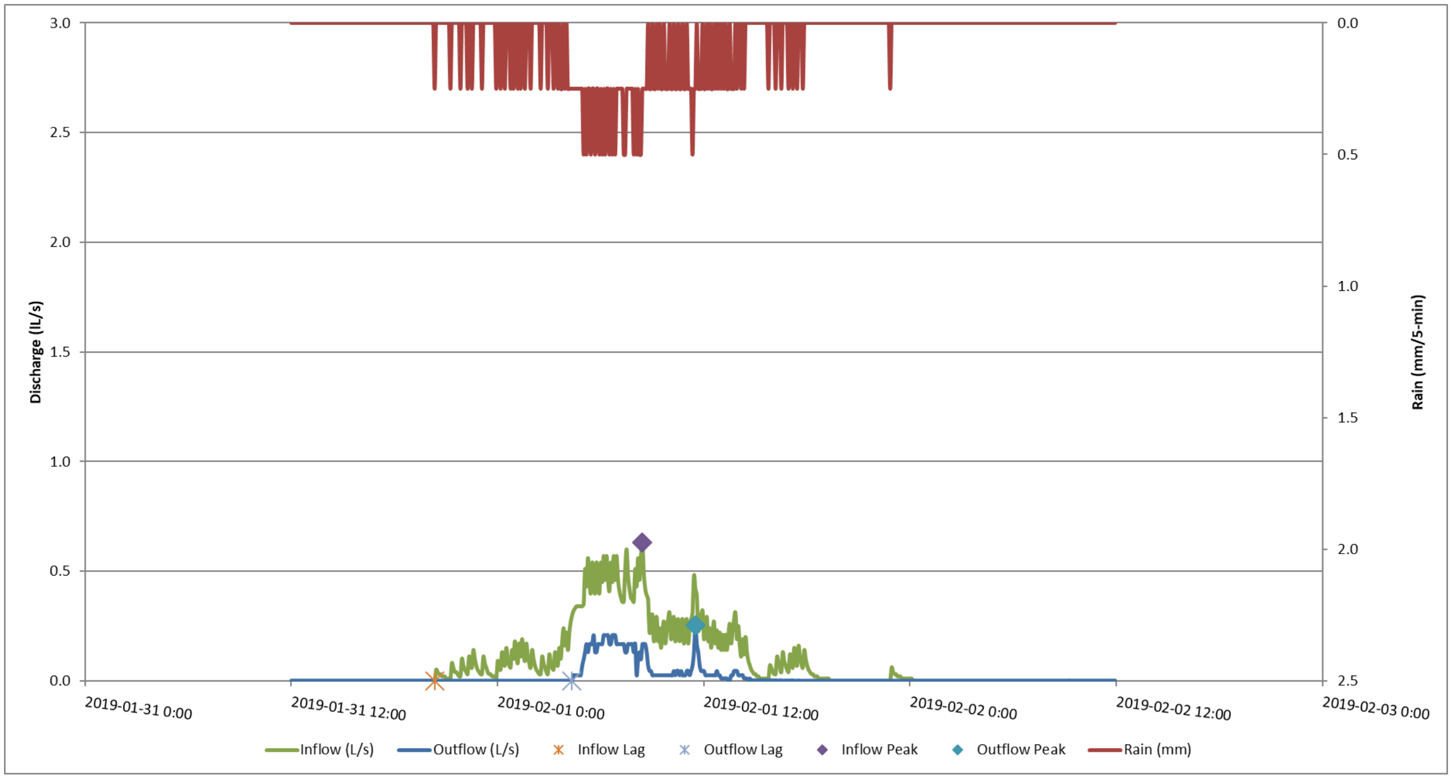

Storm ID: 2019-2-19-11

Dates for Graph	
Beginning	2019-02-19 0:00
End	2019-02-20 5:55
Inflow Peak	2019-02-19 15:30
Outflow Peak	2019-02-19 15:30
Inflow Lag	2019-02-19 12:50
Outflow Lag	2019-02-19 15:15

Performance		
Total Inflow (m^3|L)	2.6	2,595
Total Outflow (m^3|L)	0.2	168
Volume Reduction	93.5%	93.5%
Peak Flow Reduction	83.9%	83.9%
Lag Time (min|hours)	145.00	2.4
Total Rainfall (mm)	6.3	6.3
Storm Duration (hours|days)	5.8	0.2
ADP (hours|days)	71.3	3.0
Max Rain Intensity (mm/hr)	3.0	3.0

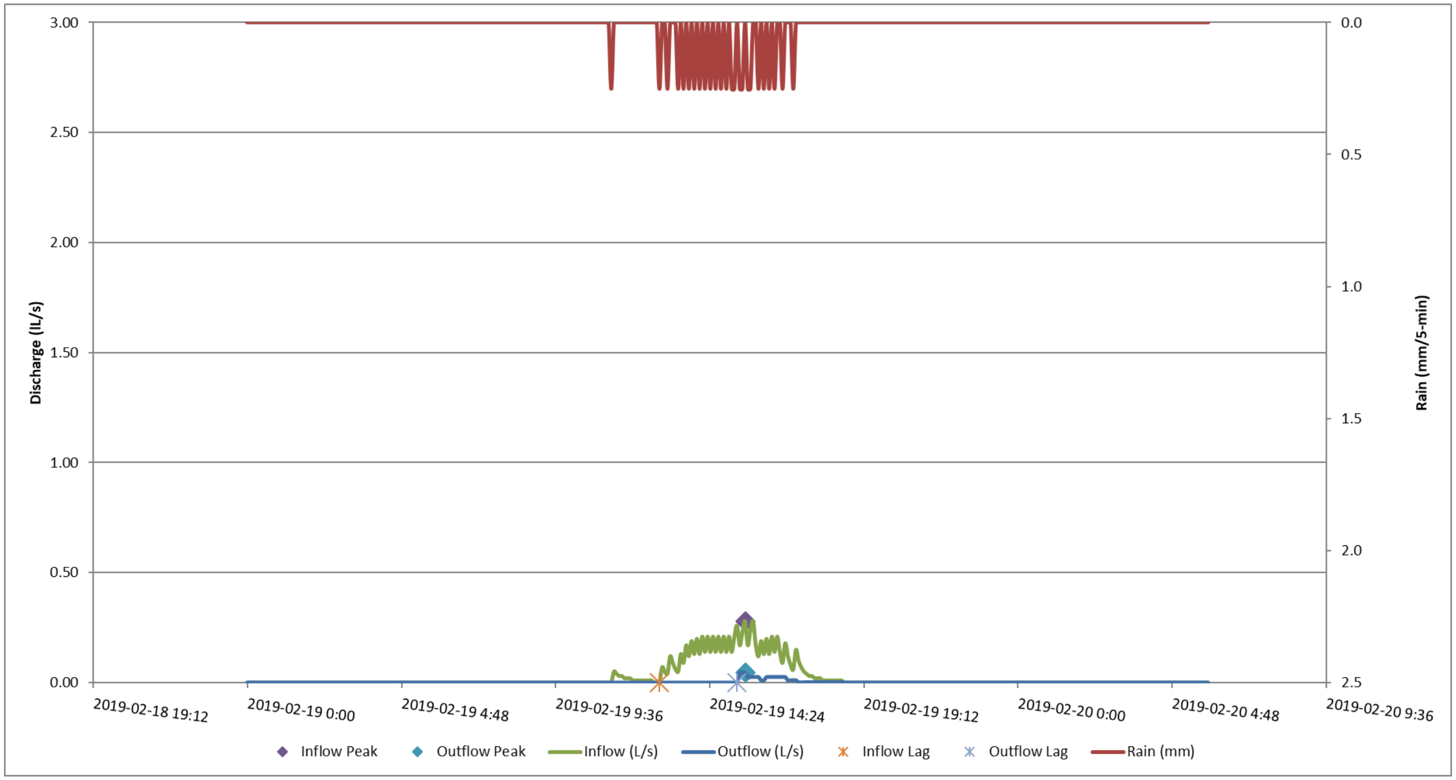

Storm ID: 2019-2-22-5

Dates for Graph	
Beginning	2019-02-22 3:00
End	2019-02-22 22:00
Inflow Peak	2019-02-22 15:00
Outflow Peak	2019-02-22 15:05
Inflow Lag	2019-02-22 14:45
Outflow Lag	2019-02-22 14:55

Performance		
Total Inflow (m^3|L)	5.8	5,814
Total Outflow (m^3|L)	0.5	463
Volume Reduction	92.0%	92.0%
Peak Flow Reduction	96.3%	96.3%
Lag Time (min|hours)	10.00	0.2
Total Rainfall (mm)	16.3	16.3
Storm Duration (hours|days)	17.7	0.7
ADP (hours|days)	60.8	2.5
Max Rain Intensity (mm/hr)	12.0	12.0

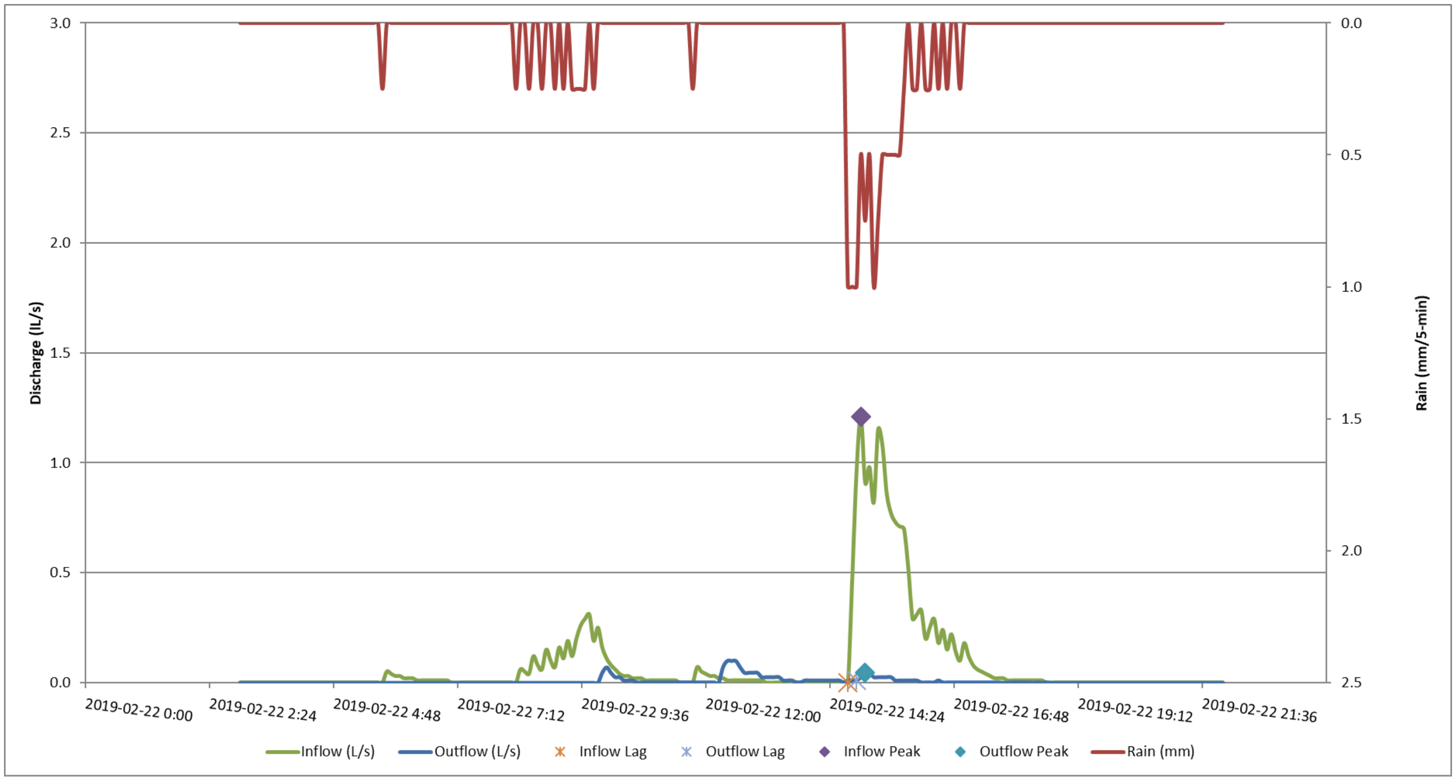

Storm ID: 2019-2-23-8

Dates for Graph	
Beginning	2019-02-23 6:00
End	2019-02-23 16:00
Inflow Peak	2019-02-23 10:00
Outflow Peak	2019-02-23 10:00
Inflow Lag	2019-02-23 8:15
Outflow Lag	2019-02-23 9:50

Performance		
Total Inflow (m^3|L)	2.0	1,962
Total Outflow (m^3|L)	0.4	441
Volume Reduction	77.5%	77.5%
Peak Flow Reduction	59.0%	59.0%
Lag Time (min|hours)	95.00	1.6
Total Rainfall (mm)	4.8	4.8
Storm Duration (hours|days)	5.0	0.2
ADP (hours|days)	8.9	0.4
Max Rain Intensity (mm/hr)	6.0	6.0

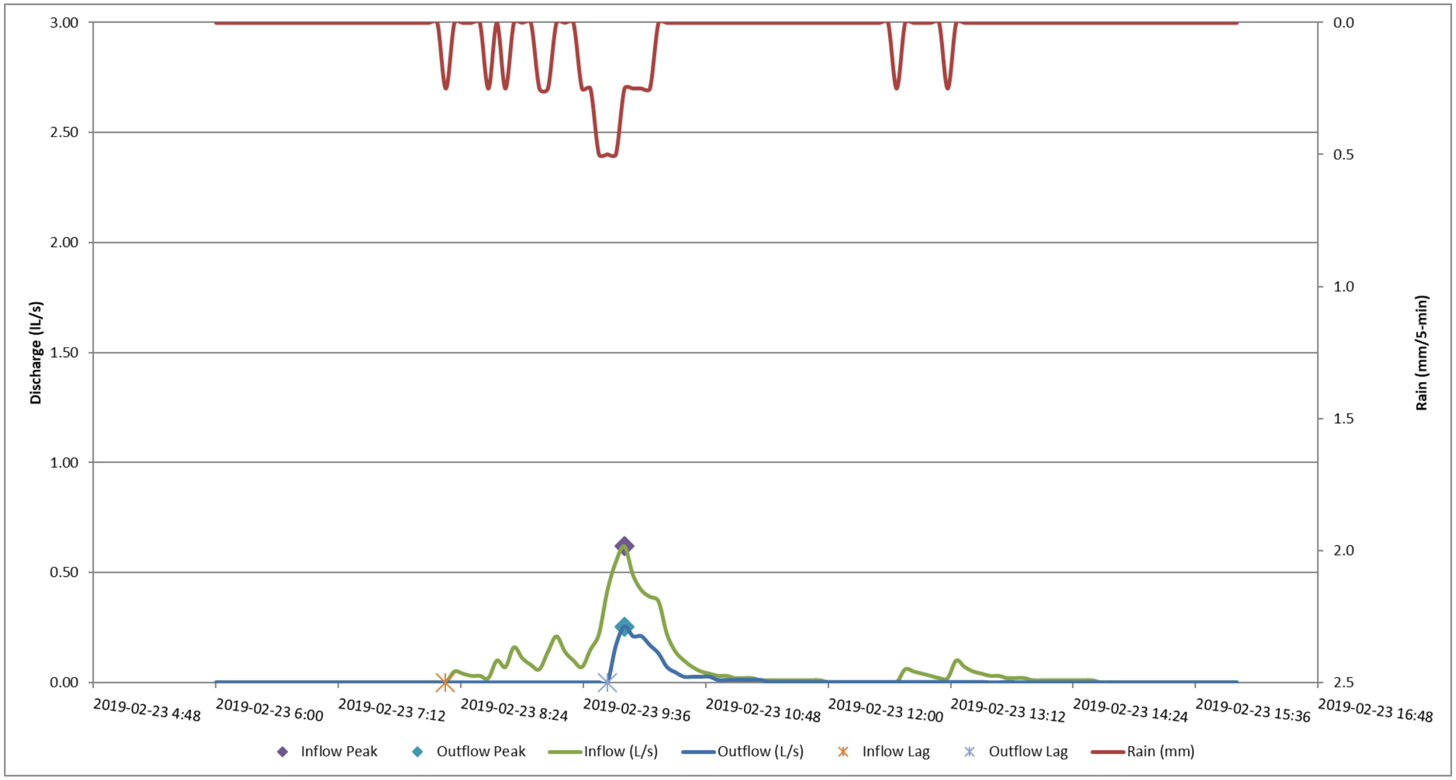

I.3 Checks: Simple Method and Rational Method

Normal events table:

Storm Date	Total Rainfall (mm)	Total Inflow Error Check	Peak Flow Check	Comment
2018-11-29 23:00	2.3	0%	17%	*no outflow
2018-11-24 12:00	2.5	4%	88%	*no outflow
2018-12-08 5:00	2.5	2%	135%	*no outflow
2018-12-22 4:00	3.0	5%	73%	*no outflow
2018-12-01 1:00	3.5	4%	0%	
2019-02-23 8:00	4.8	5%	6%	
2018-12-18 14:00	5.3	4%	39%	
2018-11-30 13:00	5.5	5%	12%	
2018-11-09 3:00	5.8	9%	10%	
2019-02-19 11:00	6.3	5%	17%	
2018-11-27 14:00	6.8	4%	64%	
2018-12-20 18:00	6.8	5%	11%	
2018-12-26 0:00	7.8	5%	60%	
2019-01-18 18:00	7.8	5%	49%	
2018-11-28 9:00	8.8	4%	93%	
2018-11-15 8:00	11.8	5%	3%	
2018-12-29 7:00	12.5	5%	10%	
2019-01-05 18:00	14.8	5%	15%	
2019-02-22 5:00	16.3	10%	9%	
2018-12-15 22:00	17.5	5%	0%	
2019-01-08 15:00	18.0	5%	24%	
2018-12-20 1:00	18.3	5%	41%	
Average		5%	35%	

Large events table:

Storm Date	Total Rainfall (mm)	Total Inflow Error Check	Peak Flow Check	Comment
2018-12-17 16:00	29.0	5%	15%	
2018-12-22 17:00	30.5	579%	119%	
2019-01-17 4:00	30.5	5%	10%	
2018-11-13 17:00	35.5	5%	2%	
2018-12-09 6:00	36.3	5%	4%	
2019-01-31 22:00	36.8	5%	4%	
2018-12-28 0:00	39.3	5%	29%	
2019-01-22 5:00	41.8	5%	26%	
Average		77%	26%	

Extreme events table:

Storm Date	Total Rainfall (mm)	Total Inflow Error Check	Peak Flow Check	Comment
2018-11-21 7:00	55.0	5%	24%	
2018-12-10 22:00	66.5	5%	3%	
2019-01-02 12:00	98.5	5%	10%	
2018-11-25 10:00	98.8	5%	18%	
2018-12-12 13:00	118.3	5%	5%	
Average		5%	12%	

Appendix J: Water quality analysis results from CARO Labs

Reports compiled in chronological order of collection.

Left blank intentionally

CARO ANALYTICAL SERVICES

CERTIFICATE OF ANALYSIS

REPORTED TO	Vancouver, City of (Green Infrastructure Branch) 305- 456 W. Broadway Vancouver,, BC V5Y 1R3		
ATTENTION	Osvaldo Vega	**WORK ORDER**	8111366
PO NUMBER		**RECEIVED / TEMP**	2018-11-15 13:55 / 13°C
PROJECT	110007	**REPORTED**	2018-11-28 14:58
PROJECT INFO		**COC NUMBER**	No #

Introduction:

CARO Analytical Services is a testing laboratory full of smart, engaged scientists driven to make the world a safer and healthier place. Through our clients' projects we become an essential element for a better world. We employ methods conducted in accordance with recognized professional standards using accepted testing methodologies and quality control efforts. CARO is accredited by the Canadian Association for Laboratories Accreditation (CALA) to ISO 17025:2005 for specific tests listed in the scope of accreditation approved by CALA.

Big Picture Sidekicks

You know that the sample you collected after snowshoeing to site, digging 5 meters, and racing to get it on a plane so you can submit it to the lab for time sensitive results needed to make important and expensive decisions (whew) is VERY important. We know that too.

We've Got Chemistry

It's simple. We figure the more you enjoy working with our fun and engaged team members; the more likely you are to give us continued opportunities to support you.

Ahead of the Curve

Through research, regulation knowledge, and instrumentation, we are your analytical centre for the technical knowledge you need, BEFORE you need it, so you can stay up to date and in the know.

If you have any questions or concerns, please contact me at bshaw@caro.ca

Authorized By:

Bryan Shaw, Ph.D., P.Chem.
Client Service Coordinator

CARO
ANALYTICAL SERVICES

TEST RESULTS

REPORTED TO	Vancouver, City of (Green Infrastructure Branch)	**WORK ORDER**	8111366
PROJECT	110007	**REPORTED**	2018-11-28 14:58

Analyte	Result	Guideline	RL	Units	Analyzed	Qualifier
in-001 (8111366-01) | Matrix: Water | Sampled: 2018-11-15 10:45						
Anions						
Nitrate+Nitrite (as N)	**0.449**	N/A	0.0050	mg/L	2018-11-22	
Calculated Parameters						
Carbon, Total	**18.0**	N/A	0.500	mg/L	N/A	
Hardness, Total (as CaCO3)	**45.2**	N/A	0.500	mg/L	N/A	
General Parameters						
Carbon, Total Inorganic	**8.55**	N/A	0.50	mg/L	2018-11-22	
Carbon, Total Organic	**9.41**	N/A	0.50	mg/L	2018-11-22	
Conductivity (EC)	**169**	200	2.0	µS/cm	2018-11-19	
Nitrogen, Total Kjeldahl	**2.26**	N/A	0.050	mg/L	2018-11-21	
Oxygen, Dissolved	**7.7**	6.5	1.0	mg/L	2018-11-22	HT2
pH	**6.94**	6.5-9.0	0.10	pH units	2018-11-21	HT2
Phosphorus, Total (as P)	**0.186**	N/A	0.0020	mg/L	2018-11-20	
Solids, Total Suspended	**81.6**	N/A	2.0	mg/L	2018-11-21	
Total Metals						
Aluminum, total	**1.65**	0.005	0.0050	mg/L	2018-11-20	
Antimony, total	**0.0134**	N/A	0.00020	mg/L	2018-11-20	
Arsenic, total	**0.00190**	0.005	0.00050	mg/L	2018-11-20	
Barium, total	**0.0783**	N/A	0.0050	mg/L	2018-11-20	
Beryllium, total	< 0.00010	N/A	0.00010	mg/L	2018-11-20	
Bismuth, total	**0.0131**	N/A	0.00010	mg/L	2018-11-20	
Boron, total	**0.0328**	1.5	0.0050	mg/L	2018-11-20	
Cadmium, total	**0.00139**	0.00009	0.000010	mg/L	2018-11-20	
Calcium, total	**15.7**	N/A	0.20	mg/L	2018-11-20	
Chromium, total	**0.00849**	N/A	0.00050	mg/L	2018-11-20	
Cobalt, total	**0.00117**	N/A	0.00010	mg/L	2018-11-20	
Copper, total	**0.0594**	0.002	0.00040	mg/L	2018-11-20	
Iron, total	**2.42**	0.3	0.010	mg/L	2018-11-20	
Lead, total	**0.0107**	0.001	0.00020	mg/L	2018-11-20	
Lithium, total	**0.00223**	N/A	0.00010	mg/L	2018-11-20	
Magnesium, total	**1.46**	N/A	0.010	mg/L	2018-11-20	
Manganese, total	**0.0563**	N/A	0.00020	mg/L	2018-11-20	
Mercury, total	**0.000041**	0.000026	0.000040	mg/L	2018-11-20	CT5
Molybdenum, total	**0.00383**	0.073	0.00010	mg/L	2018-11-20	
Nickel, total	**0.00645**	0.025	0.00040	mg/L	2018-11-20	
Phosphorus, total	**0.177**	N/A	0.050	mg/L	2018-11-20	
Potassium, total	**2.10**	N/A	0.10	mg/L	2018-11-20	
Selenium, total	< 0.00050	0.001	0.00050	mg/L	2018-11-20	
Silicon, total	**6.3**	N/A	1.0	mg/L	2018-11-20	
Silver, total	**0.000097**	0.00025	0.000050	mg/L	2018-11-20	
Sodium, total	**12.5**	N/A	0.10	mg/L	2018-11-20	

CARO
ANALYTICAL SERVICES

TEST RESULTS

REPORTED TO	Vancouver, City of (Green Infrastructure Branch)	**WORK ORDER**	8111366
PROJECT	110007	**REPORTED**	2018-11-28 14:58

Analyte	Result	Guideline	RL	Units	Analyzed	Qualifier
in-001 (8111366-01) | Matrix: Water | Sampled: 2018-11-15 10:45, Continued						
Total Metals, Continued						
Strontium, total	**0.118**	N/A	0.0010	mg/L	2018-11-20	
Sulfur, total	**4.2**	N/A	3.0	mg/L	2018-11-20	
Tellurium, total	< 0.00050	N/A	0.00050	mg/L	2018-11-20	
Thallium, total	**0.000039**	0.0008	0.000020	mg/L	2018-11-20	
Thorium, total	< 0.00010	N/A	0.00010	mg/L	2018-11-20	
Tin, total	**0.00490**	N/A	0.00020	mg/L	2018-11-20	
Titanium, total	**0.0766**	N/A	0.0050	mg/L	2018-11-20	
Tungsten, total	< 0.0010	N/A	0.0010	mg/L	2018-11-20	
Uranium, total	**0.000111**	0.015	0.000020	mg/L	2018-11-20	
Vanadium, total	**0.0100**	N/A	0.0010	mg/L	2018-11-20	
Zinc, total	**0.236**	0.03	0.0040	mg/L	2018-11-20	
Zirconium, total	**0.00223**	N/A	0.00010	mg/L	2018-11-20	

Sample Qualifiers:

CT5	This sample has been incorrectly preserved for Mercury analysis
HT2	The 15 minute recommended holding time (from sampling to analysis) has been exceeded - field analysis is recommended.

CARO ANALYTICAL SERVICES

APPENDIX 1: SUPPORTING INFORMATION

REPORTED TO	Vancouver, City of (Green Infrastructure Branch)	**WORK ORDER**	8111366
PROJECT	110007	**REPORTED**	2018-11-28 14:58

Analysis Description	Method Ref.	Technique	Location
Carbon, Total Inorganic in Water	SM 5310 B (2011)	Combustion, Infrared CO2 Detection	Kelowna
Carbon, Total Organic in Water	SM 5310 B (2011)	Combustion, Infrared CO2 Detection	Kelowna
Conductivity in Water	SM 2510 B (2011)	Conductivity Meter	Richmond
Dissolved Oxygen in Water	SM 4500-O G (2011)	Membrane Electrode	Richmond
Hardness in Water	SM 2340 B* (2011)	Calculation: 2.497 [total Ca] + 4.118 [total Mg] (Est)	N/A
Nitrate+Nitrite in Water	SM 4500-NO3- F (2011)	Automated Colorimetry (Cadmium Reduction)	Kelowna
Nitrogen, Total Kjeldahl in Water	SM 4500-Norg D* (2011)	Block Digestion and Flow Injection Analysis	Kelowna
pH in Water	SM 4500-H+ B (2011)	Electrometry	Richmond
Phosphorus, Total in Water	SM 4500-P B.5* (2011) / SM 4500-P F (2011)	Persulfate Digestion / Automated Colorimetry (Ascorbic Acid)	Kelowna
Solids, Total Suspended in Water	SM 2540 D* (2011)	Gravimetry (Dried at 103-105C)	Richmond
Total Metals in Water	EPA 200.2* / EPA 6020B	HNO3+HCl Hot Block Digestion / Inductively Coupled Plasma-Mass Spectroscopy (ICP-MS)	Richmond

Note: An asterisk in the Method Reference indicates that the CARO method has been modified from the reference method

Glossary of Terms:

RL	Reporting Limit (default)
<	Less than the specified Reporting Limit (RL) - the actual RL may be higher than the default RL due to various factors
mg/L	Milligrams per litre
pH units	pH < 7 = acidic, ph > 7 = basic
µS/cm	Microsiemens per centimetre
EPA	United States Environmental Protection Agency Test Methods
SM	Standard Methods for the Examination of Water and Wastewater, American Public Health Association

Guidelines Referenced in this Report:

CCME CEQG Residential/Parkland/Aquatic (Lowest)

Metro Van MAMFS Regulations

Note: In some cases, the values displayed on the report represent the lowest guideline and are to be verified by the end user

General Comments:

The results in this report apply to the samples analyzed in accordance with the Chain of Custody document. This analytical report must be reproduced in its entirety. CARO is not responsible for any loss or damage resulting directly or indirectly from error or omission in the conduct of testing. Liability is limited to the cost of analysis. Samples will be disposed of 30 days after the test report has been issued unless otherwise agreed to in writing. The quality control (QC) data is available upon request

CARO
ANALYTICAL SERVICES

CERTIFICATE OF ANALYSIS

REPORTED TO	Vancouver, City of (Green Infrastructure Branch) 305- 456 W. Broadway Vancouver,, BC V5Y 1R3		
ATTENTION	Osvaldo Vega	**WORK ORDER**	8112040
PO NUMBER	vancouver.ca	**RECEIVED / TEMP**	2018-11-26 11:03 / 10°C
PROJECT	110007	**REPORTED**	2018-12-03 17:14
PROJECT INFO		**COC NUMBER**	No #

Introduction:

CARO Analytical Services is a testing laboratory full of smart, engaged scientists driven to make the world a safer and healthier place. Through our clients' projects we become an essential element for a better world. We employ methods conducted in accordance with recognized professional standards using accepted testing methodologies and quality control efforts. CARO is accredited by the Canadian Association for Laboratories Accreditation (CALA) to ISO 17025:2005 for specific tests listed in the scope of accreditation approved by CALA.

Big Picture Sidekicks

You know that the sample you collected after snowshoeing to site, digging 5 meters, and racing to get it on a plane so you can submit it to the lab for time sensitive results needed to make important and expensive decisions (whew) is VERY important. We know that too.

We've Got Chemistry

It's simple. We figure the more you enjoy working with our fun and engaged team members; the more likely you are to give us continued opportunities to support you.

Ahead of the Curve

Through research, regulation knowledge, and instrumentation, we are your analytical centre for the technical knowledge you need, BEFORE you need it, so you can stay up to date and in the know.

If you have any questions or concerns, please contact me at bshaw@caro.ca

Authorized By:

Bryan Shaw, Ph.D., P.Chem.
Client Service Coordinator

CARO ANALYTICAL SERVICES

TEST RESULTS

REPORTED TO	Vancouver, City of (Green Infrastructure Branch)	**WORK ORDER**	8112040
PROJECT	110007	**REPORTED**	2018-12-03 17:14

Analyte	Result	Guideline	RL	Units	Analyzed	Qualifier
in-002 (8112040-01) | Matrix: Water | Sampled: 2018-11-26 09:40						
Anions						
Nitrate (as N)	**0.040**	57.6	0.010	mg/L	2018-11-30	HT1
Nitrite (as N)	**0.011**	0.06	0.010	mg/L	2018-11-30	HT1
Calculated Parameters						
Carbon, Total	**4.44**	N/A	0.500	mg/L	N/A	
Hardness, Total (as CaCO3)	**21.2**	N/A	0.500	mg/L	N/A	
Nitrate+Nitrite (as N)	**0.0511**	N/A	0.0200	mg/L	N/A	
General Parameters						
Carbon, Total Inorganic	**2.04**	N/A	0.50	mg/L	2018-11-30	
Carbon, Total Organic	**2.40**	N/A	0.50	mg/L	2018-12-03	
Conductivity (EC)	**28.5**	200	2.0	µS/cm	2018-11-28	
Nitrogen, Total Kjeldahl	**1.12**	N/A	0.050	mg/L	2018-11-29	
Oxygen, Dissolved	**9.3**	6.5	1.0	mg/L	2018-11-30	HT2
pH	**6.61**	6.5-9.0	0.10	pH units	2018-11-28	HT2
Phosphorus, Total (as P)	**0.109**	N/A	0.0020	mg/L	2018-11-30	
Solids, Total Suspended	**90.3**	N/A	2.0	mg/L	2018-11-27	
Total Metals						
Aluminum, total	**2.00**	0.005	0.0050	mg/L	2018-11-29	
Antimony, total	**0.00330**	N/A	0.00020	mg/L	2018-11-29	
Arsenic, total	**0.00081**	0.005	0.00050	mg/L	2018-11-29	
Barium, total	**0.0565**	N/A	0.0050	mg/L	2018-11-29	
Beryllium, total	< 0.00010	N/A	0.00010	mg/L	2018-11-29	
Bismuth, total	**0.00934**	N/A	0.00010	mg/L	2018-11-29	
Boron, total	**0.0648**	1.5	0.0050	mg/L	2018-11-29	
Cadmium, total	**0.000141**	0.00009	0.000010	mg/L	2018-11-29	
Calcium, total	**7.20**	N/A	0.20	mg/L	2018-11-29	
Chromium, total	**0.00657**	N/A	0.00050	mg/L	2018-11-29	
Cobalt, total	**0.00099**	N/A	0.00010	mg/L	2018-11-29	
Copper, total	**0.0395**	0.002	0.00040	mg/L	2018-11-29	
Iron, total	**2.28**	0.3	0.010	mg/L	2018-11-29	
Lead, total	**0.00652**	0.001	0.00020	mg/L	2018-11-29	
Lithium, total	**0.00101**	N/A	0.00010	mg/L	2018-11-29	
Magnesium, total	**0.782**	N/A	0.010	mg/L	2018-11-29	
Manganese, total	**0.0522**	N/A	0.00020	mg/L	2018-11-29	
Mercury, total	< 0.000040	0.000026	0.000040	mg/L	2018-11-29	CT5
Molybdenum, total	**0.00114**	0.073	0.00010	mg/L	2018-11-29	
Nickel, total	**0.00303**	0.025	0.00040	mg/L	2018-11-29	
Phosphorus, total	**0.126**	N/A	0.050	mg/L	2018-11-29	
Potassium, total	**1.04**	N/A	0.10	mg/L	2018-11-29	
Selenium, total	< 0.00050	0.001	0.00050	mg/L	2018-11-29	
Silicon, total	**3.3**	N/A	1.0	mg/L	2018-11-29	

CARO ANALYTICAL SERVICES

TEST RESULTS

REPORTED TO	Vancouver, City of (Green Infrastructure Branch)	**WORK ORDER**	8112040
PROJECT	110007	**REPORTED**	2018-12-03 17:14

Analyte	Result	Guideline	RL	Units	Analyzed	Qualifier
in-002 (8112040-01) | Matrix: Water | Sampled: 2018-11-26 09:40, Continued						
Total Metals, Continued						
Silver, total	< 0.000050	0.00025	0.000050	mg/L	2018-11-29	
Sodium, total	**1.18**	N/A	0.10	mg/L	2018-11-29	
Strontium, total	**0.0271**	N/A	0.0010	mg/L	2018-11-29	
Sulfur, total	< 3.0	N/A	3.0	mg/L	2018-11-29	
Tellurium, total	< 0.00050	N/A	0.00050	mg/L	2018-11-29	
Thallium, total	< 0.000020	0.0008	0.000020	mg/L	2018-11-29	
Thorium, total	< 0.00010	N/A	0.00010	mg/L	2018-11-29	
Tin, total	**0.00426**	N/A	0.00020	mg/L	2018-11-29	
Titanium, total	**0.0759**	N/A	0.0050	mg/L	2018-11-29	
Tungsten, total	< 0.0010	N/A	0.0010	mg/L	2018-11-29	
Uranium, total	**0.000071**	0.015	0.000020	mg/L	2018-11-29	
Vanadium, total	**0.0060**	N/A	0.0010	mg/L	2018-11-29	
Zinc, total	**0.130**	0.03	0.0040	mg/L	2018-11-29	
Zirconium, total	**0.00102**	N/A	0.00010	mg/L	2018-11-29	
out-002 (8112040-02) | Matrix: Water | Sampled: 2018-11-26 09:55						
Anions						
Nitrate+Nitrite (as N)	**0.280**	N/A	0.0050	mg/L	2018-11-29	
Nitrate (as N)	**0.294**	57.6	0.010	mg/L	2018-11-30	HT1
Nitrite (as N)	< 0.010	0.06	0.010	mg/L	2018-11-30	HT1
Calculated Parameters						
Carbon, Total	**19.4**	N/A	0.500	mg/L	N/A	
Hardness, Total (as CaCO3)	**35.4**	N/A	0.500	mg/L	N/A	
Nitrate+Nitrite (as N)	**0.294**	N/A	0.0200	mg/L	N/A	
General Parameters						
Carbon, Total Inorganic	**6.87**	N/A	0.50	mg/L	2018-11-30	
Carbon, Total Organic	**12.5**	N/A	0.50	mg/L	2018-12-03	
Conductivity (EC)	**111**	200	2.0	µS/cm	2018-11-28	
Nitrogen, Total Kjeldahl	**1.60**	N/A	0.050	mg/L	2018-11-29	
Oxygen, Dissolved	**9.7**	6.5	1.0	mg/L	2018-11-30	HT2
pH	**6.94**	6.5-9.0	0.10	pH units	2018-11-28	HT2
Phosphorus, Total (as P)	**1.30**	N/A	0.0020	mg/L	2018-11-30	
Solids, Total Suspended	**11.3**	N/A	2.0	mg/L	2018-11-27	
Total Metals						
Aluminum, total	**0.578**	0.005	0.0050	mg/L	2018-11-29	
Antimony, total	**0.00093**	N/A	0.00020	mg/L	2018-11-29	
Arsenic, total	**0.0102**	0.005	0.00050	mg/L	2018-11-29	
Barium, total	**0.0154**	N/A	0.0050	mg/L	2018-11-29	
Beryllium, total	< 0.00010	N/A	0.00010	mg/L	2018-11-29	

CARO ANALYTICAL SERVICES

TEST RESULTS

REPORTED TO	Vancouver, City of (Green Infrastructure Branch)	**WORK ORDER**	8112040
PROJECT	110007	**REPORTED**	2018-12-03 17:14

Analyte	Result	Guideline	RL	Units	Analyzed	Qualifier
out-002 (8112040-02) | Matrix: Water | Sampled: 2018-11-26 09:55, Continued						
Total Metals, Continued						
Bismuth, total	**0.00095**	N/A	0.00010	mg/L	2018-11-29	
Boron, total	**0.0755**	1.5	0.0050	mg/L	2018-11-29	
Cadmium, total	**0.000030**	0.00009	0.000010	mg/L	2018-11-29	
Calcium, total	**11.1**	N/A	0.20	mg/L	2018-11-29	
Chromium, total	**0.00232**	N/A	0.00050	mg/L	2018-11-29	
Cobalt, total	**0.00039**	N/A	0.00010	mg/L	2018-11-29	
Copper, total	**0.00877**	0.002	0.00040	mg/L	2018-11-29	
Iron, total	**0.603**	0.3	0.010	mg/L	2018-11-29	
Lead, total	**0.00085**	0.001	0.00020	mg/L	2018-11-29	
Lithium, total	**0.00062**	N/A	0.00010	mg/L	2018-11-29	
Magnesium, total	**1.87**	N/A	0.010	mg/L	2018-11-29	
Manganese, total	**0.0223**	N/A	0.00020	mg/L	2018-11-29	
Mercury, total	< 0.000040	0.000026	0.000040	mg/L	2018-11-29	CT5
Molybdenum, total	**0.00231**	0.073	0.00010	mg/L	2018-11-29	
Nickel, total	**0.00214**	0.025	0.00040	mg/L	2018-11-29	
Phosphorus, total	**1.36**	N/A	0.050	mg/L	2018-11-29	
Potassium, total	**14.5**	N/A	0.10	mg/L	2018-11-29	
Selenium, total	< 0.00050	0.001	0.00050	mg/L	2018-11-29	
Silicon, total	**2.3**	N/A	1.0	mg/L	2018-11-29	
Silver, total	< 0.000050	0.00025	0.000050	mg/L	2018-11-29	
Sodium, total	**2.11**	N/A	0.10	mg/L	2018-11-29	
Strontium, total	**0.0275**	N/A	0.0010	mg/L	2018-11-29	
Sulfur, total	**4.2**	N/A	3.0	mg/L	2018-11-29	
Tellurium, total	< 0.00050	N/A	0.00050	mg/L	2018-11-29	
Thallium, total	< 0.000020	0.0008	0.000020	mg/L	2018-11-29	
Thorium, total	< 0.00010	N/A	0.00010	mg/L	2018-11-29	
Tin, total	**0.00167**	N/A	0.00020	mg/L	2018-11-29	
Titanium, total	**0.0157**	N/A	0.0050	mg/L	2018-11-29	
Tungsten, total	< 0.0010	N/A	0.0010	mg/L	2018-11-29	
Uranium, total	**0.000055**	0.015	0.000020	mg/L	2018-11-29	
Vanadium, total	**0.0044**	N/A	0.0010	mg/L	2018-11-29	
Zinc, total	**0.0201**	0.03	0.0040	mg/L	2018-11-29	
Zirconium, total	**0.00022**	N/A	0.00010	mg/L	2018-11-29	

Sample Qualifiers:

CT5	This sample has been incorrectly preserved for Mercury analysis
HT1	The sample was prepared and/or analyzed past the recommended holding time.
HT2	The 15 minute recommended holding time (from sampling to analysis) has been exceeded - field analysis is recommended.

CARO ANALYTICAL SERVICES

APPENDIX 1: SUPPORTING INFORMATION

REPORTED TO	Vancouver, City of (Green Infrastructure Branch)	**WORK ORDER**	8112040
PROJECT	110007	**REPORTED**	2018-12-03 17:14

Analysis Description	Method Ref.	Technique	Location
Anions in Water	SM 4110 B (2011)	Ion Chromatography	Kelowna
Carbon, Total Inorganic in Water	SM 5310 B (2011)	Combustion, Infrared CO2 Detection	Kelowna
Carbon, Total Organic in Water	SM 5310 B (2011)	Combustion, Infrared CO2 Detection	Kelowna
Conductivity in Water	SM 2510 B (2011)	Conductivity Meter	Richmond
Dissolved Oxygen in Water	SM 4500-O G (2011)	Membrane Electrode	Richmond
Hardness in Water	SM 2340 B* (2011)	Calculation: 2.497 [total Ca] + 4.118 [total Mg] (Est)	N/A
Nitrate+Nitrite in Water	SM 4500-NO3- F (2011)	Automated Colorimetry (Cadmium Reduction)	Kelowna
Nitrogen, Total Kjeldahl in Water	SM 4500-Norg D* (2011)	Block Digestion and Flow Injection Analysis	Kelowna
pH in Water	SM 4500-H+ B (2011)	Electrometry	Richmond
Phosphorus, Total in Water	SM 4500-P B.5* (2011) / SM 4500-P F (2011)	Persulfate Digestion / Automated Colorimetry (Ascorbic Acid)	Kelowna
Solids, Total Suspended in Water	SM 2540 D* (2011)	Gravimetry (Dried at 103-105C)	Richmond
Total Metals in Water	EPA 200.2* / EPA 6020B	HNO3+HCl Hot Block Digestion / Inductively Coupled Plasma-Mass Spectroscopy (ICP-MS)	Richmond

Note: An asterisk in the Method Reference indicates that the CARO method has been modified from the reference method

Glossary of Terms:

RL	Reporting Limit (default)
<	Less than the specified Reporting Limit (RL) - the actual RL may be higher than the default RL due to various factors
mg/L	Milligrams per litre
pH units	pH < 7 = acidic, ph > 7 = basic
µS/cm	Microsiemens per centimetre
EPA	United States Environmental Protection Agency Test Methods
SM	Standard Methods for the Examination of Water and Wastewater, American Public Health Association

Guidelines Referenced in this Report:

CCME CEQG Residential/Parkland/Aquatic (Lowest)
Metro Van MAMFS Regulations

Note: In some cases, the values displayed on the report represent the lowest guideline and are to be verified by the end user

General Comments:

The results in this report apply to the samples analyzed in accordance with the Chain of Custody document. This analytical report must be reproduced in its entirety. CARO is not responsible for any loss or damage resulting directly or indirectly from error or omission in the conduct of testing. Liability is limited to the cost of analysis. Samples will be disposed of 30 days after the test report has been issued unless otherwise agreed to in writing. The quality control (QC) data is available upon request

CARO
ANALYTICAL SERVICES

CERTIFICATE OF ANALYSIS

REPORTED TO	Vancouver, City of (Green Infrastructure Branch) 305- 456 W. Broadway Vancouver,, BC V5Y 1R3		
ATTENTION	Osvaldo Vega	**WORK ORDER**	8112083
PO NUMBER	vancouver.ca	**RECEIVED / TEMP**	2018-11-27 10:35 / 12°C
PROJECT	Rainwater	**REPORTED**	2018-12-04 15:13
PROJECT INFO		**COC NUMBER**	No #

Introduction:

CARO Analytical Services is a testing laboratory full of smart, engaged scientists driven to make the world a safer and healthier place. Through our clients' projects we become an essential element for a better world. We employ methods conducted in accordance with recognized professional standards using accepted testing methodologies and quality control efforts. CARO is accredited by the Canadian Association for Laboratories Accreditation (CALA) to ISO 17025:2005 for specific tests listed in the scope of accreditation approved by CALA.

Big Picture Sidekicks

You know that the sample you collected after snowshoeing to site, digging 5 meters, and racing to get it on a plane so you can submit it to the lab for time sensitive results needed to make important and expensive decisions (whew) is VERY important. We know that too.

We've Got Chemistry

It's simple. We figure the more you enjoy working with our fun and engaged team members; the more likely you are to give us continued opportunities to support you.

Ahead of the Curve

Through research, regulation knowledge, and instrumentation, we are your analytical centre for the technical knowledge you need, BEFORE you need it, so you can stay up to date and in the know.

If you have any questions or concerns, please contact me at bshaw@caro.ca

Authorized By:

Bryan Shaw, Ph.D., P.Chem.
Client Service Coordinator

CARO
ANALYTICAL SERVICES

TEST RESULTS

REPORTED TO	Vancouver, City of (Green Infrastructure Branch)	**WORK ORDER**	8112083
PROJECT	Rainwater	**REPORTED**	2018-12-04 15:13

Analyte	Result	Guideline	RL	Units	Analyzed	Qualifier
vancity-001 (8112083-01) | Matrix: Water | Sampled: 2018-11-27 09:50						
Anions						
Nitrate (as N)	**0.038**	57.6	0.010	mg/L	2018-11-30	
Nitrite (as N)	< 0.010	0.06	0.010	mg/L	2018-11-30	
Calculated Parameters						
Carbon, Total	**1.40**	N/A	0.500	mg/L	N/A	
Hardness, Total (as CaCO3)	< 0.500	N/A	0.500	mg/L	N/A	
Nitrate+Nitrite (as N)	**0.0380**	N/A	0.0200	mg/L	N/A	
General Parameters						
Carbon, Total Inorganic	< 0.50	N/A	0.50	mg/L	2018-12-04	
Carbon, Total Organic	**1.40**	N/A	0.50	mg/L	2018-12-04	
Conductivity (EC)	**4.3**	200	2.0	µS/cm	2018-12-04	
Nitrogen, Total Kjeldahl	**0.158**	N/A	0.050	mg/L	2018-11-29	
Oxygen, Dissolved	**9.9**	6.5	1.0	mg/L	2018-11-30	HT2
pH	**5.24**	6.5-9.0	0.10	pH units	2018-11-28	HT2
Phosphorus, Total (as P)	< 0.0020	N/A	0.0020	mg/L	2018-11-30	
Solids, Total Suspended	< 2.0	N/A	2.0	mg/L	2018-11-27	
Total Metals						
Aluminum, total	**0.0082**	0.005	0.0050	mg/L	2018-12-02	
Antimony, total	< 0.00020	N/A	0.00020	mg/L	2018-12-02	
Arsenic, total	< 0.00050	0.005	0.00050	mg/L	2018-12-02	
Barium, total	< 0.0050	N/A	0.0050	mg/L	2018-12-02	
Beryllium, total	< 0.00010	N/A	0.00010	mg/L	2018-12-02	
Bismuth, total	< 0.00010	N/A	0.00010	mg/L	2018-12-02	
Boron, total	**0.0086**	1.5	0.0050	mg/L	2018-12-02	
Cadmium, total	< 0.000010	0.00009	0.000010	mg/L	2018-12-02	
Calcium, total	< 0.20	N/A	0.20	mg/L	2018-12-02	
Chromium, total	< 0.00050	N/A	0.00050	mg/L	2018-12-02	
Cobalt, total	< 0.00010	N/A	0.00010	mg/L	2018-12-02	
Copper, total	**0.00093**	0.002	0.00040	mg/L	2018-12-02	
Iron, total	< 0.010	0.3	0.010	mg/L	2018-12-02	
Lead, total	< 0.00020	0.001	0.00020	mg/L	2018-12-02	
Lithium, total	< 0.00010	N/A	0.00010	mg/L	2018-12-02	
Magnesium, total	**0.038**	N/A	0.010	mg/L	2018-12-02	
Manganese, total	**0.00030**	N/A	0.00020	mg/L	2018-12-02	
Mercury, total	< 0.000040	0.000026	0.000040	mg/L	2018-12-02	CT5
Molybdenum, total	< 0.00010	0.073	0.00010	mg/L	2018-12-02	
Nickel, total	< 0.00040	0.025	0.00040	mg/L	2018-12-02	
Phosphorus, total	< 0.050	N/A	0.050	mg/L	2018-12-02	
Potassium, total	< 0.10	N/A	0.10	mg/L	2018-12-02	
Selenium, total	< 0.00050	0.001	0.00050	mg/L	2018-12-02	
Silicon, total	< 1.0	N/A	1.0	mg/L	2018-12-02	

CARO ANALYTICAL SERVICES

TEST RESULTS

REPORTED TO	Vancouver, City of (Green Infrastructure Branch)	**WORK ORDER**	8112083
PROJECT	Rainwater	**REPORTED**	2018-12-04 15:13

Analyte	Result	Guideline	RL	Units	Analyzed	Qualifier
vancity-001 (8112083-01) | Matrix: Water | Sampled: 2018-11-27 09:50, Continued						
Total Metals, Continued						
Silver, total	< 0.000050	0.00025	0.000050	mg/L	2018-12-02	
Sodium, total	**0.29**	N/A	0.10	mg/L	2018-12-02	
Strontium, total	< 0.0010	N/A	0.0010	mg/L	2018-12-02	
Sulfur, total	< 3.0	N/A	3.0	mg/L	2018-12-02	
Tellurium, total	< 0.00050	N/A	0.00050	mg/L	2018-12-02	
Thallium, total	< 0.000020	0.0008	0.000020	mg/L	2018-12-02	
Thorium, total	< 0.00010	N/A	0.00010	mg/L	2018-12-02	
Tin, total	< 0.00020	N/A	0.00020	mg/L	2018-12-02	
Titanium, total	< 0.0050	N/A	0.0050	mg/L	2018-12-02	
Tungsten, total	< 0.0010	N/A	0.0010	mg/L	2018-12-02	
Uranium, total	< 0.000020	0.015	0.000020	mg/L	2018-12-02	
Vanadium, total	< 0.0010	N/A	0.0010	mg/L	2018-12-02	
Zinc, total	**0.0066**	0.03	0.0040	mg/L	2018-12-02	
Zirconium, total	< 0.00010	N/A	0.00010	mg/L	2018-12-02	

Sample Qualifiers:

CT5 This sample has been incorrectly preserved for Mercury analysis

HT2 The 15 minute recommended holding time (from sampling to analysis) has been exceeded - field analysis is recommended.

CARO
ANALYTICAL SERVICES

APPENDIX 1: SUPPORTING INFORMATION

REPORTED TO	Vancouver, City of (Green Infrastructure Branch)	**WORK ORDER**	8112083
PROJECT	Rainwater	**REPORTED**	2018-12-04 15:13

Analysis Description	Method Ref.	Technique	Location
Anions in Water	SM 4110 B (2011)	Ion Chromatography	Kelowna
Carbon, Total Inorganic in Water	SM 5310 B (2011)	Combustion, Infrared CO2 Detection	Kelowna
Carbon, Total Organic in Water	SM 5310 B (2011)	Combustion, Infrared CO2 Detection	Kelowna
Conductivity in Water	SM 2510 B (2011)	Conductivity Meter	Richmond
Dissolved Oxygen in Water	SM 4500-O G (2011)	Membrane Electrode	Richmond
Hardness in Water	SM 2340 B* (2011)	Calculation: 2.497 [total Ca] + 4.118 [total Mg] (Est)	N/A
Nitrogen, Total Kjeldahl in Water	SM 4500-Norg D* (2011)	Block Digestion and Flow Injection Analysis	Kelowna
pH in Water	SM 4500-H+ B (2011)	Electrometry	Richmond
Phosphorus, Total in Water	SM 4500-P B.5* (2011) / SM 4500-P F (2011)	Persulfate Digestion / Automated Colorimetry (Ascorbic Acid)	Kelowna
Solids, Total Suspended in Water	SM 2540 D* (2011)	Gravimetry (Dried at 103-105C)	Richmond
Total Metals in Water	EPA 200.2* / EPA 6020B	HNO3+HCl Hot Block Digestion / Inductively Coupled Plasma-Mass Spectroscopy (ICP-MS)	Richmond

Note: An asterisk in the Method Reference indicates that the CARO method has been modified from the reference method

Glossary of Terms:

RL	Reporting Limit (default)
<	Less than the specified Reporting Limit (RL) - the actual RL may be higher than the default RL due to various factors
mg/L	Milligrams per litre
pH units	pH < 7 = acidic, ph > 7 = basic
µS/cm	Microsiemens per centimetre
EPA	United States Environmental Protection Agency Test Methods
SM	Standard Methods for the Examination of Water and Wastewater, American Public Health Association

Guidelines Referenced in this Report:

CCME CEQG Residential/Parkland/Aquatic (Lowest)
Metro Van MAMFS Regulations

Note: In some cases, the values displayed on the report represent the lowest guideline and are to be verified by the end user

General Comments:

The results in this report apply to the samples analyzed in accordance with the Chain of Custody document. This analytical report must be reproduced in its entirety. CARO is not responsible for any loss or damage resulting directly or indirectly from error or omission in the conduct of testing. Liability is limited to the cost of analysis. Samples will be disposed of 30 days after the test report has been issued unless otherwise agreed to in writing. The quality control (QC) data is available upon request

CARO
ANALYTICAL SERVICES

CERTIFICATE OF ANALYSIS

REPORTED TO	Vancouver, City of (Green Infrastructure Branch) 305- 456 W. Broadway Vancouver,, BC V5Y 1R3		
ATTENTION	Osvaldo Vega	**WORK ORDER**	8120889
PO NUMBER		**RECEIVED / TEMP**	2018-12-11 13:10 / 6°C
PROJECT	110007	**REPORTED**	2018-12-18 16:20
PROJECT INFO			

Introduction:

CARO Analytical Services is a testing laboratory full of smart, engaged scientists driven to make the world a safer and healthier place. Through our clients' projects we become an essential element for a better world. We employ methods conducted in accordance with recognized professional standards using accepted testing methodologies and quality control efforts. CARO is accredited by the Canadian Association for Laboratories Accreditation (CALA) to ISO 17025:2005 for specific tests listed in the scope of accreditation approved by CALA.

Big Picture Sidekicks

You know that the sample you collected after snowshoeing to site, digging 5 meters, and racing to get it on a plane so you can submit it to the lab for time sensitive results needed to make important and expensive decisions (whew) is VERY important. We know that too.

We've Got Chemistry

It's simple. We figure the more you enjoy working with our fun and engaged team members; the more likely you are to give us continued opportunities to support you.

Ahead of the Curve

Through research, regulation knowledge, and instrumentation, we are your analytical centre for the technical knowledge you need, BEFORE you need it, so you can stay up to date and in the know.

If you have any questions or concerns, please contact me at teamcaro@caro.ca

Authorized By:

Team CARO
Client Service Representative

CARO ANALYTICAL SERVICES

TEST RESULTS

REPORTED TO	Vancouver, City of (Green Infrastructure Branch)	**WORK ORDER**	8120889
PROJECT	110007	**REPORTED**	2018-12-18 16:20

Analyte	Result	Guideline	RL	Units	Analyzed	Qualifier
IN-003 (8120889-01) | Matrix: Water | Sampled: 2018-12-11 09:59						
Anions						
Nitrate (as N)	**0.048**	57.6	0.010	mg/L	2018-12-13	
Nitrite (as N)	**0.011**	0.06	0.010	mg/L	2018-12-13	
Calculated Parameters						
Carbon, Total	**4.38**	N/A	0.500	mg/L	N/A	
Hardness, Total (as CaCO3)	**12.4**	N/A	0.500	mg/L	N/A	
Nitrate+Nitrite (as N)	**0.0589**	N/A	0.0200	mg/L	N/A	
General Parameters						
Carbon, Total Inorganic	**1.87**	N/A	0.50	mg/L	2018-12-17	
Carbon, Total Organic	**2.51**	N/A	0.50	mg/L	2018-12-13	
Conductivity (EC)	**41.4**	200	2.0	µS/cm	2018-12-18	
Nitrogen, Total Kjeldahl	**0.703**	N/A	0.050	mg/L	2018-12-14	
Oxygen, Dissolved	**9.8**	6.5	1.0	mg/L	2018-12-18	HT1
pH	**7.10**	6.5-9.0	0.10	pH units	2018-12-13	HT2
Phosphorus, Total (as P)	**0.0922**	N/A	0.0020	mg/L	2018-12-16	
Solids, Total Suspended	**90.8**	N/A	2.0	mg/L	2018-12-17	
Total Metals						
Aluminum, total	**1.32**	0.005	0.0050	mg/L	2018-12-16	
Antimony, total	**0.00213**	N/A	0.00020	mg/L	2018-12-16	
Arsenic, total	**0.00054**	0.005	0.00050	mg/L	2018-12-16	
Barium, total	**0.0409**	N/A	0.0050	mg/L	2018-12-16	
Beryllium, total	< 0.00010	N/A	0.00010	mg/L	2018-12-16	
Bismuth, total	**0.00566**	N/A	0.00010	mg/L	2018-12-16	
Boron, total	< 0.0050	1.5	0.0050	mg/L	2018-12-16	
Cadmium, total	**0.000128**	0.00009	0.000010	mg/L	2018-12-16	
Calcium, total	**4.08**	N/A	0.20	mg/L	2018-12-16	
Chromium, total	**0.00418**	N/A	0.00050	mg/L	2018-12-16	
Cobalt, total	**0.00067**	N/A	0.00010	mg/L	2018-12-16	
Copper, total	**0.0341**	0.002	0.00040	mg/L	2018-12-16	
Iron, total	**1.52**	0.3	0.010	mg/L	2018-12-16	
Lead, total	**0.00540**	0.001	0.00020	mg/L	2018-12-16	
Lithium, total	**0.00095**	N/A	0.00010	mg/L	2018-12-16	
Magnesium, total	**0.543**	N/A	0.010	mg/L	2018-12-16	
Manganese, total	**0.0356**	N/A	0.00020	mg/L	2018-12-16	
Mercury, total	< 0.000010	0.000026	0.000010	mg/L	2018-12-18	
Molybdenum, total	**0.00077**	0.073	0.00010	mg/L	2018-12-16	
Nickel, total	**0.00185**	0.025	0.00040	mg/L	2018-12-16	
Phosphorus, total	**0.091**	N/A	0.050	mg/L	2018-12-16	
Potassium, total	**0.34**	N/A	0.10	mg/L	2018-12-16	
Selenium, total	< 0.00050	0.001	0.00050	mg/L	2018-12-16	
Silicon, total	**2.2**	N/A	1.0	mg/L	2018-12-16	

TEST RESULTS

REPORTED TO	Vancouver, City of (Green Infrastructure Branch)	**WORK ORDER**	8120889
PROJECT	110007	**REPORTED**	2018-12-18 16:20

Analyte	Result	Guideline	RL	Units	Analyzed	Qualifier
IN-003 (8120889-01) | Matrix: Water | Sampled: 2018-12-11 09:59, Continued						
Total Metals, Continued						
Silver, total	< 0.000050	0.00025	0.000050	mg/L	2018-12-16	
Sodium, total	**3.94**	N/A	0.10	mg/L	2018-12-16	
Strontium, total	**0.0205**	N/A	0.0010	mg/L	2018-12-16	
Sulfur, total	< 3.0	N/A	3.0	mg/L	2018-12-16	
Tellurium, total	< 0.00050	N/A	0.00050	mg/L	2018-12-16	
Thallium, total	< 0.000020	0.0008	0.000020	mg/L	2018-12-16	
Thorium, total	< 0.00010	N/A	0.00010	mg/L	2018-12-16	
Tin, total	**0.00267**	N/A	0.00020	mg/L	2018-12-16	
Titanium, total	**0.0502**	N/A	0.0050	mg/L	2018-12-16	
Tungsten, total	< 0.0010	N/A	0.0010	mg/L	2018-12-16	
Uranium, total	**0.000051**	0.015	0.000020	mg/L	2018-12-16	
Vanadium, total	**0.0044**	N/A	0.0010	mg/L	2018-12-16	
Zinc, total	**0.102**	0.03	0.0040	mg/L	2018-12-16	
Zirconium, total	**0.00084**	N/A	0.00010	mg/L	2018-12-16	
OUT-003 (8120889-02) | Matrix: Water | Sampled: 2018-12-11 10:09						
Anions						
Nitrate (as N)	**0.445**	57.6	0.010	mg/L	2018-12-13	
Nitrite (as N)	< 0.010	0.06	0.010	mg/L	2018-12-13	
Calculated Parameters						
Carbon, Total	**16.3**	N/A	0.500	mg/L	N/A	
Hardness, Total (as CaCO3)	**26.4**	N/A	0.500	mg/L	N/A	
Nitrate+Nitrite (as N)	**0.445**	N/A	0.0200	mg/L	N/A	
General Parameters						
Carbon, Total Inorganic	**5.24**	N/A	0.50	mg/L	2018-12-17	
Carbon, Total Organic	**11.1**	N/A	0.50	mg/L	2018-12-13	
Conductivity (EC)	**107**	200	2.0	µS/cm	2018-12-18	
Nitrogen, Total Kjeldahl	**1.28**	N/A	0.050	mg/L	2018-12-14	
Oxygen, Dissolved	**11.0**	6.5	1.0	mg/L	2018-12-18	HT1
pH	**7.55**	6.5-9.0	0.10	pH units	2018-12-12	HT2
Phosphorus, Total (as P)	**1.16**	N/A	0.0020	mg/L	2018-12-16	
Solids, Total Suspended	**12.0**	N/A	2.0	mg/L	2018-12-17	
Total Metals						
Aluminum, total	**0.446**	0.005	0.0050	mg/L	2018-12-16	
Antimony, total	**0.00077**	N/A	0.00020	mg/L	2018-12-16	
Arsenic, total	**0.00748**	0.005	0.00050	mg/L	2018-12-16	
Barium, total	**0.0128**	N/A	0.0050	mg/L	2018-12-16	
Beryllium, total	< 0.00010	N/A	0.00010	mg/L	2018-12-16	
Bismuth, total	**0.00074**	N/A	0.00010	mg/L	2018-12-16	

TEST RESULTS

REPORTED TO	Vancouver, City of (Green Infrastructure Branch)	**WORK ORDER**	8120889
PROJECT	110007	**REPORTED**	2018-12-18 16:20

Analyte	Result	Guideline	RL	Units	Analyzed	Qualifier
OUT-003 (8120889-02) | Matrix: Water | Sampled: 2018-12-11 10:09, Continued						
Total Metals, Continued						
Boron, total	**0.0313**	1.5	0.0050	mg/L	2018-12-16	
Cadmium, total	**0.000302**	0.00009	0.000010	mg/L	2018-12-16	
Calcium, total	**7.26**	N/A	0.20	mg/L	2018-12-16	
Chromium, total	**0.00146**	N/A	0.00050	mg/L	2018-12-16	
Cobalt, total	**0.00031**	N/A	0.00010	mg/L	2018-12-16	
Copper, total	**0.00938**	0.002	0.00040	mg/L	2018-12-16	
Iron, total	**0.486**	0.3	0.010	mg/L	2018-12-16	
Lead, total	**0.00081**	0.001	0.00020	mg/L	2018-12-16	
Lithium, total	**0.00070**	N/A	0.00010	mg/L	2018-12-16	
Magnesium, total	**2.00**	N/A	0.010	mg/L	2018-12-16	
Manganese, total	**0.0202**	N/A	0.00020	mg/L	2018-12-16	
Mercury, total	< 0.000010	0.000026	0.000010	mg/L	2018-12-18	
Molybdenum, total	**0.00166**	0.073	0.00010	mg/L	2018-12-16	
Nickel, total	**0.00162**	0.025	0.00040	mg/L	2018-12-16	
Phosphorus, total	**1.18**	N/A	0.050	mg/L	2018-12-16	
Potassium, total	**10.3**	N/A	0.10	mg/L	2018-12-16	
Selenium, total	< 0.00050	0.001	0.00050	mg/L	2018-12-16	
Silicon, total	**1.9**	N/A	1.0	mg/L	2018-12-16	
Silver, total	< 0.000050	0.00025	0.000050	mg/L	2018-12-16	
Sodium, total	**4.01**	N/A	0.10	mg/L	2018-12-16	
Strontium, total	**0.0229**	N/A	0.0010	mg/L	2018-12-16	
Sulfur, total	< 3.0	N/A	3.0	mg/L	2018-12-16	
Tellurium, total	< 0.00050	N/A	0.00050	mg/L	2018-12-16	
Thallium, total	< 0.000020	0.0008	0.000020	mg/L	2018-12-16	
Thorium, total	< 0.00010	N/A	0.00010	mg/L	2018-12-16	
Tin, total	**0.00025**	N/A	0.00020	mg/L	2018-12-16	
Titanium, total	**0.0101**	N/A	0.0050	mg/L	2018-12-16	
Tungsten, total	< 0.0010	N/A	0.0010	mg/L	2018-12-16	
Uranium, total	**0.000039**	0.015	0.000020	mg/L	2018-12-16	
Vanadium, total	**0.0037**	N/A	0.0010	mg/L	2018-12-16	
Zinc, total	**0.0148**	0.03	0.0040	mg/L	2018-12-16	
Zirconium, total	< 0.00010	N/A	0.00010	mg/L	2018-12-16	

Sample Qualifiers:

HT1 The sample was prepared and/or analyzed past the recommended holding time.

HT2 The 15 minute recommended holding time (from sampling to analysis) has been exceeded - field analysis is recommended.

CARO ANALYTICAL SERVICES

APPENDIX 1: SUPPORTING INFORMATION

REPORTED TO	Vancouver, City of (Green Infrastructure Branch)	**WORK ORDER**	8120889
PROJECT	110007	**REPORTED**	2018-12-18 16:20

Analysis Description	Method Ref.	Technique	Location
Anions in Water	SM 4110 B (2011)	Ion Chromatography	Kelowna
Carbon, Total Inorganic in Water	SM 5310 B (2011)	Combustion, Infrared CO2 Detection	Kelowna
Carbon, Total Organic in Water	SM 5310 B (2011)	Combustion, Infrared CO2 Detection	Kelowna
Conductivity in Water	SM 2510 B (2011)	Conductivity Meter	Richmond
Dissolved Oxygen in Water	SM 4500-O G (2011)	Membrane Electrode	Richmond
Hardness in Water	SM 2340 B* (2011)	Calculation: 2.497 [total Ca] + 4.118 [total Mg] (Est)	N/A
Mercury, total in Water	EPA 245.7*	BrCl2 Oxidation / Cold Vapor Atomic Fluorescence Spectrometry (CVAFS)	Richmond
Nitrogen, Total Kjeldahl in Water	SM 4500-Norg D* (2011)	Block Digestion and Flow Injection Analysis	Kelowna
pH in Water	SM 4500-H+ B (2011)	Electrometry	Richmond
Phosphorus, Total in Water	SM 4500-P B.5* (2011) / SM 4500-P F (2011)	Persulfate Digestion / Automated Colorimetry (Ascorbic Acid)	Kelowna
Solids, Total Suspended in Water	SM 2540 D* (2011)	Gravimetry (Dried at 103-105C)	Richmond
Total Metals in Water	EPA 200.2* / EPA 6020B	HNO3+HCl Hot Block Digestion / Inductively Coupled Plasma-Mass Spectroscopy (ICP-MS)	Richmond

Note: An asterisk in the Method Reference indicates that the CARO method has been modified from the reference method

Glossary of Terms:

RL	Reporting Limit (default)
<	Less than the specified Reporting Limit (RL) - the actual RL may be higher than the default RL due to various factors
mg/L	Milligrams per litre
pH units	pH < 7 = acidic, ph > 7 = basic
µS/cm	Microsiemens per centimetre
EPA	United States Environmental Protection Agency Test Methods
SM	Standard Methods for the Examination of Water and Wastewater, American Public Health Association

Guidelines Referenced in this Report:

CCME CEQG Residential/Parkland/Aquatic (Lowest)
Metro Van MAMFS Regulations

Note: In some cases, the values displayed on the report represent the lowest guideline and are to be verified by the end user

General Comments:

The results in this report apply to the samples analyzed in accordance with the Chain of Custody document. This analytical report must be reproduced in its entirety. CARO is not responsible for any loss or damage resulting directly or indirectly from error or omission in the conduct of testing. Liability is limited to the cost of analysis. Samples will be disposed of 30 days after the test report has been issued unless otherwise agreed to in writing. The quality control (QC) data is available upon request

CARO ANALYTICAL SERVICES

CERTIFICATE OF ANALYSIS

REPORTED TO	Vancouver, City of (Green Infrastructure Branch) 305- 456 W. Broadway Vancouver,, BC V5Y 1R3		
ATTENTION	Osvaldo Vega	**WORK ORDER**	8121139
PO NUMBER		**RECEIVED / TEMP**	2018-12-13 13:50 / 8°C
PROJECT	110006	**REPORTED**	2018-12-20 14:08
PROJECT INFO		**COC NUMBER**	No #

Introduction:

CARO Analytical Services is a testing laboratory full of smart, engaged scientists driven to make the world a safer and healthier place. Through our clients' projects we become an essential element for a better world. We employ methods conducted in accordance with recognized professional standards using accepted testing methodologies and quality control efforts. CARO is accredited by the Canadian Association for Laboratories Accreditation (CALA) to ISO 17025:2005 for specific tests listed in the scope of accreditation approved by CALA.

Big Picture Sidekicks

You know that the sample you collected after snowshoeing to site, digging 5 meters, and racing to get it on a plane so you can submit it to the lab for time sensitive results needed to make important and expensive decisions (whew) is VERY important. We know that too.

We've Got Chemistry

It's simple. We figure the more you enjoy working with our fun and engaged team members; the more likely you are to give us continued opportunities to support you.

Ahead of the Curve

Through research, regulation knowledge, and instrumentation, we are your analytical centre for the technical knowledge you need, BEFORE you need it, so you can stay up to date and in the know.

If you have any questions or concerns, please contact me at teamcaro@caro.ca

Authorized By:

Team CARO
Client Service Representative

CARO
ANALYTICAL SERVICES

TEST RESULTS

REPORTED TO Vancouver, City of (Green Infrastructure Branch)
PROJECT 110006

WORK ORDER 8121139
REPORTED 2018-12-20 14:08

Analyte	Result	Guideline	RL	Units	Analyzed	Qualifier
in-001 (8121139-01) | Matrix: Water | Sampled: 2018-12-13 11:00						
Anions						
Nitrate (as N)	**0.071**	57.6	0.010	mg/L	2018-12-14	
Nitrite (as N)	**0.015**	0.06	0.010	mg/L	2018-12-14	
Calculated Parameters						
Carbon, Total	**3.11**	N/A	0.500	mg/L	N/A	
Hardness, Total (as CaCO3)	**8.96**	N/A	0.500	mg/L	N/A	
Nitrate+Nitrite (as N)	**0.0858**	N/A	0.0200	mg/L	N/A	
General Parameters						
Carbon, Total Inorganic	**0.93**	N/A	0.50	mg/L	2018-12-17	
Carbon, Total Organic	**2.18**	N/A	0.50	mg/L	2018-12-17	
Conductivity (EC)	**29.1**	200	2.0	µS/cm	2018-12-18	
Nitrogen, Total Kjeldahl	**0.498**	N/A	0.050	mg/L	2018-12-17	
Oxygen, Dissolved	**10.9**	6.5	1.0	mg/L	2018-12-18	HT1
pH	**6.54**	6.5-9.0	0.10	pH units	2018-12-19	HT2
Phosphorus, Total (as P)	**0.0506**	N/A	0.0020	mg/L	2018-12-16	
Solids, Total Suspended	**47.0**	N/A	2.0	mg/L	2018-12-19	
Total Metals						
Aluminum, total	**0.760**	0.005	0.0050	mg/L	2018-12-19	
Antimony, total	**0.00173**	N/A	0.00020	mg/L	2018-12-19	
Arsenic, total	< 0.00050	0.005	0.00050	mg/L	2018-12-19	
Barium, total	**0.0252**	N/A	0.0050	mg/L	2018-12-19	
Beryllium, total	< 0.00010	N/A	0.00010	mg/L	2018-12-19	
Bismuth, total	**0.00063**	N/A	0.00010	mg/L	2018-12-19	
Boron, total	**0.0140**	1.5	0.0050	mg/L	2018-12-19	
Cadmium, total	**0.000125**	0.00009	0.000010	mg/L	2018-12-19	
Calcium, total	**3.00**	N/A	0.20	mg/L	2018-12-19	
Chromium, total	**0.00399**	N/A	0.00050	mg/L	2018-12-19	
Cobalt, total	**0.00101**	N/A	0.00010	mg/L	2018-12-19	
Copper, total	**0.0309**	0.002	0.00040	mg/L	2018-12-19	
Iron, total	**0.911**	0.3	0.010	mg/L	2018-12-19	
Lead, total	**0.00469**	0.001	0.00020	mg/L	2018-12-19	
Lithium, total	**0.00071**	N/A	0.00010	mg/L	2018-12-19	
Magnesium, total	**0.351**	N/A	0.010	mg/L	2018-12-19	
Manganese, total	**0.0261**	N/A	0.00020	mg/L	2018-12-19	
Mercury, total	< 0.000040	0.000026	0.000040	mg/L	2018-12-19	CT5
Molybdenum, total	**0.00051**	0.073	0.00010	mg/L	2018-12-19	
Nickel, total	**0.00165**	0.025	0.00040	mg/L	2018-12-19	
Phosphorus, total	**0.053**	N/A	0.050	mg/L	2018-12-19	
Potassium, total	**0.22**	N/A	0.10	mg/L	2018-12-19	
Selenium, total	< 0.00050	0.001	0.00050	mg/L	2018-12-19	
Silicon, total	**1.2**	N/A	1.0	mg/L	2018-12-19	

TEST RESULTS

REPORTED TO	Vancouver, City of (Green Infrastructure Branch)	**WORK ORDER**	8121139
PROJECT	110006	**REPORTED**	2018-12-20 14:08

Analyte	Result	Guideline	RL	Units	Analyzed	Qualifier
in-001 (8121139-01) | Matrix: Water | Sampled: 2018-12-13 11:00, Continued						
Total Metals, Continued						
Silver, total	< 0.000050	0.00025	0.000050	mg/L	2018-12-19	
Sodium, total	**2.57**	N/A	0.10	mg/L	2018-12-19	
Strontium, total	**0.0119**	N/A	0.0010	mg/L	2018-12-19	
Sulfur, total	< 3.0	N/A	3.0	mg/L	2018-12-19	
Tellurium, total	< 0.00050	N/A	0.00050	mg/L	2018-12-19	
Thallium, total	< 0.000020	0.0008	0.000020	mg/L	2018-12-19	
Thorium, total	< 0.00010	N/A	0.00010	mg/L	2018-12-19	
Tin, total	**0.00156**	N/A	0.00020	mg/L	2018-12-19	
Titanium, total	**0.0310**	N/A	0.0050	mg/L	2018-12-19	
Tungsten, total	< 0.0010	N/A	0.0010	mg/L	2018-12-19	
Uranium, total	**0.000037**	0.015	0.000020	mg/L	2018-12-19	
Vanadium, total	**0.0018**	N/A	0.0010	mg/L	2018-12-19	
Zinc, total	**0.0810**	0.03	0.0040	mg/L	2018-12-19	
Zirconium, total	**0.00058**	N/A	0.00010	mg/L	2018-12-19	
out-001 (8121139-02) | Matrix: Water | Sampled: 2018-12-13 11:04						
Anions						
Nitrate (as N)	**8.17**	57.6	0.010	mg/L	2018-12-14	
Nitrite (as N)	**0.010**	0.06	0.010	mg/L	2018-12-14	
Calculated Parameters						
Carbon, Total	**35.3**	N/A	5.00	mg/L	N/A	
Hardness, Total (as CaCO3)	**71.8**	N/A	0.500	mg/L	N/A	
Nitrate+Nitrite (as N)	**8.18**	N/A	0.0200	mg/L	N/A	
General Parameters						
Carbon, Total Inorganic	**11.3**	N/A	0.50	mg/L	2018-12-17	
Carbon, Total Organic	**24.0**	N/A	0.50	mg/L	2018-12-17	
Conductivity (EC)	**311**	200	2.0	µS/cm	2018-12-18	
Nitrogen, Total Kjeldahl	**11.0**	N/A	0.050	mg/L	2018-12-17	
Oxygen, Dissolved	**10.1**	6.5	1.0	mg/L	2018-12-18	HT1
pH	**7.17**	6.5-9.0	0.10	pH units	2018-12-19	HT2
Phosphorus, Total (as P)	**4.17**	N/A	0.0020	mg/L	2018-12-16	
Solids, Total Suspended	**26.0**	N/A	2.0	mg/L	2018-12-19	
Total Metals						
Aluminum, total	**0.859**	0.005	0.0050	mg/L	2018-12-19	
Antimony, total	**0.00062**	N/A	0.00020	mg/L	2018-12-19	
Arsenic, total	**0.00939**	0.005	0.00050	mg/L	2018-12-19	
Barium, total	**0.0472**	N/A	0.0050	mg/L	2018-12-19	
Beryllium, total	< 0.00010	N/A	0.00010	mg/L	2018-12-19	
Bismuth, total	< 0.00010	N/A	0.00010	mg/L	2018-12-19	

TEST RESULTS

REPORTED TO	Vancouver, City of (Green Infrastructure Branch)	**WORK ORDER**	8121139
PROJECT	110006	**REPORTED**	2018-12-20 14:08

Analyte	Result	Guideline	RL	Units	Analyzed	Qualifier
out-001 (8121139-02) | Matrix: Water | Sampled: 2018-12-13 11:04, Continued						
Total Metals, Continued						
Boron, total	**0.0339**	1.5	0.0050	mg/L	2018-12-19	
Cadmium, total	**0.000735**	0.00009	0.000010	mg/L	2018-12-19	
Calcium, total	**21.2**	N/A	0.20	mg/L	2018-12-19	
Chromium, total	**0.00219**	N/A	0.00050	mg/L	2018-12-19	
Cobalt, total	**0.00160**	N/A	0.00010	mg/L	2018-12-19	
Copper, total	**0.0258**	0.002	0.00040	mg/L	2018-12-19	
Iron, total	**1.06**	0.3	0.010	mg/L	2018-12-19	
Lead, total	**0.00110**	0.001	0.00020	mg/L	2018-12-19	
Lithium, total	**0.00088**	N/A	0.00010	mg/L	2018-12-19	
Magnesium, total	**4.56**	N/A	0.010	mg/L	2018-12-19	
Manganese, total	**0.0658**	N/A	0.00020	mg/L	2018-12-19	
Mercury, total	< 0.000040	0.000026	0.000040	mg/L	2018-12-19	CT5
Molybdenum, total	**0.00294**	0.073	0.00010	mg/L	2018-12-19	
Nickel, total	**0.00540**	0.025	0.00040	mg/L	2018-12-19	
Phosphorus, total	**4.67**	N/A	0.050	mg/L	2018-12-19	
Potassium, total	**34.6**	N/A	0.10	mg/L	2018-12-19	
Selenium, total	< 0.00050	0.001	0.00050	mg/L	2018-12-19	
Silicon, total	**4.1**	N/A	1.0	mg/L	2018-12-19	
Silver, total	**0.000104**	0.00025	0.000050	mg/L	2018-12-19	
Sodium, total	**12.9**	N/A	0.10	mg/L	2018-12-19	
Strontium, total	**0.0821**	N/A	0.0010	mg/L	2018-12-19	
Sulfur, total	**3.7**	N/A	3.0	mg/L	2018-12-19	
Tellurium, total	< 0.00050	N/A	0.00050	mg/L	2018-12-19	
Thallium, total	**0.000026**	0.0008	0.000020	mg/L	2018-12-19	
Thorium, total	< 0.00010	N/A	0.00010	mg/L	2018-12-19	
Tin, total	< 0.00020	N/A	0.00020	mg/L	2018-12-19	
Titanium, total	**0.0301**	N/A	0.0050	mg/L	2018-12-19	
Tungsten, total	< 0.0010	N/A	0.0010	mg/L	2018-12-19	
Uranium, total	**0.000140**	0.015	0.000020	mg/L	2018-12-19	
Vanadium, total	**0.0063**	N/A	0.0010	mg/L	2018-12-19	
Zinc, total	**0.0225**	0.03	0.0040	mg/L	2018-12-19	
Zirconium, total	**0.00103**	N/A	0.00010	mg/L	2018-12-19	

Sample Qualifiers:

CT5	This sample has been incorrectly preserved for Mercury analysis
HT1	The sample was prepared and/or analyzed past the recommended holding time.
HT2	The 15 minute recommended holding time (from sampling to analysis) has been exceeded - field analysis is recommended.

CARO
ANALYTICAL SERVICES

APPENDIX 1: SUPPORTING INFORMATION

REPORTED TO	Vancouver, City of (Green Infrastructure Branch)	**WORK ORDER**	8121139
PROJECT	110006	**REPORTED**	2018-12-20 14:08

Analysis Description	Method Ref.	Technique	Location
Anions in Water	SM 4110 B (2011)	Ion Chromatography	Kelowna
Carbon, Total Inorganic in Water	SM 5310 B (2011)	Combustion, Infrared CO2 Detection	Kelowna
Carbon, Total Organic in Water	SM 5310 B (2011)	Combustion, Infrared CO2 Detection	Kelowna
Conductivity in Water	SM 2510 B (2011)	Conductivity Meter	Richmond
Dissolved Oxygen in Water	SM 4500-O G (2011)	Membrane Electrode	Richmond
Hardness in Water	SM 2340 B* (2011)	Calculation: 2.497 [total Ca] + 4.118 [total Mg] (Est)	N/A
Nitrogen, Total Kjeldahl in Water	SM 4500-Norg D* (2011)	Block Digestion and Flow Injection Analysis	Kelowna
pH in Water	SM 4500-H+ B (2011)	Electrometry	Richmond
Phosphorus, Total in Water	SM 4500-P B.5* (2011) / SM 4500-P F (2011)	Persulfate Digestion / Automated Colorimetry (Ascorbic Acid)	Kelowna
Solids, Total Suspended in Water	SM 2540 D* (2011)	Gravimetry (Dried at 103-105C)	Richmond
Total Metals in Water	EPA 200.2* / EPA 6020B	HNO3+HCl Hot Block Digestion / Inductively Coupled Plasma-Mass Spectroscopy (ICP-MS)	Richmond

Note: An asterisk in the Method Reference indicates that the CARO method has been modified from the reference method

Glossary of Terms:

RL	Reporting Limit (default)
<	Less than the specified Reporting Limit (RL) - the actual RL may be higher than the default RL due to various factors
mg/L	Milligrams per litre
pH units	pH < 7 = acidic, ph > 7 = basic
µS/cm	Microsiemens per centimetre
EPA	United States Environmental Protection Agency Test Methods
SM	Standard Methods for the Examination of Water and Wastewater, American Public Health Association

Guidelines Referenced in this Report:

CCME CEQG Residential/Parkland/Aquatic (Lowest)
Metro Van MAMFS Regulations

Note: In some cases, the values displayed on the report represent the lowest guideline and are to be verified by the end user

General Comments:

The results in this report apply to the samples analyzed in accordance with the Chain of Custody document. This analytical report must be reproduced in its entirety. CARO is not responsible for any loss or damage resulting directly or indirectly from error or omission in the conduct of testing. Liability is limited to the cost of analysis. Samples will be disposed of 30 days after the test report has been issued unless otherwise agreed to in writing. The quality control (QC) data is available upon request

CARO ANALYTICAL SERVICES

CERTIFICATE OF ANALYSIS

REPORTED TO	Vancouver, City of (Green Infrastructure Branch) 305- 456 W. Broadway Vancouver,, BC V5Y 1R3		
ATTENTION	Osvaldo Vega	**WORK ORDER**	9010123
PO NUMBER		**RECEIVED / TEMP**	2019-01-03 11:05 / 8°C
PROJECT	320004	**REPORTED**	2019-01-10 15:14
PROJECT INFO		**COC NUMBER**	No #

Introduction:

CARO Analytical Services is a testing laboratory full of smart, engaged scientists driven to make the world a safer and healthier place. Through our clients' projects we become an essential element for a better world. We employ methods conducted in accordance with recognized professional standards using accepted testing methodologies and quality control efforts. CARO is accredited by the Canadian Association for Laboratories Accreditation (CALA) to ISO 17025:2005 for specific tests listed in the scope of accreditation approved by CALA.

Big Picture Sidekicks

You know that the sample you collected after snowshoeing to site, digging 5 meters, and racing to get it on a plane so you can submit it to the lab for time sensitive results needed to make important and expensive decisions (whew) is VERY important. We know that too.

We've Got Chemistry

It's simple. We figure the more you enjoy working with our fun and engaged team members; the more likely you are to give us continued opportunities to support you.

Ahead of the Curve

Through research, regulation knowledge, and instrumentation, we are your analytical centre for the technical knowledge you need, BEFORE you need it, so you can stay up to date and in the know.

If you have any questions or concerns, please contact me at teamcaro@caro.ca

Authorized By:

Team CARO
Client Service Representative

CARO ANALYTICAL SERVICES

TEST RESULTS

REPORTED TO Vancouver, City of (Green Infrastructure Branch)
PROJECT 320004

WORK ORDER 9010123
REPORTED 2019-01-10 15:14

Analyte	Result	Guideline	RL	Units	Analyzed	Qualifier
in-001 (9010123-01) | Matrix: Water | Sampled: 2019-01-03 10:03						
Anions						
Nitrate (as N)	**0.055**	57.6	0.010	mg/L	2019-01-05	
Nitrite (as N)	< 0.010	0.06	0.010	mg/L	2019-01-05	
Calculated Parameters						
Carbon, Total	**3.17**	N/A	0.500	mg/L	N/A	
Hardness, Total (as CaCO3)	**6.15**	N/A	0.500	mg/L	N/A	
Nitrate+Nitrite (as N)	**0.0553**	N/A	0.0200	mg/L	N/A	
General Parameters						
Carbon, Total Inorganic	**1.33**	N/A	0.50	mg/L	2019-01-10	
Carbon, Total Organic	**1.84**	N/A	0.50	mg/L	2019-01-07	
Conductivity (EC)	**31.7**	200	2.0	µS/cm	2019-01-03	
Nitrogen, Total Kjeldahl	**0.334**	N/A	0.050	mg/L	2019-01-07	
Oxygen, Dissolved	**10.0**	6.5	1.0	mg/L	2019-01-07	HT2
pH	**7.33**	6.5-9.0	0.10	pH units	2019-01-04	HT2
Phosphorus, Total (as P)	**0.0510**	N/A	0.0020	mg/L	2019-01-05	
Solids, Total Suspended	**29.8**	N/A	2.0	mg/L	2019-01-04	
Total Metals						
Aluminum, total	**0.439**	0.005	0.0050	mg/L	2019-01-05	
Antimony, total	**0.00128**	N/A	0.00020	mg/L	2019-01-05	
Arsenic, total	< 0.00050	0.005	0.00050	mg/L	2019-01-05	
Barium, total	**0.0162**	N/A	0.0050	mg/L	2019-01-05	
Beryllium, total	< 0.00010	N/A	0.00010	mg/L	2019-01-05	
Bismuth, total	**0.00044**	N/A	0.00010	mg/L	2019-01-05	
Boron, total	< 0.0050	1.5	0.0050	mg/L	2019-01-05	
Cadmium, total	**0.000152**	0.00009	0.000010	mg/L	2019-01-05	
Calcium, total	**2.07**	N/A	0.20	mg/L	2019-01-05	
Chromium, total	**0.00186**	N/A	0.00050	mg/L	2019-01-05	
Cobalt, total	**0.00030**	N/A	0.00010	mg/L	2019-01-05	
Copper, total	**0.0181**	0.002	0.00040	mg/L	2019-01-05	
Iron, total	**0.581**	0.3	0.010	mg/L	2019-01-05	
Lead, total	**0.00217**	0.001	0.00020	mg/L	2019-01-05	
Lithium, total	**0.00042**	N/A	0.00010	mg/L	2019-01-05	
Magnesium, total	**0.238**	N/A	0.010	mg/L	2019-01-05	
Manganese, total	**0.0185**	N/A	0.00020	mg/L	2019-01-05	
Mercury, total	< 0.000040	0.000026	0.000040	mg/L	2019-01-05	CT5
Molybdenum, total	**0.00045**	0.073	0.00010	mg/L	2019-01-05	
Nickel, total	**0.00122**	0.025	0.00040	mg/L	2019-01-05	
Phosphorus, total	< 0.050	N/A	0.050	mg/L	2019-01-05	
Potassium, total	**0.18**	N/A	0.10	mg/L	2019-01-05	
Selenium, total	< 0.00050	0.001	0.00050	mg/L	2019-01-05	
Silicon, total	< 1.0	N/A	1.0	mg/L	2019-01-05	

CARO ANALYTICAL SERVICES

TEST RESULTS

REPORTED TO	Vancouver, City of (Green Infrastructure Branch)	**WORK ORDER**	9010123
PROJECT	320004	**REPORTED**	2019-01-10 15:14

Analyte	Result	Guideline	RL	Units	Analyzed	Qualifier
in-001 (9010123-01) | Matrix: Water | Sampled: 2019-01-03 10:03, Continued						
Total Metals, Continued						
Silver, total	< 0.000050	0.00025	0.000050	mg/L	2019-01-05	
Sodium, total	**3.50**	N/A	0.10	mg/L	2019-01-05	
Strontium, total	**0.0080**	N/A	0.0010	mg/L	2019-01-05	
Sulfur, total	< 3.0	N/A	3.0	mg/L	2019-01-05	
Tellurium, total	< 0.00050	N/A	0.00050	mg/L	2019-01-05	
Thallium, total	< 0.000020	0.0008	0.000020	mg/L	2019-01-05	
Thorium, total	< 0.00010	N/A	0.00010	mg/L	2019-01-05	
Tin, total	**0.00165**	N/A	0.00020	mg/L	2019-01-05	
Titanium, total	**0.0174**	N/A	0.0050	mg/L	2019-01-05	
Tungsten, total	< 0.0010	N/A	0.0010	mg/L	2019-01-05	
Uranium, total	**0.000025**	0.015	0.000020	mg/L	2019-01-05	
Vanadium, total	**0.0011**	N/A	0.0010	mg/L	2019-01-05	
Zinc, total	**0.0629**	0.03	0.0040	mg/L	2019-01-05	
Zirconium, total	**0.00132**	N/A	0.00010	mg/L	2019-01-05	
out-001 (9010123-02) | Matrix: Water | Sampled: 2019-01-03 10:13						
Anions						
Nitrate (as N)	**0.267**	57.6	0.010	mg/L	2019-01-05	
Nitrite (as N)	< 0.010	0.06	0.010	mg/L	2019-01-05	
Calculated Parameters						
Carbon, Total	**3.59**	N/A	0.500	mg/L	N/A	
Hardness, Total (as CaCO3)	**7.56**	N/A	0.500	mg/L	N/A	
Nitrate+Nitrite (as N)	**0.267**	N/A	0.0200	mg/L	N/A	
General Parameters						
Carbon, Total Inorganic	**1.44**	N/A	0.50	mg/L	2019-01-10	
Carbon, Total Organic	**2.15**	N/A	0.50	mg/L	2019-01-07	
Conductivity (EC)	**43.2**	200	2.0	µS/cm	2019-01-03	
Nitrogen, Total Kjeldahl	**0.165**	N/A	0.050	mg/L	2019-01-07	
Oxygen, Dissolved	**10.6**	6.5	1.0	mg/L	2019-01-07	HT2
pH	**6.93**	6.5-9.0	0.10	pH units	2019-01-04	HT2
Phosphorus, Total (as P)	**0.0331**	N/A	0.0020	mg/L	2019-01-05	
Solids, Total Suspended	**11.6**	N/A	2.0	mg/L	2019-01-04	
Total Metals						
Aluminum, total	**0.202**	0.005	0.0050	mg/L	2019-01-05	
Antimony, total	**0.00078**	N/A	0.00020	mg/L	2019-01-05	
Arsenic, total	< 0.00050	0.005	0.00050	mg/L	2019-01-05	
Barium, total	**0.0102**	N/A	0.0050	mg/L	2019-01-05	
Beryllium, total	< 0.00010	N/A	0.00010	mg/L	2019-01-05	
Bismuth, total	**0.00018**	N/A	0.00010	mg/L	2019-01-05	

TEST RESULTS

REPORTED TO	Vancouver, City of (Green Infrastructure Branch)	**WORK ORDER**	9010123
PROJECT	320004	**REPORTED**	2019-01-10 15:14

Analyte	Result	Guideline	RL	Units	Analyzed	Qualifier
out-001 (9010123-02) | Matrix: Water | Sampled: 2019-01-03 10:13, Continued						
Total Metals, Continued						
Boron, total	< 0.0050	1.5	0.0050	mg/L	2019-01-05	
Cadmium, total	**0.000030**	0.00009	0.000010	mg/L	2019-01-05	
Calcium, total	**2.56**	N/A	0.20	mg/L	2019-01-05	
Chromium, total	**0.00110**	N/A	0.00050	mg/L	2019-01-05	
Cobalt, total	**0.00015**	N/A	0.00010	mg/L	2019-01-05	
Copper, total	**0.00852**	0.002	0.00040	mg/L	2019-01-05	
Iron, total	**0.216**	0.3	0.010	mg/L	2019-01-05	
Lead, total	**0.00098**	0.001	0.00020	mg/L	2019-01-05	
Lithium, total	**0.00032**	N/A	0.00010	mg/L	2019-01-05	
Magnesium, total	**0.283**	N/A	0.010	mg/L	2019-01-05	
Manganese, total	**0.0101**	N/A	0.00020	mg/L	2019-01-05	
Mercury, total	< 0.000040	0.000026	0.000040	mg/L	2019-01-05	CT5
Molybdenum, total	**0.00036**	0.073	0.00010	mg/L	2019-01-05	
Nickel, total	**0.00062**	0.025	0.00040	mg/L	2019-01-05	
Phosphorus, total	< 0.050	N/A	0.050	mg/L	2019-01-05	
Potassium, total	**0.63**	N/A	0.10	mg/L	2019-01-05	
Selenium, total	< 0.00050	0.001	0.00050	mg/L	2019-01-05	
Silicon, total	< 1.0	N/A	1.0	mg/L	2019-01-05	
Silver, total	< 0.000050	0.00025	0.000050	mg/L	2019-01-05	
Sodium, total	**3.80**	N/A	0.10	mg/L	2019-01-05	
Strontium, total	**0.0100**	N/A	0.0010	mg/L	2019-01-05	
Sulfur, total	< 3.0	N/A	3.0	mg/L	2019-01-05	
Tellurium, total	< 0.00050	N/A	0.00050	mg/L	2019-01-05	
Thallium, total	< 0.000020	0.0008	0.000020	mg/L	2019-01-05	
Thorium, total	< 0.00010	N/A	0.00010	mg/L	2019-01-05	
Tin, total	**0.00066**	N/A	0.00020	mg/L	2019-01-05	
Titanium, total	**0.0096**	N/A	0.0050	mg/L	2019-01-05	
Tungsten, total	< 0.0010	N/A	0.0010	mg/L	2019-01-05	
Uranium, total	< 0.000020	0.015	0.000020	mg/L	2019-01-05	
Vanadium, total	< 0.0010	N/A	0.0010	mg/L	2019-01-05	
Zinc, total	**0.0251**	0.03	0.0040	mg/L	2019-01-05	
Zirconium, total	**0.00035**	N/A	0.00010	mg/L	2019-01-05	

Sample Qualifiers:

CT5	This sample has been incorrectly preserved for Mercury analysis
HT2	The 15 minute recommended holding time (from sampling to analysis) has been exceeded - field analysis is recommended.

CARO
ANALYTICAL SERVICES

APPENDIX 1: SUPPORTING INFORMATION

REPORTED TO	Vancouver, City of (Green Infrastructure Branch)	**WORK ORDER**	9010123
PROJECT	320004	**REPORTED**	2019-01-10 15:14

Analysis Description	Method Ref.	Technique	Location
Anions in Water	SM 4110 B (2011)	Ion Chromatography	Kelowna
Carbon, Total Inorganic in Water	SM 5310 B (2011)	Combustion, Infrared CO2 Detection	Kelowna
Carbon, Total Organic in Water	SM 5310 B (2011)	Combustion, Infrared CO2 Detection	Kelowna
Conductivity in Water	SM 2510 B (2011)	Conductivity Meter	Richmond
Dissolved Oxygen in Water	SM 4500-O G (2011)	Membrane Electrode	Richmond
Hardness in Water	SM 2340 B* (2011)	Calculation: 2.497 [total Ca] + 4.118 [total Mg] (Est)	N/A
Nitrogen, Total Kjeldahl in Water	SM 4500-Norg D* (2011)	Block Digestion and Flow Injection Analysis	Kelowna
pH in Water	SM 4500-H+ B (2011)	Electrometry	Richmond
Phosphorus, Total in Water	SM 4500-P B.5* (2011) / SM 4500-P F (2011)	Persulfate Digestion / Automated Colorimetry (Ascorbic Acid)	Kelowna
Solids, Total Suspended in Water	SM 2540 D* (2011)	Gravimetry (Dried at 103-105C)	Richmond
Total Metals in Water	EPA 200.2* / EPA 6020B	HNO3+HCl Hot Block Digestion / Inductively Coupled Plasma-Mass Spectroscopy (ICP-MS)	Richmond

Note: An asterisk in the Method Reference indicates that the CARO method has been modified from the reference method

Glossary of Terms:

RL	Reporting Limit (default)
<	Less than the specified Reporting Limit (RL) - the actual RL may be higher than the default RL due to various factors
mg/L	Milligrams per litre
pH units	pH < 7 = acidic, ph > 7 = basic
µS/cm	Microsiemens per centimetre
EPA	United States Environmental Protection Agency Test Methods
SM	Standard Methods for the Examination of Water and Wastewater, American Public Health Association

Guidelines Referenced in this Report:

CCME CEQG Residential/Parkland/Aquatic (Lowest)
Metro Van MAMFS Regulations

Note: In some cases, the values displayed on the report represent the lowest guideline and are to be verified by the end user

General Comments:

The results in this report apply to the samples analyzed in accordance with the Chain of Custody document. This analytical report must be reproduced in its entirety. CARO is not responsible for any loss or damage resulting directly or indirectly from error or omission in the conduct of testing. Liability is limited to the cost of analysis. Samples will be disposed of 30 days after the test report has been issued unless otherwise agreed to in writing. The quality control (QC) data is available upon request

CARO ANALYTICAL SERVICES

CERTIFICATE OF ANALYSIS

REPORTED TO	Vancouver, City of (Green Infrastructure Branch) 305- 456 W. Broadway Vancouver,, BC V5Y 1R3		
ATTENTION	Osvaldo Vega	**WORK ORDER**	9020070
PO NUMBER	vancouver.ca	**RECEIVED / TEMP**	2019-02-01 14:35 / 7°C
PROJECT	320004	**REPORTED**	2019-02-08 13:11
PROJECT INFO		**COC NUMBER**	No #

Introduction:

CARO Analytical Services is a testing laboratory full of smart, engaged scientists driven to make the world a safer and healthier place. Through our clients' projects we become an essential element for a better world. We employ methods conducted in accordance with recognized professional standards using accepted testing methodologies and quality control efforts. CARO is accredited by the Canadian Association for Laboratories Accreditation (CALA) to ISO 17025:2005 for specific tests listed in the scope of accreditation approved by CALA.

Big Picture Sidekicks

You know that the sample you collected after snowshoeing to site, digging 5 meters, and racing to get it on a plane so you can submit it to the lab for time sensitive results needed to make important and expensive decisions (whew) is VERY important. We know that too.

We've Got Chemistry

It's simple. We figure the more you enjoy working with our fun and engaged team members; the more likely you are to give us continued opportunities to support you.

Ahead of the Curve

Through research, regulation knowledge, and instrumentation, we are your analytical centre for the technical knowledge you need, BEFORE you need it, so you can stay up to date and in the know.

If you have any questions or concerns, please contact me at teamcaro@caro.ca

Authorized By:

Team CARO
Client Service Representative

CARO ANALYTICAL SERVICES

TEST RESULTS

REPORTED TO	Vancouver, City of (Green Infrastructure Branch)	**WORK ORDER**	9020070
PROJECT	320004	**REPORTED**	2019-02-08 13:11

Analyte	Result	Guideline	RL	Units	Analyzed	Qualifier
in-002 (9020070-01) | Matrix: Water | Sampled: 2019-02-01 11:47						
Anions						
Nitrate (as N)	**0.175**	57.6	0.010	mg/L	2019-02-03	
Nitrite (as N)	**0.024**	0.06	0.010	mg/L	2019-02-03	
Calculated Parameters						
Carbon, Total	**7.59**	N/A	0.500	mg/L	N/A	
Hardness, Total (as CaCO3)	**26.3**	N/A	0.500	mg/L	N/A	
Nitrate+Nitrite (as N)	**0.199**	N/A	0.0200	mg/L	N/A	
General Parameters						
Carbon, Total Inorganic	**3.63**	N/A	0.50	mg/L	2019-02-07	
Carbon, Total Organic	**3.96**	N/A	0.50	mg/L	2019-02-05	
Conductivity (EC)	**114**	200	2.0	µS/cm	2019-02-07	
Nitrogen, Total Kjeldahl	**2.39**	N/A	0.050	mg/L	2019-02-03	
Oxygen, Dissolved	**9.9**	6.5	1.0	mg/L	2019-02-07	HT2
pH	**7.21**	6.5-9.0	0.10	pH units	2019-02-07	HT2
Phosphorus, Total (as P)	**0.193**	N/A	0.0020	mg/L	2019-02-05	
Solids, Total Suspended	**137**	N/A	2.0	mg/L	2019-02-06	
Total Metals						
Aluminum, total	**2.16**	0.005	0.0050	mg/L	2019-02-07	
Antimony, total	**0.00227**	N/A	0.00020	mg/L	2019-02-07	
Arsenic, total	**0.00102**	0.005	0.00050	mg/L	2019-02-07	
Barium, total	**0.0809**	N/A	0.0050	mg/L	2019-02-07	
Beryllium, total	< 0.00010	N/A	0.00010	mg/L	2019-02-07	
Bismuth, total	**0.00081**	N/A	0.00010	mg/L	2019-02-07	
Boron, total	**0.0118**	1.5	0.0050	mg/L	2019-02-07	
Cadmium, total	**0.000252**	0.00009	0.000010	mg/L	2019-02-07	
Calcium, total	**9.05**	N/A	0.20	mg/L	2019-02-07	
Chromium, total	**0.00684**	N/A	0.00050	mg/L	2019-02-07	
Cobalt, total	**0.00176**	N/A	0.00010	mg/L	2019-02-07	
Copper, total	**0.0901**	0.002	0.00040	mg/L	2019-02-07	
Iron, total	**3.26**	0.3	0.010	mg/L	2019-02-07	
Lead, total	**0.0120**	0.001	0.00020	mg/L	2019-02-07	
Lithium, total	**0.00165**	N/A	0.00010	mg/L	2019-02-07	
Magnesium, total	**0.895**	N/A	0.010	mg/L	2019-02-07	
Manganese, total	**0.0895**	N/A	0.00020	mg/L	2019-02-07	
Mercury, total	< 0.000010	0.000026	0.000010	mg/L	2019-02-06	
Molybdenum, total	**0.00088**	0.073	0.00010	mg/L	2019-02-07	
Nickel, total	**0.00567**	0.025	0.00040	mg/L	2019-02-07	
Phosphorus, total	**0.221**	N/A	0.050	mg/L	2019-02-07	
Potassium, total	**0.62**	N/A	0.10	mg/L	2019-02-07	
Selenium, total	< 0.00050	0.001	0.00050	mg/L	2019-02-07	
Silicon, total	**3.7**	N/A	1.0	mg/L	2019-02-07	

CARO ANALYTICAL SERVICES

TEST RESULTS

REPORTED TO	Vancouver, City of (Green Infrastructure Branch)	**WORK ORDER**	9020070
PROJECT	320004	**REPORTED**	2019-02-08 13:11

Analyte	Result	Guideline	RL	Units	Analyzed	Qualifier
in-002 (9020070-01) | Matrix: Water | Sampled: 2019-02-01 11:47, Continued						
Total Metals, Continued						
Silver, total	**0.000066**	0.00025	0.000050	mg/L	2019-02-07	
Sodium, total	**14.1**	N/A	0.10	mg/L	2019-02-07	
Strontium, total	**0.0398**	N/A	0.0010	mg/L	2019-02-07	
Sulfur, total	< 3.0	N/A	3.0	mg/L	2019-02-07	
Tellurium, total	< 0.00050	N/A	0.00050	mg/L	2019-02-07	
Thallium, total	< 0.000020	0.0008	0.000020	mg/L	2019-02-07	
Thorium, total	< 0.00010	N/A	0.00010	mg/L	2019-02-07	
Tin, total	**0.00308**	N/A	0.00020	mg/L	2019-02-07	
Titanium, total	**0.0782**	N/A	0.0050	mg/L	2019-02-07	
Tungsten, total	< 0.0010	N/A	0.0010	mg/L	2019-02-07	
Uranium, total	**0.000191**	0.015	0.000020	mg/L	2019-02-07	
Vanadium, total	**0.0060**	N/A	0.0010	mg/L	2019-02-07	
Zinc, total	**0.276**	0.03	0.0040	mg/L	2019-02-07	
Zirconium, total	**0.00140**	N/A	0.00010	mg/L	2019-02-07	
out-002 (9020070-02) | Matrix: Water | Sampled: 2019-02-01 11:47						
Anions						
Nitrate (as N)	**0.396**	57.6	0.010	mg/L	2019-02-03	
Nitrite (as N)	**0.022**	0.06	0.010	mg/L	2019-02-03	
Calculated Parameters						
Carbon, Total	**8.10**	N/A	0.500	mg/L	N/A	
Hardness, Total (as CaCO3)	**16.6**	N/A	0.500	mg/L	N/A	
Nitrate+Nitrite (as N)	**0.418**	N/A	0.0200	mg/L	N/A	
General Parameters						
Carbon, Total Inorganic	**3.78**	N/A	0.50	mg/L	2019-02-07	
Carbon, Total Organic	**4.32**	N/A	0.50	mg/L	2019-02-05	
Conductivity (EC)	**124**	200	2.0	µS/cm	2019-02-07	
Nitrogen, Total Kjeldahl	**0.642**	N/A	0.050	mg/L	2019-02-03	
Oxygen, Dissolved	**10.6**	6.5	1.0	mg/L	2019-02-07	HT2
pH	**7.14**	6.5-9.0	0.10	pH units	2019-02-07	HT2
Phosphorus, Total (as P)	**0.0496**	N/A	0.0020	mg/L	2019-02-05	
Solids, Total Suspended	**18.4**	N/A	2.0	mg/L	2019-02-06	
Total Metals						
Aluminum, total	**0.378**	0.005	0.0050	mg/L	2019-02-07	
Antimony, total	**0.00164**	N/A	0.00020	mg/L	2019-02-07	
Arsenic, total	< 0.00050	0.005	0.00050	mg/L	2019-02-07	
Barium, total	**0.0208**	N/A	0.0050	mg/L	2019-02-07	
Beryllium, total	< 0.00010	N/A	0.00010	mg/L	2019-02-07	
Bismuth, total	**0.00028**	N/A	0.00010	mg/L	2019-02-07	

CARO
ANALYTICAL SERVICES

TEST RESULTS

REPORTED TO	Vancouver, City of (Green Infrastructure Branch)	**WORK ORDER**	9020070
PROJECT	320004	**REPORTED**	2019-02-08 13:11

out-002 (9020070-02) | Matrix: Water | Sampled: 2019-02-01 11:47, Continued

Analyte	Result	Guideline	RL	Units	Analyzed	Qualifier
Total Metals, Continued						
Boron, total	**0.0086**	1.5	0.0050	mg/L	2019-02-07	
Cadmium, total	**0.000069**	0.00009	0.000010	mg/L	2019-02-07	
Calcium, total	**5.92**	N/A	0.20	mg/L	2019-02-07	
Chromium, total	**0.00232**	N/A	0.00050	mg/L	2019-02-07	
Cobalt, total	**0.00023**	N/A	0.00010	mg/L	2019-02-07	
Copper, total	**0.0174**	0.002	0.00040	mg/L	2019-02-07	
Iron, total	**0.390**	0.3	0.010	mg/L	2019-02-07	
Lead, total	**0.00193**	0.001	0.00020	mg/L	2019-02-07	
Lithium, total	**0.00076**	N/A	0.00010	mg/L	2019-02-07	
Magnesium, total	**0.452**	N/A	0.010	mg/L	2019-02-07	
Manganese, total	**0.0149**	N/A	0.00020	mg/L	2019-02-07	
Mercury, total	< 0.000010	0.000026	0.000010	mg/L	2019-02-06	
Molybdenum, total	**0.00079**	0.073	0.00010	mg/L	2019-02-07	
Nickel, total	**0.00091**	0.025	0.00040	mg/L	2019-02-07	
Phosphorus, total	< 0.050	N/A	0.050	mg/L	2019-02-07	
Potassium, total	**0.98**	N/A	0.10	mg/L	2019-02-07	
Selenium, total	< 0.00050	0.001	0.00050	mg/L	2019-02-07	
Silicon, total	**1.3**	N/A	1.0	mg/L	2019-02-07	
Silver, total	< 0.000050	0.00025	0.000050	mg/L	2019-02-07	
Sodium, total	**14.2**	N/A	0.10	mg/L	2019-02-07	
Strontium, total	**0.0246**	N/A	0.0010	mg/L	2019-02-07	
Sulfur, total	< 3.0	N/A	3.0	mg/L	2019-02-07	
Tellurium, total	< 0.00050	N/A	0.00050	mg/L	2019-02-07	
Thallium, total	< 0.000020	0.0008	0.000020	mg/L	2019-02-07	
Thorium, total	< 0.00010	N/A	0.00010	mg/L	2019-02-07	
Tin, total	**0.00066**	N/A	0.00020	mg/L	2019-02-07	
Titanium, total	**0.0133**	N/A	0.0050	mg/L	2019-02-07	
Tungsten, total	< 0.0010	N/A	0.0010	mg/L	2019-02-07	
Uranium, total	**0.000028**	0.015	0.000020	mg/L	2019-02-07	
Vanadium, total	**0.0019**	N/A	0.0010	mg/L	2019-02-07	
Zinc, total	**0.0472**	0.03	0.0040	mg/L	2019-02-07	
Zirconium, total	**0.00089**	N/A	0.00010	mg/L	2019-02-07	

Sample Qualifiers:

HT2 The 15 minute recommended holding time (from sampling to analysis) has been exceeded - field analysis is recommended.

CARO ANALYTICAL SERVICES

APPENDIX 1: SUPPORTING INFORMATION

REPORTED TO	Vancouver, City of (Green Infrastructure Branch)	**WORK ORDER**	9020070
PROJECT	320004	**REPORTED**	2019-02-08 13:11

Analysis Description	Method Ref.	Technique	Location
Anions in Water	SM 4110 B (2011)	Ion Chromatography	Kelowna
Carbon, Total Inorganic in Water	SM 5310 B (2011)	Combustion, Infrared CO2 Detection	Kelowna
Carbon, Total Organic in Water	SM 5310 B (2011)	Combustion, Infrared CO2 Detection	Kelowna
Conductivity in Water	SM 2510 B (2011)	Conductivity Meter	Richmond
Dissolved Oxygen in Water	SM 4500-O G (2011)	Membrane Electrode	Richmond
Hardness in Water	SM 2340 B* (2011)	Calculation: 2.497 [total Ca] + 4.118 [total Mg] (Est)	N/A
Mercury, total in Water	EPA 245.7*	BrCl2 Oxidation / Cold Vapor Atomic Fluorescence Spectrometry (CVAFS)	Richmond
Nitrogen, Total Kjeldahl in Water	SM 4500-Norg D* (2011)	Block Digestion and Flow Injection Analysis	Kelowna
pH in Water	SM 4500-H+ B (2011)	Electrometry	Richmond
Phosphorus, Total in Water	SM 4500-P B.5* (2011) / SM 4500-P F (2011)	Persulfate Digestion / Automated Colorimetry (Ascorbic Acid)	Kelowna
Solids, Total Suspended in Water	SM 2540 D* (2011)	Gravimetry (Dried at 103-105C)	Richmond
Total Metals in Water	EPA 200.2* / EPA 6020B	HNO3+HCl Hot Block Digestion / Inductively Coupled Plasma-Mass Spectroscopy (ICP-MS)	Richmond

Note: An asterisk in the Method Reference indicates that the CARO method has been modified from the reference method

Glossary of Terms:

RL	Reporting Limit (default)
<	Less than the specified Reporting Limit (RL) - the actual RL may be higher than the default RL due to various factors
mg/L	Milligrams per litre
pH units	pH < 7 = acidic, ph > 7 = basic
µS/cm	Microsiemens per centimetre
EPA	United States Environmental Protection Agency Test Methods
SM	Standard Methods for the Examination of Water and Wastewater, American Public Health Association

Guidelines Referenced in this Report:

CCME CEQG Residential/Parkland/Aquatic (Lowest)
Metro Van MAMFS Regulations

Note: In some cases, the values displayed on the report represent the lowest guideline and are to be verified by the end user

General Comments:

The results in this report apply to the samples analyzed in accordance with the Chain of Custody document. This analytical report must be reproduced in its entirety. CARO is not responsible for any loss or damage resulting directly or indirectly from error or omission in the conduct of testing. Liability is limited to the cost of analysis. Samples will be disposed of 30 days after the test report has been issued unless otherwise agreed to in writing. The quality control (QC) data is available upon request

CARO
ANALYTICAL SERVICES

CERTIFICATE OF ANALYSIS

REPORTED TO	Vancouver, City of (Green Infrastructure Branch) 305- 456 W. Broadway Vancouver,, BC V5Y 1R3		
ATTENTION	Osvaldo Vega	**WORK ORDER**	9021944
PO NUMBER	vancouver.ca	**RECEIVED / TEMP**	2019-02-28 10:20 / 20°C
PROJECT	Fieldblank	**REPORTED**	2019-03-08 14:37
PROJECT INFO		**COC NUMBER**	No #

Introduction:

CARO Analytical Services is a testing laboratory full of smart, engaged scientists driven to make the world a safer and healthier place. Through our clients' projects we become an essential element for a better world. We employ methods conducted in accordance with recognized professional standards using accepted testing methodologies and quality control efforts. CARO is accredited by the Canadian Association for Laboratories Accreditation (CALA) to ISO 17025:2005 for specific tests listed in the scope of accreditation approved by CALA.

Big Picture Sidekicks

You know that the sample you collected after snowshoeing to site, digging 5 meters, and racing to get it on a plane so you can submit it to the lab for time sensitive results needed to make important and expensive decisions (whew) is VERY important. We know that too.

We've Got Chemistry

It's simple. We figure the more you enjoy working with our fun and engaged team members; the more likely you are to give us continued opportunities to support you.

Ahead of the Curve

Through research, regulation knowledge, and instrumentation, we are your analytical centre for the technical knowledge you need, BEFORE you need it, so you can stay up to date and in the know.

If you have any questions or concerns, please contact me at teamcaro@caro.ca

Authorized By:

Team CARO
Client Service Representative

CARO ANALYTICAL SERVICES

TEST RESULTS

REPORTED TO	Vancouver, City of (Green Infrastructure Branch)	**WORK ORDER**	9021944
PROJECT	Fieldblank	**REPORTED**	2019-03-08 14:37

Analyte	Result	Guideline	RL	Units	Analyzed	Qualifier
in-001 (9021944-01) | Matrix: Water | Sampled: 2019-02-28 09:30						
Anions						
Nitrate+Nitrite (as N)	**0.0138**	N/A	0.0050	mg/L	2019-03-03	
Calculated Parameters						
Carbon, Total	**0.642**	N/A	0.500	mg/L	N/A	
Hardness, Total (as CaCO3)	< 0.500	N/A	0.500	mg/L	N/A	
Nitrogen, Total	< 0.0500	N/A	0.0500	mg/L	N/A	
General Parameters						
Carbon, Total Inorganic	< 0.50	N/A	0.50	mg/L	2019-03-04	
Carbon, Total Organic	**0.64**	N/A	0.50	mg/L	2019-03-01	
Conductivity (EC)	**2.2**	200	2.0	µS/cm	2019-03-05	
Nitrogen, Total Kjeldahl	< 0.050	N/A	0.050	mg/L	2019-03-02	
Oxygen, Dissolved	**10.6**	6.5	1.0	mg/L	2019-03-06	HT2
pH	**4.78**	6.5-9.0	0.10	pH units	2019-03-05	HT2
Phosphorus, Total (as P)	**0.0117**	N/A	0.0020	mg/L	2019-03-03	
Solids, Total Suspended	< 2.0	N/A	2.0	mg/L	2019-03-06	
Total Metals						
Aluminum, total	**0.0209**	0.005	0.0050	mg/L	2019-03-04	
Antimony, total	< 0.00020	N/A	0.00020	mg/L	2019-03-04	
Arsenic, total	< 0.00050	0.005	0.00050	mg/L	2019-03-04	
Barium, total	< 0.0050	N/A	0.0050	mg/L	2019-03-04	
Beryllium, total	< 0.00010	N/A	0.00010	mg/L	2019-03-04	
Bismuth, total	< 0.00010	N/A	0.00010	mg/L	2019-03-04	
Boron, total	< 0.0050	1.5	0.0050	mg/L	2019-03-04	
Cadmium, total	**0.000033**	0.00009	0.000010	mg/L	2019-03-04	
Calcium, total	< 0.20	N/A	0.20	mg/L	2019-03-04	
Chromium, total	< 0.00050	N/A	0.00050	mg/L	2019-03-04	
Cobalt, total	< 0.00010	N/A	0.00010	mg/L	2019-03-04	
Copper, total	**0.00154**	0.002	0.00040	mg/L	2019-03-04	
Iron, total	**0.010**	0.3	0.010	mg/L	2019-03-04	
Lead, total	< 0.00020	0.001	0.00020	mg/L	2019-03-04	
Lithium, total	< 0.00010	N/A	0.00010	mg/L	2019-03-04	
Magnesium, total	< 0.010	N/A	0.010	mg/L	2019-03-04	
Manganese, total	**0.00042**	N/A	0.00020	mg/L	2019-03-04	
Mercury, total	< 0.000040	0.000026	0.000040	mg/L	2019-03-04	CT5
Molybdenum, total	< 0.00010	0.073	0.00010	mg/L	2019-03-04	
Nickel, total	< 0.00040	0.025	0.00040	mg/L	2019-03-04	
Phosphorus, total	**0.109**	N/A	0.050	mg/L	2019-03-04	
Potassium, total	< 0.10	N/A	0.10	mg/L	2019-03-04	
Selenium, total	< 0.00050	0.001	0.00050	mg/L	2019-03-04	
Silicon, total	< 1.0	N/A	1.0	mg/L	2019-03-04	
Silver, total	< 0.000050	0.00025	0.000050	mg/L	2019-03-04	

CARO
ANALYTICAL SERVICES

TEST RESULTS

REPORTED TO	Vancouver, City of (Green Infrastructure Branch)	**WORK ORDER**	9021944
PROJECT	Fieldblank	**REPORTED**	2019-03-08 14:37

Analyte	Result	Guideline	RL	Units	Analyzed	Qualifier
in-001 (9021944-01) | Matrix: Water | Sampled: 2019-02-28 09:30, Continued						
Total Metals, Continued						
Sodium, total	< 0.10	N/A	0.10	mg/L	2019-03-04	
Strontium, total	< 0.0010	N/A	0.0010	mg/L	2019-03-04	
Sulfur, total	< 3.0	N/A	3.0	mg/L	2019-03-04	
Tellurium, total	< 0.00050	N/A	0.00050	mg/L	2019-03-04	
Thallium, total	< 0.000020	0.0008	0.000020	mg/L	2019-03-04	
Thorium, total	< 0.00010	N/A	0.00010	mg/L	2019-03-04	
Tin, total	< 0.00020	N/A	0.00020	mg/L	2019-03-04	
Titanium, total	< 0.0050	N/A	0.0050	mg/L	2019-03-04	
Tungsten, total	< 0.0010	N/A	0.0010	mg/L	2019-03-04	
Uranium, total	< 0.000020	0.015	0.000020	mg/L	2019-03-04	
Vanadium, total	< 0.0010	N/A	0.0010	mg/L	2019-03-04	
Zinc, total	**0.0092**	0.03	0.0040	mg/L	2019-03-04	
Zirconium, total	< 0.00010	N/A	0.00010	mg/L	2019-03-04	
out-001 (9021944-02) | Matrix: Water | Sampled: 2019-02-28 09:30						
Anions						
Nitrate+Nitrite (as N)	< 0.0050	N/A	0.0050	mg/L	2019-03-03	
Calculated Parameters						
Carbon, Total	**0.570**	N/A	0.500	mg/L	N/A	
Hardness, Total (as CaCO3)	< 0.500	N/A	0.500	mg/L	N/A	
Nitrogen, Total	< 0.0500	N/A	0.0500	mg/L	N/A	
General Parameters						
Carbon, Total Inorganic	< 0.50	N/A	0.50	mg/L	2019-03-04	
Carbon, Total Organic	**0.57**	N/A	0.50	mg/L	2019-03-01	
Conductivity (EC)	< 2.0	200	2.0	µS/cm	2019-03-05	
Nitrogen, Total Kjeldahl	< 0.050	N/A	0.050	mg/L	2019-03-02	
Oxygen, Dissolved	**10.8**	6.5	1.0	mg/L	2019-03-06	HT2
pH	**4.81**	6.5-9.0	0.10	pH units	2019-03-05	HT2
Phosphorus, Total (as P)	**0.0228**	N/A	0.0020	mg/L	2019-03-03	
Solids, Total Suspended	**2.0**	N/A	2.0	mg/L	2019-03-06	
Total Metals						
Aluminum, total	**0.0127**	0.005	0.0050	mg/L	2019-03-04	
Antimony, total	< 0.00020	N/A	0.00020	mg/L	2019-03-04	
Arsenic, total	< 0.00050	0.005	0.00050	mg/L	2019-03-04	
Barium, total	< 0.0050	N/A	0.0050	mg/L	2019-03-04	
Beryllium, total	< 0.00010	N/A	0.00010	mg/L	2019-03-04	
Bismuth, total	< 0.00010	N/A	0.00010	mg/L	2019-03-04	
Boron, total	< 0.0050	1.5	0.0050	mg/L	2019-03-04	
Cadmium, total	**0.000029**	0.00009	0.000010	mg/L	2019-03-04	

CARO
ANALYTICAL SERVICES

TEST RESULTS

REPORTED TO	Vancouver, City of (Green Infrastructure Branch)	**WORK ORDER**	9021944
PROJECT	Fieldblank	**REPORTED**	2019-03-08 14:37

Analyte	Result	Guideline	RL	Units	Analyzed	Qualifier
out-001 (9021944-02) | Matrix: Water | Sampled: 2019-02-28 09:30, Continued						
Total Metals, Continued						
Calcium, total	< 0.20	N/A	0.20	mg/L	2019-03-04	
Chromium, total	< 0.00050	N/A	0.00050	mg/L	2019-03-04	
Cobalt, total	< 0.00010	N/A	0.00010	mg/L	2019-03-04	
Copper, total	**0.00137**	0.002	0.00040	mg/L	2019-03-04	
Iron, total	**0.021**	0.3	0.010	mg/L	2019-03-04	
Lead, total	**0.00024**	0.001	0.00020	mg/L	2019-03-04	
Lithium, total	< 0.00010	N/A	0.00010	mg/L	2019-03-04	
Magnesium, total	< 0.010	N/A	0.010	mg/L	2019-03-04	
Manganese, total	**0.00055**	N/A	0.00020	mg/L	2019-03-04	
Mercury, total	< 0.000010	0.000026	0.000010	mg/L	2019-03-05	
Molybdenum, total	< 0.00010	0.073	0.00010	mg/L	2019-03-04	
Nickel, total	< 0.00040	0.025	0.00040	mg/L	2019-03-04	
Phosphorus, total	**0.174**	N/A	0.050	mg/L	2019-03-04	
Potassium, total	< 0.10	N/A	0.10	mg/L	2019-03-04	
Selenium, total	< 0.00050	0.001	0.00050	mg/L	2019-03-04	
Silicon, total	< 1.0	N/A	1.0	mg/L	2019-03-04	
Silver, total	< 0.000050	0.00025	0.000050	mg/L	2019-03-04	
Sodium, total	< 0.10	N/A	0.10	mg/L	2019-03-04	
Strontium, total	< 0.0010	N/A	0.0010	mg/L	2019-03-04	
Sulfur, total	< 3.0	N/A	3.0	mg/L	2019-03-04	
Tellurium, total	< 0.00050	N/A	0.00050	mg/L	2019-03-04	
Thallium, total	< 0.000020	0.0008	0.000020	mg/L	2019-03-04	
Thorium, total	< 0.00010	N/A	0.00010	mg/L	2019-03-04	
Tin, total	< 0.00020	N/A	0.00020	mg/L	2019-03-04	
Titanium, total	< 0.0050	N/A	0.0050	mg/L	2019-03-04	
Tungsten, total	< 0.0010	N/A	0.0010	mg/L	2019-03-04	
Uranium, total	< 0.000020	0.015	0.000020	mg/L	2019-03-04	
Vanadium, total	< 0.0010	N/A	0.0010	mg/L	2019-03-04	
Zinc, total	**0.0084**	0.03	0.0040	mg/L	2019-03-04	
Zirconium, total	< 0.00010	N/A	0.00010	mg/L	2019-03-04	

Sample Qualifiers:

CT5	This sample has been incorrectly preserved for Mercury analysis
HT2	The 15 minute recommended holding time (from sampling to analysis) has been exceeded - field analysis is recommended.

CARO
ANALYTICAL SERVICES

APPENDIX 1: SUPPORTING INFORMATION

REPORTED TO	Vancouver, City of (Green Infrastructure Branch)	**WORK ORDER**	9021944
PROJECT	Fieldblank	**REPORTED**	2019-03-08 14:37

Analysis Description	Method Ref.	Technique	Location
Carbon, Total Inorganic in Water	SM 5310 B (2011)	Combustion, Infrared CO2 Detection	Kelowna
Carbon, Total Organic in Water	SM 5310 B (2011)	Combustion, Infrared CO2 Detection	Kelowna
Conductivity in Water	SM 2510 B (2011)	Conductivity Meter	Richmond
Dissolved Oxygen in Water	SM 4500-O G (2011)	Membrane Electrode	Richmond
Hardness in Water	SM 2340 B* (2011)	Calculation: 2.497 [total Ca] + 4.118 [total Mg] (Est)	N/A
Mercury, total in Water	EPA 245.7*	BrCl2 Oxidation / Cold Vapor Atomic Fluorescence Spectrometry (CVAFS)	Richmond
Nitrate+Nitrite in Water	SM 4500-NO3- F (2011)	Automated Colorimetry (Cadmium Reduction)	Kelowna
Nitrogen, Total Kjeldahl in Water	SM 4500-Norg D* (2011)	Block Digestion and Flow Injection Analysis	Kelowna
pH in Water	SM 4500-H+ B (2011)	Electrometry	Richmond
Phosphorus, Total in Water	SM 4500-P B.5* (2011) / SM 4500-P F (2011)	Persulfate Digestion / Automated Colorimetry (Ascorbic Acid)	Kelowna
Solids, Total Suspended in Water	SM 2540 D* (2011)	Gravimetry (Dried at 103-105C)	Richmond
Total Metals in Water	EPA 200.2* / EPA 6020B	HNO3+HCl Hot Block Digestion / Inductively Coupled Plasma-Mass Spectroscopy (ICP-MS)	Richmond

Note: An asterisk in the Method Reference indicates that the CARO method has been modified from the reference method

Glossary of Terms:

RL	Reporting Limit (default)
<	Less than the specified Reporting Limit (RL) - the actual RL may be higher than the default RL due to various factors
mg/L	Milligrams per litre
pH units	pH < 7 = acidic, ph > 7 = basic
µS/cm	Microsiemens per centimetre
EPA	United States Environmental Protection Agency Test Methods
SM	Standard Methods for the Examination of Water and Wastewater, American Public Health Association

Guidelines Referenced in this Report:

CCME CEQG Residential/Parkland/Aquatic (Lowest)
Metro Van MAMFS Regulations

Note: In some cases, the values displayed on the report represent the lowest guideline and are to be verified by the end user

General Comments:

The results in this report apply to the samples analyzed in accordance with the Chain of Custody document. This analytical report must be reproduced in its entirety. CARO is not responsible for any loss or damage resulting directly or indirectly from error or omission in the conduct of testing. Liability is limited to the cost of analysis. Samples will be disposed of 30 days after the test report has been issued unless otherwise agreed to in writing. The quality control (QC) data is available upon request

Results in **Bold** indicate values that are above CARO's method reporting limits. Any results that are above regulatory limits are highlighted **red**. Please note that results will only be highlighted red if the regulatory limits are included on the CARO report. Any Bold and/or highlighted results do not take into account method uncertainty. If you would like method